Analysis of the impact of climate change on hydrological processes in Iceland. A case study.

Philippe Crochet

Report number: 2023-RD-01	Date: August 2023	Number of pages:180	Distribution: Public

Report title:
Analysis of the impact of climate change on hydrological processes in Iceland. A case study.

Author:
Philippe Crochet
philippec@simnet.is

Abstract:

This study presents a comparative analysis of the hydrological response of three Icelandic river catchments to projected climate change in the 21st century. Daily streamflow series were simulated for the period 1981-2100 with the HYPE hydrological model forced with an ensemble of regional climate projections from CORDEX, considering two greenhouse gas emission scenarios. Changes affecting near surface air temperature and precipitation and their impact on mean and extreme streamflow characteristics were analysed. There is a general consensus that air temperature will rise in the future and that precipitation will likely increase in summer and autumn. Projected climate change, if it realises, is expected to have a significant impact on the hydrological characteristics of the three catchments in the future. However, the timing, magnitude and direction of the hydrological response are expected to be different from season to season and from one catchment to another because their characteristics differ.

Prepared for:
The research fund of the Icelandic Road and Coastal Administration

Keywords:
Iceland - Hydrology - Climate change - CORDEX - HYPE model

Executive summary

This study presents an analysis of the hydrological response of three Icelandic river catchments to projected climate change in the 21st century. The Þverá catchment is located near the coast in the Westfjords; The Markarfljót catchment is located in the southern highlands, in the region of Myrdalsjökull ice cap, and has a 13% glacier coverage; The Kreppa catchment is located in the northeast central highlands, in the region of Vatnajökull ice cap, and has a 51% glacier coverage.

An ensemble of daily streamflow series was simulated for the period 1981-2100, with the HYPE hydrological model forced with locally-adjusted temperature and precipitation outputs from an ensemble of CORDEX climate projections, considering two greenhouse gas emission scenarios referred to as Representative Concentration Pathways (RCPs 4.5 and 8.5). Projected changes affecting near surface air temperature, precipitation, snow storage, snow and glacier melt, and their impact on mean and extreme streamflow characteristics were analysed, considering moving 30-year time-windows. The reference period was taken as 1981-2010.

A significant warming is projected over the course of the 21st century, more or less pronounced according to the season, catchment location and emission scenario (0.29°C/decade for the RCP4.5 emission scenario and 0.46°C/decade for the RCP8.5 emission scenario, on average over all months and catchments). Precipitation variations are characterised by decadal to multi-decadal oscillations reflecting natural climate variability. The different precipitation projections do not always fluctuate in phase with each other, which sometimes leads to large uncertainties regarding both direction and magnitude of changes in annual and seasonal means, depending on the future time-windows under consideration. Despite these large fluctuations, mean precipitation is projected to significantly increase in summer and autumn in the future in the three catchments, especially under the RCP8.5 emission scenario, and decrease in winter in the Markarfljót catchment.

Projected climate change, if it realises, is expected to have a significant impact on the hydrological characteristics of the three studied catchments in the future. The main driver of these changes is the projected warming, which is expected to lead to more rainfall at the expense of snowfall, to a decrease in snow storage and to changes in snow and glacier melt. The magnitude of the hydrological response varies over the course of the 21st century and is different from one catchment to another because their characteristics differ. In summary, results indicate that mean seasonal streamflow is likely to increase in all seasons in the future in the Kreppa catchment, whereas in the Þverá and Markarfljót catchments, mean streamflow is projected to i) increase in autumn and winter, ii) increase in spring under both emission scenarios but decrease towards the end of the century under the RCP8.5 emission scenario, iii) decrease in summer.

Projected climate change will also have an impact on flood risk in the future. Changes in the seasonal frequency of occurrence of annual maximum floods are expected in the Þverá and Markarfljót catchments with an increase in autumn/winter and a decrease in spring/summer. An increase in the magnitude of annual maximum floods is also expected in the Kreppa and Markarfljót catchments.

1 Introduction

Global warming caused by human influence is unequivocal (IPCC 2021). The study of climate change due to anthropogenic greenhouse gas emissions and its potential impact on ecosystems and societies has become a subject of primary concern. In particular, numerous studies have investigated the impact of projected climate change on the hydrological characteristics of river basins worldwide and associated extreme events such as floods and droughts (e.g. Habets et al. 2013; Arheimer and Lindström 2015; Vetter et al. 2015; Vormoor et al. 2015; Wanders and Wada 2015; Naz et al. 2016; Frans et al. 2018; Osuch et al. 2018; Wan et al. 2018; Somers et al. 2019; Zhao et al. 2019; Lane and Kay 2021; and many others). In Iceland, several studies have analysed recent climate variations and projected climate changes in the 21st century and their impact on glaciers and hydrology. Results indicate that climate warming is expected to lead to more rainfall at the expense of snowfall, shorter snow seasons and less snow storage, retreat of glaciers, and to changes in the seasonality of streamflow in snow-dominated and glacier-fed river basins (e.g. Jóhannesson et al. 2007; Einarsson and Jónsson 2010; Thorsteinsson and Björnsson Eds. 2011; Björnsson et al. 2018; Aðalgeirsdóttir et al. 2020; Crochet 2013, 2020, 2021, 2022).

Projected changes affecting hydrological characteristics of river basins are likely to have consequences on water resources management, operation of reservoirs and existing hydropower installations and flood and drought risks. Therefore, studying the potential impact of projected climate change on hydrological processes is necessary in order to help identify the most appropriate adaptation strategies and mitigating actions to be deployed to insure resilience of society in the future.

The aim of this study is to continue the work of Crochet (2020, 2021, 2022) and document the likely hydrological response to projected climate change in Iceland in the 21st century. Following the same procedure as in Crochet (2022), an ensemble of daily hydrological series was simulated for the period 1981-2100, in three river catchments located in different regions of the country. The HYPE hydrological model was used for that purpose and forced with locally-adjusted temperature and precipitation outputs from an ensemble of climate projections from CORDEX, considering two greenhouse gas emission scenarios. Projected changes affecting near surface air temperature, precipitation, snow storage, snow and glacier melt, and their impact on mean and extreme streamflow characteristics were analysed.

This report is organised as follows. Section 2 presents the studied catchments and Section 3 presents the data and methods. Section 4 is dedicated to the calibration of the hydrological model and Section 5 to the analysis of the climate projections. The hydrological response to projected climate change is analysed in Sections 6 and 7 and Section 8 concludes this report.

2 The investigated catchments

The three river catchments are situated in different regions of the country (Figure 1 and Table 1). The Þverá catchment is located close to the coast in the Westfjords; The Markarfljót catchment is partly-glaciated and located in the southern highlands, in the region of Myrdalsjökull ice-cap; The Kreppa catchment is partly-glaciated and located in the northeast central highlands, in the region of Vatnajökull ice-cap. The delineation of the drainage areas of these catchments was made with a digital elevation model (DEM) from ArcticDEM (Porter et al., 2018) but the average elevations given in Table 1 were estimated with the DEM from the National Land Survey of Iceland (see Section 3-6 below), which can explain the differences between these estimates and those given in Hróðmarsson and Þórarinsdóttir (2018) or Massad et al. (2022), especially in the case of the Kreppa catchment due to its large glaciated extent. The streamflow gauging stations located in these catchments are monitored by Veðurstofa Íslands (Icelandic Met. Office).

Icelandic rivers are usually classified in three main categories according to the origin of flow, direct runoff rivers (D), glacial fed rivers (J), groundwater fed rivers (L) and whether they flow through lakes (S). In practise, rivers are often a combination of several of these categories. According to Hróðmarsson and Þórarinsdóttir (2018), the Þverá river at gauging site vhm38 is a combination of two categories (D, S), the Kreppa river at gauging site vhm233 is a combination of two categories (J, D) and the Markarfljót river at gauging site vhm218 is a combination of three categories (J, D, L). According to the Corine Land Cover data (Árnason and Matthíasson, 2017), the Þverá catchment contains several lakes and is partly covered with mosses, poor heathland and with partly vegetated land; The Markarfljót catchment is partly glaciated (ca. 13%) and the land area is partly covered with mosses, poor heathland and with barren areas; The Kreppa catchment is partly glaciated (ca. 51%) and the land area is mostly barren. According to the soil map of Iceland (Arnalds and Óskarsson, 2009; Arnalds, 2015), the prevailing soil types found in the Þverá catchment are composed of i) a complex of Brown Andosol, Gleyic Andosol and Histosol, and ii) Cambic Vitrisol; The prevailing soil types found in the Markarfljót catchment are composed of i) Cambic Vitrisol, ii) Brown Andosol, iii) Arenic Vitrisol, iv) a complex of Cambic and Arenic Vitrisols, v) Leptosols and vi) a complex of Arenic Vitrisol and Leptosol; The prevailing soil types found in the Kreppa catchment are composed of i) a complex of Cambic and Arenic Vitrisols, ii) Cambic Vitrisol, iii) a complex of Arenic Vitrisol and Leptosol, and iv) Brown Andosol.

Table 1: Discharge gauging stations and main characteristics of catchments

Name of river and location of gauging station	**ID**	**River type**	**Drainage area (km²)**	**Average elevation (m.a.s.l)**
Þverá, Langadalsströnd; Nauteyri	vhm38	D, S	41	428
Markarfljót; Emstrur	vhm218	J, D, L	516	728
Kreppa, Krepputungu; Lónshnjúkur	vhm233	J, D	1126	1034

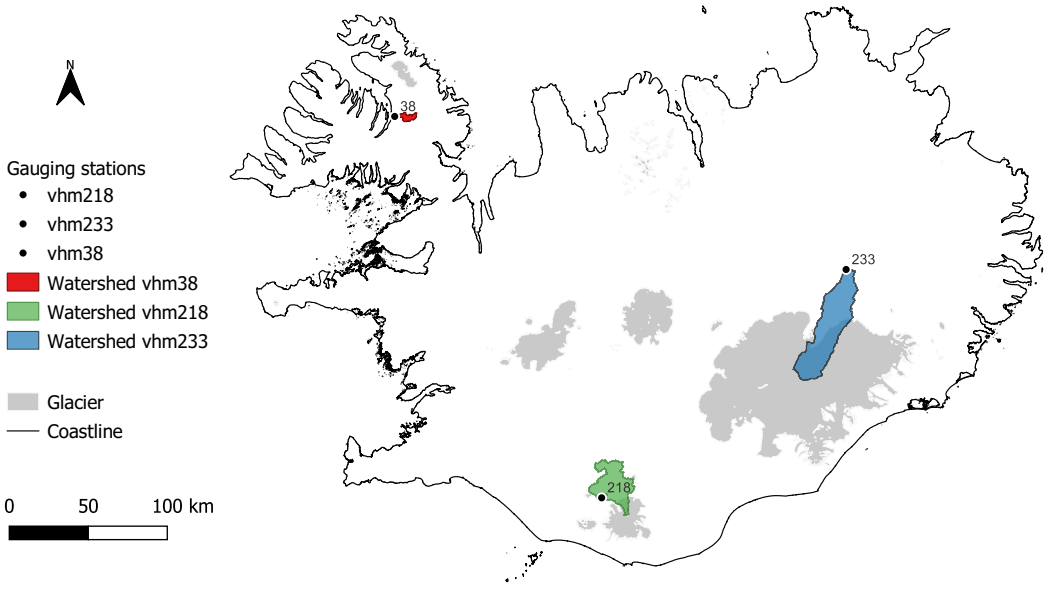

Figure 1: Overview of the studied catchments. Glaciers and coastline from National Land Survey of Iceland. Catchment delineation based on ArcticDEM (Porter et al., 2018).

3 Data and methods

The text below is mostly taken from Crochet (2022), since the same hydrological model, climate data and methodology are used.

3-1 Method overview

The following modelling chain was used to produce an ensemble of daily hydrological projections for the period 1981-2100:

"Greenhouse gas emission scenario → global climate model → regional downscaling → local adjustment / bias correction → hydrological model → analysis"

The climate forcing was provided by an ensemble of six regional climate projections from the CORDEX framework for two possible greenhouse gas emission scenarios (see Section 3-3). These climate projections were obtained from four regional climate models (RCMs) driven by two global climate models (GCMs) and their precipitation and temperature outputs were then locally adjusted using a statistical technique to improve their applicability at the catchment scale (see Section 3-7). Using an ensemble of climate projections rather than a single one gives a better representation of possible future states of the climate system under study and allows a more reliable evaluation of its future temporal evolution.

The HYPE hydrological model was used in this study (see Section 3-2). The model was calibrated over two consecutive periods, leading to two parameter sets. This approach is expected to improve the reliability of the hydrological simulations. In total, an ensemble of twelve daily hydrological projections (or twelve ensemble members) was obtained for the period 1981-2100 and each emission scenario (six climate projections × two HYPE parameter sets). The spread of the hydrological projections is expected to provide a plausible estimate of the uncertainty range associated with future hydrological characteristics.

Various hydro-climatic indicators were extracted from these projections and their characteristics analysed considering a moving time-window approach based on 30-year periods (1981-2010; 1991-2020; 2001-2030; 2011-2040; 2021-2050; 2031-2060; 2041-2070; 2051-2080; 2061-2090; 2071-2100). The reference or baseline period is defined as 1981-2010.

The hydro-climatic indicators considered in this study are:

- Near surface air temperature (catchment-averaged)
- Precipitation (catchment-averaged)
- Rainfall (catchment-averaged) (liquid fraction of precipitation)
- Snowfall (catchment-averaged) (solid fraction of precipitation)
- Snow storage, in snow water equivalent (SWE, catchment-averaged)
- Snow and glacier melt (catchment-averaged)
- River discharge at the catchment outlet

For each hydro-climatic indicator (except snow storage), monthly and/or seasonal and annual values were calculated each year, by averaging daily values from each month, season and water year, respectively, and their 30-year mean estimated in each 30-year time-window. The water-year is defined from October of year *i* to September of year *i*+1 and the four seasons are October to December (OND), January to March (JFM), April to June (AMJ) and July to September (JAS). These seasons will sometimes be referred to as autumn, winter, spring and summer, respectively. In order to analyse changes in more details, 30-year mean daily discharge and snow storage were also calculated for each day of the water year.

The annual maxima of the daily river discharge series (annual maximum floods, AMFs) were also extracted in each water-year and changes in the timing and magnitude of these extreme events examined. Changes in the timing of AMFs were analysed in order to examine possible changes in the flood-generating mechanisms. To do so, the day in the water-year when annual maximum discharge occurred was assigned to the corresponding season. The frequency with which AMFs occurred in each season was then calculated in each 30-year time-window. To analyse changes in the magnitude of extreme flood events, a Gumbel distribution was fitted to the AMFs (Stephenson 2002; Delignette-Muller and Dutang 2015) in each 30-year time-window and the magnitude of the T-year floods (for T=10 and 50 years) estimated. Finally, the flood magnitude Q was fixed and the corresponding return period T(Q) estimated in each 30-year time-window.

Changes affecting the statistical characteristics of each hydro-climatic indicator between the reference (1981-2010) and future 30-year periods were evaluated. A two-sided Mann-Whitney test with a 5% significance level was used to compare the 30-year mean daily snow storage and river discharge ensembles, respectively, between the reference and future periods. The null hypothesis being that the ensembles in the reference and future periods are drawn from populations having the same distribution and the alternative hypothesis being that the two populations differ. Two one-sided Mann-Whitney tests with a 5% significance level were used to compare the ensembles of 30-year mean seasonal and annual temperature, precipitation, rainfall, snowfall, snow and glacier melt, discharge, the T-year flood ensembles and the seasonal frequencies of occurrence of AMFs, respectively, between the reference and future periods. The null hypothesis being that the ensembles in the reference and future periods are drawn from populations having the same distribution and the alternative hypothesis either being that the population in the future period tends to be shifted towards larger values (increase) or towards lower values (decrease), compared to the population in the reference period. The two one-sided tests were run consecutively. When the null hypothesis was not rejected by both tests, it was reasonably concluded that the ensemble members from the two periods had been drawn from the same population, and no change was likely projected between the two periods. When the null hypothesis was rejected in favour of one of the alternative hypothesis, it was reasonably concluded that either an increase or decrease had likely been projected in the future period, compared to the reference period, depending on the selected alternative hypothesis.

For the projected return period T(Q), changes between the reference and future periods were considered significant when at least two-thirds of the ensemble members were shifted in the same direction (T(Q) increase or decrease).

Then, changes affecting the 30-year mean (annual, seasonal and/or daily) values of each hydro-climatic indicator and the T-year flood magnitude between reference and future periods were quantified. To do so, the future values of each ensemble member were compared with the value of the same member in the reference period, by calculating the difference (future minus reference) or relative difference in percent (100×(future minus reference)/reference), and the ensemble median of the difference or relative difference calculated.

The multi-model ensemble approach used in this study takes into consideration various sources of uncertainties in the modelling chain (future emission scenarios, global and regional climate modelling, hydrological model parameterisation). Other sources of uncertainty not included in the present study may also play some role in the overall uncertainty (e.g. local bias adjustment method, hydrological model structure, hydrological model calibration strategy). Velázquez et al. (2013) found that the added-value of using several hydrological models in climate change impact studies depended on the hydrological indicator considered and the region investigated. Their results suggested that the use of several types of hydrological models should be considered for the study of low flow, whilst most hydrological models tested by these authors led to comparable results in the case of high flow. Concerning mean flow, their results were found to depend on the region considered which led them to recommend to use several types of hydrological models, as for the study of low flow. Gosling et al. (2011) also found that the uncertainty associated with the type of hydrological model used could be substantial but still relatively small compared to the one arising from the use of multiple GCMs, in a study of projected changes of mean annual as well as high and low monthly runoff. The introduction of more components in the modelling chain would come at the cost of extra computational efforts and its added-value regarding the estimation of the overall uncertainty range would need to be evaluated for each catchment. A detailed analysis of the contribution of individual sources of uncertainty in the modelling chain to the overall hydrological uncertainty is beyond the focus of this study and therefore not undertaken. It is simply assumed that the modelling chain used in this study offers a reasonable trade-off between complexity and reliability.

3-2 The HYPE hydrological model

HYPE (Hydrological Predictions for the Environment) is a semi-distributed hydrological model developed by the Swedish Meteorological and Hydrological Institute (SMHI) to assess water resources and water quality. It is forced with time series of precipitation and near surface air temperature, typically on a daily time step, to simulate water flow and nutrients concentrations at the catchment scale. The catchment to be modelled may be divided into sub-catchments which, in turn, are divided into land cover and soil type classes. The soil classes can contain up to three

layers. A detailed description of the model can be found in Lindström et al. (2010) and on the HYPE wiki page (http://www.smhi.net/hype/wiki/doku.php).

3-3 Climate projections

The climate projections for daily precipitation and near surface air temperature used to force the hydrological model are based on the CORDEX framework (Coordinated Regional Climate Downscaling Experiment) (www.cordex.org). This framework has provided an ensemble of high-resolution regional climate projections over several regions of the world for use in impact and adaptation studies (Giorgi et al., 2009). The CORDEX projections were obtained by dynamical downscaling of a set of coarse global climate simulations made with different global climate models (GCMs), with a set of regional climate models (RCMs), assuming various greenhouse gas emission scenarios referred to as Representative Concentration Pathways (RCPs). The set of global climate model simulations used within CORDEX are part of the fifth phase of the Climate Model Inter-comparison Project (referred to as CMIP5), planned in support of the IPCC Fifth Assessment Report. The RCPs correspond to prescribed greenhouse-gas concentration pathways throughout the 21st century leading to different radiative forcing levels by the year 2100, relative to pre-industrial conditions (see for instance Giorgi et al., 2009; Benestad et al., 2017). Two RCPs emission scenarios are considered in this study in order to account for the uncertainty about future emissions. The first one (RCP4.5) assumes a warming scenario with a stabilisation of radiative forcing by the end of the 21st century at 4.5 W/m² and the second one (RCP8.5) represents very high greenhouse gas emissions and assumes a radiative forcing by the end of 21st century at 8.5 W/m² which continues to rise after 2100. In this project, the climate projections are taken from the European branch of CORDEX, EURO-CORDEX (www.euro-cordex.net) (Jacob *et al.*, 2014), as this region includes Iceland and is available at a very high horizontal resolution (0.11°, about 12.5 km).

The CORDEX projections consist of a historical period (1976-2005) and a projection period (2006-2100) assuming a given RCP. The projections in the historical period (1976-2005) do not correspond to the actual reality as it took place day after day but represent a possible realisation of what could have taken place. Evaluation series driven by the European Centre for Medium-Range Weather Forecasts (ECMWF) ERA-Interim reanalyses (Dee et al., 2011) and dynamically downscaled with the selected RCMs are available for the 1981-2010 period and have been used in this study to investigate the intrinsic quality of these RCMs.

Tables 2 and 3 present the GCMs and RCMs used in this study. The two selected GCMs are those suggested by Gosseling (2017) as the best GCMs for the Icelandic domain, namely MOHC-HadGEM2-ES and MPI-ESM-LR. Each CORDEX projection is considered equally likely.

Table 2: List of CORDEX GCMs and RCMs

Model	Type	Institution	Reference
ERA-Interim	Reanalysis	ECMWF	Dee et al. (2011)
MOHC-HadGEM2-ES	GCM	Met Office Hadley Centre	Jones et al. (2011)
MPI-ESM-LR	GCM	ESM of the Max-Planck-Institut fur Meteorologie	Giorgetta et al. (2013)
CCLM4-8-17	RCM	CLMcom: Climate Limited-area modelling community (CLM-Community)	Rockel et al. (2008)
RCA4	RCM	SMHI	Kupiainen et al. (2011) Samuelsson et al. (2011)
RACMO22E	RCM	KNMI	van Meijgaard et al. (2012)
REMO2009	RCM	MPI-CSC	Jacob et al. (2012)

Table 3: List of CORDEX GCM-RCM combinations and emission scenarios (RCP)

		RCP	RCM			
			CCLM4-8-17	RCA4	RACMO22E	REMO2009
Forcing GCM	ERA-Interim (evaluation)		x	x	x	x
	MOHC-HadGEM2-ES	RCP4.5 & RCP8.5	x	x	x	
	MPI-ESM-LR	RCP4.5 & RCP8.5	x	x		x

3-4 Reference climate data

Daily precipitation and 2m-temperature from the high-resolution (2.5 km) ICRA climate reanalysis (Nawri et al., 2017) produced by Veðurstofa Íslands constitute the historical meteorological data of reference (1981-2017) used i) as input to calibrate the HYPE hydrological model ii) to verify the credibility of the CORDEX climate projections in the historical period and iii) to statistically bias-correct the CORDEX climate projections prior to use them as input to the hydrological model.

3-5 Hydrological data

Daily-averaged discharge series from three gauging stations monitored by Veðurstofa Íslands (Fig. 1) were used to calibrate HYPE and verify the credibility of the simulated streamflow series in the historical period when the hydrological model was forced with the CORDEX climate projections.

3-6 Other data

The hydrological modelling with HYPE requires the use of a land cover map and a soil map. The Corine Land Cover data updated for the reference year 2012 (Árnason and Matthíasson, 2017) were used and obtained from the download page of the National Land Survey of Iceland. The soil map of Iceland compiled by the Agricultural University of Iceland (Arnalds and Óskarsson, 2009; Arnalds, 2015) was used and downloaded from http://rangarvellir.ru.is. A digital elevation model (DEM) with resolution 10m obtained from ArcticDEM (Porter et al., 2018) was used for the delineation of the catchments and sub-catchments borders and extraction of various hydrologic and physiographic information. A DEM with resolution 10m obtained from the download page of the National Land Survey of Iceland (http://atlas.lmi.is/LmiData/) was used to calculate the average elevation of the catchments (cf. Table 1). Additional information about coastline, glaciers and water bodies were also obtained from the download page of the National Land Survey of Iceland. The delineation of the catchment borders and extraction of all required hydrologic and physiographic information was done with QGIS.

3-7 Local bias-adjustment method

The CORDEX daily precipitation and air temperature projections have been locally adjusted prior to be used as input to the hydrological model. This adjustment is necessary in order to correct systematic biases and guaranty consistency between the climate projections and the ICRA reference climate used in the calibration of the HYPE model. The local adjustment is based on quantile mapping (QM) (Gudmundsson et al. 2012; Gudmundsson 2016), which is a distribution-based adjustment method. A specific QM adjustment was defined for each month. The adjustment coefficients were estimated by comparing the CORDEX climate series to the ICRA climate reanalysis in the common 1981-2005 period. The adjustment was then applied to the entire projection period (1976-2100).

4 Calibration and validation of the hydrological model

For the hydrological modelling, the Þverá catchment (vhm38) was divided into two sub-basins, the Kreppa catchment (vhm233) was divided into four sub-basins and the Markarfljót catchment (vhm218) was divided into twelve sub-basins.

The HYPE model parameters were inferred through optimisation using the PEST software package (Doherty, 2021). The SCEUA_P global optimisation scheme, where SCE stands for "Shuffled Complex Evolution" and UA stands for "University of Arizona", was used, considering the root-mean-square error (RMSE) between observed and simulated discharges as the objective function. In order to deal with the uncertainty of model parameters, the calibration was performed over two consecutive periods of similar duration, leading to two best performing parameter sets and therefore two simulated discharge series for each simulation period. Among the optimised parameters, a correction for precipitation was included, meaning that after passage into the hydrological model, the two output precipitation series will be different.

The model validation was then performed for different periods. Tables 4 to 7 summarise the results of the daily discharge simulations for the different calibration/validation periods (water years). Figs. 2 to 8 present the results for the longest validation period. The criteria are i) the Nash and Sutcliffe efficiency criterion, NSE (Nash and Sutcliffe 1970) and ii) the percent bias (RE):

$$NSE = 1 - \frac{\sum_{i=1}^{n} \left(Qsim_i - Qobs_i\right)^2}{\sum_{i=1}^{n} \left(Qobs_i - E[Qobs]\right)^2} \qquad (1)$$

$$RE(\%) = 100 \times \frac{\sum_{i=1}^{n} \left(Qsim_i - Qobs_i\right)}{\sum_{i=1}^{n} Qobs_i} \qquad (2)$$

where *Qobs* and *Qsim* denote observed and simulated discharge respectively and *n* the number of time steps (days). The NSE criterion evaluates the performance of the HYPE discharge simulations by comparing it to the performance of a benchmark estimate obtained by assigning the mean of the discharge observations (E[Qobs]) to each time step. The NSE criterion can take values ranging from $-\infty$ to 1. A value lower than 0 indicates that HYPE is less accurate than the benchmark estimate, a value of 0 means that HYPE is as accurate as the benchmark estimate, a value greater than 0 indicates that HYPE is more accurate than the benchmark estimate and a value of 1 corresponds to a perfect simulation of observed discharges.

The overall NSE and RE criteria were calculated using all available daily discharge observations in each validation period, whereas the annual NSE was only calculated in water years for which daily discharge observations were available in more than 300 days.

- Daily discharge simulations
    - Kreppa catchment (vhm233)

The HYPE model simulations perform reasonably well with respect to NSE in the different validation periods and the results obtained with the two parameter sets are of similar quality. The percent bias varies within [−3.3%;+11.8%] but is mostly positive. The seasonality of mean daily flow in the period 1981-2016 is also reasonably well reproduced.

    - Markarfljót catchment (vhm218)

The HYPE model simulations perform reasonably well with respect to NSE in the different validation periods and the results obtained with the two parameter sets are of similar quality. The streamflow simulations are unbiased on average in most validation periods and the percent bias varies within [−2.6%;−0.7%]. The seasonality of mean daily flow in the water years 1981-2016 is also reasonably well reproduced.

    - Þverá catchment (vhm38)

The HYPE model simulations perform reasonably well with respect to NSE but the results obtained with the first parameter set are of slightly better quality than those obtained with the second parameter set. The percent bias varies with the validation period and is within [−15.9%; +5.9%]. The streamflow simulations are relatively unbiased, except in the period 1981-1995 where a negative bias is observed with both streamflow simulations. The seasonality of mean daily flow in the water years 1981-2016 is also reasonably well reproduced by both simulated series.

- Annual Maximum Floods (AMFs)

The plots of the magnitude versus occurrence day of AMFs are shown in Figs. 6 to 8 and Appendix 1 presents the plots of simulated vs. observed magnitude of AMFs. Only water years for which daily discharge observations are available in more than 300 days are considered. Different generating mechanisms (rainfall, snowmelt, glacier melt, combined rainfall and snowmelt) are associated with the AMFs depending on catchment and season of occurrence. AMFs occurring in autumn are expected to be primarily generated by rainfall, sometimes combined with snowmelt. AMFs occurring in winter are expected to be generated by a combination of rainfall and snowmelt. AMFs occurring in spring are expected to be primarily generated by snowmelt, sometimes combined with rain. AMFs occurring in summer are expected to be primarily generated by rainfall, sometimes combined with snowmelt (and glacier melt in glaciated catchments). In the Kreppa catchment (vhm233), observed AMFs occurred from July to September and were primarily caused by glacier melt. In the Markarfljót catchment (vhm218), observed AMFs occurred in all seasons but with a majority in June-July. In the Þverá catchment (vhm38), observed AMFs occurred in all seasons with a majority in May-June.

The seasonality of the timing of AMFs is usually well reproduced by the HYPE simulations in the Kreppa catchment but some AMFs are simulated in May-June whilst none are observed in these

months. In the Markarfljót catchment, AMFs are simulated in all seasons, as observed. In the Þverá catchment, the concentration of AMFs occurring in June has been well detected by the HYPE simulations but those observed in other months have often not been detected by the simulations and most of those simulated in July-August do not correspond to any observation, especially with the model calibrated in 2003-2009.

The magnitude of AMFs is reasonably well simulated by HYPE in the Kreppa catchment but the most extremes ones (some of which could have been caused by jökulhlaup and not by the meteorological situation) are underestimated by both model simulations. The magnitude of AMFs tends to be underestimated by the model simulations in the Markarfljót and Þverá catchments.

- Conclusion

The HYPE hydrological model simulations reproduce observed daily streamflow characteristics reasonably well but the magnitude of AMFs tends to be underestimated in the Markarfljót and Þverá catchments. The performances of the daily model simulations in the validation periods are usually consistent with their performances in the calibration periods which suggests that the model parameters are sufficiently robust to natural variations in climatic conditions. The robustness of hydrological model parameters for climate change impact studies is an important issue (see e.g. Brigode et al. 2013; Vormoor et al. 2015).

Table 4: Catchment vhm233 (Kreppa): HYPE discharge simulations: Validation results for a daily time step (text in bold indicates when the calibration and validation periods are the same).

vhm233				
	Calibration period 1996-2002		Calibration period 2003-2009	
Validation period	NSE	RE (%)	NSE	RE (%)
1981-2016	0.79	1.9	0.78	7.02
1981-1995	0.68	6.6	0.67	11.8
1996-2002	**0.84**	**0.22**	0.83	5.25
2003-2009	0.89	-3.3	**0.89**	**1.98**
2010-2016	0.76	2.5	0.74	7.6

Table 5: Catchment vhm218 (Markarfljót): HYPE discharge simulations: Validation results for a daily time step (text in bold indicates when the calibration and validation periods are the same).

vhm218				
	Calibration period 1996-2002		Calibration period 2003-2009	
Validation period	NSE	RE (%)	NSE	RE (%)
1981-2016	0.73	-1.5	0.73	-1.53
1981-1995	0.75	-0.71	0.74	-0.7
1996-2002	**0.72**	**-2.1**	0.72	-2.3
2003-2009	0.7	-1.4	**0.72**	**-1.3**
2010-2016	0.72	-2.5	0.73	-2.6

Table 6: Catchment vhm38 (Þverá): HYPE discharge simulations: Validation results for a daily time step (text in bold indicates when the calibration and validation periods are the same).

vhm38				
	Calibration period 1996-2002		Calibration period 2003-2009	
Validation period	NSE	RE (%)	NSE	RE (%)
1981-2016	0.77	-3.1	0.71	-7.8
1981-1995	0.77	-12.4	0.68	-15.9
1996-2002	**0.69**	**-0.06**	0.63	-4.6
2003-2009	0.77	5.2	**0.8**	**-1.3**
2010-2016	0.79	5.9	0.73	0.15

Table 7: HYPE discharge simulations: Annual NSE statistics for water years with more than 300 valid daily discharge observations. Validation results for a daily time step.

Validation		
vhm233 (1981-2016)	Calibration period: 1996-2002	Calibration period: 2003-2009
NSE min	-0.04	-0.14
NSE median	0.81	0.80
NSE max	0.94	0.93
vhm218 (1981-2016)	Calibration period: 1996-2002	Calibration period: 2003-2009
NSE min	0.38	0.21
NSE median	0.73	0.74
NSE max	0.83	0.85
vhm38 (1981-2016)	Calibration period: 1996-2002	Calibration period 2003-2009
NSE min	0.46	0.14
NSE median	0.79	0.75
NSE max	0.89	0.89

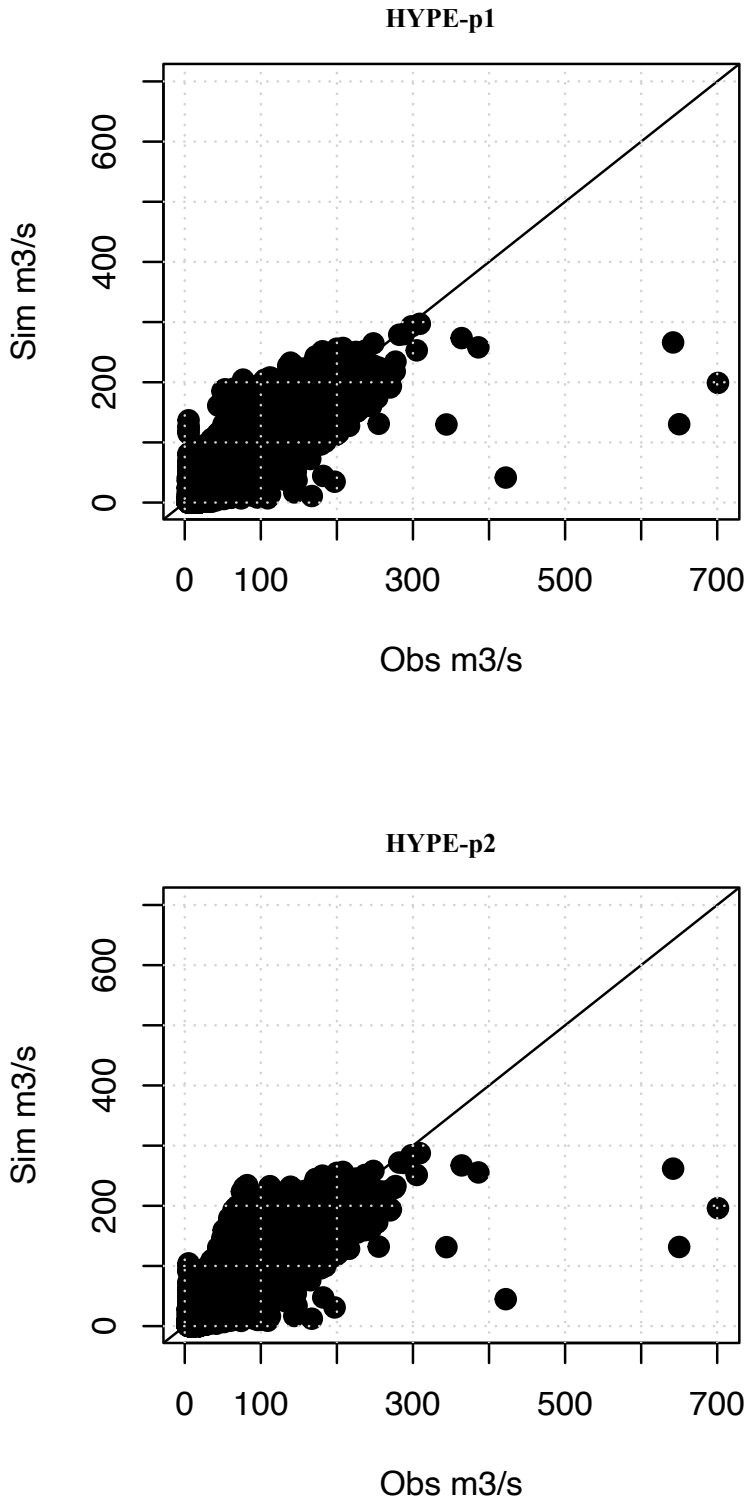

Fig. 2: Catchment vhm233 (Kreppa): Simulated vs. observed daily discharge in the water years 1981-2016. Top: HYPE with parameter set calibrated in 1996-2002. Bottom: HYPE with parameter set calibrated in 2003-2009.

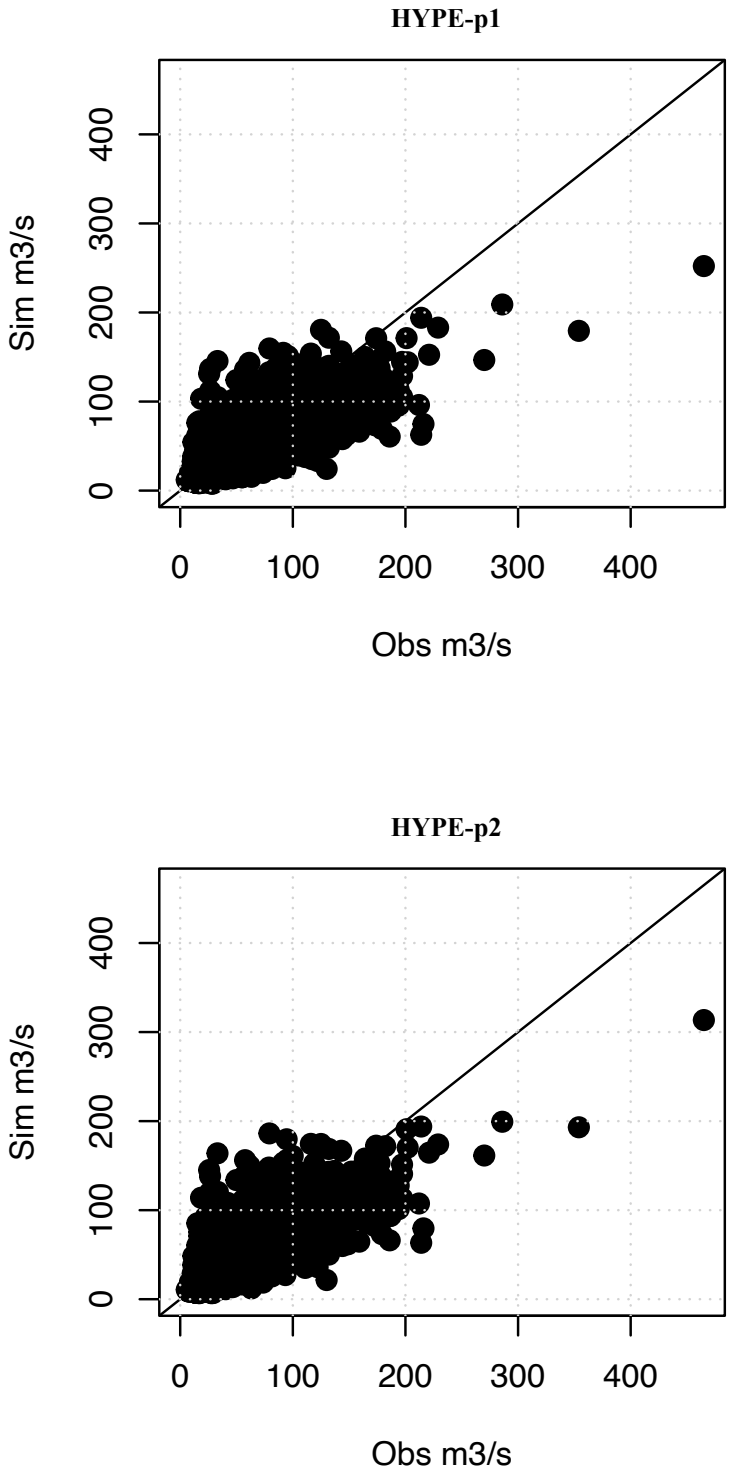

Fig. 3: Catchment vhm218 (Markarfljót): Simulated vs. observed daily discharge in the water years 1981-2016. Top: HYPE with parameter set calibrated in 1996-2002. Bottom: HYPE with parameter set calibrated in 2003-2009.

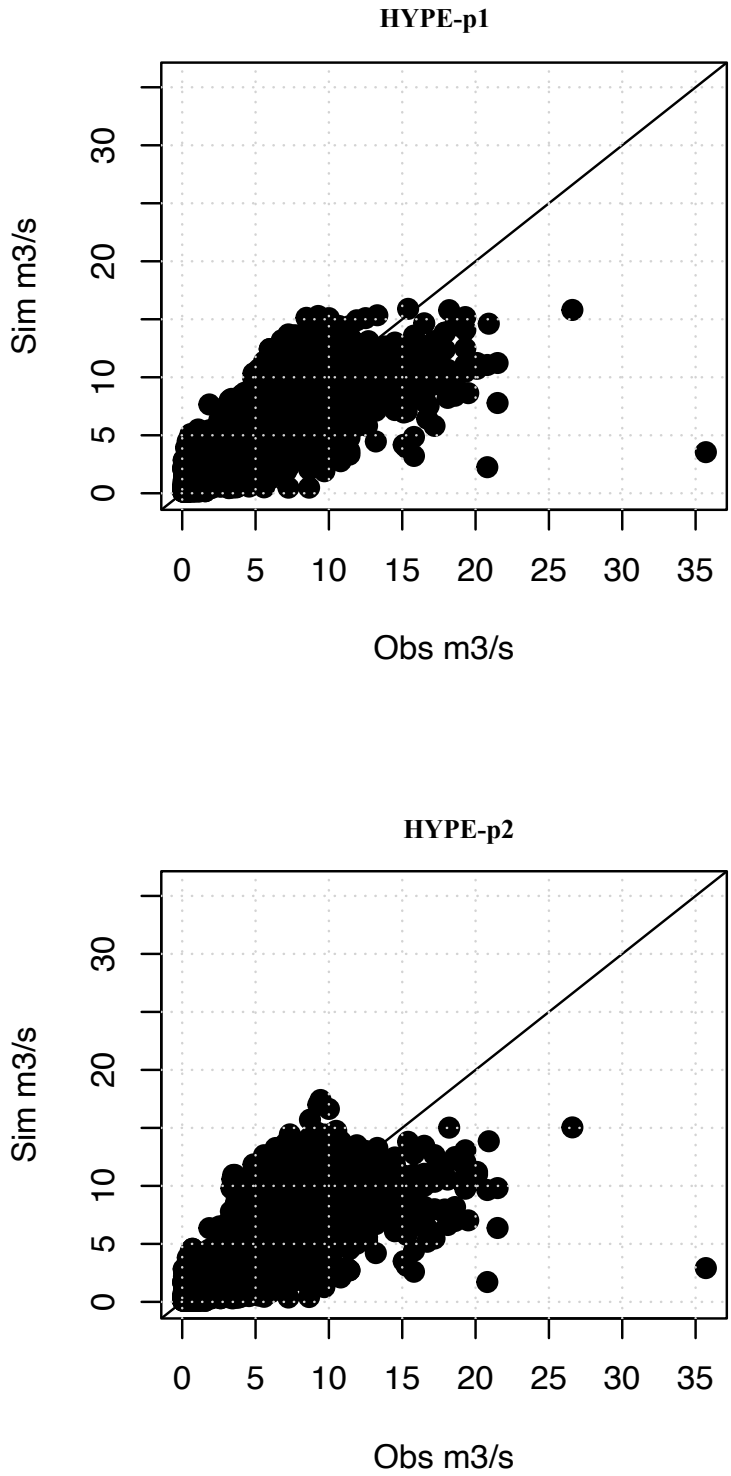

Fig. 4: Catchment vhm38 (Þverá): Simulated vs. observed daily discharge in the water years 1981-2016. Top: HYPE with parameter set calibrated in 1996-2002. Bottom: HYPE with parameter set calibrated in 2003-2009.

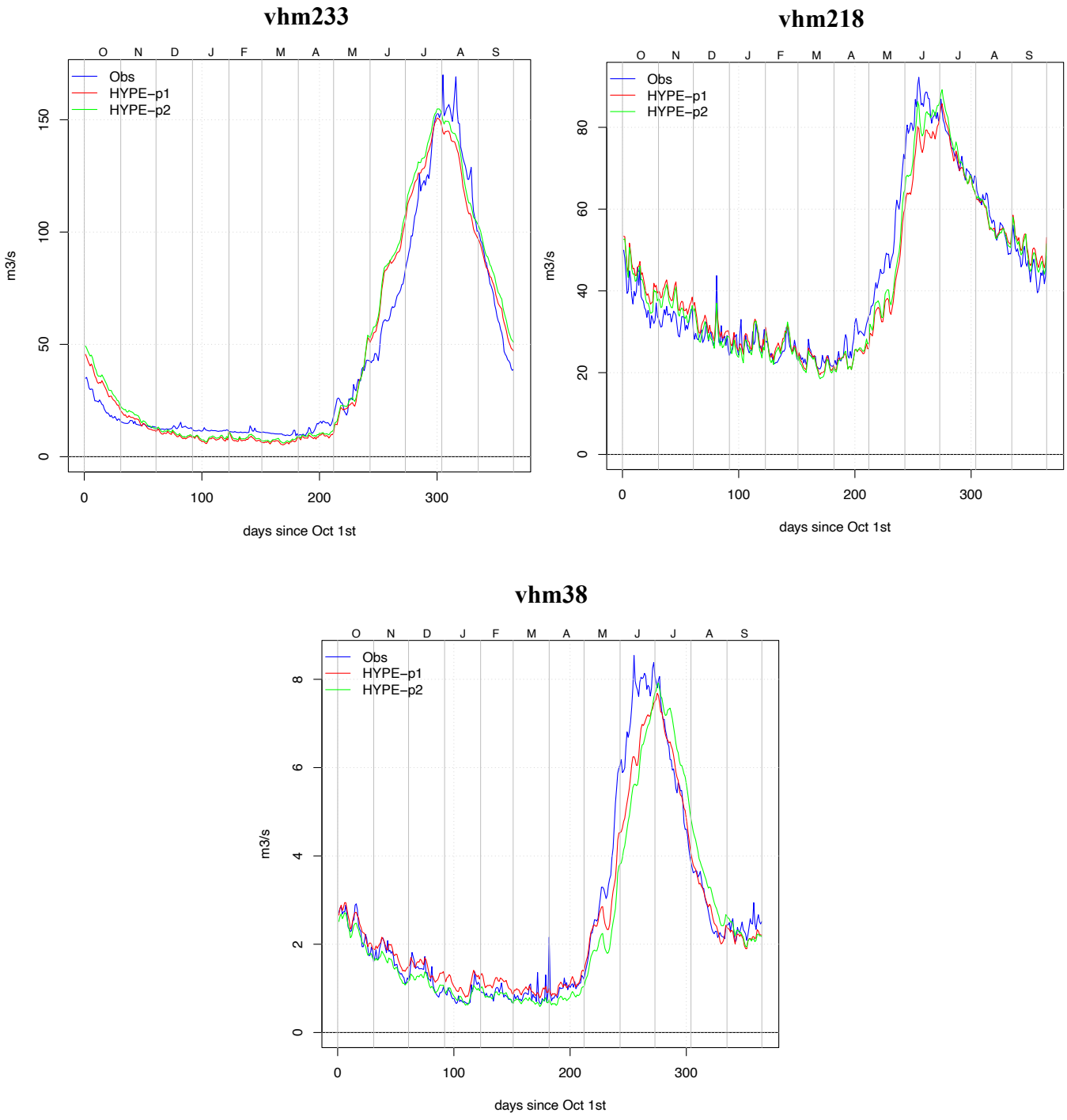

Fig. 5: Seasonality of mean daily discharge (1981-2016). Observed discharge (blue), HYPE discharge simulations using first (red) and second (green) parameter sets; vhm233 (top-left); vhm218 (top-right); vhm38 (bottom). The day=1 for October 1st and 365 for September 30th.

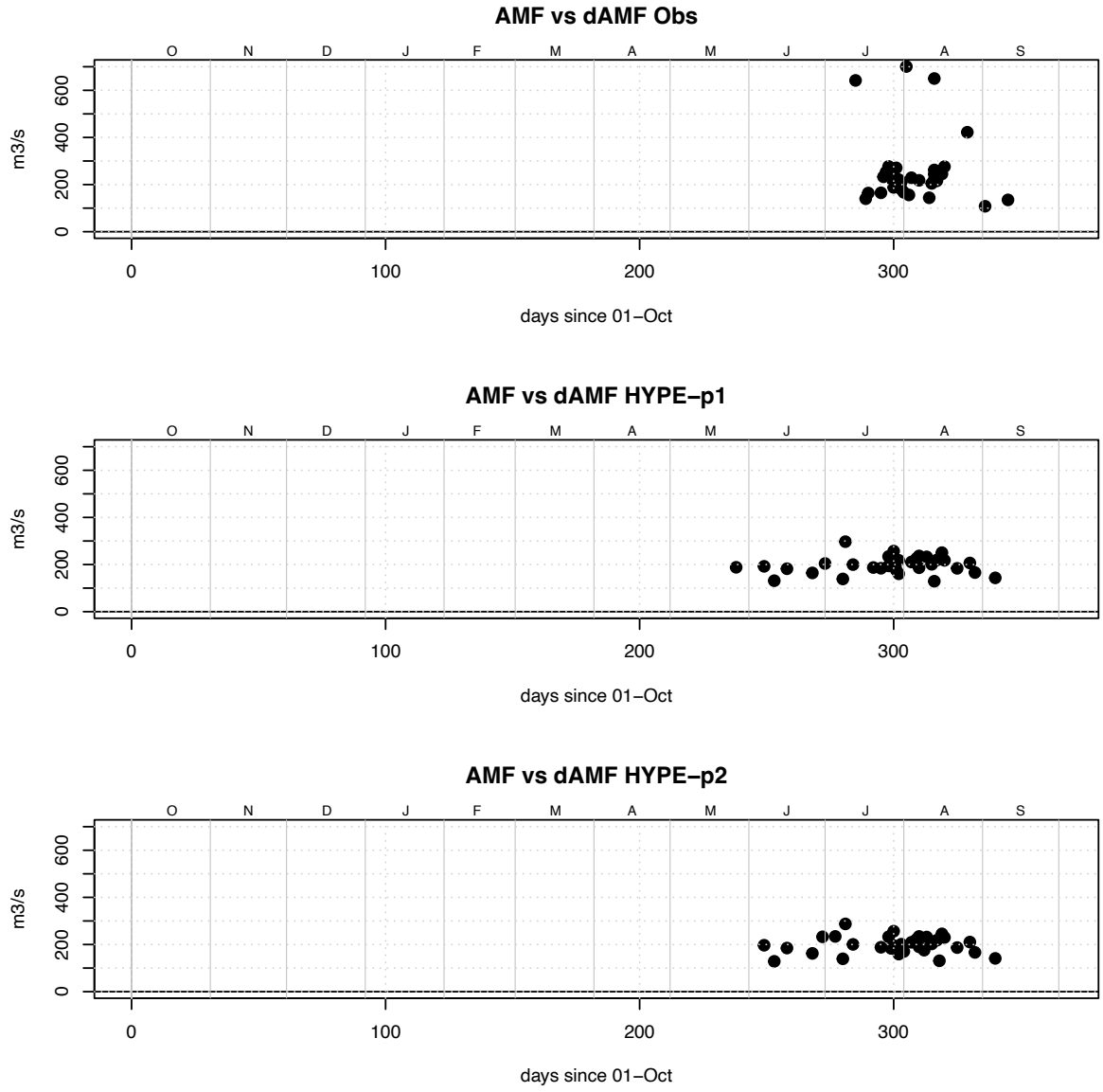

Fig. 6: Catchment vhm233 (Kreppa): Magnitude vs. day of occurrence of AMFs (water years 1981-2016). Observed (top), HYPE with parameter set calibrated in 1996-2002 (middle), HYPE with parameter set calibrated in 2003-2009 (bottom). The day=1 for October 1st and 365 for September 30th.

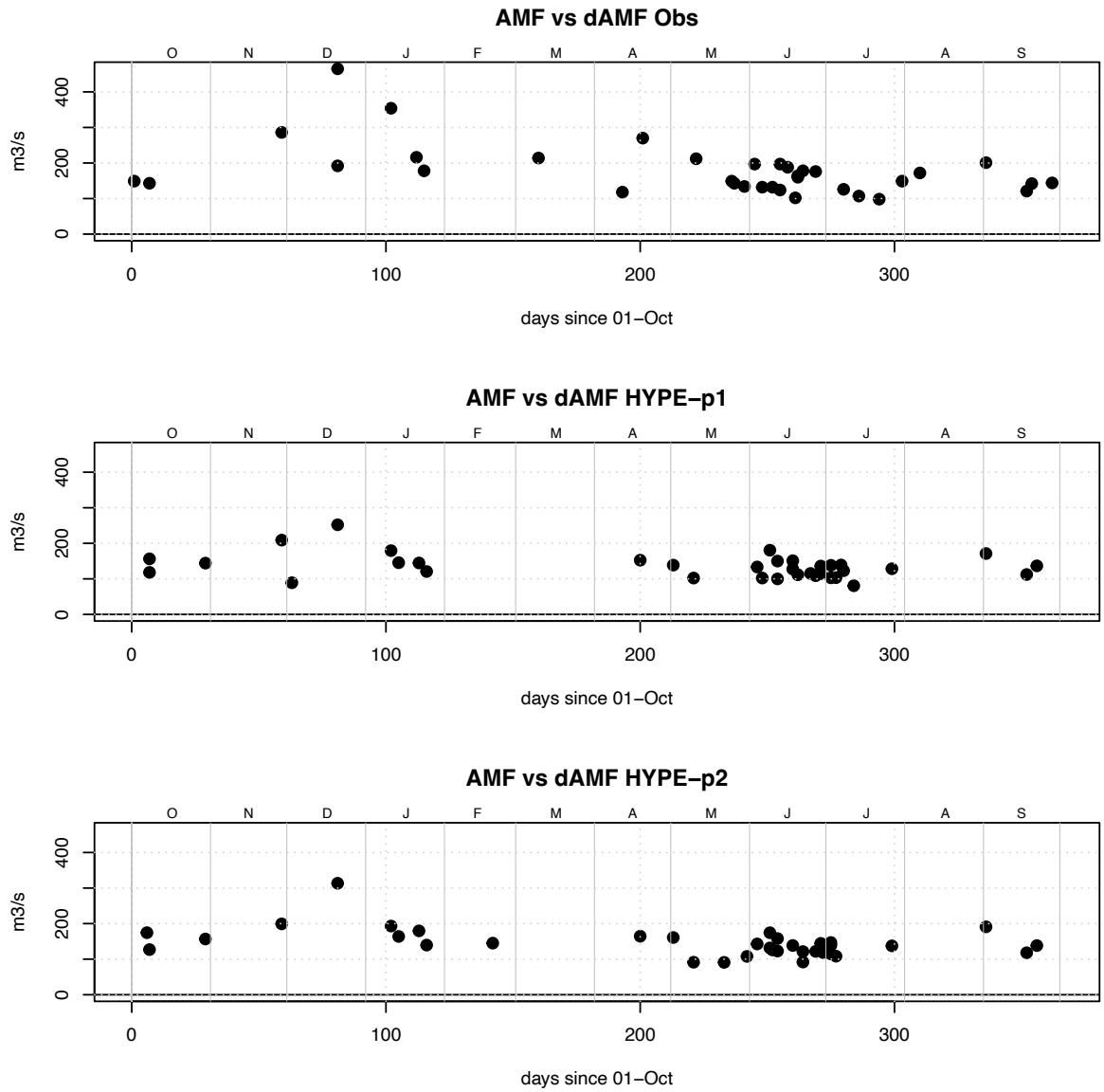

Fig. 7: Catchment vhm218 (Markarfljót): Magnitude vs. day of occurrence of AMFs (water years 1981-2016). Observed (top), HYPE with parameter set calibrated in 1996-2002 (middle), HYPE with parameter set calibrated in 2003-2009 (bottom-right). The day=1 for October 1st and 365 for September 30th.

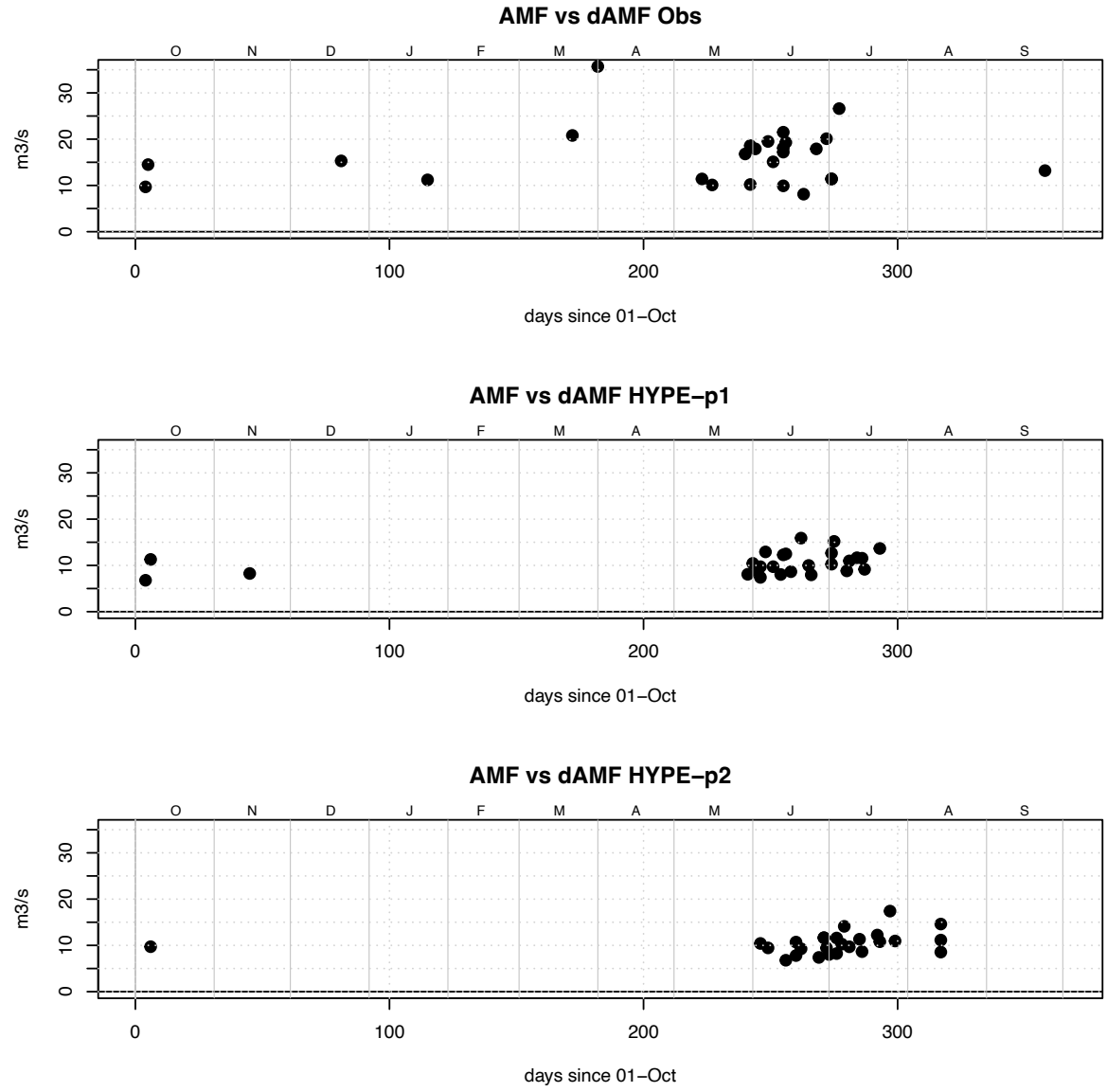

Fig. 8: Catchment vhm38 (Þverá): Magnitude vs. day of occurrence of AMFs (water years 1981-2016). Observed (top), HYPE with parameter set calibrated in 1996-2002 (middle), HYPE with parameter set calibrated in 2003-2009 (bottom). The day=1 for October 1st and 365 for September 30th.

5 EURO-CORDEX climate projections

The ICRA and CORDEX precipitation and temperature series were first area-averaged over each sub-basin and then a specific QM-based adjustment was defined for each month and sub-basin (see section 3-7). The results presented in this section correspond to the ICRA temperature and precipitation series and the corresponding QM-adjusted CORDEX projections, before their passage into the hydrological model. The ICRA and QM-adjusted CORDEX precipitation series will then be further corrected by the the HYPE hydrological model with a coefficient that depends on each calibration period (these results are presented in Section 6).

5-1 RCMs evaluation and skill of the local bias-adjustment method

In order to evaluate the intrinsic quality of the different RCMs and the skill of the QM adjustment method at removing local biases, a comparison was made between the ICRA reanalysis and the CORDEX evaluation series obtained by dynamical downscaling of ERA-interim reanalyses with the selected RCMs (see Tables 2 and 3). The CORDEX evaluation series are synchronised with observed climate, making a direct comparison with ICRA reanalysis possible. The QM-based adjustment coefficients were defined by comparing the ICRA data in the 1981-2010 period to the CORDEX evaluation series in the available period (1981-2010 or 1989-2008, depending on the RCM). The results presented here are for daily temperature and precipitation area-averaged over the entire catchments.

The following evaluation statistics were calculated in the period 1989-2008 common to all daily temperature and precipitation evaluation series:

$$\text{Mean error: } ME = E[CORDEX - ICRA] \tag{3}$$

$$\text{Root-mean-square error: } RMSE = \sqrt{E[(CORDEX - ICRA)^2]} \tag{4}$$

5-1-1 Temperature

The seasonality of ME and RMSE before and after local bias-adjustment is presented in Appendix 2. The CCLM-4-8-17 evaluation series display a positive temperature bias in all three catchments in spring/summer and are relatively unbiased in other months. The REMO2009 evaluation series display a positive temperature bias in all three catchments in spring/summer and are slightly negatively biased in autumn/winter. The RCA4 and RACMO22E evaluation series are negatively biased in all months in the Kreppa (vhm233) and Markarfljót (vhm218) catchments and relatively unbiased or slightly positively biased in the Þverá (vhm38) catchment. These biases are partly related to differences between the ICRA and CORDEX terrain elevations caused by a difference of spatial resolutions. Quantile mapping eliminates the bias, on average, and reduces RMSE in months where ME was large. After bias-correction, the different evaluation series are relatively similar in terms of RMSE, with a slight advantage for CCLM-4-8-17 and RACMO22E.

5-1-2 Precipitation

The seasonality of ME and RMSE before and after local bias-adjustment is presented in Appendix 3. The results vary with the catchments and RCMs. The biases are usually not of a systematic nature as for temperature and the scatter plots indicate over- or under-estimation depending on the days (not shown). For the Kreppa catchment (vhm233), two RCMs (RCA4 and RACMO22E) are relatively unbiased on average whereas CCLM-4-8-17 is positively biased in autumn/winter and unbiased in other months, and REMO2009 is slightly negatively biased in autumn/winter and unbiased in other months. Precipitation over the Markarfljót catchment (vhm218) is unbiased on average with RACMO22E, underestimated on average with REMO2009, especially in autumn/winter, and overestimated on average with RCA4 and CCLM-4-8-17. Precipitation over the Þverá catchment (vhm38) is underestimated on average in all months with REMO2009, especially in autumn/winter, slightly overestimated in a majority of months with CCLM-4-8-17, slightly overestimated in spring/summer and underestimated in winter with RCA4, underestimated in autumn/winter and unbiased in other months with RACMO22E. Quantile mapping eliminates the bias, on average and either reduces RMSE, when the bias is large and systematic, or keeps it similar to its original level or even increase it slightly, when the bias is low. Overall, the different bias-corrected evaluation series are relatively similar in terms of RMSE but with a slight advantage for CCLM-4-8-17 in a majority of months in catchments vhm218 and vhm38.

5-2 Climate projections

Comparisons between CORDEX and ICRA mean monthly temperature and precipitation in the 1981-2010 period confirms i) the presence of biases in the original CORDEX temperature and precipitation series and ii) the efficiency of the QM adjustment method at eliminating these biases on average (see Appendix 4 and 5). The biases depend both on the RCM and the driving GCM. After local bias-adjustment, a temporal trend test based on ordinary least squares linear regression was applied to catchment-averaged monthly temperature and precipitation series in the 1981-2100 period and the significance of the trend estimated at a 5% significance level (p value lower than 0.05).

5-2-1 Temperature trends

A significant warming is projected in all months and catchments, more or less pronounced according to the emission scenario and the month under consideration (see Table 8). On average over all months and catchments, a warming rate of 0.29°C/decade is projected with the RCP4.5 emission scenario and 0.46°C/decade with the RCP8.5 emission scenario. The lowest average warming rate is projected in the Markarfljót catchment (vhm218) and the highest one is projected in the Þverá catchment (vhm38). The warming rate is usually larger for scenarios driven by HadGEM2ES GCM than for those driven by MPI−ESM−LR GCM (not shown). Note also that the warming rate estimated from the locally-adjusted temperature series is slightly greater than the one derived from the original temperature series (0.27°C/decade under RCP4.5 and 0.42°C/decade under RCP8.5). These results are similar to those observed in the analysis of other catchments (see Crochet 2020, 2021, 2022).

In addition to the presence of long-term trends, oscillations are observed in the temperature series reflecting natural climate variability (not shown). The locally-adjusted temperature series are more or less grouped according to the driving GCM and the two groups of projections do not necessarily vary in phase with each other. The projected warming in the 21st century is also well reflected in the evolution of the mean monthly temperature cycle (see Appendix 6).

5-2-2 Precipitation trends

As already observed in the analysis of other catchments (see Crochet 2020, 2021, 2022), monthly precipitation projections do not exhibit any significant linear trend in most months and studied catchments (see Table 9). The main features characterising the variability of monthly precipitation projections are decadal to multi-decadal oscillations, especially in autumn/winter, corresponding to a succession of “wet” and “dry” periods. These oscillations are characteristic of the natural variability of precipitation in the Icelandic domain (see for instance Crochet, 2007). The oscillations often depend on the driving GCM and the two groups of precipitation projections driven by the two GCMs do not always vary in phase with each other. The lack of significant linear precipitation trend does not mean that no significant change will be affecting precipitation in some future periods. Changes in 30-year mean annual and seasonal precipitation are studied in Section 6 using the Mann-Whitney test.

To illustrate the temporal variability of precipitation, Appendix 7 presents the time-series of locally-adjusted monthly precipitation in February, June and October for the RCP4.5 scenario. A 5-year moving average was applied to the monthly series in order to make the oscillations appear more clearly. Similar results were observed for the RCP8.5 scenario (not shown).

Table 8: Ensemble average warming rate in degree Celsius/decade estimated from the locally-adjusted monthly temperature series (1981-2100). All six ensemble members display a statistically significant trend (slope of the linear regression statistically different from zero at the 5% level). The average warming rate estimated from the original temperature series before local bias-adjustment is also given for comparison (Mean DMO).

Month	vhm233		vhm218		vhm38	
	RCP4.5	RCP8.5	RCP4.5	RCP8.5	RCP4.5	RCP8.5
Jan	0.290	0.373	0.265	0.334	0.324	0.445
Feb	0.279	0.444	0.259	0.400	0.305	0.499
Mar	0.266	0.414	0.259	0.382	0.313	0.511
Apr	0.239	0.351	0.230	0.348	0.298	0.464
May	0.260	0.455	0.247	0.404	0.312	0.455
Jun	0.303	0.526	0.315	0.502	0.306	0.445
Jul	0.308	0.568	0.346	0.591	0.336	0.538
Agu	0.290	0.574	0.301	0.576	0.304	0.545
Sep	0.309	0.509	0.251	0.393	0.298	0.454
Oct	0.343	0.537	0.280	0.426	0.327	0.478
Nov	0.278	0.480	0.240	0.414	0.279	0.458
Dec	0.286	0.448	0.239	0.376	0.307	0.488
Mean	**0.288**	**0.473**	**0.269**	**0.429**	**0.309**	**0.482**
Mean DMO	**0.258**	**0.418**	**0.250**	**0.389**	**0.301**	**0.459**

Table 9: Locally-adjusted monthly precipitation projections (1981-2100): Average trend (mm/day / decade) when more than 50% of the six ensemble members have a statistically significant trend (slope of the linear regression statistically different from zero at the 5% level). Number of members with a significant trend is given in brackets.

Month	vhm233		vhm218		vhm38	
	RCP4.5	RCP8.5	RCP4.5	RCP8.5	RCP4.5	RCP8.5
Jan	/	/	/	/	/	/
Feb	/	/	/	/	/	/
Mar	/	/	/	/	/	/
Apr	/	/	/	/	/	/
May	/	/	/	/	/	/
Jun	/	/	/	/	/	/
Jul	/	/	/	/	/	/
Agu	/	/	/	/	/	/
Sep	/	/	/	/	/	0.185 (6)
Oct	/	/	/	/	/	/
Nov	/	/	/	0.182 (4)	/	/
Dec	/	0.143 (4)	/	/	/	0.131 (5)

6 Hydrological projections

An ensemble of twelve daily hydrological projections was obtained for the period 1981-2100 and each emission scenario, by forcing HYPE with the ensemble of locally-adjusted CORDEX daily precipitation and temperature projections (six climate projections × two HYPE parameter sets).

6-1 Comparison with reference hydrological series

The hydrological series obtained by forcing HYPE with the CORDEX projections in the reference period (1981-2010) were compared to the reference series obtained by forcing HYPE with the ICRA reanalysis in the same period. These comparisons allow to evaluate how the local adjustments of CORDEX precipitation and temperature projections by quantile mapping propagate into the hydrological modelling chain. Figs 9 to 11 present the seasonality of mean daily discharge and snow storage (snow water equivalent, SWE). Appendix 8 presents the comparisons of the seasonal frequencies of occurrence of AMFs and the comparisons of the empirical cumulative frequency distributions of the magnitude of AMFs. The hydrological projections are identical in the 1981-2005 historical period but differ thereafter because the CORDEX RCPs 4.5 and 8.5 emission scenarios differ, hence results from the two RCPs are presented.

The current streamflow seasonality of the Þverá catchment is governed by the seasonality of snow accumulation and melt, leading to a strong contrast between low flows in winter when snow accumulates and high flows in spring/summer when snow melts. The Kreppa and Markarfljót catchments which are partly glaciated have low flows in winter when snow accumulates and high flows in spring/summer when snow and then later ice melt. The Markarfljót catchment has also some substantial groundwater flow so that the contrast between low winter flow and high spring/ summer flows is not as marked as in the Kreppa catchment. The seasonality of mean daily flow and SWE projections in the 1981-2010 reference period offers a reliable estimation of the seasonality of the reference mean daily flow and SWE in that period. The seasonal frequencies of occurrence of AMFs and the empirical cumulative frequency distributions of the magnitude of AMFs are usually reasonably well reproduced when the HYPE hydrological model is forced with the locally-adjusted CORDEX projections in the reference period (1981-2010), although some overestimation in the magnitude of AMFs is observed in the Markarfljót (vhm218) and Þverá (vhm38) catchments compared to the reference simulations (note however that in these two catchments, the magnitude of AMFs is often underestimated by the HYPE simulations forced with ICRA, as compared to observed AMFs, see Section 4). The spread of the hydrological ensembles reflects the uncertainties associated with the different climate projections, their local-adjustment, and the hydrological model parameterisation. Overall, these results give credibility to the local-adjustment by quantile mapping applied to the CORDEX climate projections. It is assumed in the rest of the study that the local-adjustments of CORDEX precipitation and air temperature hold for the entire projection period and that the HYPE parameter sets are sufficiently robust to be transferable over the entire projection period.

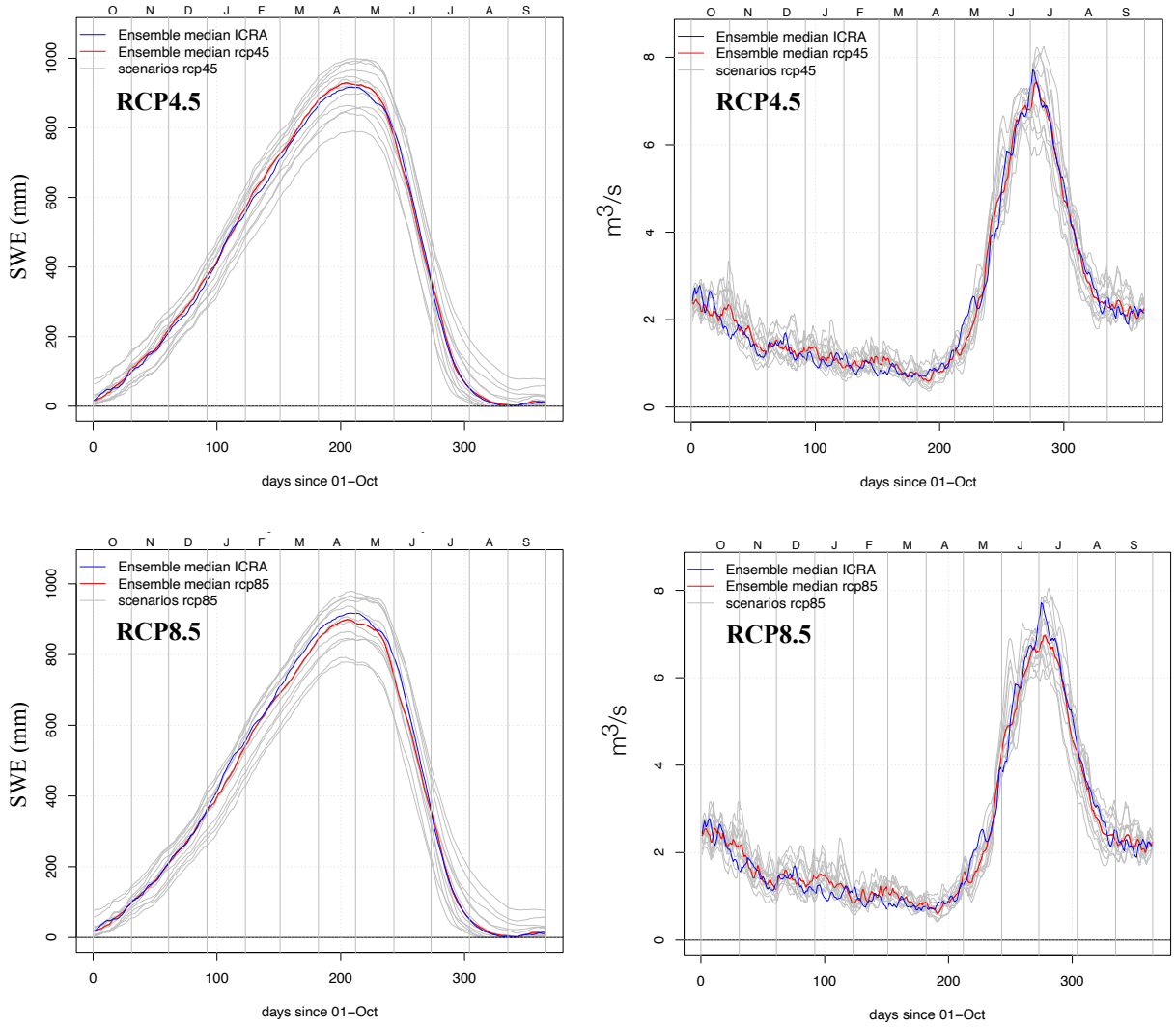

Fig. 9: Þverá catchment (vhm38): Mean daily snow storage (SWE) (left panel) and river discharge (right panel). Estimations derived from the HYPE hydrological model forced with the ICRA reanalysis (blue line) and with the locally-adjusted CORDEX projections (grey lines) in the 1981-2010 period (RCPs 4.5 & 8.5). The ensemble median of the mean daily projections is coloured in red. HYPE model forced with CORDEX RCP4.5 series (top) and CORDEX RCP8.5 series (bottom). The day=1 for October 1st and 365 for September 30th.

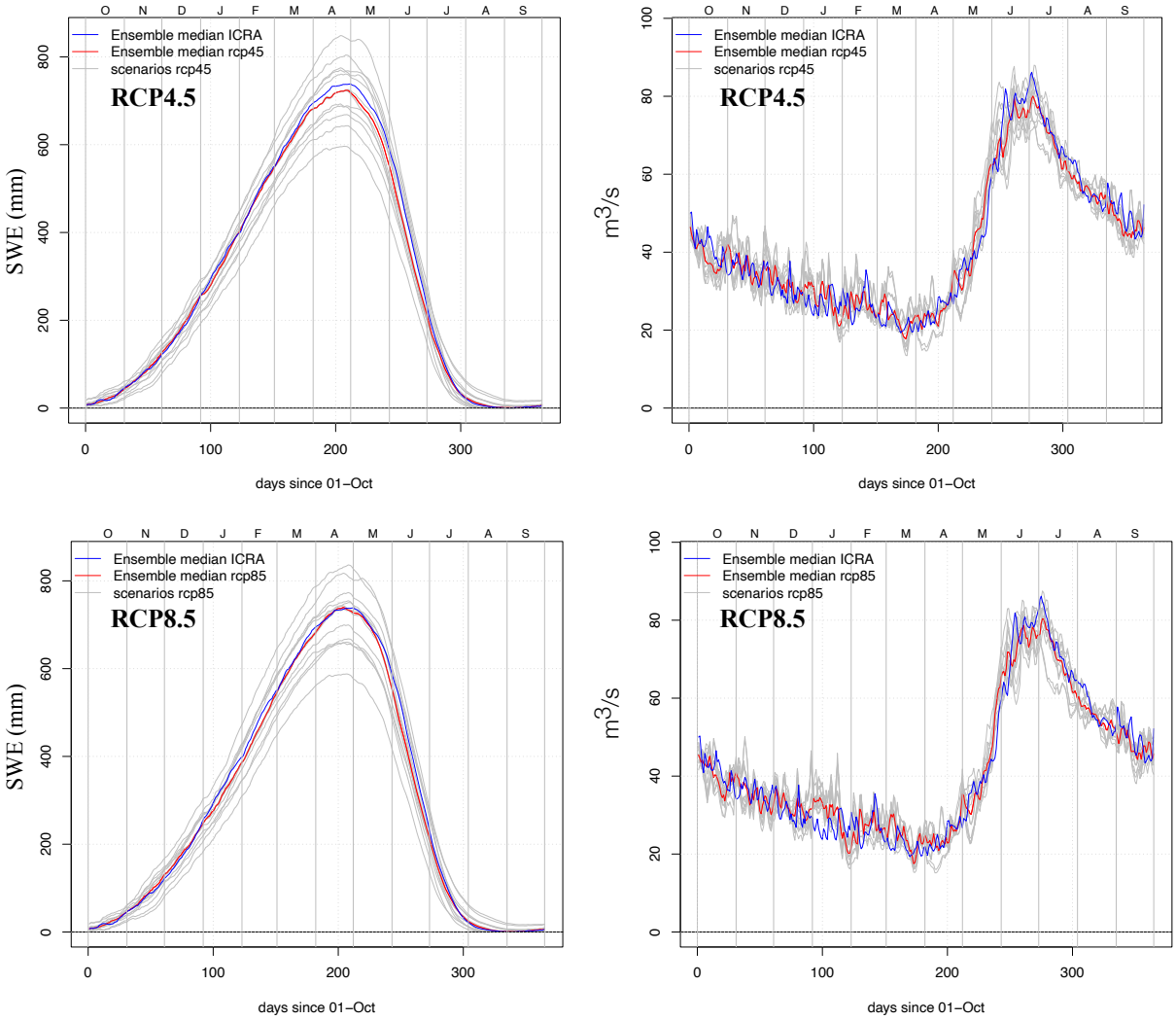

Fig. 10: Markarfljót catchment (vhm218): Mean daily snow storage (SWE) (left panel) and river discharge (right panel). Estimations derived from the HYPE hydrological model forced with the ICRA reanalysis (blue line) and with the locally-adjusted CORDEX projections (grey lines) in the 1981-2010 period (RCPs 4.5 & 8.5). The ensemble median of the mean daily projections is coloured in red. HYPE model forced with CORDEX RCP4.5 series (top) and CORDEX RCP8.5 series (bottom). The day=1 for October 1st and 365 for September 30th.

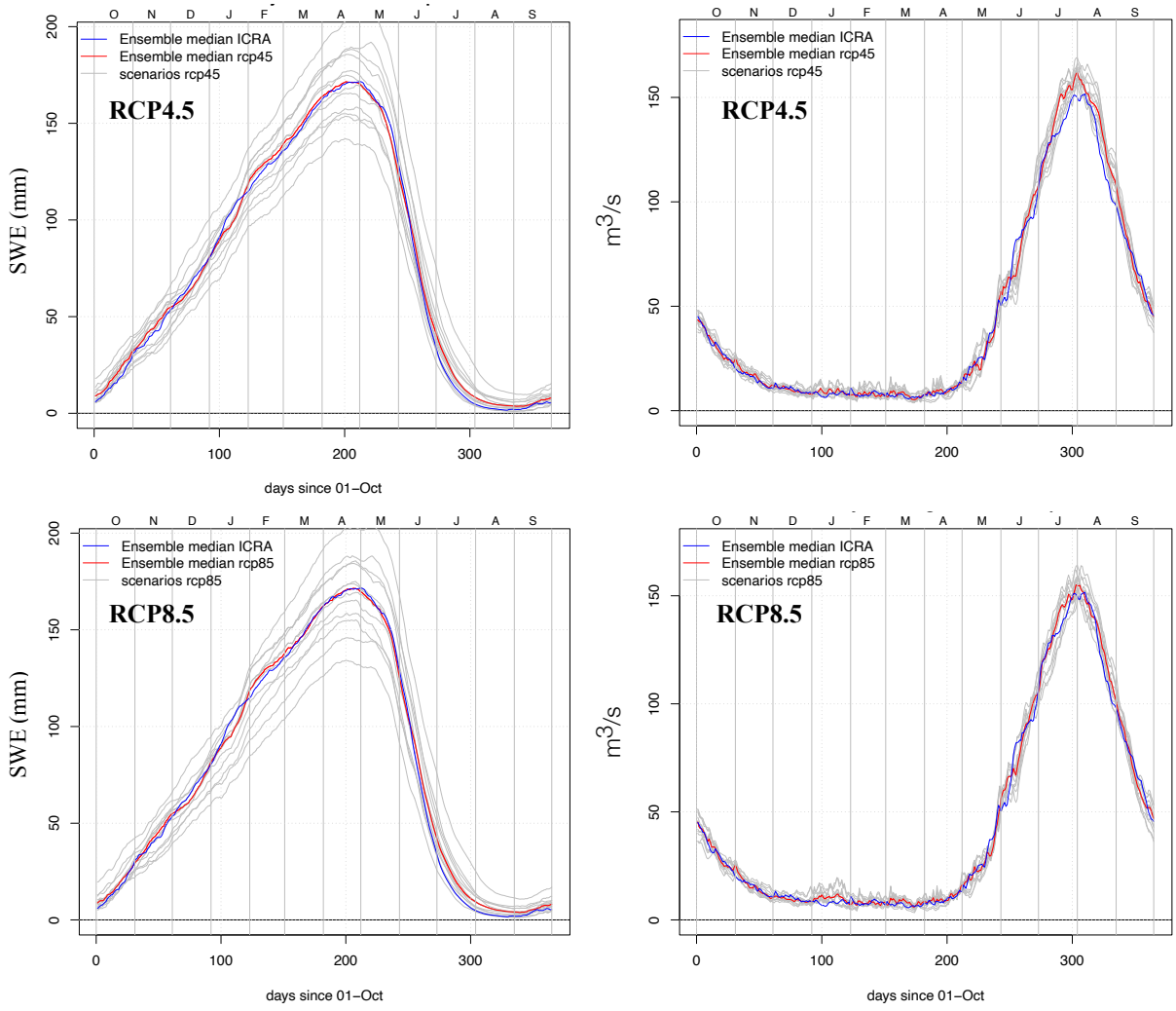

Fig. 11: Kreppa catchment (vhm233): Mean daily snow storage (SWE) (left panel) and river discharge (right panel). Estimations derived from the HYPE hydrological model forced with the ICRA reanalysis (blue line) and with the locally-adjusted CORDEX projections (grey lines) in the 1981-2010 period (RCPs 4.5 & 8.5). The ensemble median of the mean daily projections is coloured in red. HYPE model forced with CORDEX RCP4.5 series (top) and CORDEX RCP8.5 series (bottom). The day=1 for October 1st and 365 for September 30th.

6-2 Hydrological response to projected climate change

This section examines the hydrological impact of projected climate change in the 21st century.

6-2-1 Changes in the seasonality of mean daily snow storage and river flow

Projected changes in the seasonality of mean daily snow storage and river discharge are presented in Figs. 12 to 23. First, the ensemble median is presented for all 30-year periods and then results with all the ensemble members are presented for two periods: near future (2021-2050) and far future (2071-2100). The overall uncertainty associated with these projections can be estimated by the spread of the ensemble. The percentage of days in the water year for which the mean daily snow storage or discharge ensembles significantly differ between the reference (1981-2010) and these two future periods is also indicated. The larger warming projected with the RCP8.5 emission scenario leads to larger hydrological changes in the three catchments than the RCP4.5 emission scenario.

In the Þverá (vhm38) and Markarfljót (vhm218) catchments, the projected rise in temperatures (see Section 5-2-1 and Appendix 6) gradually leads to shorter snow seasons and less snow storage. By the end of the 21st century, mean daily snow storage is projected to strongly deplete on these two catchments, especially under the RCP8.5 emission scenario. Results look quite different in the Kreppa (vhm233) catchment where mean daily snow storage is apparently projected to increase under both emission scenarios. To explain this result, it should be mentioned that HYPE converts all the snow falling onto the glaciers into ice, and snow is only accumulated by the model for the land area outside the glaciers (snow accumulation is assumed to be null on the glacier since snow is converted into ice). As temperature is rising, the glacier is projected to progressively retreat and the land area increase (not shown). Therefore, when averaged over the entire catchment, snow storage is projected to increase because of the increase in land area (where additional snow storage is accounted for), and not because more snow will accumulate over the initial land area. To verify this assumption, HYPE was re-run without glacier in order to calculate snow storage over the entire catchment during the entire projection period (not shown). Results indicate that snow storage over the entire Kreppa catchment is projected to decrease during the 21st century, which was expected as a reduction of catchment-averaged snowfall is projected in the future (see Section 6-2-2 below). Note that for the Markarfljót catchment, the glacier is also projected to progressively retreat and the land area increase (not shown), however, as the glacier coverage on the Markarfljót catchment is much smaller than on the Kreppa catchment (ca. 13% vs. 51% at the start of the simulations), the gain in land area where additional snow storage is accounted for is obviously not sufficient to compensate for the reduction of snow storage over the initial land area, owing to the projected warming, so that overall, snow storage averaged over the entire catchment is projected to decrease.

As the projection horizon increases, the mean daily streamflow seasonality pattern of the three catchments is projected to change in response to rising temperatures and subsequent changes in snow (and glacier) melt. In the Þverá and Markarfljót catchments, mean daily discharge is

projected to increase more or less progressively between October and May, likely because the number of rainfall and/or snowmelt events will increase with projected warming, and decrease more or less progressively between June and August in relation to snow storage depletion and subsequent snowmelt reduction. The peak of mean daily discharge caused by snowmelt in spring or early summer is projected to gradually decrease and shift earlier in these two catchments under both emission scenarios because the projected snow storage reduction will lead to less snowmelt in spring/summer and the onset of spring snowmelt will start earlier. In the Þverá catchment, the peak of mean daily discharge originally observed in late June-early July is projected to disappear towards the end of the century under the RCP8.5 emission scenario and a new peak caused by rainfall will emerge in October/November. Furthermore, in that catchment, a period of low flow is projected to develop in Jul/Aug towards the end of the century under both emission scenarios. The lowest mean daily flow is observed in Mar/Apr in the 1981-2010 reference period whereas in 2071-2100, the lowest mean daily flow is projected to occur in Jul/Aug.

In the Markarfljót catchment, the seasonal differences in mean daily flow are projected to remain substantial during the entire projection period under the RCP4.5 emission scenario, whereas under the RCP8.5 emission scenario, projected mean daily flow becomes more evenly distributed within the water-year, towards the end of the 21st century. In particular, glacier melt and groundwater flow will maintain a relatively high flow in summer, although reduced compared to what is observed in the 1981-2010 reference period.

Results for the Kreppa catchment indicate a generalised increase in mean daily flow in the future, under both emission scenarios, most likely caused by an increase in rainfall, snowmelt and/or glacier melt, depending on the month under consideration, owing to the rise in temperatures. The projected increase is gradual except in Jul/Aug where after around 2041-2070/2051-2080, mean daily flow will start declining because of the decline of glacier melt, owing to the glacier retreat. Nevertheless, projected mean daily discharge in Jul/Aug will remain substantially greater than in the reference period.

Note that in practise, the retreat of glaciers could introduce some changes in the geometry and drainage area of the two glaciated catchments. This aspect was not taken into consideration in the simulations and the drainage areas were assumed to remain unchanged during the entire projection period. The uncertainty regarding this geometrical aspect may introduce some additional uncertainties in the hydro-climatic projections.

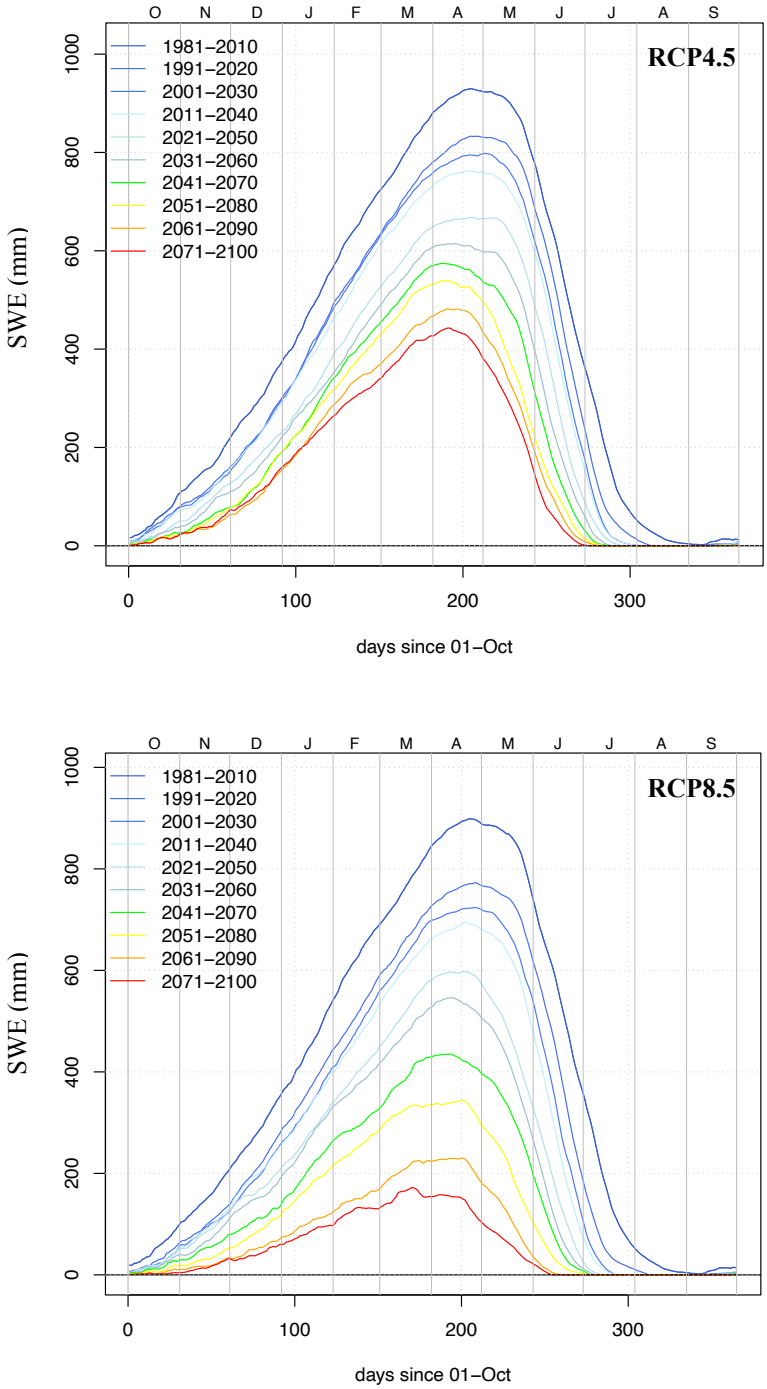

Fig. 12: Þverá catchment (vhm38): Projected seasonality of mean daily snow storage (ensemble median) under the RCP4.5 emission scenario (top) and RCP8.5 emission scenario (bottom). Each colour corresponds to a 30-year period: from dark blue (1981-2010) to red (2071-2100). The day=1 for October 1st and 365 for September 30th.

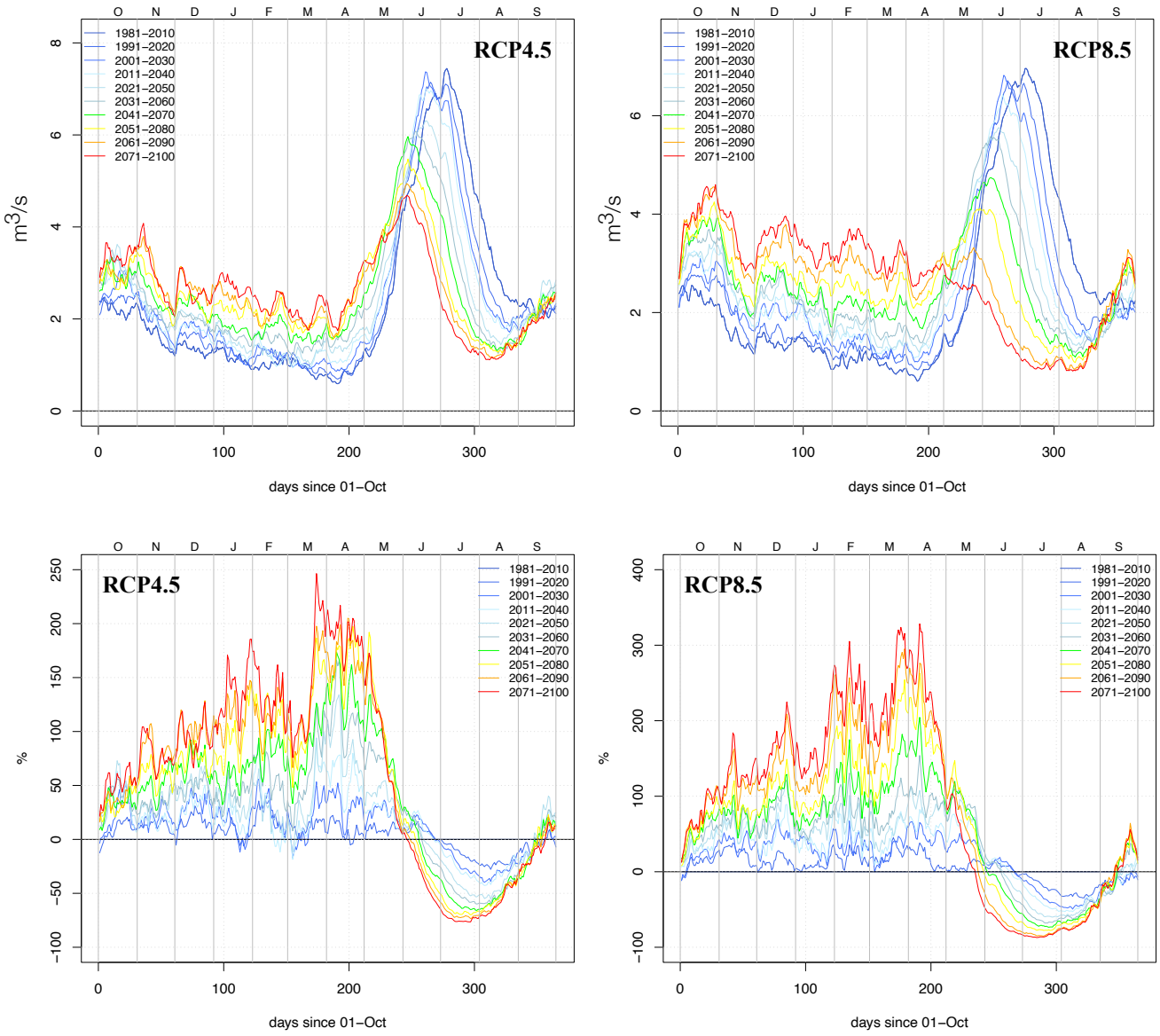

Fig. 13: Þverá catchment (vhm38). Top-panel: Projected seasonality of mean daily discharge (ensemble median). Bottom-panel: Percent change in mean daily discharge relative to the 1981-2010 reference period (ensemble median). Left-panel: RCP4.5 emission scenario. Right-panel: RCP8.5 emission scenario. Each colour corresponds to a 30-year period: from dark blue (1981-2010) to red (2071-2100). The day=1 for October 1st and 365 for September 30th.

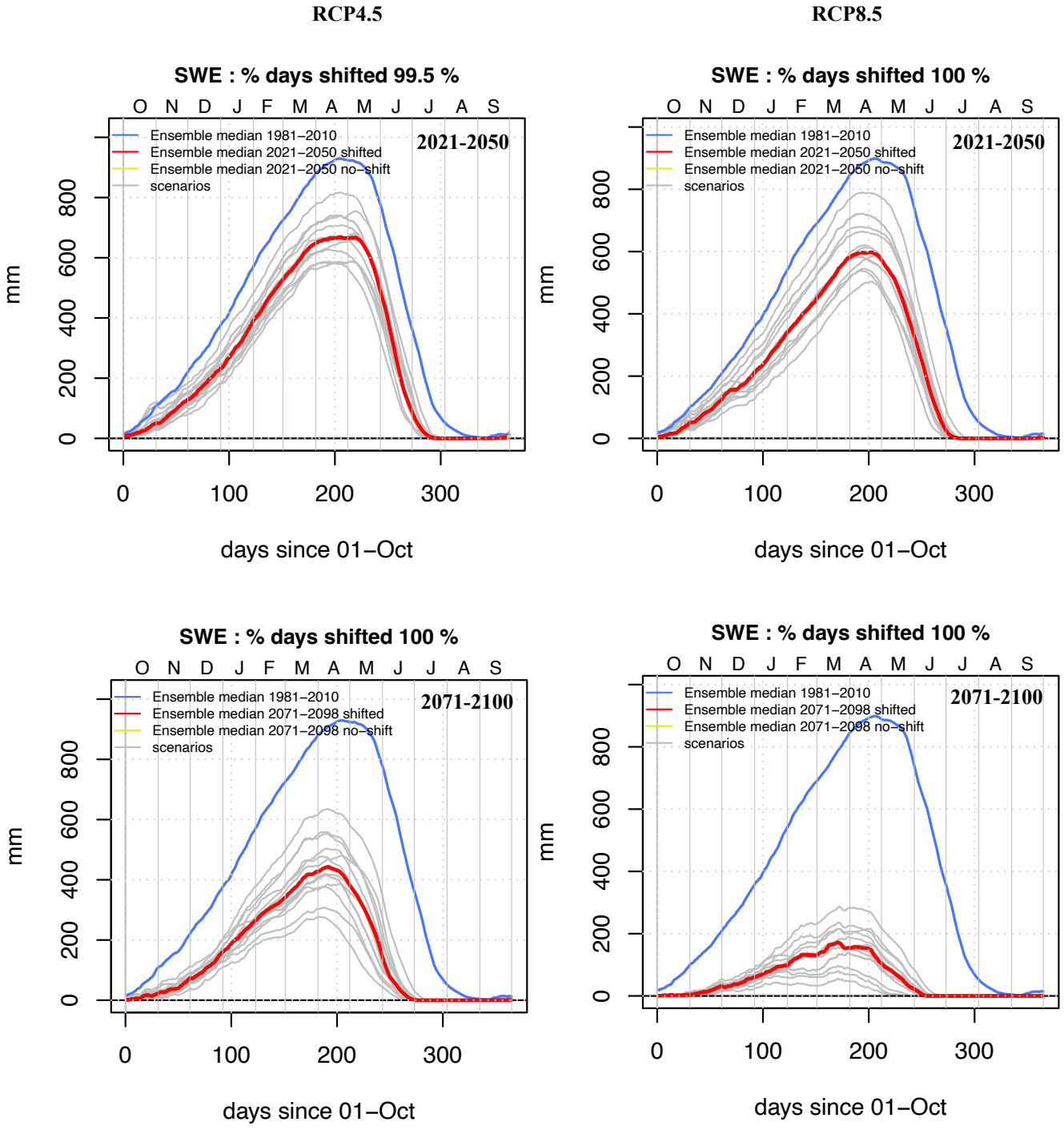

Fig. 14: Þverá catchment (vhm38): Projected seasonality of mean daily snow storage (SWE) under the RCP4.5 emission scenario (left-panel) and the RCP8.5 emission scenario (right-panel). Projection periods: 2021-2050 (top-panel) and 2071-2100 (bottom-panel). Individual ensemble members are coloured in grey. The ensemble median in each projection period is coloured in red for days when the Mann-Whitney test detected a significant shift in the mean daily snow storage ensemble, compared to the reference period (1981-2010) and yellow otherwise. The ensemble median in the reference period is shown in blue. The percentage of days in the water year when a significant shift in mean daily snow storage is detected by the Mann-Whitney test is also indicated. The day=1 for October 1st and 365 for September 30th.

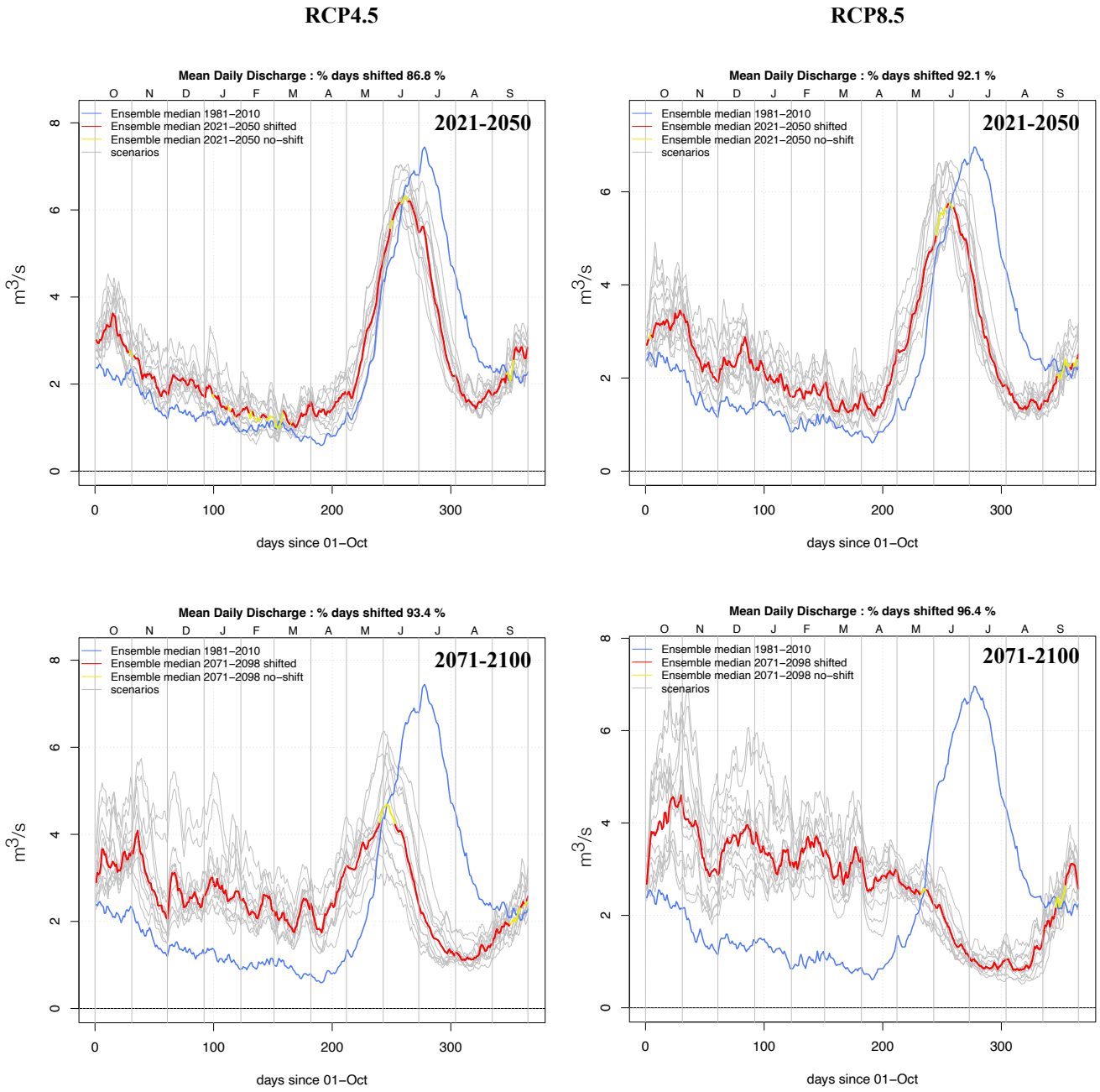

Fig. 15: Þverá catchment (vhm38): Projected seasonality of mean daily discharge under the RCP4.5 emission scenario (left-panel) and the RCP8.5 emission scenario (right-panel). Projection periods: 2021-2050 (top-panel) and 2071-2100 (bottom-panel). Individual ensemble members are coloured in grey. The ensemble median in each projection period is coloured in red for days when the Mann-Whitney test detected a significant shift in the mean daily discharge ensemble, compared to the reference period (1981-2010) and yellow otherwise. The ensemble median in the reference period is shown in blue. The percentage of days in the water year when a significant shift in mean daily discharge is detected by the Mann-Whitney test is also indicated. The day=1 for October 1st and 365 for September 30th.

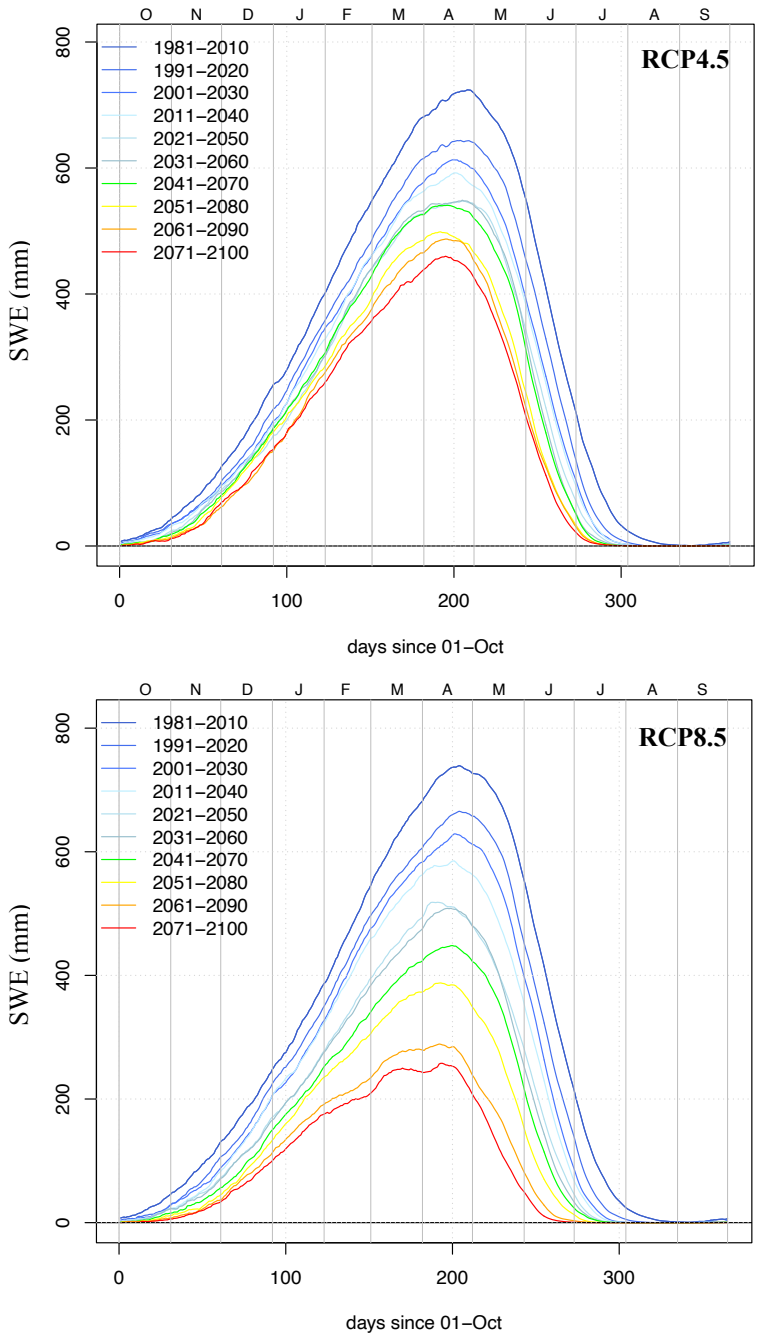

Fig. 16: Markarfljót catchment (vhm218): Projected seasonality of mean daily snow storage (ensemble median) under the RCP4.5 emission scenario (top) and RCP8.5 emission scenario (bottom). Each colour corresponds to a 30-year period: from dark blue (1981-2010) to red (2071-2100). The day=1 for October 1st and 365 for September 30th.

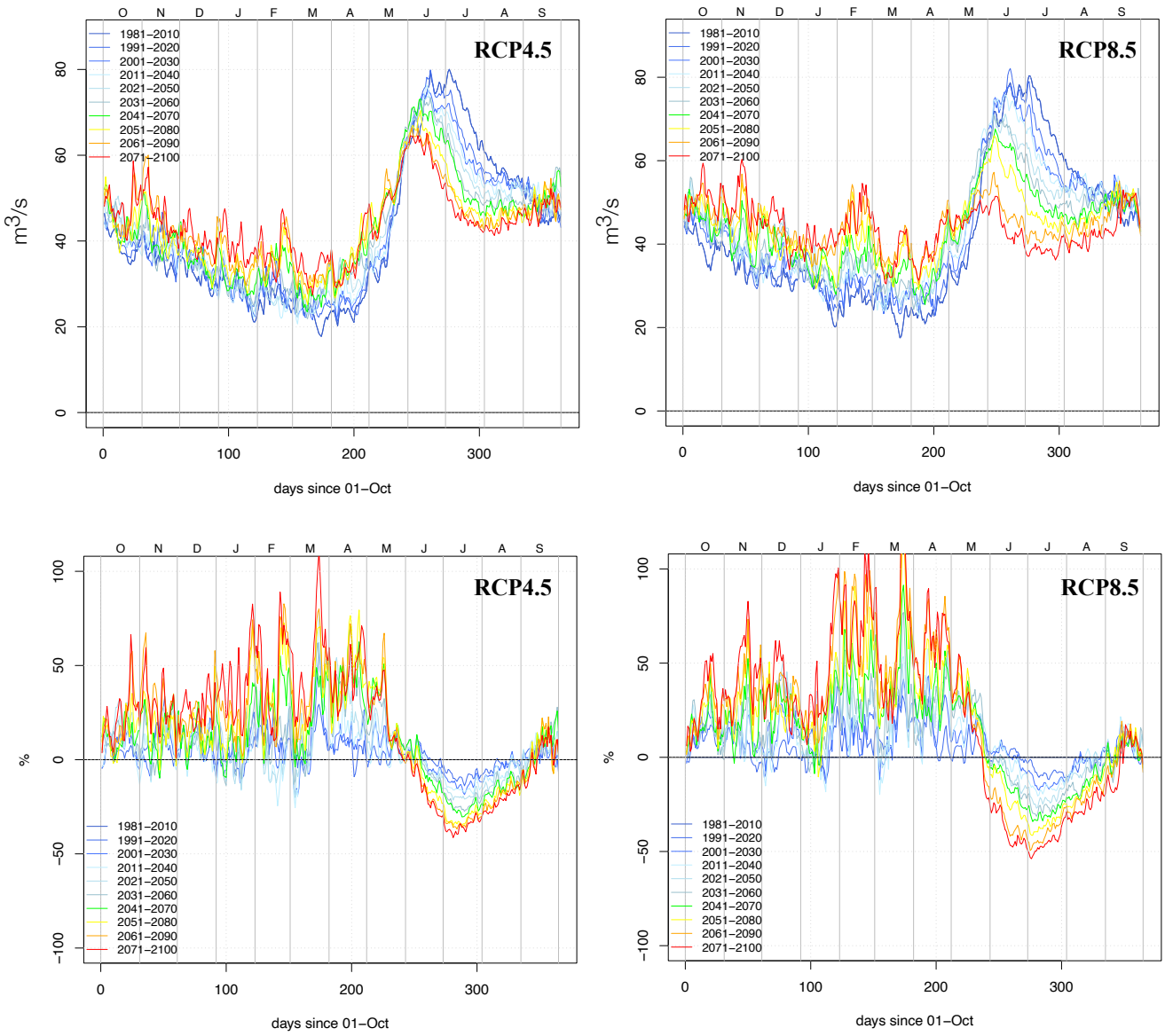

Fig. 17: Markarfljót catchment (vhm218). Top-panel: Projected seasonality of mean daily discharge (ensemble median). Bottom-panel: Percent change in mean daily discharge relative to the 1981-2010 reference period (ensemble median). Left-panel: RCP4.5 emission scenario. Right-panel: RCP8.5 emission scenario. Each colour corresponds to a 30-year period: from dark blue (1981-2010) to red (2071-2100). The day=1 for October 1st and 365 for September 30th.

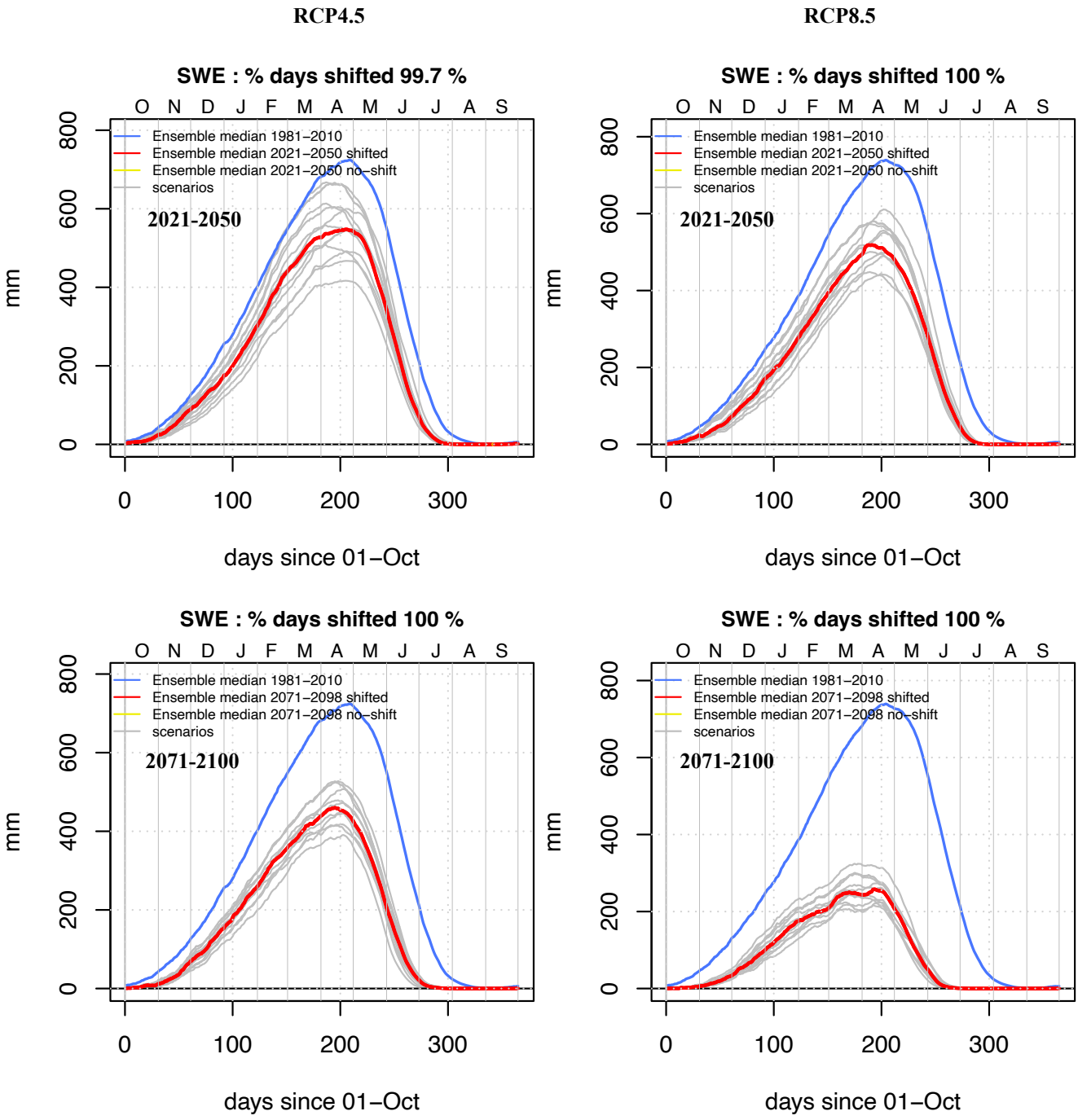

Fig. 18: Markarfljót catchment (vhm218): Projected seasonality of mean daily snow storage (SWE) under the RCP4.5 emission scenario (left-panel) and the RCP8.5 emission scenario (right-panel). Projection periods: 2021-2050 (top-panel) and 2071-2100 (bottom-panel). Individual ensemble members are coloured in grey. The ensemble median in each projection period is coloured in red for days when the Mann-Whitney test detected a significant shift in the mean daily snow storage ensemble, compared to the reference period (1981-2010) and yellow otherwise. The ensemble median in the reference period is shown in blue. The percentage of days in the water year when a significant shift in mean daily snow storage is detected by the Mann-Whitney test is also indicated. The day=1 for October 1st and 365 for September 30th.

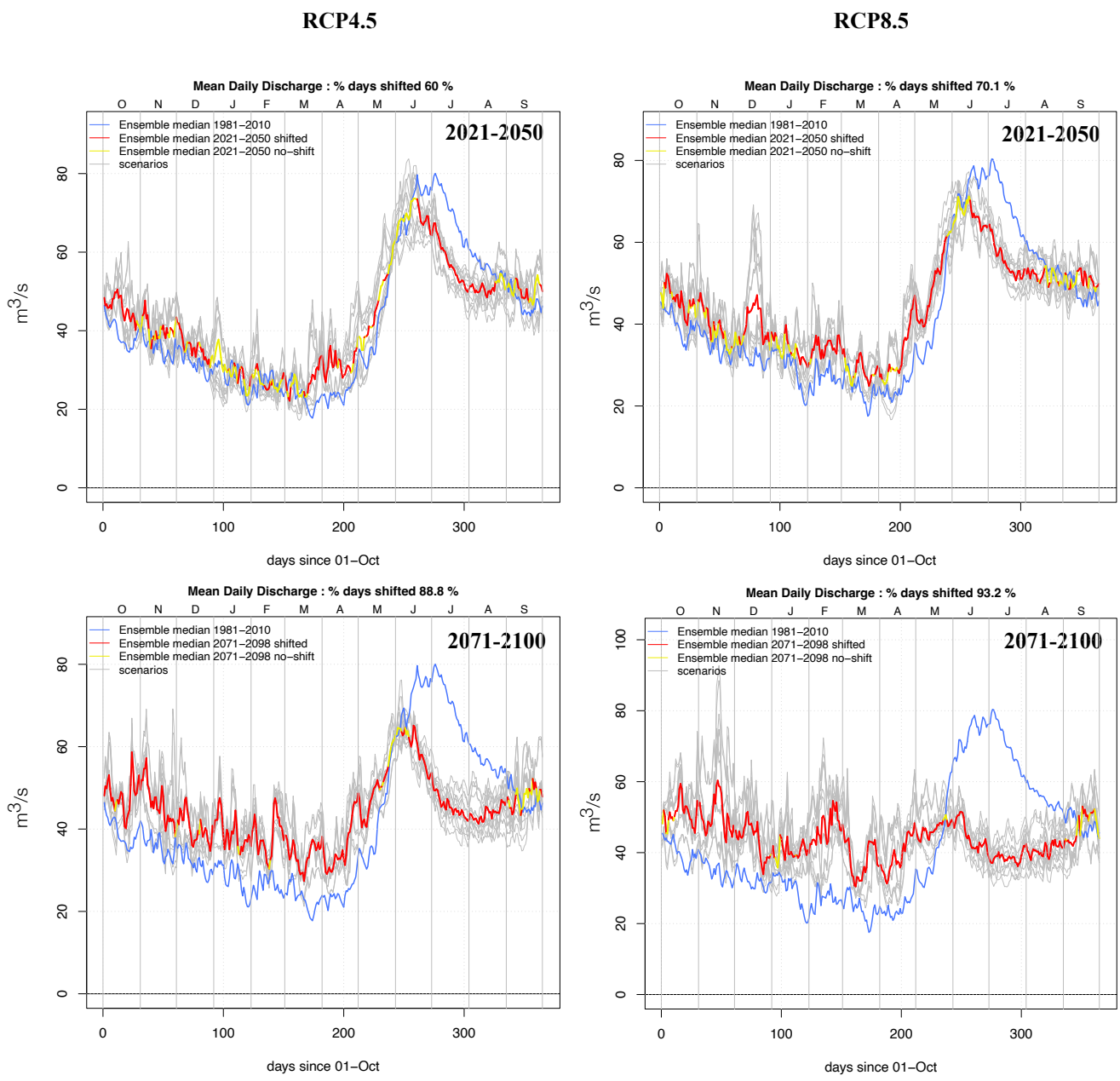

Fig. 19: Markarfljót catchment (vhm218): Projected seasonality of mean daily discharge under the RCP4.5 emission scenario (left-panel) and the RCP8.5 emission scenario (right-panel). Projection periods: 2021-2050 (top-panel) and 2071-2100 (bottom-panel). Individual ensemble members are coloured in grey. The ensemble median in each projection period is coloured in red for days when the Mann-Whitney test detected a significant shift in the mean daily discharge ensemble, compared to the reference period (1981-2010) and yellow otherwise. The ensemble median in the reference period is shown in blue. The percentage of days in the water year when a significant shift in mean daily discharge is detected by the Mann-Whitney test is also indicated. The day=1 for October 1st and 365 for September 30th.

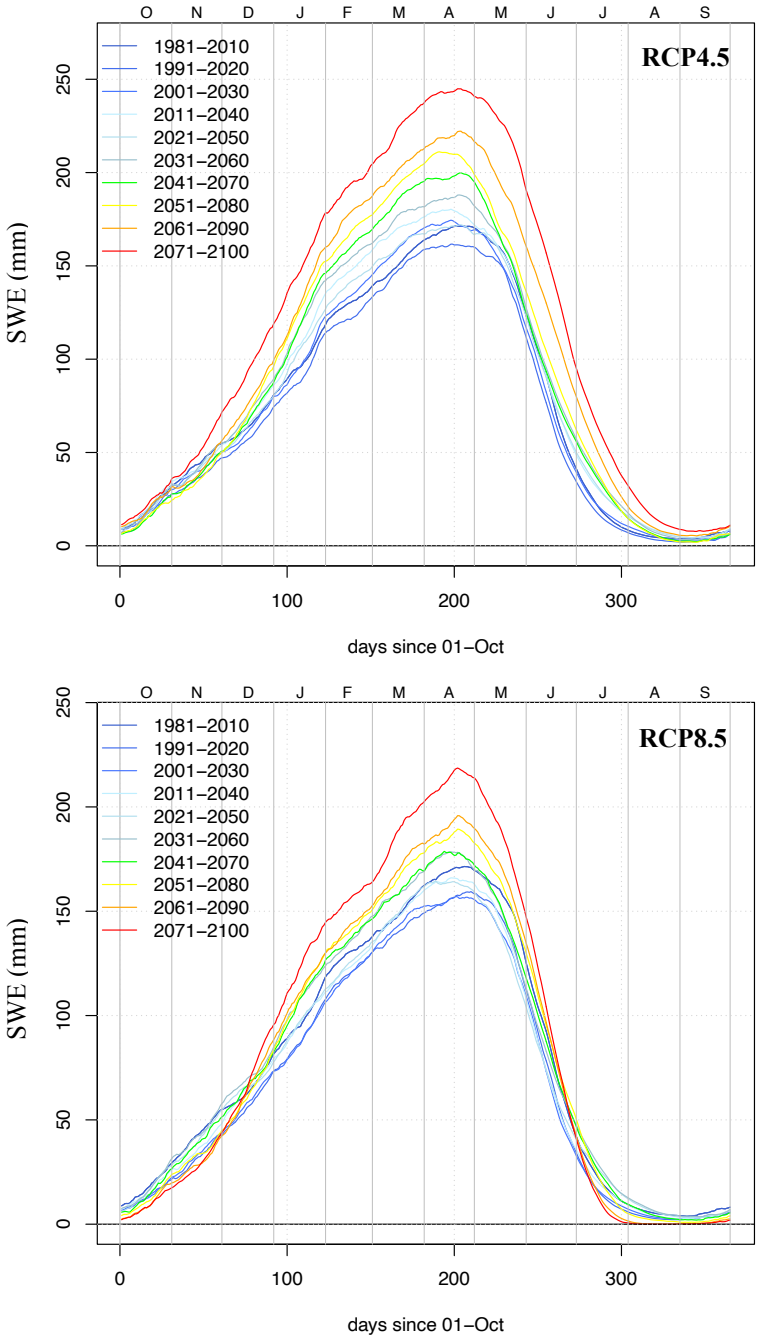

Fig. 20: Kreppa catchment (vhm233): Projected seasonality of mean daily snow storage (ensemble median) under the RCP4.5 emission scenario (top) and RCP8.5 emission scenario (bottom). Each colour corresponds to a 30-year period: from dark blue (1981-2010) to red (2071-2100). The day=1 for October 1st and 365 for September 30th.

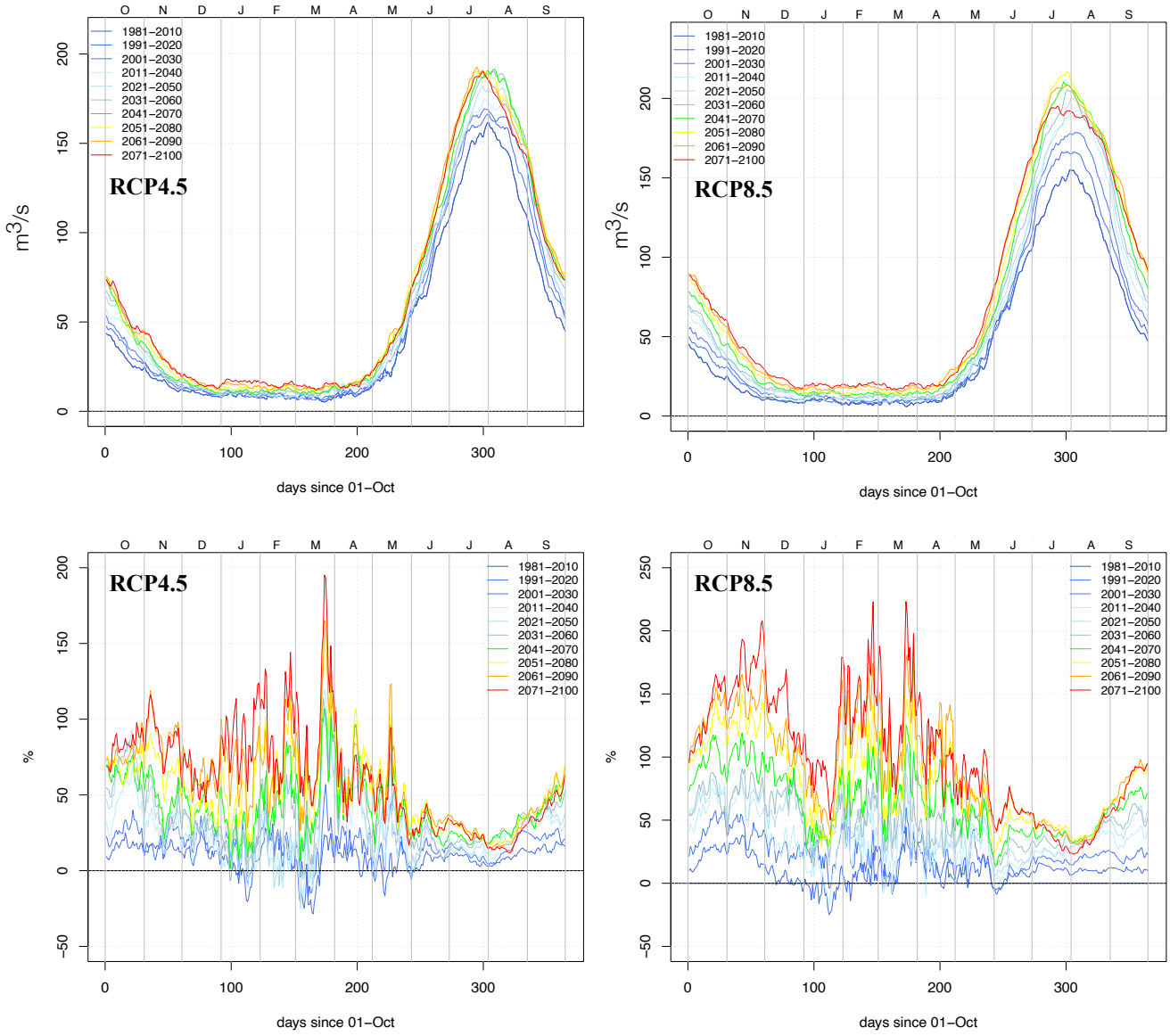

Fig. 21: Kreppa catchment (vhm233). Top-panel: Projected seasonality of mean daily discharge (ensemble median). Bottom-panel: Percent change in mean daily discharge relative to the 1981-2010 reference period (ensemble median). Left-panel: RCP4.5 emission scenario. Right-panel: RCP8.5 emission scenario. Each colour corresponds to a 30-year period: from dark blue (1981-2010) to red (2071-2100). The day=1 for October 1st and 365 for September 30th.

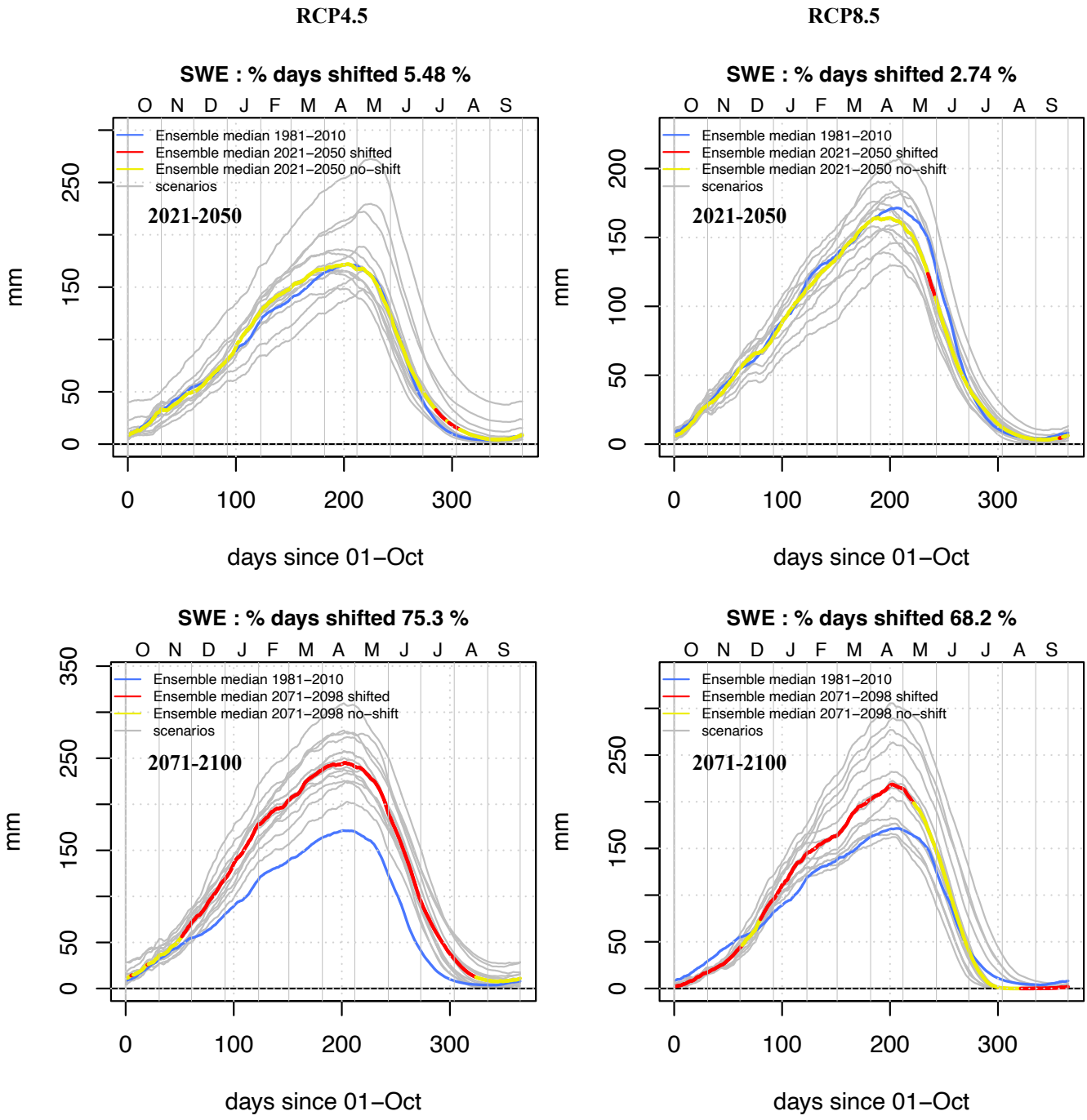

Fig. 22: Kreppa catchment (vhm233): Projected seasonality of mean daily snow storage (SWE) under the RCP4.5 emission scenario (left-panel) and the RCP8.5 emission scenario (right-panel). Projection periods: 2021-2050 (top-panel) and 2071-2100 (bottom-panel). Individual ensemble members are coloured in grey. The ensemble median in each projection period is coloured in red for days when the Mann-Whitney test detected a significant shift in the mean daily snow storage ensemble, compared to the reference period (1981-2010) and yellow otherwise. The ensemble median in the reference period is shown in blue. The percentage of days in the water year when a significant shift in mean daily snow storage is detected by the Mann-Whitney test is also indicated. The day=1 for October 1st and 365 for September 30th.

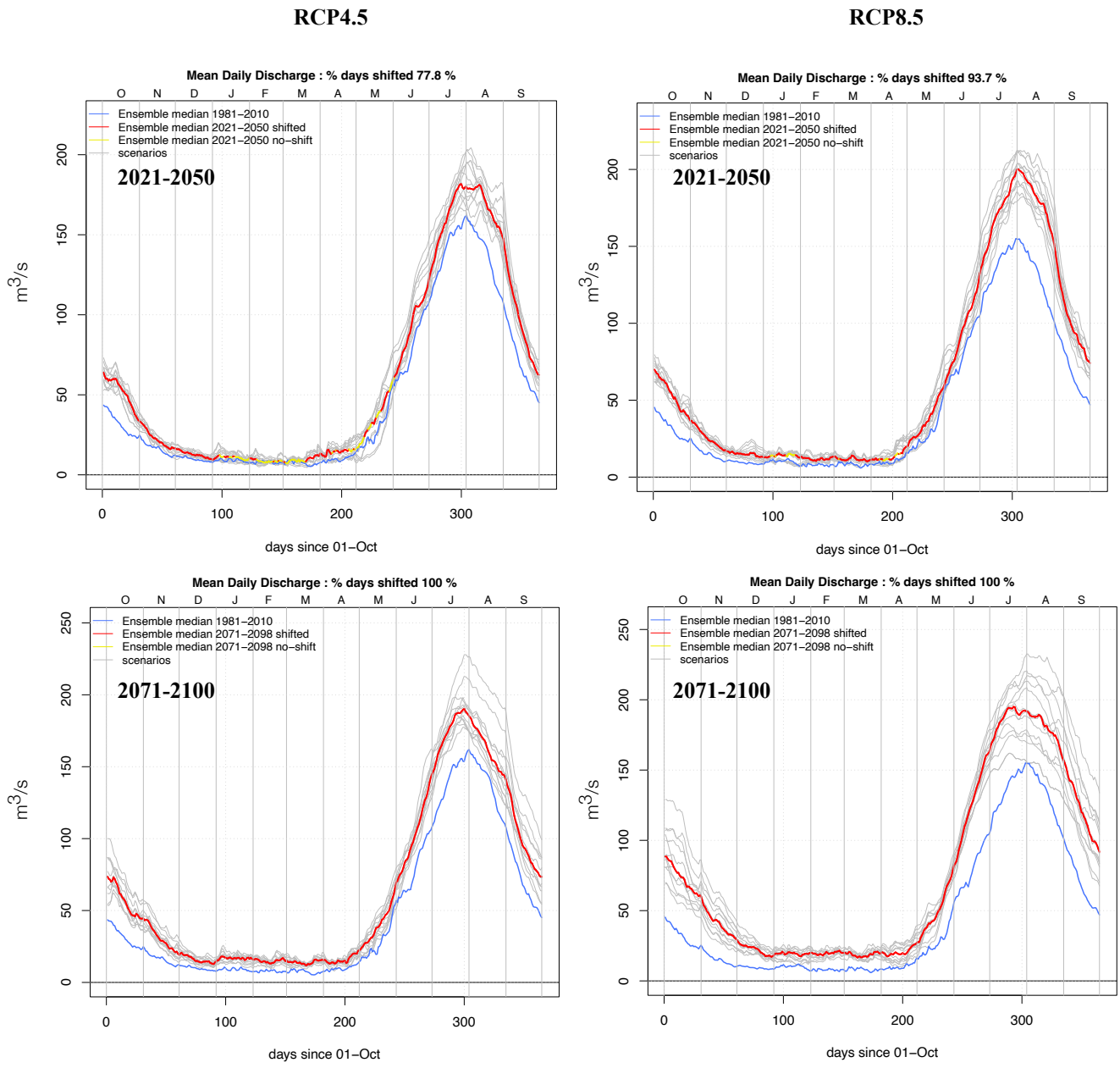

Fig. 23: Kreppa catchment (vhm233): Projected seasonality of mean daily discharge under the RCP4.5 emission scenario (left-panel) and the RCP8.5 emission scenario (right-panel). Projection periods: 2021-2050 (top-panel) and 2071-2100 (bottom-panel). Individual ensemble members are coloured in grey. The ensemble median in each projection period is coloured in red for days when the Mann-Whitney test detected a significant shift in the mean daily discharge ensemble, compared to the reference period (1981-2010) and yellow otherwise. The ensemble median in the reference period is shown in blue. The percentage of days in the water year when a significant shift in mean daily discharge is detected by the Mann-Whitney test is also indicated. The day=1 for October 1st and 365 for September 30th.

6-2-2 Changes in mean annual and seasonal hydro-climatic characteristics

In this section, the ensembles of 30-year mean annual and seasonal streamflow projections are jointly analysed with the corresponding ensembles of mean annual and seasonal temperature, precipitation, rainfall, snowfall and snow and glacier melt projections. Projected changes between reference and future 30-year periods are presented in Figs. 24 to 53. For the Markarfljót (vhm218) and Kreppa (vhm233) catchments, figures show the total changes in snow and glacier melt, and Appendix 9 and 10 present the results for snow and glacier melt separately (keep in mind that HYPE converts all snow falling onto glaciers into ice and subsequently, the model accumulates and melts snow outside the glaciers only). For temperature, the projected changes are given in degree Celsius (future minus reference) and for the other indicators, the changes are given in percent relative to the corresponding reference (100×(future minus reference)/reference). The plots also include results from the two one-sided Mann-Whitney tests used to compare the 30-year mean ensembles between reference and future periods (see Methodology in Section 3-1). The analysis below summarises the results.

- **Þverá catchment (vhm38)**
  - Mean annual and seasonal near surface air temperatures are projected to steadily rise during the 21st century. A median warming of about +2.7°C is projected from 1981-2010 to 2071-2100 under the RCP4.5 scenario and about +4.2°C to +4.6°C under the RCP8.5 scenario, depending on the season (see also Table 8).
  - A significant increase in mean annual precipitation is projected during the 21st century under both emission scenarios and concerns most ensemble members, especially under the RCP8.5 emission scenario. This increase is moderate under the RCP4.5 scenario and does not exceed a median value of +10%, whereas under the RCP8.5 scenario, the increase reaches a median value of almost +20% by the end of the century. The spread of the ensemble increases with the projection horizon under both emission scenarios. The increase in mean annual precipitation is driven by the projected increase in mean precipitation in JAS and OND. The largest increases in JAS and OND are projected towards the end of the 21st century with a median value estimated at about +20% under the RCP4.5 scenario and about +30% under the RCP8.5 scenario. Mean seasonal precipitation is not projected to change significantly in JFM and AMJ in most projection time-windows, either because the ensemble spread is large and with a lack of consensus regarding the direction of change, making the outcome uncertain, or because the projections fluctuate closely around their reference level.
  - The increase in temperature is projected to have an impact on the fractions of precipitation falling as rain or snow. Mean seasonal rainfall is projected to increase more or less gradually whereas mean seasonal snowfall is projected to decrease more or less gradually, during the 21st century and all seasons, under both emission scenarios. The increase in mean seasonal rainfall in JFM and AMJ results mainly from changes in the phase of precipitation, whereas in JAS, the rainfall increase results mainly from a precipitation increase, and in OND from both changes in the amount and phase of precipitation.

- The decrease in mean annual snowfall resulting from the projected warming leads to a reduction in snow storage (cf. Fig. 12) which, in turn, leads to a decrease in mean annual snowmelt under both emission scenarios. At the seasonal level, mean snowmelt variations are more complex: Results indicate that mean seasonal snowmelt is projected to increase in OND, progressively increase in JFM, first increase and then decrease in AMJ, and continuously decrease in JAS. The changes are usually greater under the RCP8.5 emission scenario than under the RCP4.5 emission scenario because the projected warming is greater. The projected increase in mean snowmelt in OND/JFM/AMJ is likely caused by an increase in the number of warm spells leading to intermittent snowmelt events and/or a shift earlier in the onset of the snowmelt season (JFM/AMJ), whereas the projected decrease in mean snowmelt in AMJ/JAS is owing to the projected snow storage depletion caused by the projected decrease in seasonal snowfall combined with an increased number of snowmelt events in winter destabilising the build-up of the snowpack. Note also that in OND, snowmelt increases under the RCP8.5 scenario but from 2051-2080, the rate of increase slows down, most likely indicating that less snow is available for melting because the build-up of the snowpack starts later in the season.
- Following the projected increase in mean annual precipitation, mean annual streamflow is projected to increase significantly under both emission scenarios, especially in the second half of the 21st century. The spread of the ensemble increases with the projection horizon under both emission scenarios. Note that increased evapotranspiration (not shown) caused by rising temperatures counteracts the increase in mean annual precipitation, therefore the percent increase in mean annual streamflow is slightly smaller than the percent increase in mean annual precipitation. At the seasonal level, the projections indicate a progressive increase in mean streamflow in OND and JFM under both emission scenarios, caused by the projected increase in rainfall and snowmelt. Mean streamflow is projected to increase in AMJ during most of the 21st century (except in 2071-2100) under the RCP4.5 emission scenario, with a peak in 2041-2070, whereas under the RCP8.5 emission scenario, mean streamflow will increase until 2041-2070 with a peak in 2031-2060, and decrease thereafter until the end of the century. These results in AMJ are first related to an increase in rainfall and snowmelt and then to a decrease in snowmelt not always compensated by the rainfall increase. A gradual decrease in mean streamflow is projected in JAS under both emission scenarios, caused by the snowmelt decrease and increased evapotranspiration (not shown) not compensated by the increase in rainfall. The changes are usually more pronounced with the RCP8.5 than the RCP4.5 emission scenario because the projected warming is greater and its impact on the change in the phase of precipitation and on snow accumulation and melt larger. The greatest median changes in mean seasonal streamflow projected in the 21st century have the following values:

  -RCP4.5: OND (+75%), JFM (+128%), AMJ (+27%), JAS (−55%)
  -RCP8.5: OND (+115%), JFM (+211%), AMJ (±22%), JAS (−62%)

RCP4.5

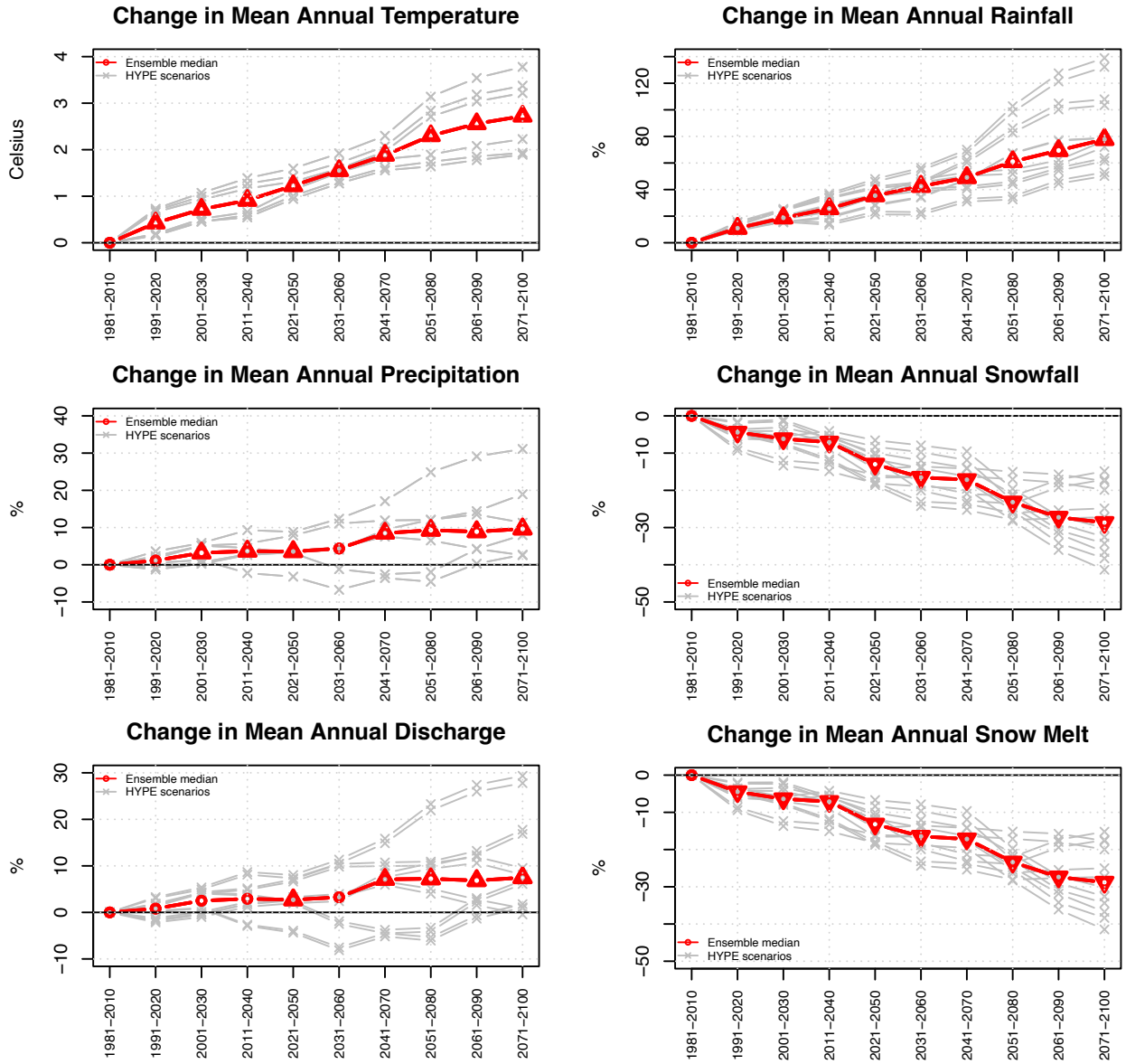

Fig. 24: Þverá catchment (vhm38): Projected changes in 30-year mean annual temperature, precipitation, rainfall, snowfall, snowmelt and river discharge under the RCP4.5 emission scenario, relative to the 1981-2010 reference period. Ensemble members (grey lines) and ensemble median (red line). The symbols on the ensemble median indicate whether the 30-year mean is projected to change significantly or to remain unchanged in future periods compared to the reference period, according to the Mann-Whitney test (triangle point-up=significant increase; triangle point down=significant decrease; open circle=no significant change).

RCP4.5

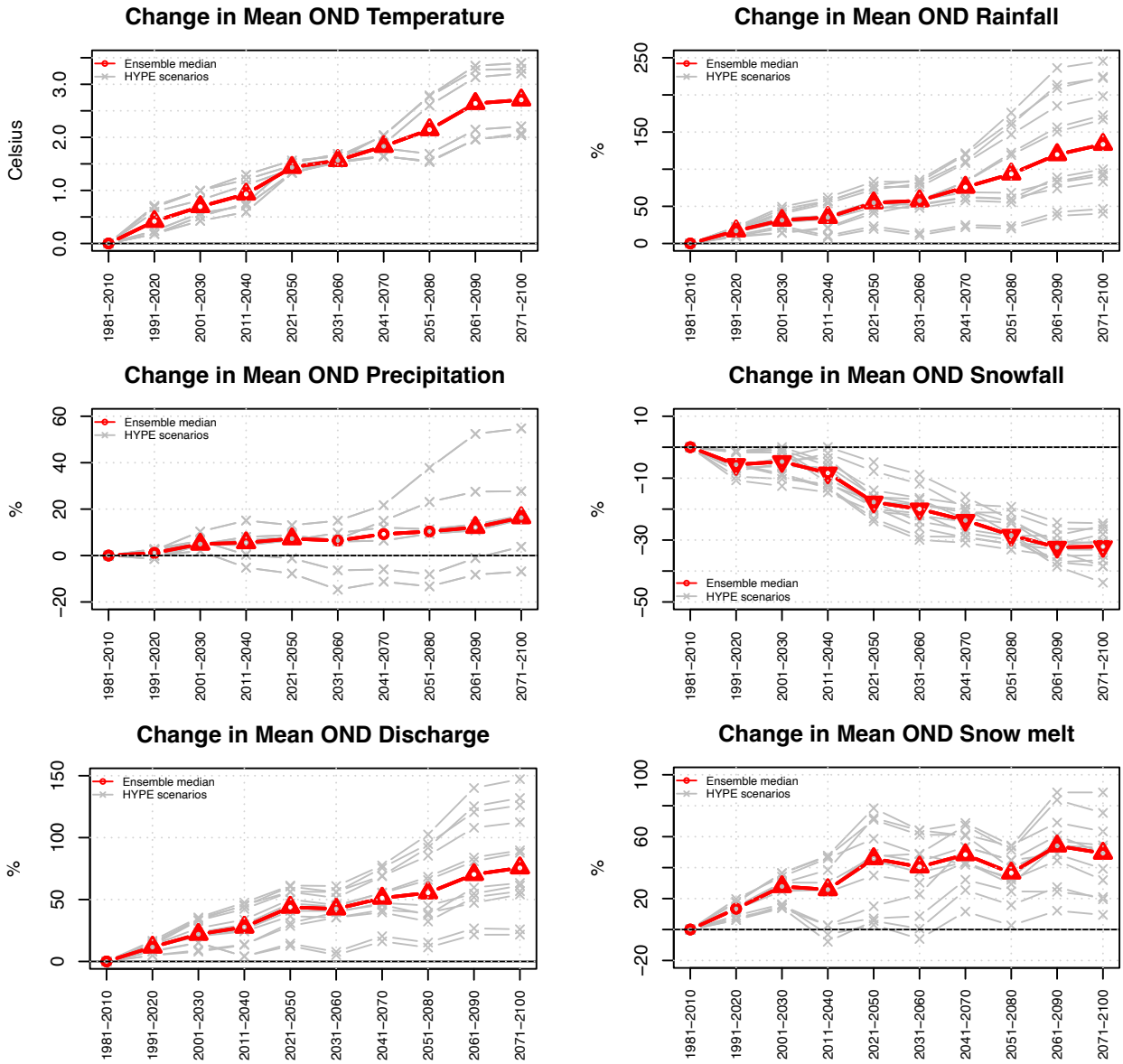

Fig. 25: Þverá catchment (vhm38): Projected changes in 30-year mean OND temperature, precipitation, rainfall, snowfall, snowmelt and river discharge under the RCP4.5 emission scenario, relative to the 1981-2010 reference period. Ensemble members (grey lines) and ensemble median (red line). The symbols on the ensemble median indicate whether the 30-year mean is projected to change significantly or to remain unchanged in future periods compared to the reference period, according to the Mann-Whitney test (triangle point-up=significant increase; triangle point down=significant decrease; open circle=no significant change).

RCP4.5

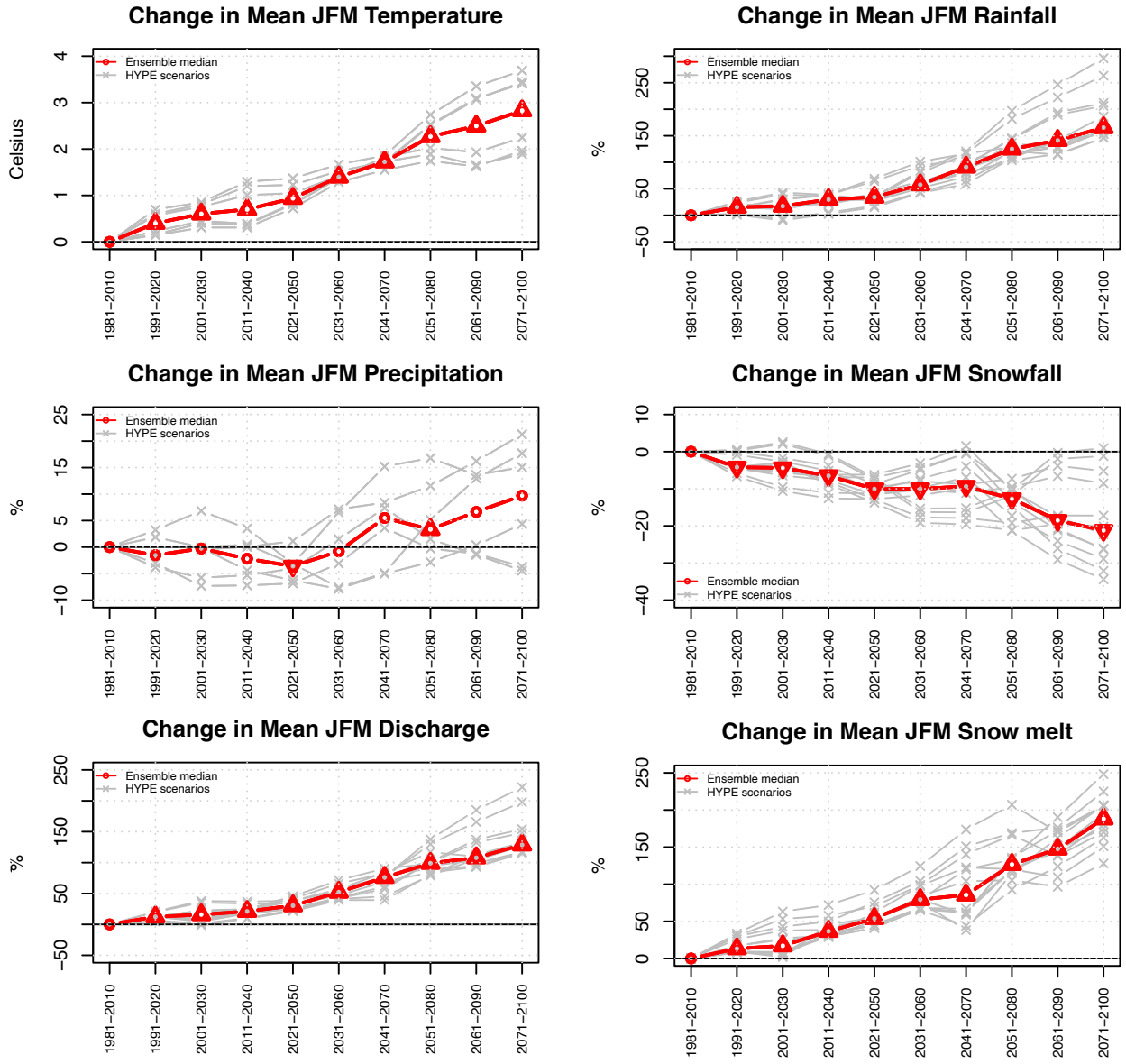

Fig. 26: Þverá catchment (vhm38): Projected changes in 30-year mean JFM temperature, precipitation, rainfall, snowfall, snowmelt and river discharge under the RCP4.5 emission scenario, relative to the 1981-2010 reference period. Ensemble members (grey lines) and ensemble median (red line). The symbols on the ensemble median indicate whether the 30-year mean is projected to change significantly or to remain unchanged in future periods compared to the reference period, according to the Mann-Whitney test (triangle point-up=significant increase; triangle point down=significant decrease; open circle=no significant change).

RCP4.5

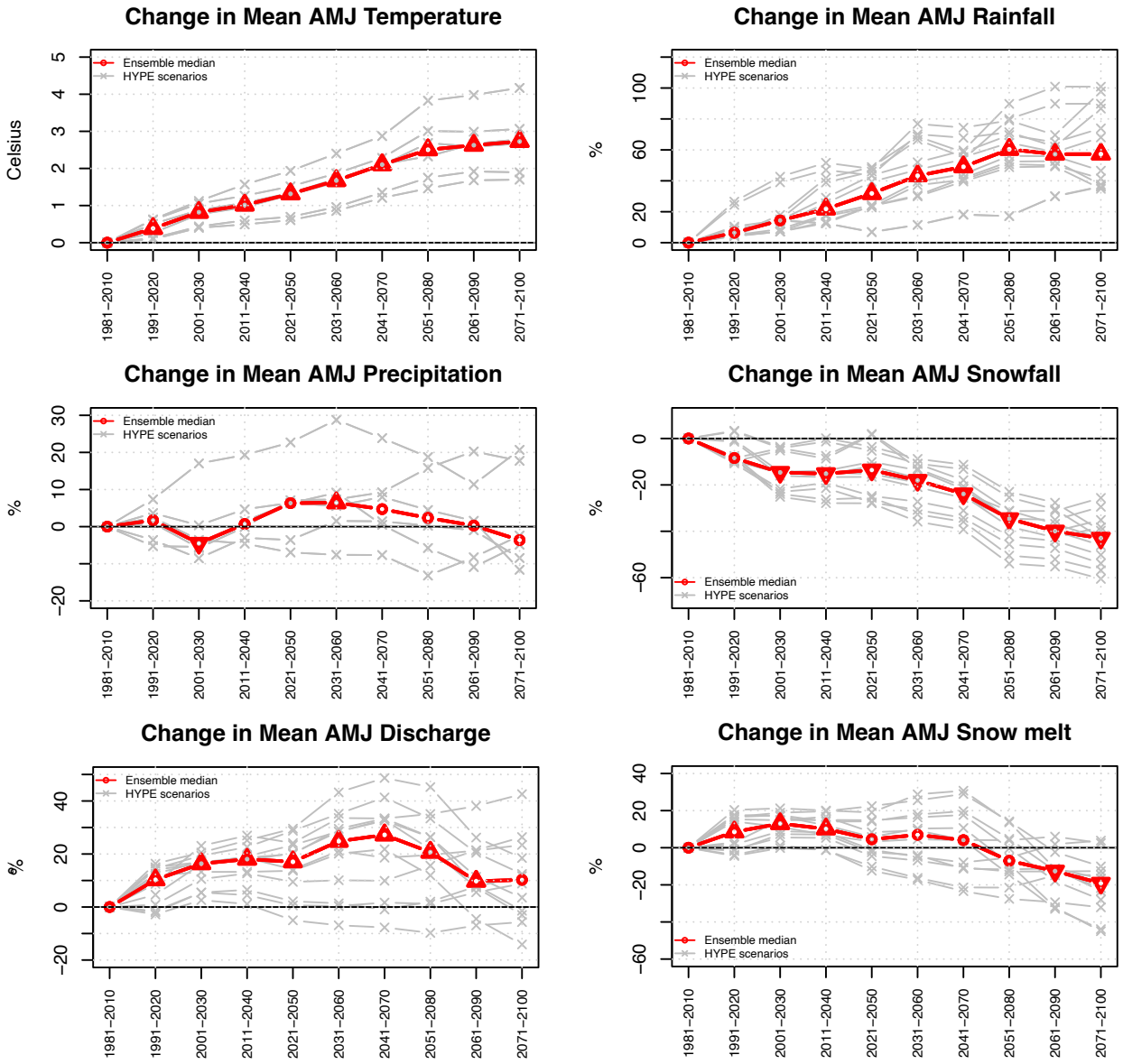

Fig. 27: Þverá catchment (vhm38): Projected changes in 30-year mean AMJ temperature, precipitation, rainfall, snowfall, snowmelt and river discharge under the RCP4.5 emission scenario, relative to the 1981-2010 reference period. Ensemble members (grey lines) and ensemble median (red line). The symbols on the ensemble median indicate whether the 30-year mean is projected to change significantly or to remain unchanged in future periods compared to the reference period, according to the Mann-Whitney test (triangle point-up=significant increase; triangle point down=significant decrease; open circle=no significant change).

RCP4.5

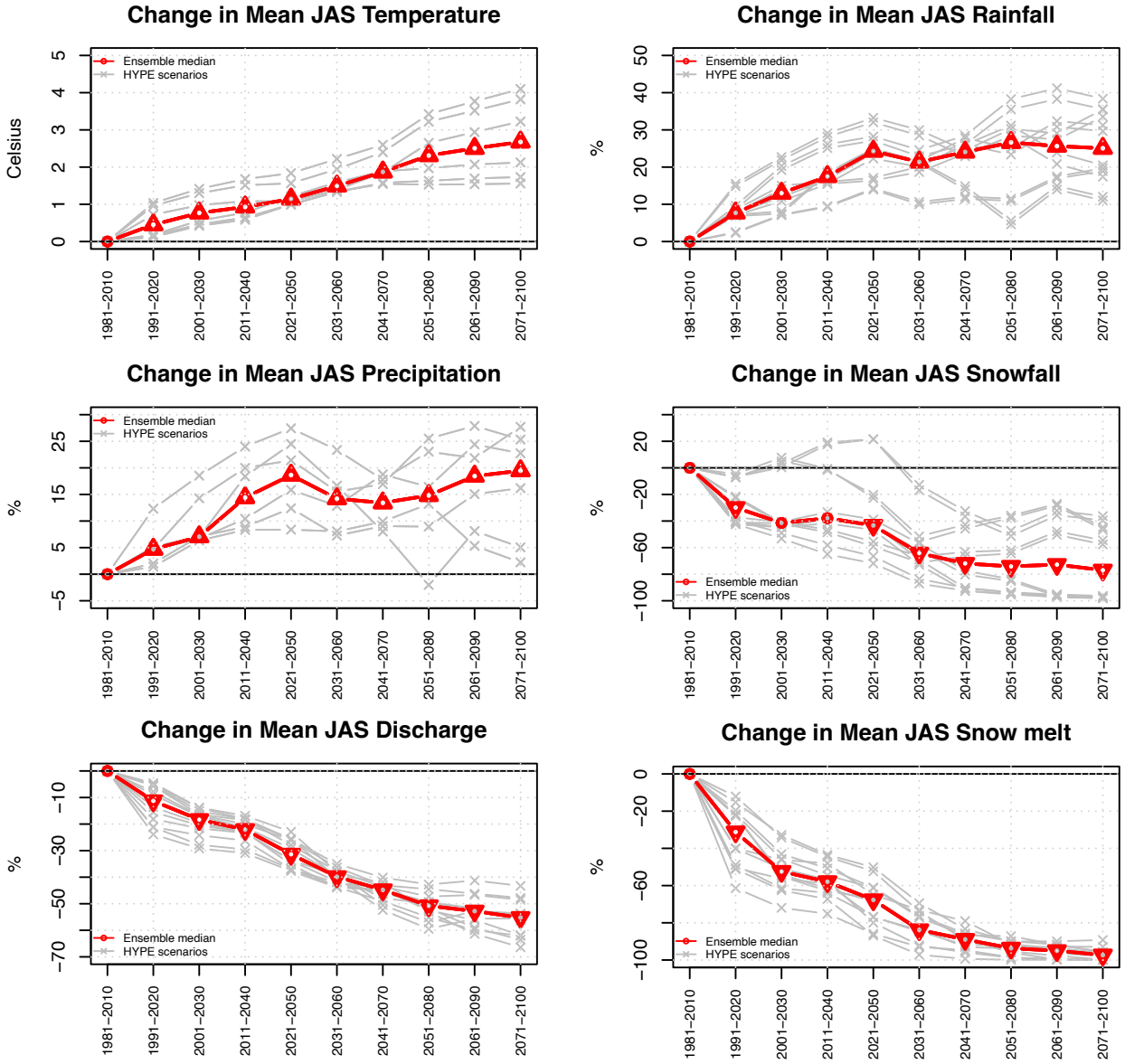

Fig. 28: Þverá catchment (vhm38): Projected changes in 30-year mean JAS temperature, precipitation, rainfall, snowfall, snowmelt and river discharge under the RCP4.5 emission scenario, relative to the 1981-2010 reference period. Ensemble members (grey lines) and ensemble median (red line). The symbols on the ensemble median indicate whether the 30-year mean is projected to change significantly or to remain unchanged in future periods compared to the reference period, according to the Mann-Whitney test (triangle point-up=significant increase; triangle point down=significant decrease; open circle=no significant change).

RCP8.5

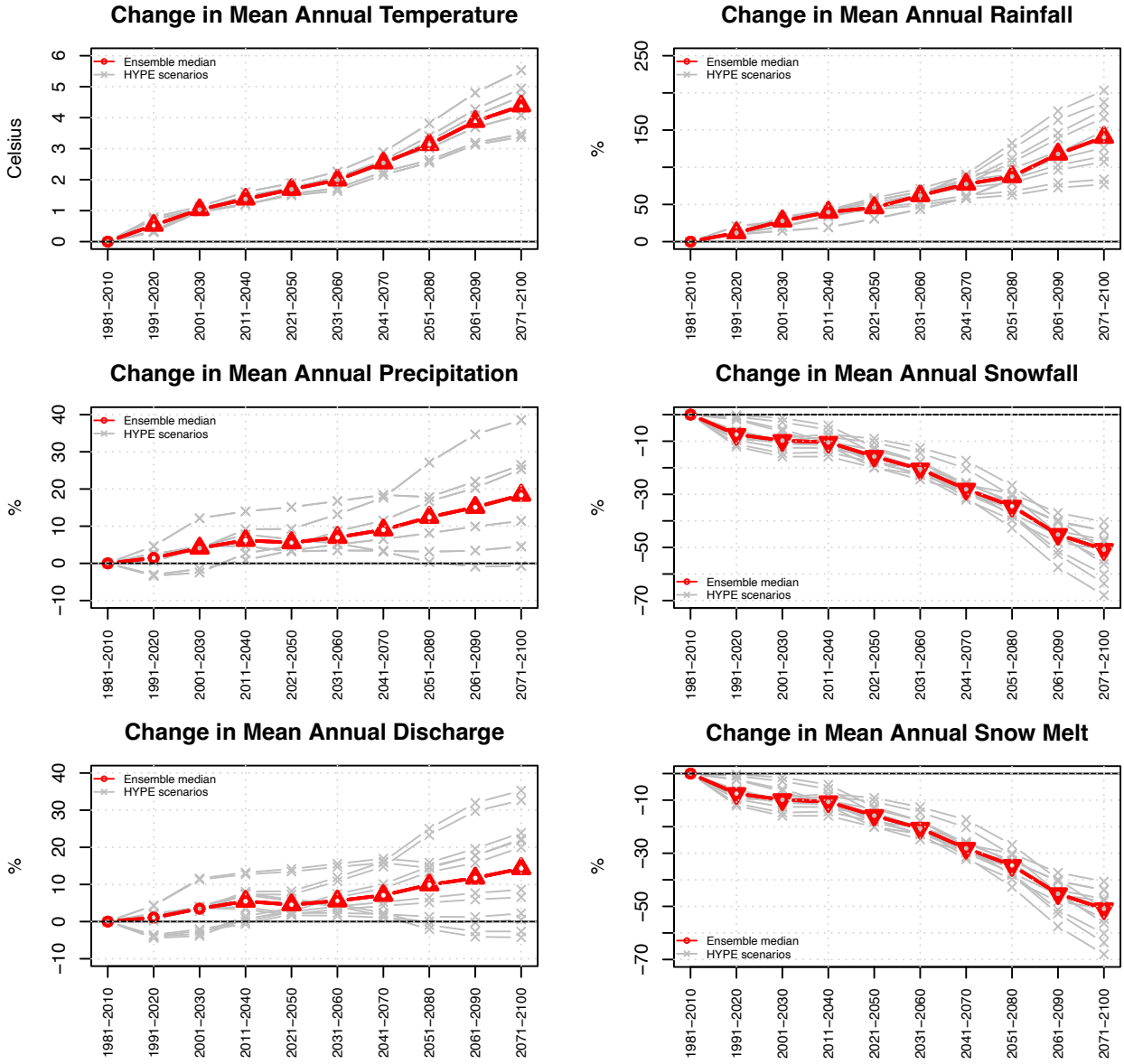

Fig. 29: Þverá catchment (vhm38): Projected changes in 30-year mean annual temperature, precipitation, rainfall, snowfall, snowmelt and river discharge under the RCP8.5 emission scenario, relative to the 1981-2010 reference period. Ensemble members (grey lines) and ensemble median (red line). The symbols on the ensemble median indicate whether the 30-year mean is projected to change significantly or to remain unchanged in future periods compared to the reference period, according to the Mann-Whitney test (triangle point-up=significant increase; triangle point down=significant decrease; open circle=no significant change).

RCP8.5

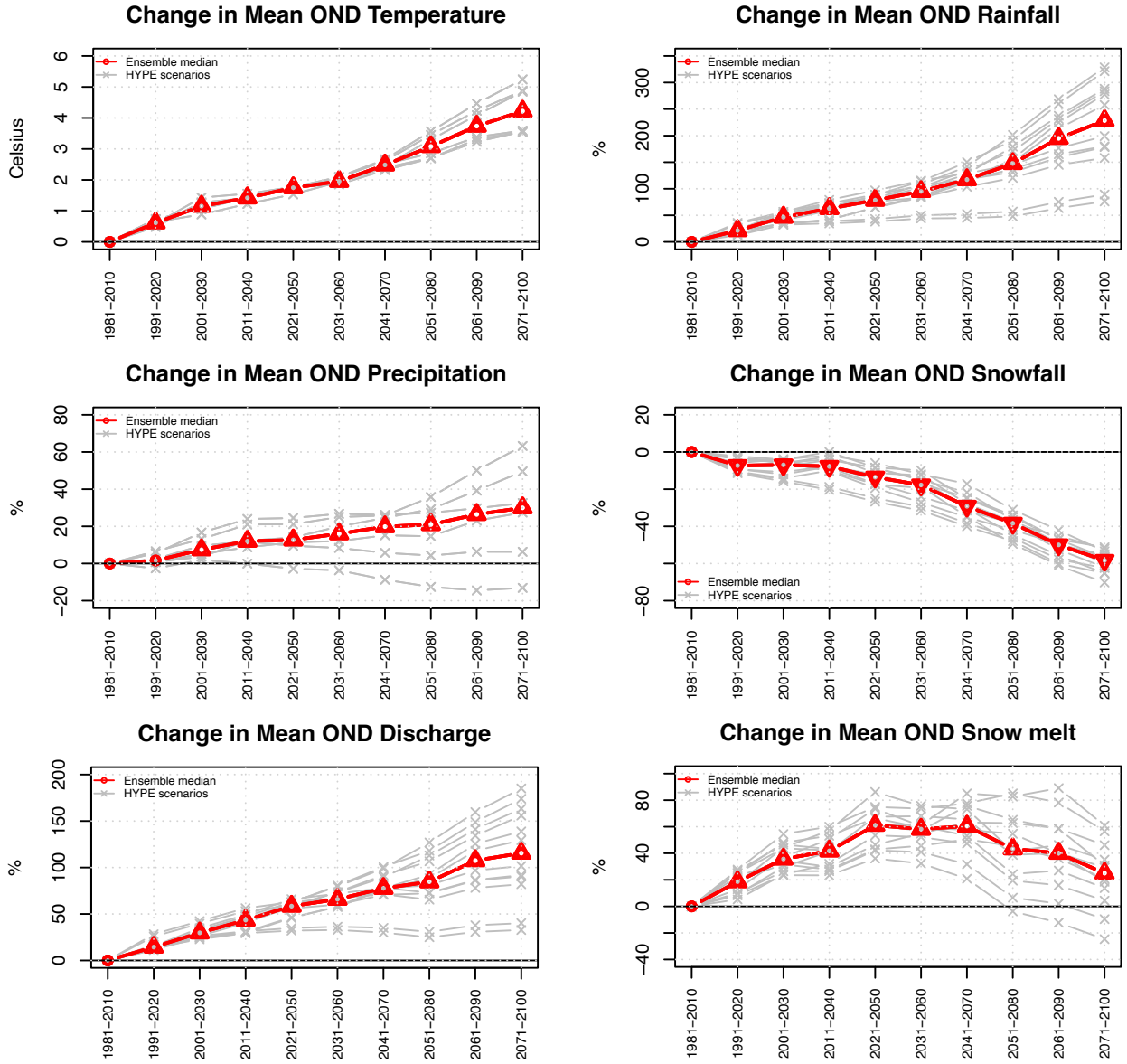

Fig. 30: Þverá catchment (vhm38): Projected changes in 30-year mean OND temperature, precipitation, rainfall, snowfall, snowmelt and river discharge under the RCP8.5 emission scenario, relative to the 1981-2010 reference period. Ensemble members (grey lines) and ensemble median (red line). The symbols on the ensemble median indicate whether the 30-year mean is projected to change significantly or to remain unchanged in future periods compared to the reference period, according to the Mann-Whitney test (triangle point-up=significant increase; triangle point down=significant decrease; open circle=no significant change).

RCP8.5

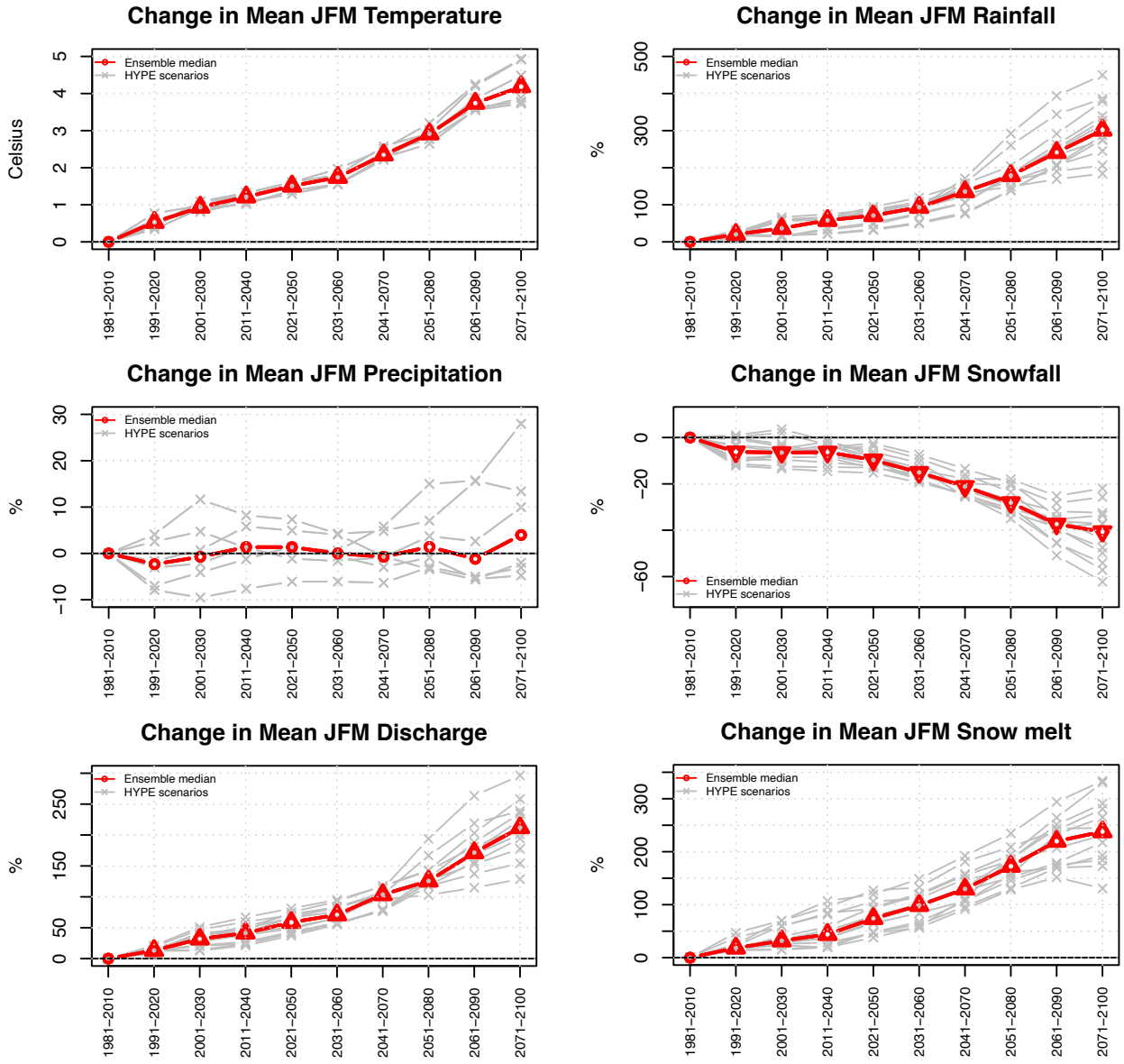

Fig. 31: Þverá catchment (vhm38): Projected changes in 30-year mean JFM temperature, precipitation, rainfall, snowfall, snowmelt and river discharge under the RCP8.5 emission scenario, relative to the 1981-2010 reference period. Ensemble members (grey lines) and ensemble median (red line). The symbols on the ensemble median indicate whether the 30-year mean is projected to change significantly or to remain unchanged in future periods compared to the reference period, according to the Mann-Whitney test (triangle point-up=significant increase; triangle point down=significant decrease; open circle=no significant change).

RCP8.5

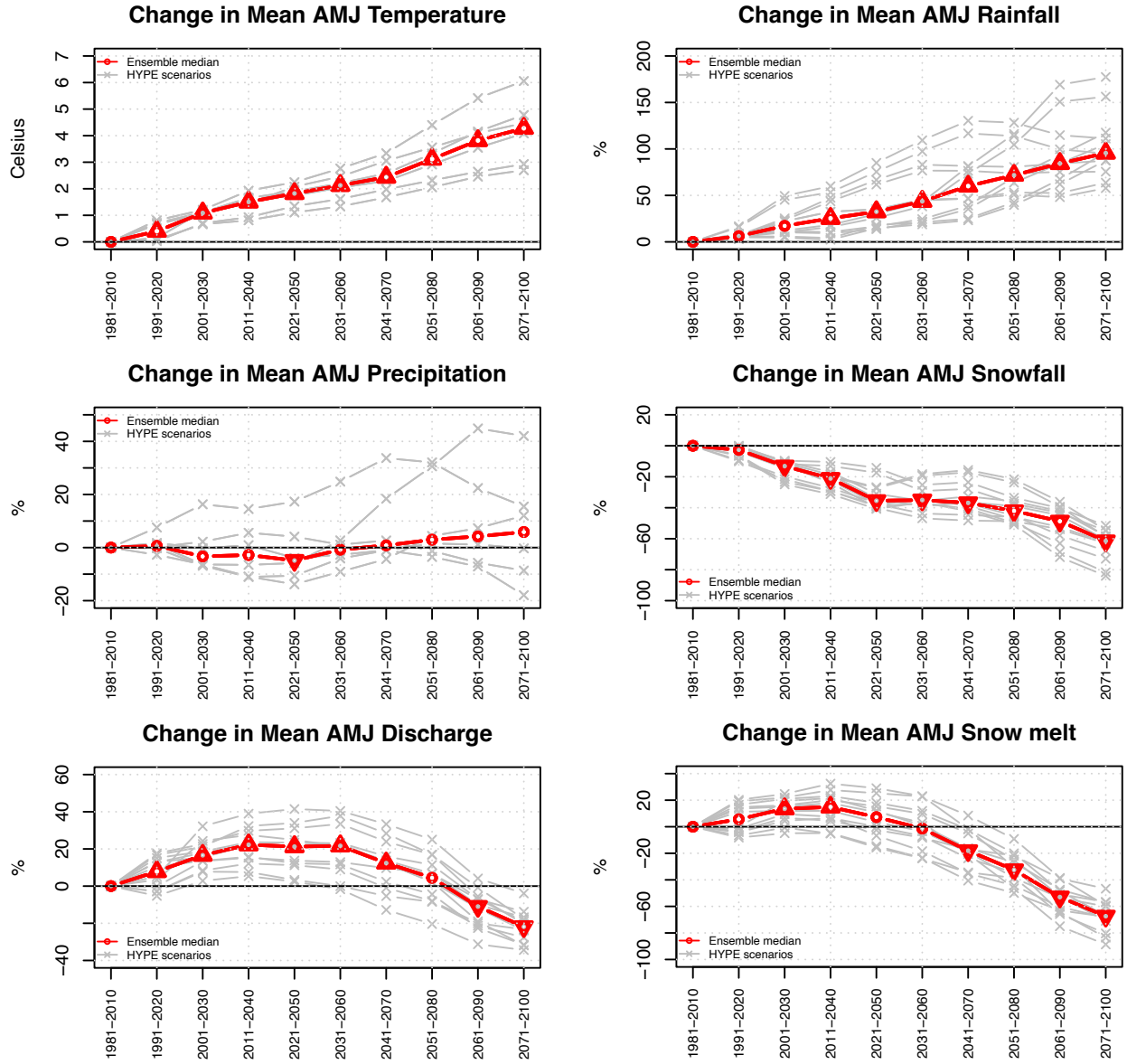

Fig. 32: Þverá catchment (vhm38): Projected changes in 30-year mean AMJ temperature, precipitation, rainfall, snowfall, snowmelt and river discharge under the RCP8.5 emission scenario, relative to the 1981-2010 reference period. Ensemble members (grey lines) and ensemble median (red line). The symbols on the ensemble median indicate whether the 30-year mean is projected to change significantly or to remain unchanged in future periods compared to the reference period, according to the Mann-Whitney test (triangle point-up=significant increase; triangle point down=significant decrease; open circle=no significant change).

RCP8.5

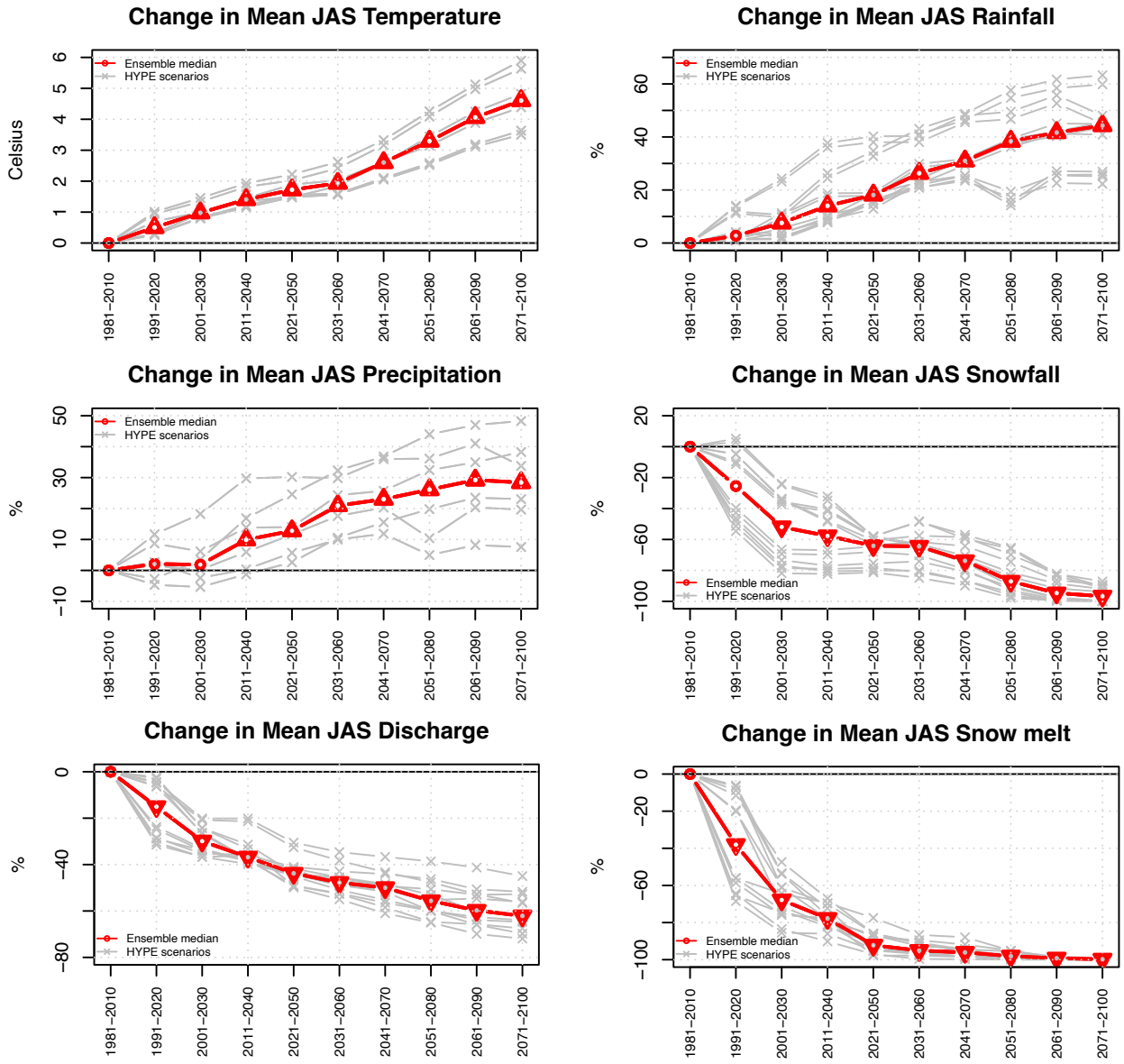

Fig. 33: Þverá catchment (vhm38): Projected changes in 30-year mean JAS temperature, precipitation, rainfall, snowfall, snowmelt and river discharge under the RCP8.5 emission scenario, relative to the 1981-2010 reference period. Ensemble members (grey lines) and ensemble median (red line). The symbols on the ensemble median indicate whether the 30-year mean is projected to change significantly or to remain unchanged in future periods compared to the reference period, according to the Mann-Whitney test (triangle point-up=significant increase; triangle point down=significant decrease; open circle=no significant change).

- **Markarfljót catchment (vhm218) (see also Appendix 9)**
  - Mean annual and seasonal near surface air temperatures are projected to progressively increase during the 21st century. A median warming of about +2.2°C to +2.4°C is projected from 1981-2010 to 2071-2100 under the RCP4.5 scenario and about +3.2°C to +4.6°C under the RCP8.5 scenario, depending on the season (see also Table 8).
  - No clear consensus is emerging regarding the direction of change in mean annual precipitation under the RCP4.5 emission scenario due to the presence of a large spread in the ensemble, leading the median change to remain close to zero, except in 2071-2100 where a small significant increase is projected. Mean annual precipitation is projected to oscillate around the reference level under the RCP8.5 emission scenario and a significant increase is projected in the early part of the 21st century only. The magnitude and direction of changes in mean seasonal precipitation vary greatly with the season and emission scenario. Under the RCP4.5 scenario, mean seasonal precipitation is projected to significantly decrease in JFM in a majority of projection time-windows depending on the amplitude of the oscillations, significantly increase in JAS until 2041-2070, whereas little or no change is projected in OND and AMJ in most projection periods. Under the RCP8.5 scenario, mean seasonal precipitation is mainly projected to significantly increase in JAS and OND and decrease in JFM, whereas little or no change is projected in AMJ.
  - The projected warming is expected to lead to an increase in mean seasonal rainfall and subsequently to a decrease in mean seasonal snowfall in all seasons, during the 21st century, under both emission scenarios. These changes are usually gradual, except for rainfall in AMJ under the RCP4.5 scenario and in JAS under the RCP8.5 scenario where the median increase becomes relatively stable from 2021-2050 until the end of the century. As these changes affect all seasons, the annual means are similarly impacted: Mean annual rainfall is projected to progressively increase whereas mean annual snowfall is projected to progressively decrease during the 21st century, under both emission scenarios.
  - Changes in mean annual snow and glacier melt are mainly driven by changes in mean annual snowmelt, which is projected to gradually decrease under both emission scenarios (cf. Appendix 9), owing to the reduction in snow storage caused by warming (cf. Fig. 16). Mean annual glacier melt is first projected to increase under both emission scenarios, following the increase in temperature, and latter decrease until the end of the 21st century because of the concomitant retreat of glaciers. The magnitude and direction of change in mean seasonal snow and glacier melt vary greatly with the season and emission scenario. Mean seasonal snowmelt is greater than glacier melt in OND, JFM and AMJ whereas in JAS, mean glacier melt is greater (not shown). Therefore, changes in mean seasonal snow and glacier melt are mainly driven by changes in mean seasonal snowmelt except in JAS where changes in mean glacier melt dominate. A significant increase in mean snow and glacier melt is projected in OND, especially in the first half of the 21st century, with a peak around 2021-2050, whereas little or no significant change is projected in the second-half of the 21st century, because the build-up of the snowpack will start later in the water-year due to the increase in temperature. A progressive increase in mean snow and glacier melt is projected in JFM under both

emission scenarios, mainly caused by an increase in mean snowmelt. Mean snow and glacier melt is projected to remain unchanged in AMJ until 2051-2080 under the RCP4.5 scenario and until 2031-2060 under the RCP8.5 scenario, and thereafter progressively decrease, owing to the decrease in both mean snowmelt and glacier melt. In JAS, mean snow and glacier melt is projected to progressively decrease under both emission scenarios, due to the snowpack reduction and the retreat of glaciers.

- Mean annual streamflow is projected to slightly increase under both emission scenarios but the spread of the ensemble increases with the projection horizon, making the outcome progressively more uncertain. The pattern of mean annual streamflow change resembles the pattern of mean annual precipitation change but is also influenced by changes in groundwater flow and glacier melt. At the seasonal level, the projections indicate a progressive increase in mean streamflow in OND and JFM, caused by the projected increase in rainfall and snowmelt; An increase in AMJ in the second half of the projection period under the RCP4.5 scenario, mainly caused by increased rainfall, an increase in the first-half of the 21st century under the RCP8.5 scenario caused by an increase in rainfall and glacier melt, followed by a return to the reference level and thereafter a decrease by the end of the century, caused by a decrease in snowmelt not balanced by the increase in rainfall; A progressive decrease in JAS, caused by the decrease in snow and glacier melt not balanced by the increase in rainfall. The changes in mean seasonal streamflow are often more severe and/or start earlier under the RCP8.5 emission scenario than under the RCP4.5 emission scenario because the projected warming is greater and its impact on the change in the phase of precipitation and on snow storage larger. The greatest median changes in mean seasonal streamflow projected in the 21st century have the following values:

  -RCP4.5: OND (+24%), JFM (+42%), AMJ (+12%), JAS (−21%)
  -RCP8.5: OND (+35%), JFM (+51%), AMJ (±8%), JAS (−26%)

Note that in practise, the retreat of glaciers could introduce some changes in the geometry and drainage area of this glaciated catchment. This aspect was not taken into consideration in the simulations and the drainage area was assumed to remain unchanged during the entire projection period. The uncertainty regarding this geometrical aspect may introduce some additional uncertainties in the hydro-climatic projections.

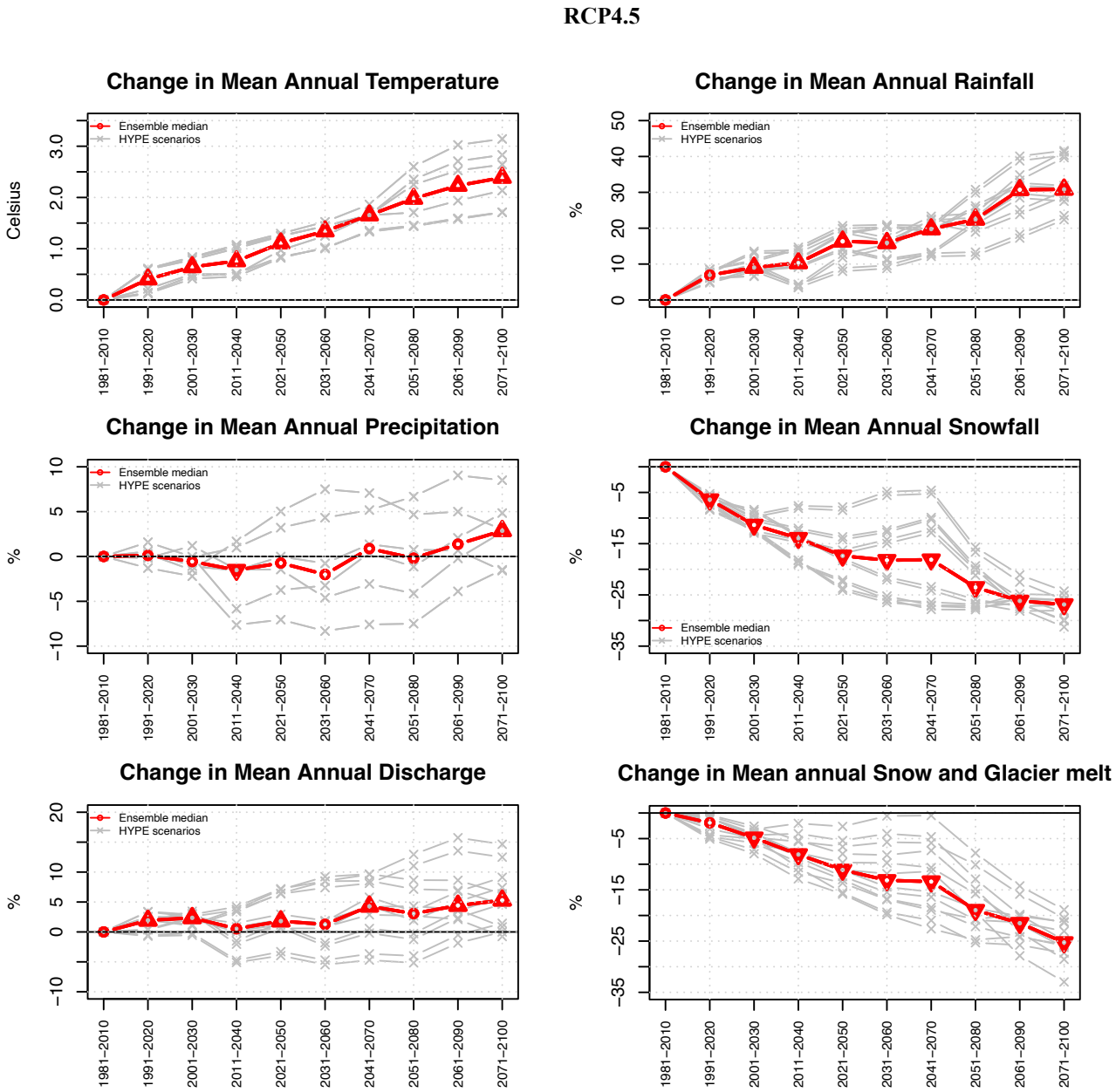

Fig. 34: Markarfljót catchment (vhm218): Projected changes in 30-year mean annual temperature, precipitation, rainfall, snowfall, snow and glacier melt and river discharge under the RCP4.5 emission scenario, relative to the 1981-2010 reference period. Ensemble members (grey lines) and ensemble median (red line). The symbols on the ensemble median indicate whether the 30-year mean is projected to change significantly or to remain unchanged in future periods compared to the reference period, according to the Mann-Whitney test (triangle point-up=significant increase; triangle point down=significant decrease; open circle=no significant change).

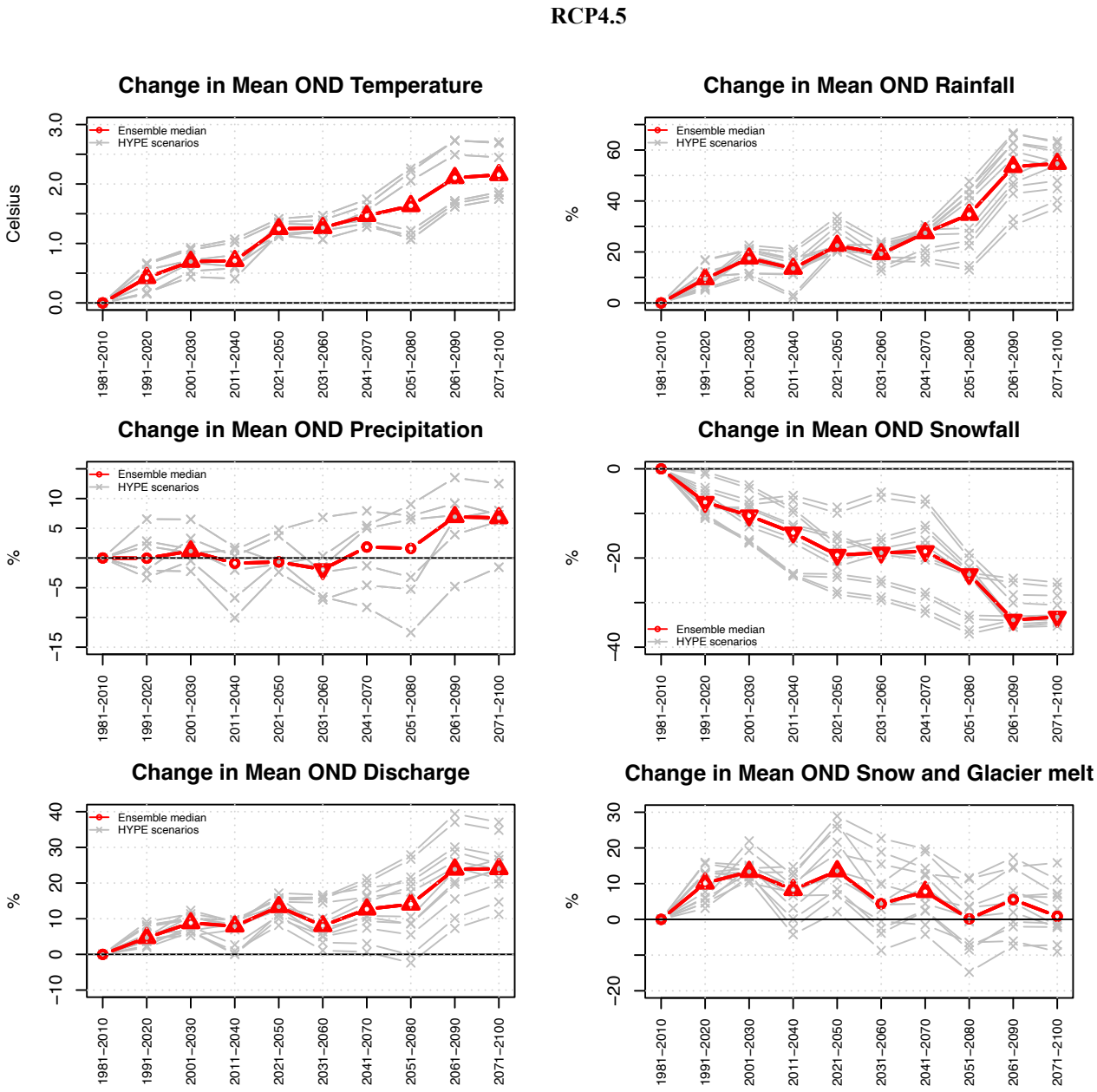

Fig. 35: Markarfljót catchment (vhm218): Projected changes in 30-year mean OND temperature, precipitation, rainfall, snowfall, snow and glacier melt and river discharge under the RCP4.5 emission scenario, relative to the 1981-2010 reference period. Ensemble members (grey lines) and ensemble median (red line). The symbols on the ensemble median indicate whether the 30-year mean is projected to change significantly or to remain unchanged in future periods compared to the reference period, according to the Mann-Whitney test (triangle point-up=significant increase; triangle point down=significant decrease; open circle=no significant change).

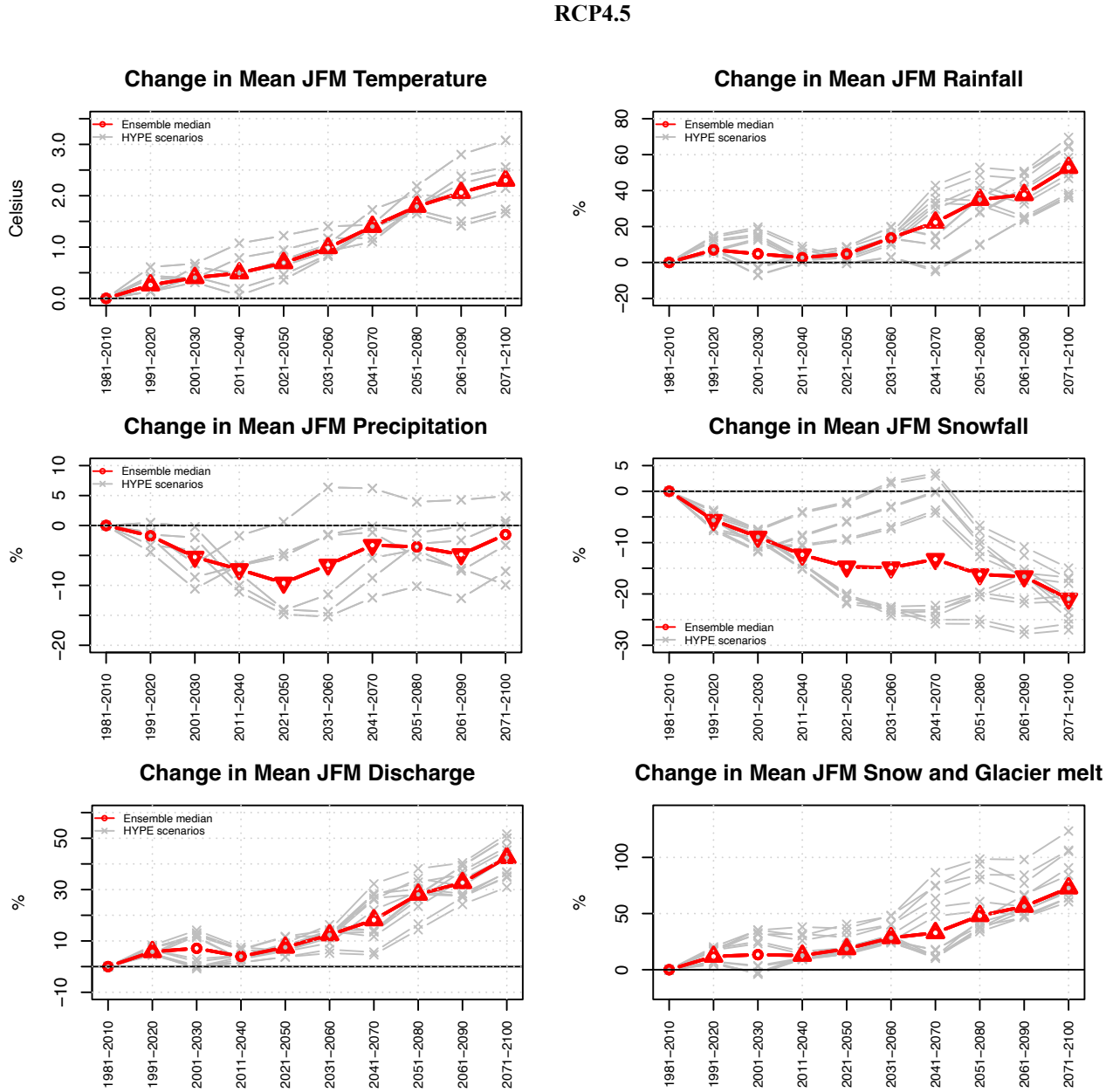

Fig. 36: Markarfljót catchment (vhm218): Projected changes in 30-year mean JFM temperature, precipitation, rainfall, snowfall, snow and glacier melt and river discharge under the RCP4.5 emission scenario, relative to the 1981-2010 reference period. Ensemble members (grey lines) and ensemble median (red line). The symbols on the ensemble median indicate whether the 30-year mean is projected to change significantly or to remain unchanged in future periods compared to the reference period, according to the Mann-Whitney test (triangle point-up=significant increase; triangle point down=significant decrease; open circle=no significant change).

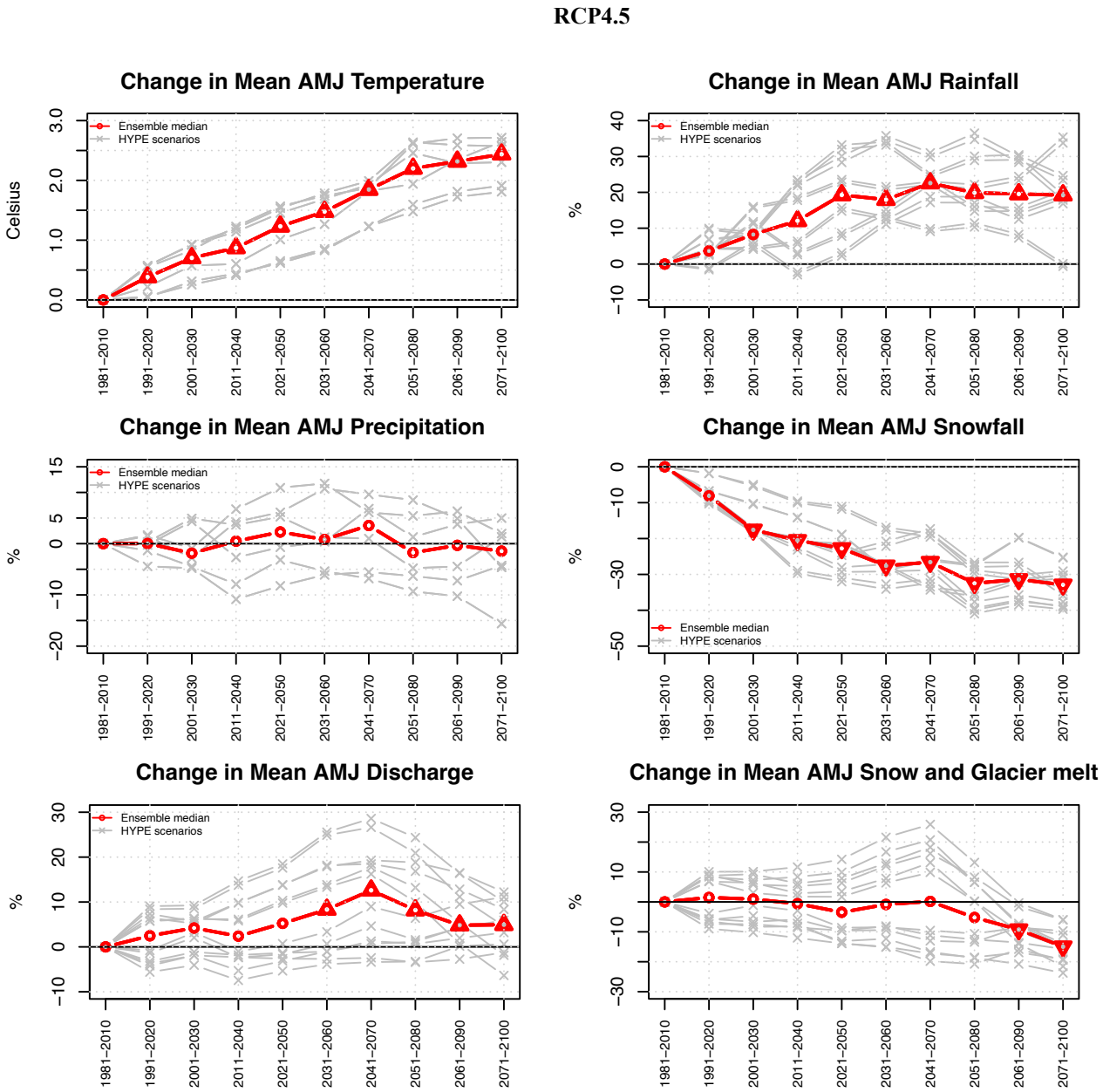

Fig. 37: Markarfljót catchment (vhm218): Projected changes in 30-year mean AMJ temperature, precipitation, rainfall, snowfall, snow and glacier melt and river discharge under the RCP4.5 emission scenario, relative to the 1981-2010 reference period. Ensemble members (grey lines) and ensemble median (red line). The symbols on the ensemble median indicate whether the 30-year mean is projected to change significantly or to remain unchanged in future periods compared to the reference period, according to the Mann-Whitney test (triangle point-up=significant increase; triangle point down=significant decrease; open circle=no significant change).

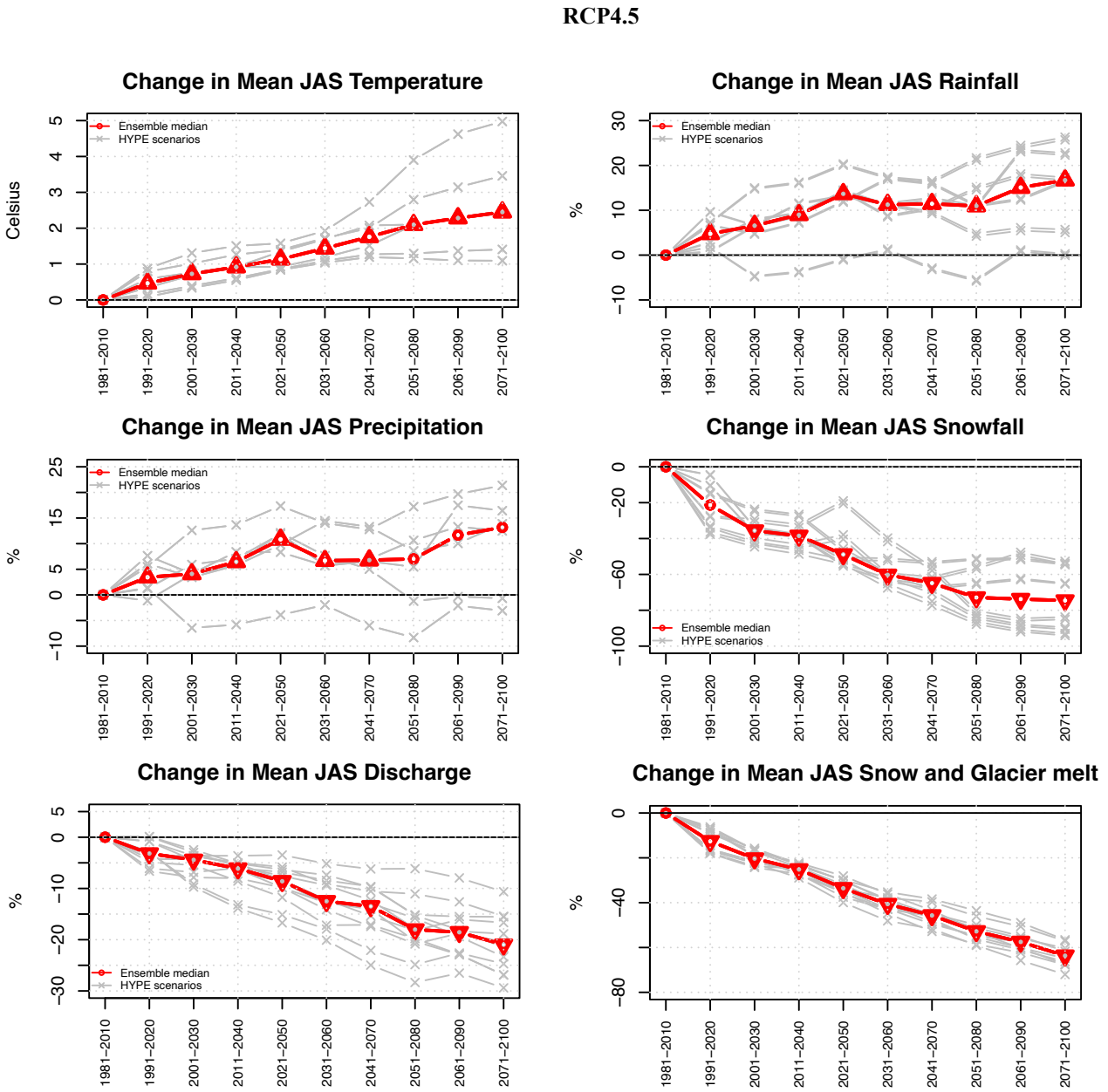

Fig. 38: Markarfljót catchment (vhm218): Projected changes in 30-year mean JAS temperature, precipitation, rainfall, snowfall, snow and glacier melt and river discharge under the RCP4.5 emission scenario, relative to the 1981-2010 reference period. Ensemble members (grey lines) and ensemble median (red line). The symbols on the ensemble median indicate whether the 30-year mean is projected to change significantly or to remain unchanged in future periods compared to the reference period, according to the Mann-Whitney test (triangle point-up=significant increase; triangle point down=significant decrease; open circle=no significant change).

RCP8.5

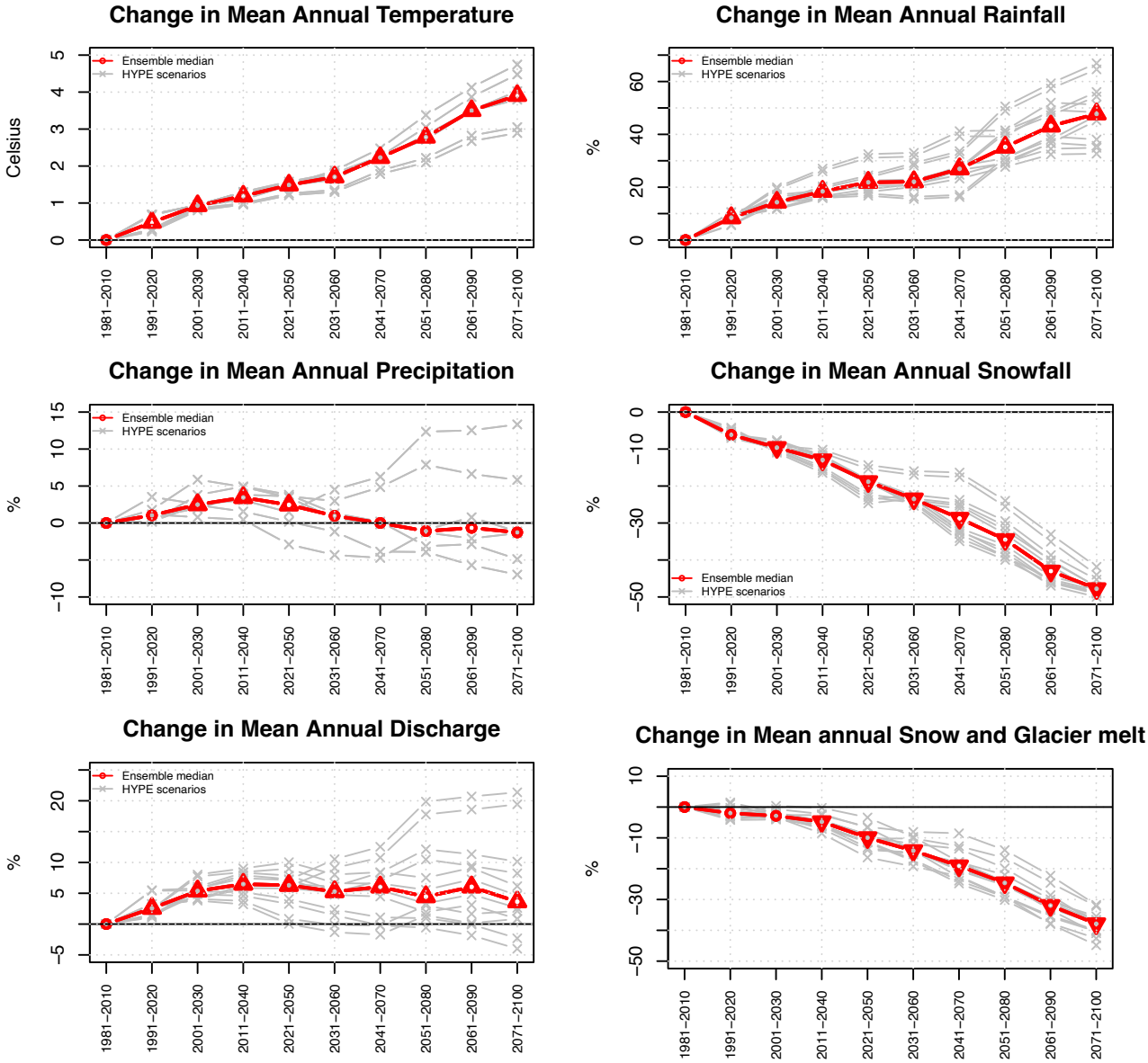

Fig. 39: Markarfljót catchment (vhm218): Projected changes in 30-year mean annual temperature, precipitation, rainfall, snowfall, snow and glacier melt and river discharge under the RCP8.5 emission scenario, relative to the 1981-2010 reference period. Ensemble members (grey lines) and ensemble median (red line). The symbols on the ensemble median indicate whether the 30-year mean is projected to change significantly or to remain unchanged in future periods compared to the reference period, according to the Mann-Whitney test (triangle point-up=significant increase; triangle point down=significant decrease; open circle=no significant change).

RCP8.5

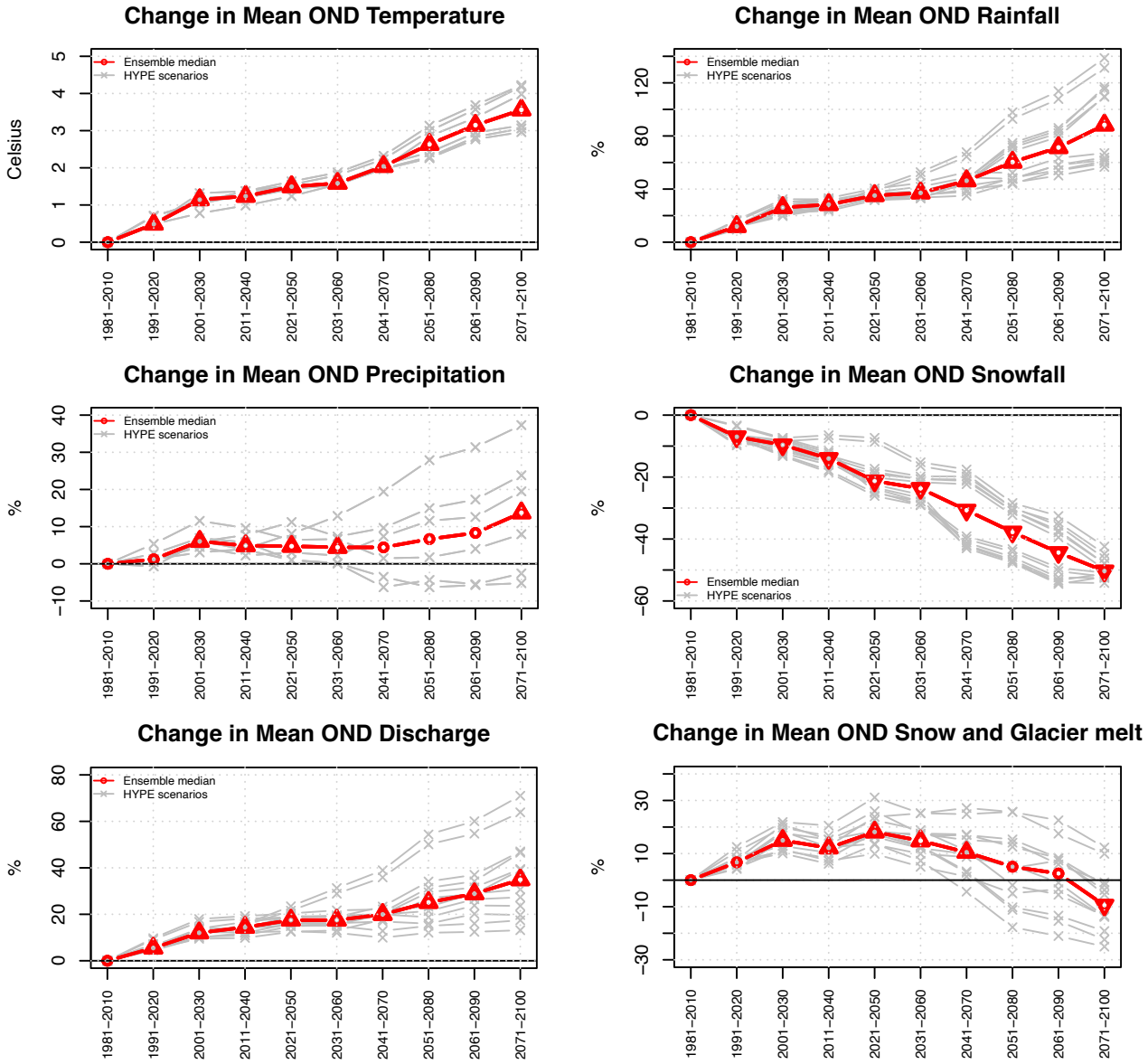

Fig. 40: Markarfljót catchment (vhm218): Projected changes in 30-year mean OND temperature, precipitation, rainfall, snowfall, snow and glacier melt and river discharge under the RCP8.5 emission scenario, relative to the 1981-2010 reference period. Ensemble members (grey lines) and ensemble median (red line). The symbols on the ensemble median indicate whether the 30-year mean is projected to change significantly or to remain unchanged in future periods compared to the reference period, according to the Mann-Whitney test (triangle point-up=significant increase; triangle point down=significant decrease; open circle=no significant change).

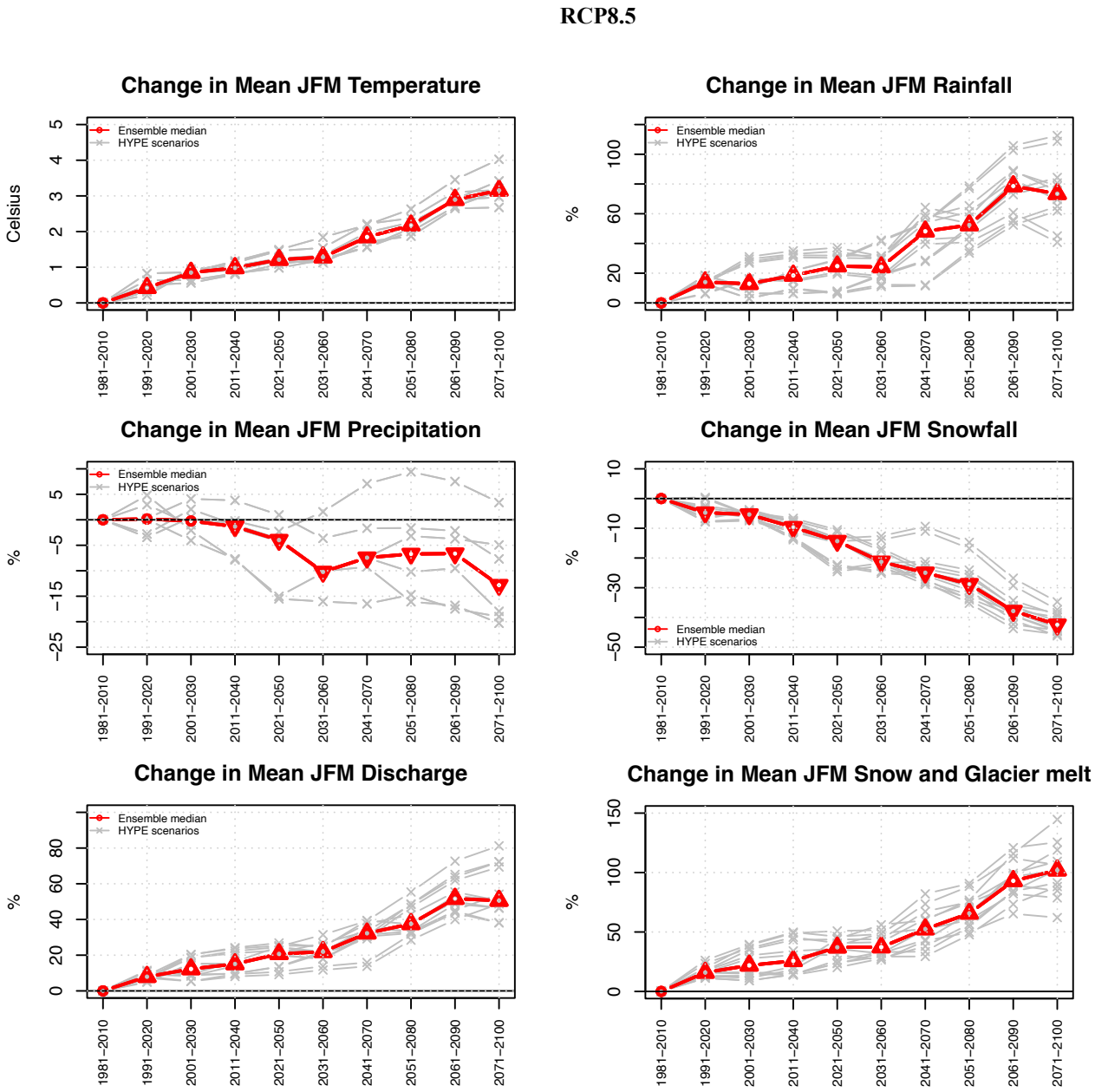

Fig. 41: Markarfljót catchment (vhm218): Projected changes in 30-year mean JFM temperature, precipitation, rainfall, snowfall, snow and glacier melt and river discharge under the RCP8.5 emission scenario, relative to the 1981-2010 reference period. Ensemble members (grey lines) and ensemble median (red line). The symbols on the ensemble median indicate whether the 30-year mean is projected to change significantly or to remain unchanged in future periods compared to the reference period, according to the Mann-Whitney test (triangle point-up=significant increase; triangle point down=significant decrease; open circle=no significant change).

RCP8.5

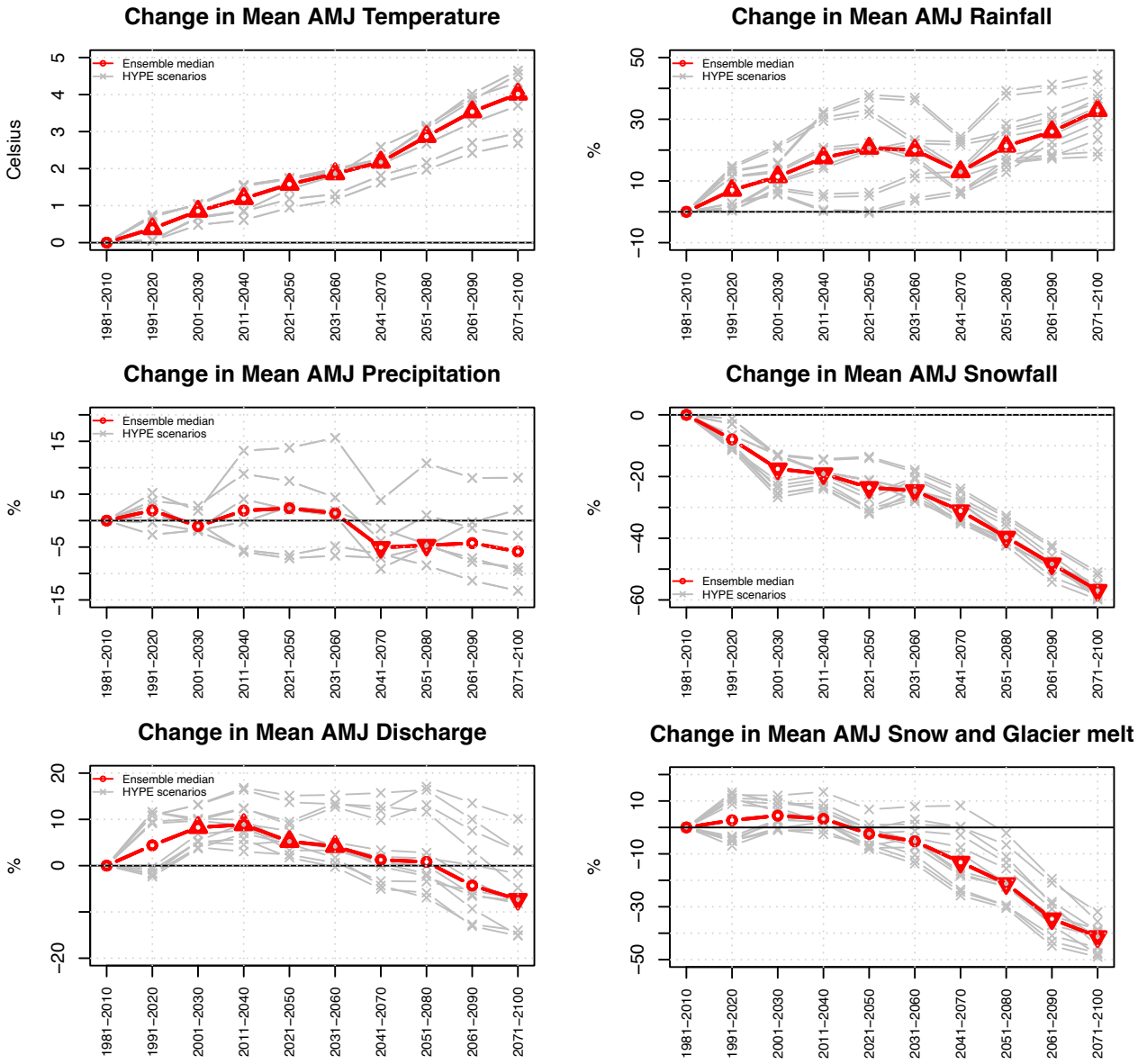

Fig. 42: Markarfljót catchment (vhm218): Projected changes in 30-year mean AMJ temperature, precipitation, rainfall, snowfall, snow and glacier melt and river discharge under the RCP8.5 emission scenario, relative to the 1981-2010 reference period. Ensemble members (grey lines) and ensemble median (red line). The symbols on the ensemble median indicate whether the 30-year mean is projected to change significantly or to remain unchanged in future periods compared to the reference period, according to the Mann-Whitney test (triangle point-up=significant increase; triangle point down=significant decrease; open circle=no significant change).

RCP8.5

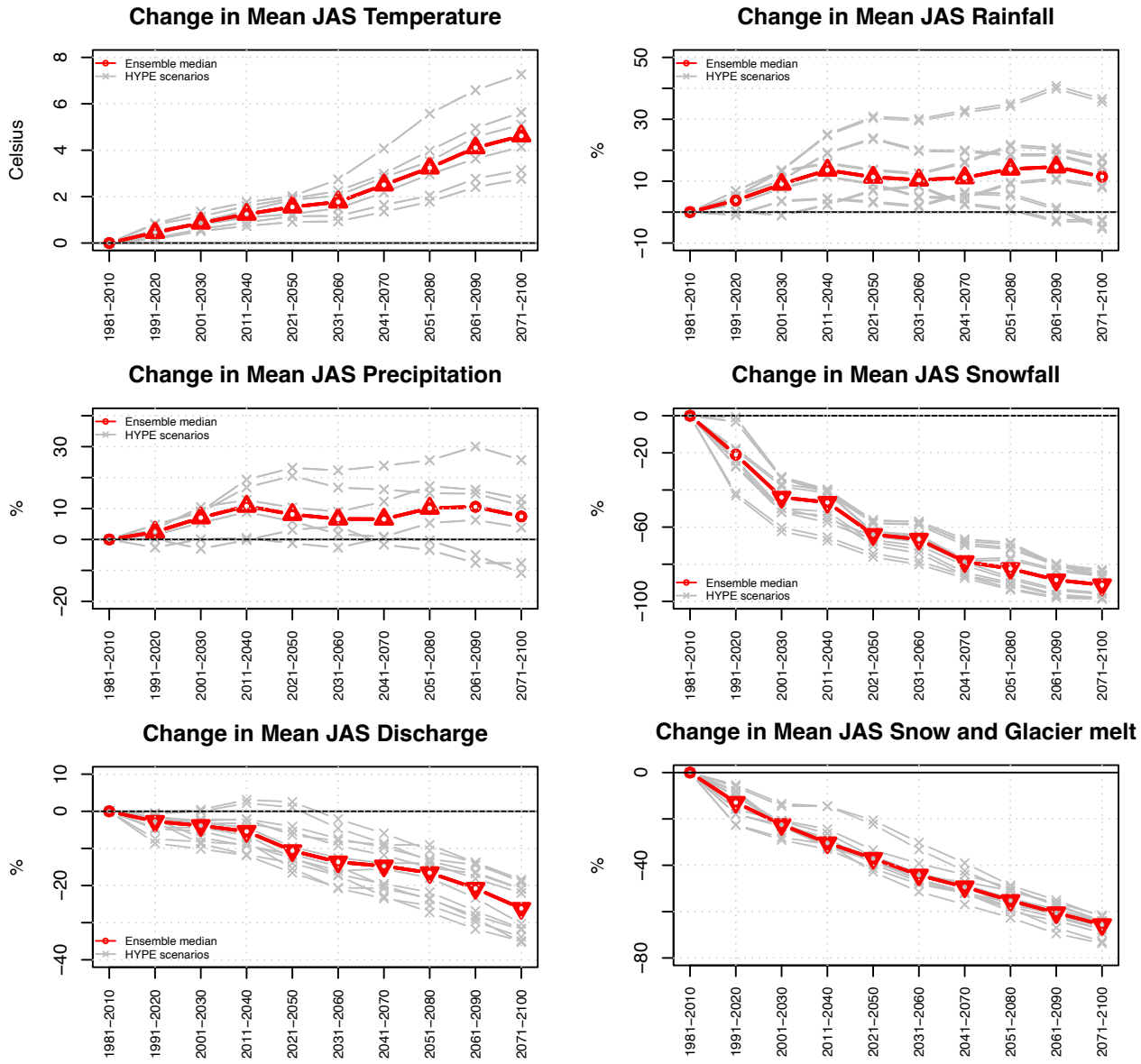

Fig. 43: Markarfljót catchment (vhm218): Projected changes in 30-year mean JAS temperature, precipitation, rainfall, snowfall, snow and glacier melt and river discharge under the RCP8.5 emission scenario, relative to the 1981-2010 reference period. Ensemble members (grey lines) and ensemble median (red line). The symbols on the ensemble median indicate whether the 30-year mean is projected to change significantly or to remain unchanged in future periods compared to the reference period, according to the Mann-Whitney test (triangle point-up=significant increase; triangle point down=significant decrease; open circle=no significant change).

- **Kreppa catchment (vhm233) (see also Appendix 10)**
  - Mean annual and seasonal near surface air temperatures are projected to rise during the 21st century. A median warming of about +2.3°C to +2.7°C is projected from 1981-2010 to 2071-2100 under the RCP4.5 scenario and about +3.6°C to +5.1°C under the RCP8.5 scenario, depending on the season (see also Table 8).
  - Mean annual precipitation is projected to increase in most projection periods under both emission scenarios but with some oscillations. A large ensemble spread increasing with the projection horizon is also observed. Mean seasonal precipitation is projected to increase in OND, remain unchanged in JFM, and oscillate around the reference level in AMJ and JAS with or without significant increase, depending on the phase and amplitude of these oscillations. The lack of consistency in the direction of change of individual members in JFM and also AMJ makes it difficult to draw any robust conclusion regarding the ensemble.
  - The rise in temperature leads to an increase in mean annual rainfall and a decrease in mean annual snowfall. At the seasonal level, changes in mean rainfall and snowfall vary according to changes in mean precipitation and temperature. Mean seasonal rainfall is projected to increase in OND, AMJ and JAS over the course of the 21st century under both emission scenarios, whereas in JFM, an increase is projected from 2051-2080 until the end of the century under the RCP4.5 scenario, and from 2021-2050 until the end of the century under the RCP8.5 scenario. Mean seasonal snowfall is projected to gradually decrease during the 21st century under both emission scenarios in JAS, decrease more or less early in OND and AMJ, depending on the emission scenario, whereas no change is projected in JFM under both emission scenarios because of the large ensemble spread and the lack of consensus among the ensemble members.
  - Mean annual glacier melt is greater than snowmelt (not shown), owing to the large glacier coverage in this catchment, therefore changes in mean annual snow and glacier melt are mainly driven by changes in mean annual glacier melt, which is projected to increase during the 21st century under both emission scenarios with a peak around 2051-2080/2061-2090 (cf. Appendix 10). Mean annual snowmelt is projected to increase in a progressive manner, due to the increase in snow storage (outside the glacier) caused by the increase in land area concomitant with the glacier retreat (not shown). Mean seasonal snow and glacier melt is projected to increase more or less progressively in all seasons under both emission scenarios, owing to an increase in both mean snowmelt and glacier melt (except snowmelt in JAS under RCP8.5 where no change is projected). In OND and AMJ, mean snowmelt and glacier melt are often of the same order of magnitude whereas in JFM, mean snowmelt is greater than mean glacier melt and in JAS, mean glacier melt is greater than mean snowmelt (not shown). The largest mean snow and glacier melt in the year occurs in JAS, mainly caused by glacier melt. A peak of mean glacier melt increase in JAS is projected around 2051-2080 / 2061-2090 (cf. Appendix 10), explaining also the peak in mean annual snow and glacier melt increase in Figs. 44 and 49.
  - Mean annual streamflow is projected to continuously increase during the 21st century under both emission scenarios, with a peak around 2051-2080 / 2061-2090, in line with the

projected increase in mean annual glacier melt. Mean seasonal streamflow is projected to progressively increase during the 21st century in all seasons, owing to the combined increase in rainfall, snow and glacier melt. According to the simulations, the order of the dominant processes causing the increase in mean seasonal streamflow varies with the season, future time-window and emission scenario (increase in rainfall, glacier melt and snowmelt in OND; increase in rainfall and snowmelt in JFM; increase in glacier melt, rainfall and snowmelt in AMJ; increase in glacier melt and rainfall in JAS). The increase in mean seasonal streamflow is usually greater under the RCP8.5 emission scenario than under the RCP4.5 emission scenario because the projected warming is greater and has a larger impact on the changes in the phase of precipitation, in snow storage and glacier melt. The greatest median changes in mean seasonal streamflow projected in the 21st century have the following values:

- RCP4.5: OND (+78%), JFM (+78%), AMJ (+40%), JAS (+29%)
- RCP8.5: OND (+138%), JFM (+117%), AMJ (+65%), JAS (+48%)

Note that in practise, the retreat of glaciers could introduce some changes in the geometry and drainage area of this glaciated catchment. This aspect was not taken into consideration in the simulations and the drainage area was assumed to remain unchanged during the entire projection period. The uncertainty regarding this geometrical aspect may introduce some additional uncertainties in the hydro-climatic projections.

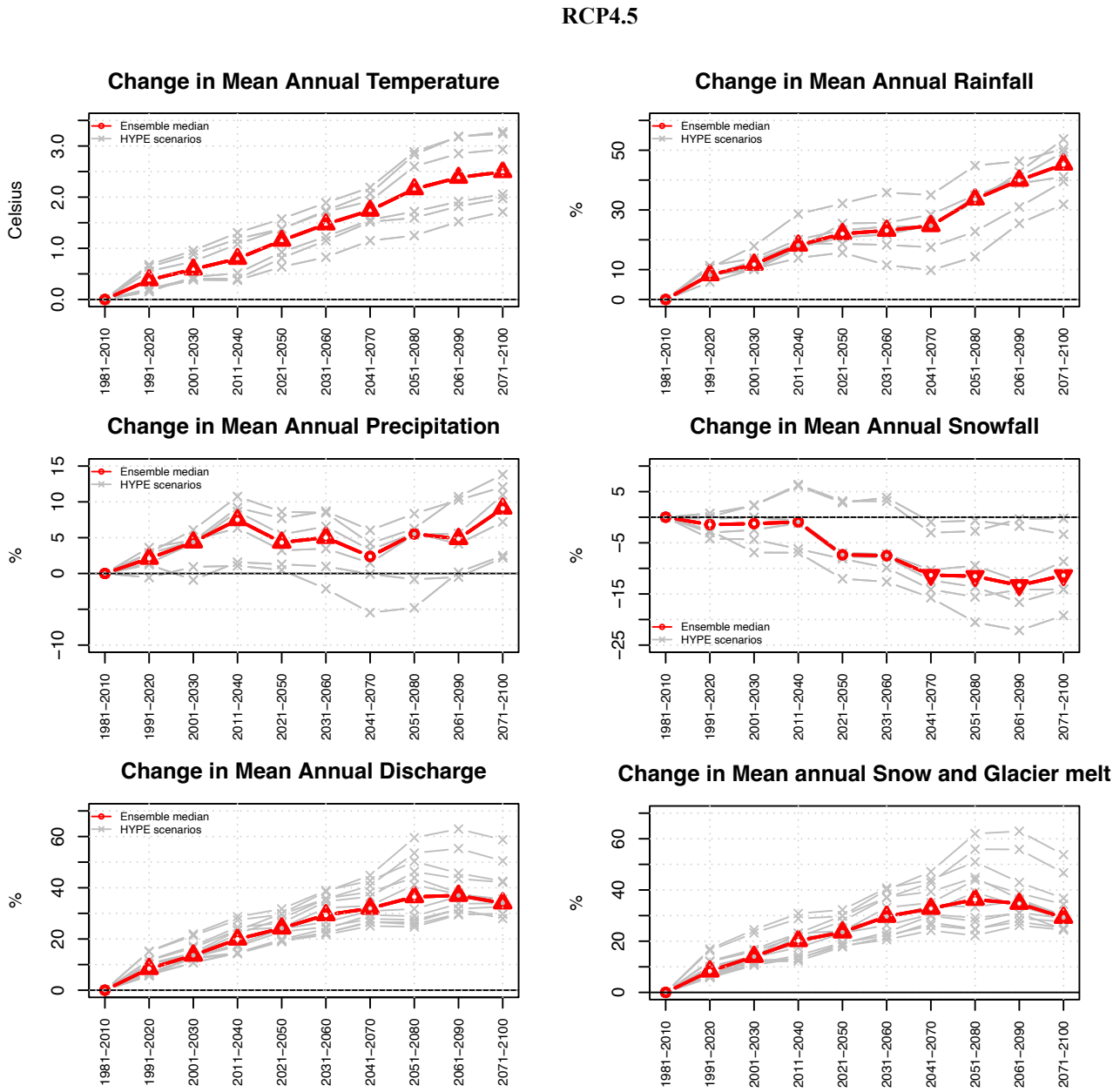

Fig. 44: Kreppa catchment (vhm233): Projected changes in 30-year mean annual temperature, precipitation, rainfall, snowfall, snow and glacier melt and river discharge under the RCP4.5 emission scenario, relative to the 1981-2010 reference period. Ensemble members (grey lines) and ensemble median (red line). The symbols on the ensemble median indicate whether the 30-year mean is projected to change significantly or to remain unchanged in future periods compared to the reference period, according to the Mann-Whitney test (triangle point-up=significant increase; triangle point down=significant decrease; open circle=no significant change).

RCP4.5

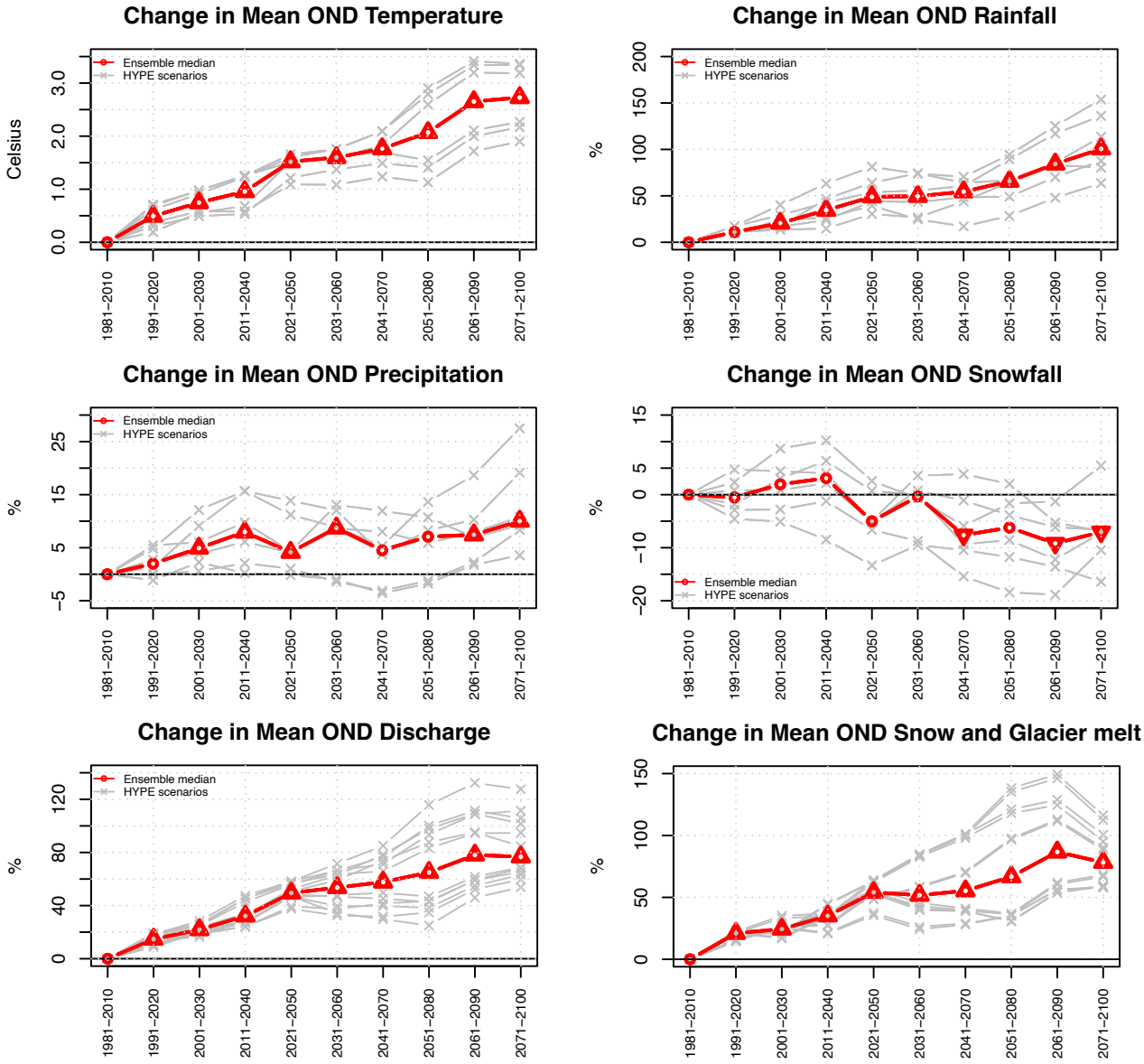

Fig. 45: Kreppa catchment (vhm233): Projected changes in 30-year mean OND temperature, precipitation, rainfall, snowfall, snow and glacier melt and river discharge under the RCP4.5 emission scenario, relative to the 1981-2010 reference period. Ensemble members (grey lines) and ensemble median (red line). The symbols on the ensemble median indicate whether the 30-year mean is projected to change significantly or to remain unchanged in future periods compared to the reference period, according to the Mann-Whitney test (triangle point-up=significant increase; triangle point down=significant decrease; open circle=no significant change).

RCP4.5

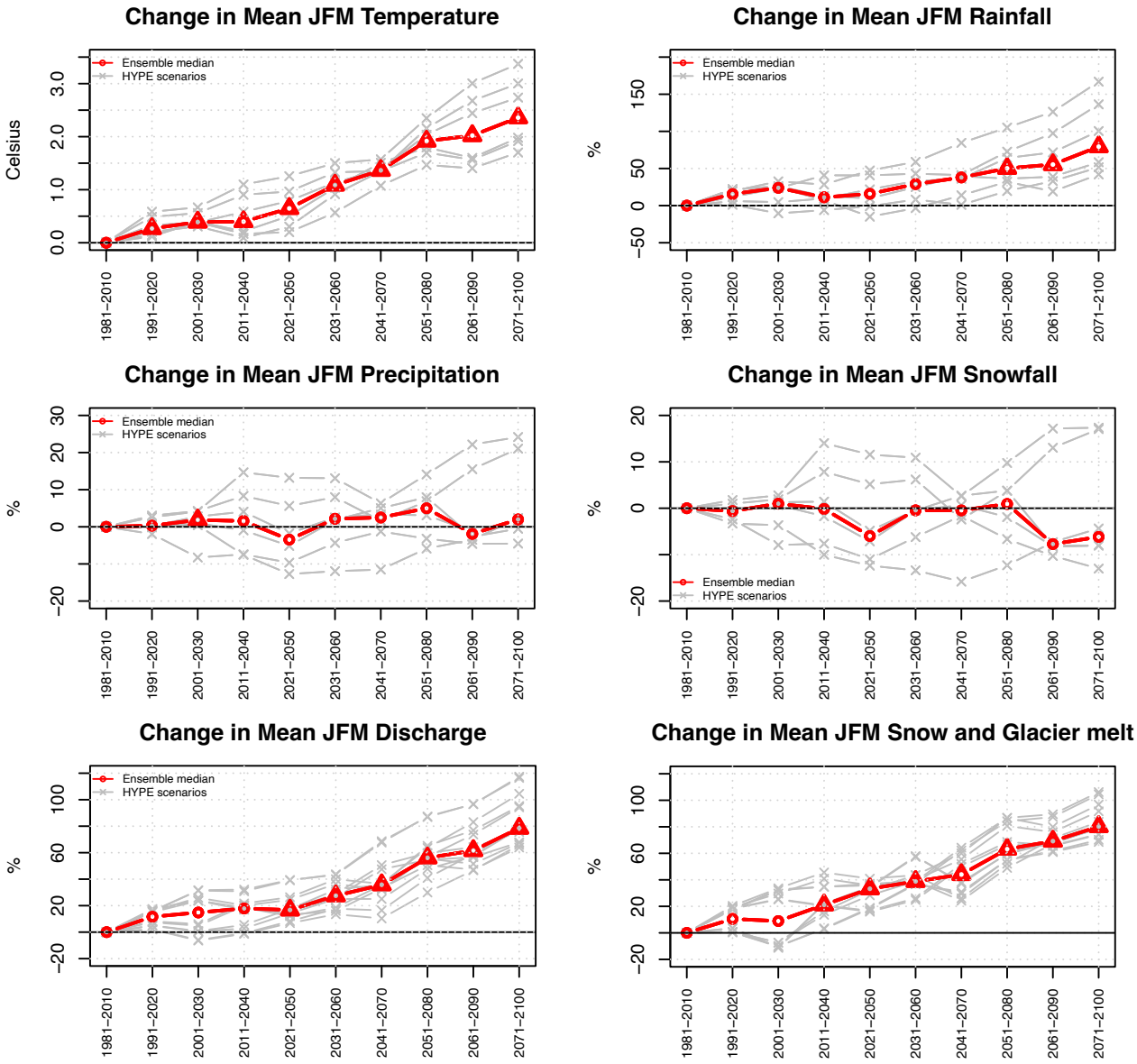

Fig. 46: Kreppa catchment (vhm233): Projected changes in 30-year mean JFM temperature, precipitation, rainfall, snowfall, snow and glacier melt and river discharge under the RCP4.5 emission scenario, relative to the 1981-2010 reference period. Ensemble members (grey lines) and ensemble median (red line). The symbols on the ensemble median indicate whether the 30-year mean is projected to change significantly or to remain unchanged in future periods compared to the reference period, according to the Mann-Whitney test (triangle point-up=significant increase; triangle point down=significant decrease; open circle=no significant change).

RCP4.5

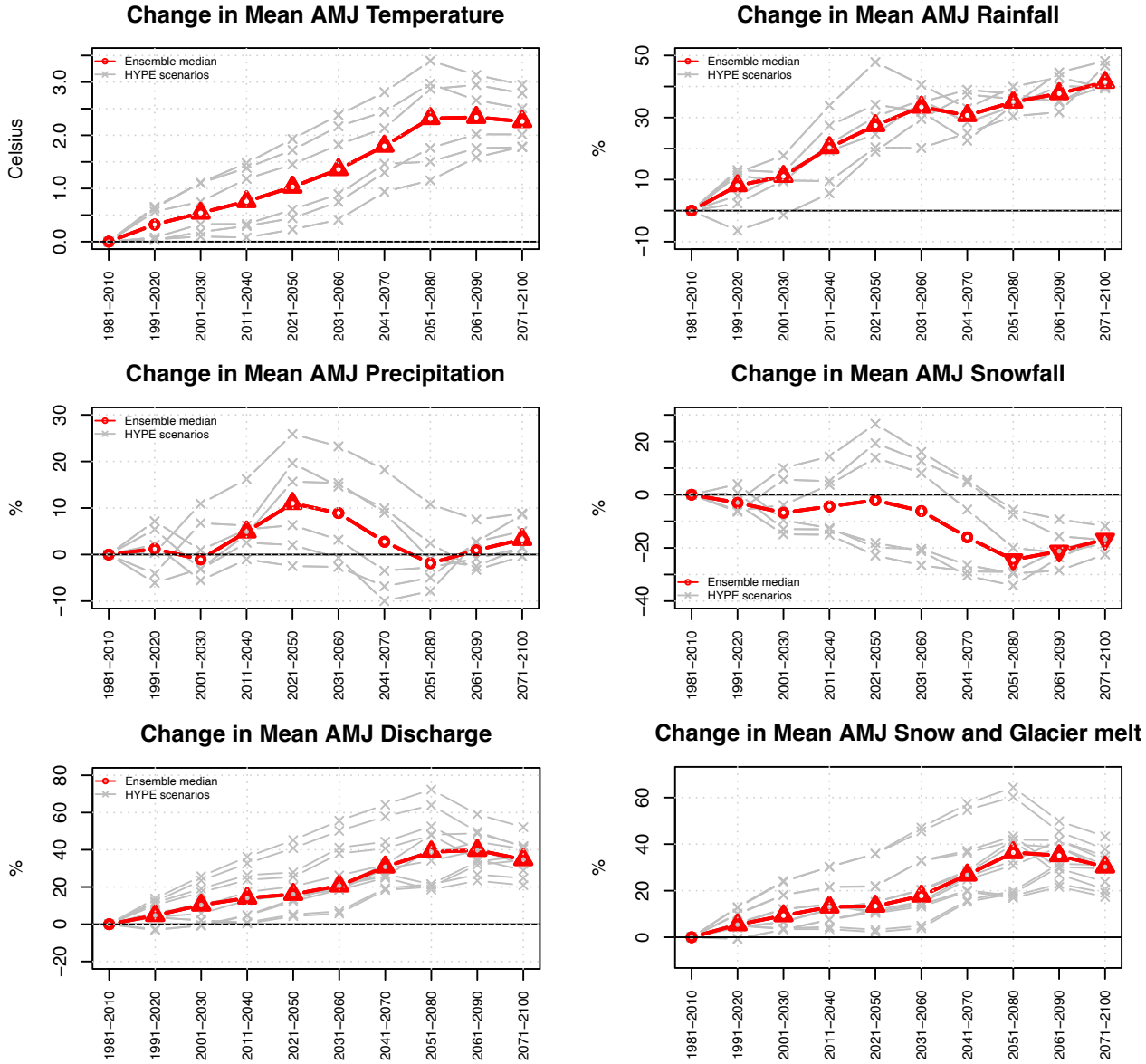

Fig. 47: Kreppa catchment (vhm233): Projected changes in 30-year mean AMJ temperature, precipitation, rainfall, snowfall, snow and glacier melt and river discharge under the RCP4.5 emission scenario, relative to the 1981-2010 reference period. Ensemble members (grey lines) and ensemble median (red line). The symbols on the ensemble median indicate whether the 30-year mean is projected to change significantly or to remain unchanged in future periods compared to the reference period, according to the Mann-Whitney test (triangle point-up=significant increase; triangle point down=significant decrease; open circle=no significant change).

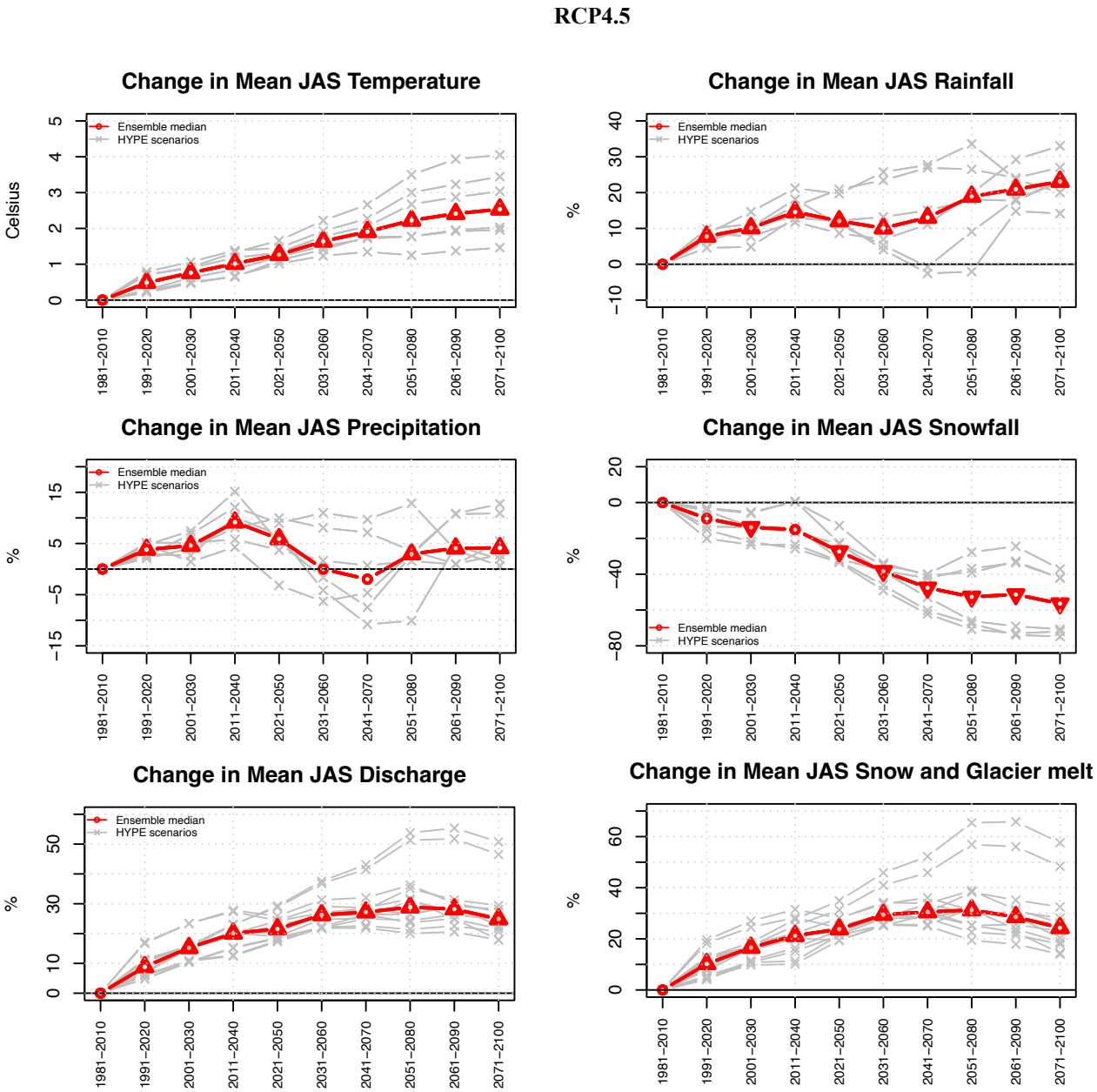

Fig. 48: Kreppa catchment (vhm233): Projected changes in 30-year mean JAS temperature, precipitation, rainfall, snowfall, snow and glacier melt and river discharge under the RCP4.5 emission scenario, relative to the 1981-2010 reference period. Ensemble members (grey lines) and ensemble median (red line). The symbols on the ensemble median indicate whether the 30-year mean is projected to change significantly or to remain unchanged in future periods compared to the reference period, according to the Mann-Whitney test (triangle point-up=significant increase; triangle point down=significant decrease; open circle=no significant change).

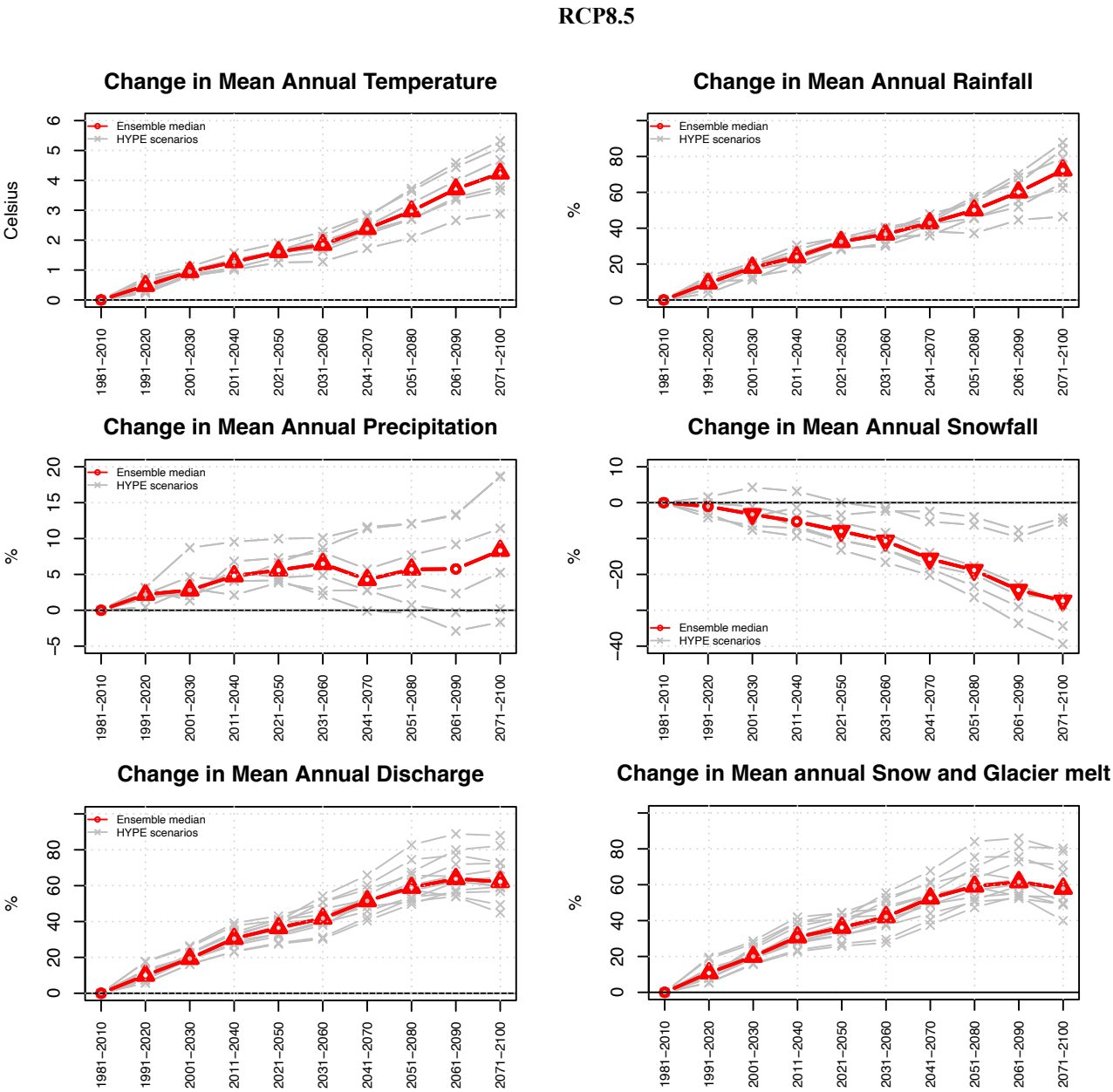

Fig. 49: Kreppa catchment (vhm233): Projected changes in 30-year mean annual temperature, precipitation, rainfall, snowfall, snow and glacier melt and river discharge under the RCP8.5 emission scenario, relative to the 1981-2010 reference period. Ensemble members (grey lines) and ensemble median (red line). The symbols on the ensemble median indicate whether the 30-year mean is projected to change significantly or to remain unchanged in future periods compared to the reference period, according to the Mann-Whitney test (triangle point-up=significant increase; triangle point down=significant decrease; open circle=no significant change).

RCP8.5

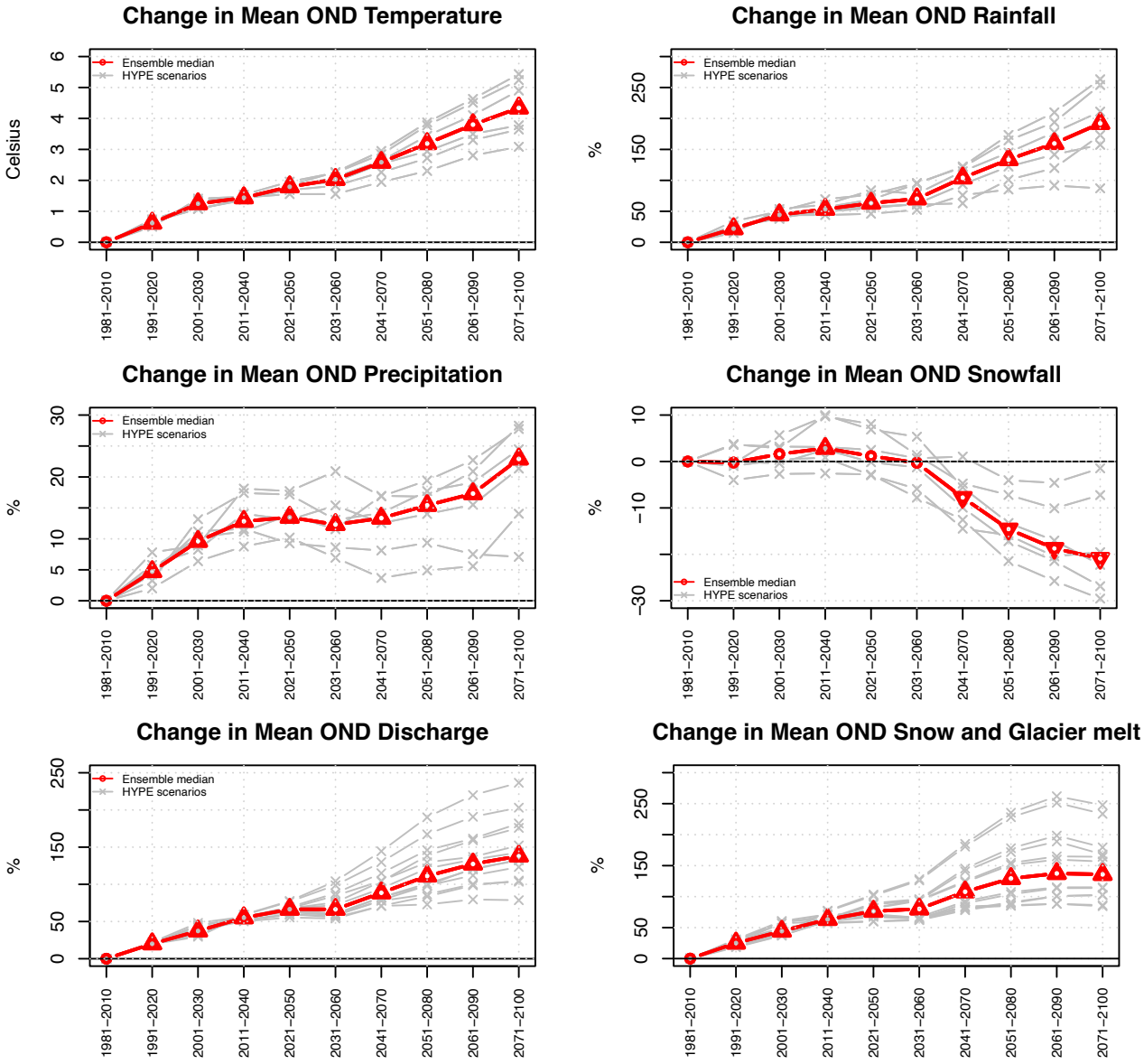

Fig. 50: Kreppa catchment (vhm233): Projected changes in 30-year mean OND temperature, precipitation, rainfall, snowfall, snow and glacier melt and river discharge under the RCP8.5 emission scenario, relative to the 1981-2010 reference period. Ensemble members (grey lines) and ensemble median (red line). The symbols on the ensemble median indicate whether the 30-year mean is projected to change significantly or to remain unchanged in future periods compared to the reference period, according to the Mann-Whitney test (triangle point-up=significant increase; triangle point down=significant decrease; open circle=no significant change).

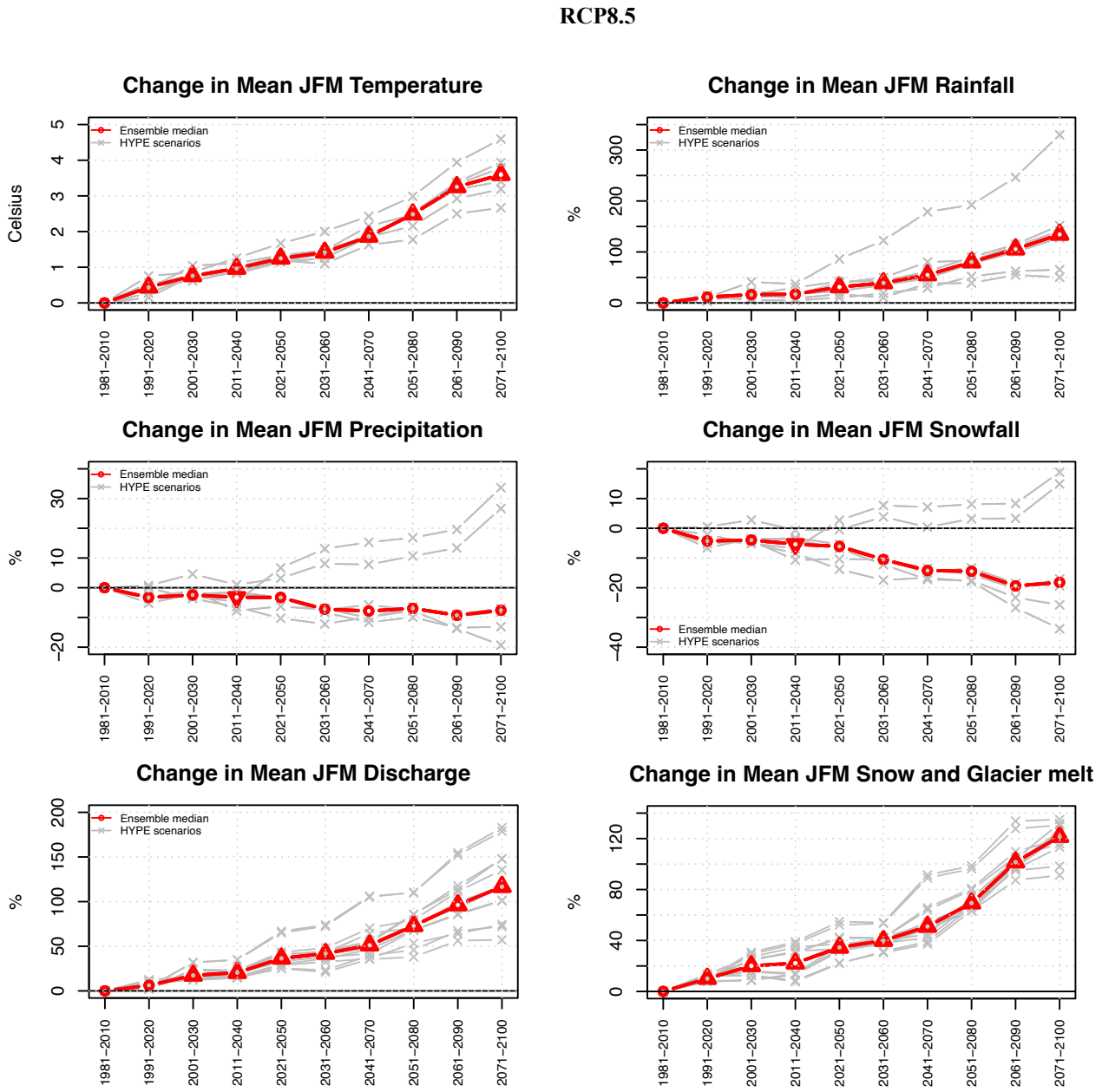

Fig. 51: Kreppa catchment (vhm233): Projected changes in 30-year mean JFM temperature, precipitation, rainfall, snowfall, snow and glacier melt and river discharge under the RCP8.5 emission scenario, relative to the 1981-2010 reference period. Ensemble members (grey lines) and ensemble median (red line). The symbols on the ensemble median indicate whether the 30-year mean is projected to change significantly or to remain unchanged in future periods compared to the reference period, according to the Mann-Whitney test (triangle point-up=significant increase; triangle point down=significant decrease; open circle=no significant change).

RCP8.5

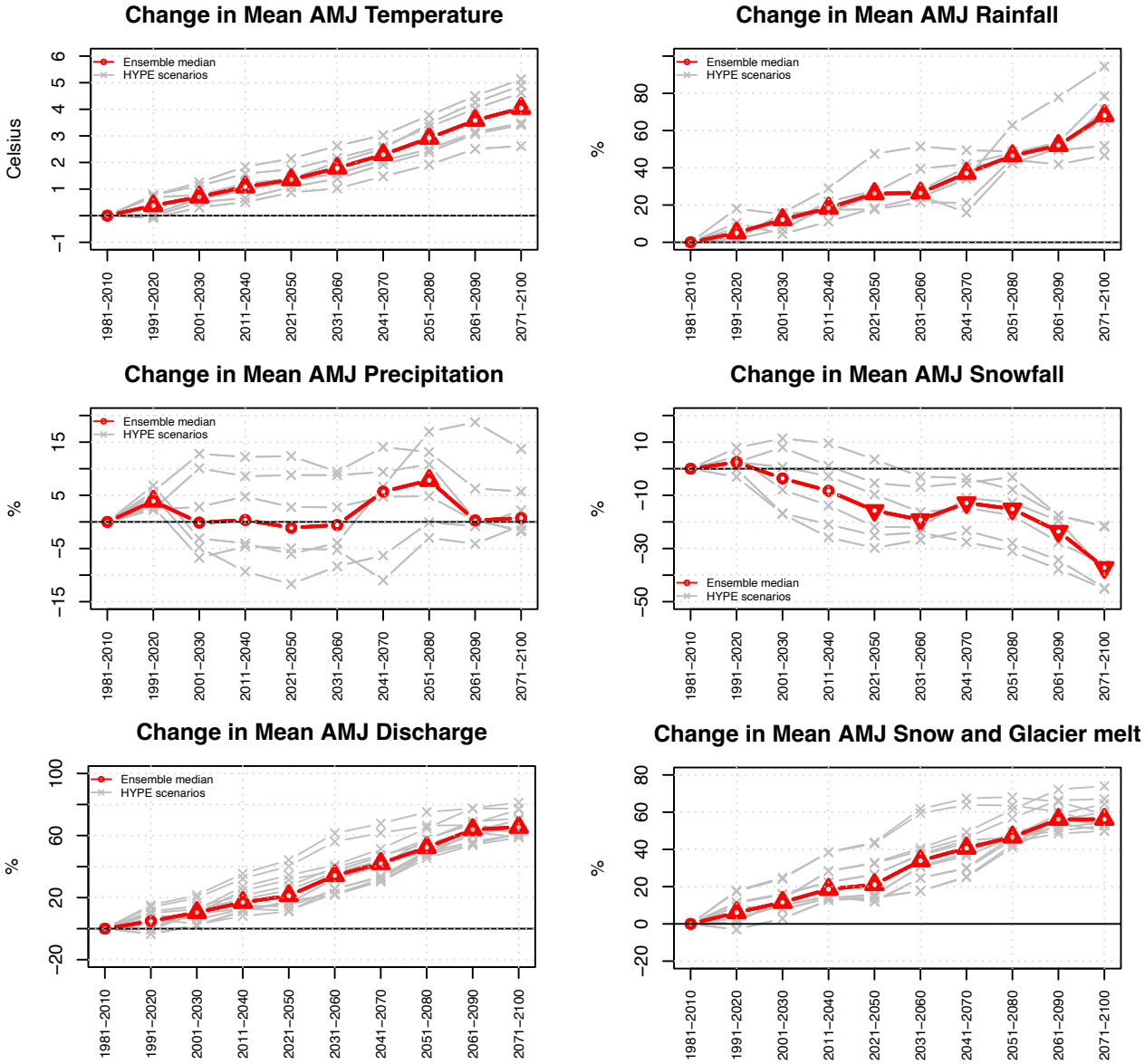

Fig. 52: Kreppa catchment (vhm233): Projected changes in 30-year mean AMJ temperature, precipitation, rainfall, snowfall, snow and glacier melt and river discharge under the RCP8.5 emission scenario, relative to the 1981-2010 reference period. Ensemble members (grey lines) and ensemble median (red line). The symbols on the ensemble median indicate whether the 30-year mean is projected to change significantly or to remain unchanged in future periods compared to the reference period, according to the Mann-Whitney test (triangle point-up=significant increase; triangle point down=significant decrease; open circle=no significant change).

RCP8.5

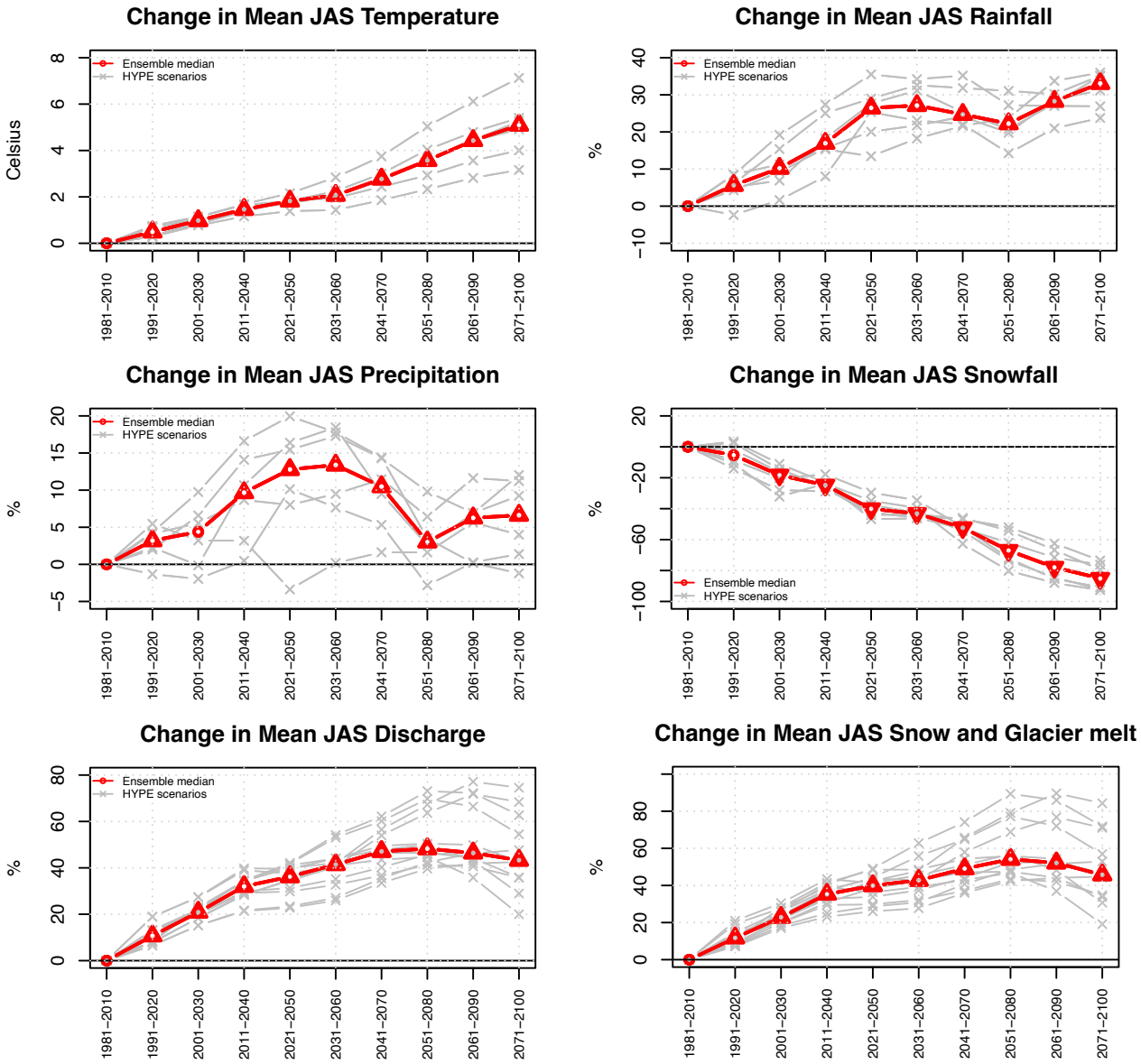

Fig. 53: Kreppa catchment (vhm233): Projected changes in 30-year mean JAS temperature, precipitation, rainfall, snowfall, snow and glacier melt and river discharge under the RCP8.5 emission scenario, relative to the 1981-2010 reference period. Ensemble members (grey lines) and ensemble median (red line). The symbols on the ensemble median indicate whether the 30-year mean is projected to change significantly or to remain unchanged in future periods compared to the reference period, according to the Mann-Whitney test (triangle point-up=significant increase; triangle point down=significant decrease; open circle=no significant change).

6-2-3 Summary and discussion

A progressive warming is projected in the 21st century, in all seasons and catchments. As expected, a greater warming is projected under the RCP8.5 emission scenario than under the RCP4.5 emission scenario. Some spatial variations are also observed in each season. The lowest warming rate is projected in the south (Markarfljót catchment) and the highest one in the northwest (Þverá catchment), on average over all months.

Mean seasonal precipitation is projected to increase in JAS and OND in the three studied catchments and this increase is usually more pronounced under the RCP8.5 scenario, which is also the warmest one. Mean seasonal precipitation projections are also characterised by oscillations reflecting long-term natural climate variability. However, the different precipitation projections do not always vary in phase with each other, leading sometimes to large uncertainties in some projection time-windows caused by the large ensemble spread. Little or no significant change is projected in JFM and AMJ because of a lack of consensus in the direction of change within the ensembles, except in JFM in the Markarfljót catchment where a significant decrease is projected.

The projected warming leads to an increase in mean seasonal and annual rainfall and subsequently to a decrease in mean seasonal and annual snowfall and shorter snow seasons. The direction of projected change in mean seasonal snowmelt varies with the season and catchment and may also vary with the projection horizon. The projected increase in mean snowmelt in OND and JFM in all catchments is likely caused by an increase in the number of intermittent snowmelt events due to warming. The projected decrease in mean snowmelt in AMJ and JAS in the Þverá and Markarfljót catchments is due to a snow storage reduction caused by warming whereas the projected increase in AMJ and JAS in the Kreppa catchment is caused by an increase in snow storage outside the glacier resulting from the increase in land area concomitant with the glacier retreat due to warming. In the Kreppa and Markarfljót catchments, mean annual glacier melt is projected to increase and reach a peak and thereafter start declining because the glaciers will retreat. The peak of glacier melt is projected to occur much earlier in the Markarfljót than Kreppa catchment. As a result, mean annual glacier melt will become lower than in the reference period in the Markarfljót catchment in the second half of the 21st century, whereas in the Kreppa catchment, it is projected to remain greater than in the reference period during the entire projection period.

Projected changes in mean seasonal rainfall, snowmelt and glacier melt due to warming lead to changes in seasonal runoff distribution, but the timing, magnitude and direction of streamflow changes vary with the season, catchment and emission scenario. Results indicated that mean seasonal streamflow is projected to increase in all seasons in the Kreppa catchment, whereas in the Þverá and Markarfljót catchments, an increase is projected in OND and JFM, a decrease is projected in JAS, and either an increase or a decrease is projected in AMJ depending on the future time-window and emission scenario under consideration. The projected changes in mean seasonal streamflow are not necessarily gradual, like warming, because precipitation oscillations contribute to modulate these changes. The projected changes are usually more severe and/or start earlier under the RCP8.5 emission scenario than under the RCP4.5 emission scenario because the warming is greater.

7 Climate change impact on flood characteristics

This section examines the impact of projected climate change on the timing and magnitude of annual maximum floods (AMFs).

7-1 Changes in the timing of annual maximum floods

To investigate changes in the timing of AMFs, the day in each water-year when annual maximum discharge occurred was extracted from the simulated daily streamflow time-series and assigned to the corresponding season. The frequency with which AMFs occurred in each season and in each 30-year time-window was then calculated for each ensemble member, and the ensemble median estimated (see Methodology in Section 3-1). Figs. 54 to 59 present the results for the ensemble median and Appendix 11 presents the results with all ensemble members. It is assumed that AMFs occurring in autumn are primarily generated by rainfall sometimes combined with snowmelt, AMFs occurring in winter are generated by a combination of rainfall and snowmelt, AMFs occurring in spring are primarily generated by snowmelt sometimes combined with rain, and AMFs occurring in summer are primarily generated by rainfall, sometimes combined with snowmelt, but primarily generated by glacier melt in the Kreppa catchment.

- **Þverá catchment (vhm38)**

In the reference period (1981-2010), AMFs primarily occurred in AMJ and JAS, whereas very few occurred in JFM and OND.

- RCP4.5 emission scenario

As the projection horizon increases, AMFs are projected to occur progressively less frequently in JAS and more often in OND and JFM, whereas little change is taking place in AMJ. By the end of the 21st century, AMFs are projected to occur as frequently in AMJ as in OND and very few will occur in JAS.

- RCP8.5 emission scenario

Results are similar to those projected with the RCP4.5 scenario except that the changes are greater, including in AMJ where a strong decrease is projected. Towards the end of the 21st century, AMFs are projected to occur most frequently in OND, followed by JFM whereas very few AMFs will occur in AMJ and JAS.

- **Markarfljót catchment (vhm218)**

In the reference period (1981-2010), AMFs occurred with a similar frequency in each season.

- RCP4.5 emission scenario

As the projection horizon increases, AMFs are projected to occur progressively more frequently in OND and less frequently in JAS first, and later in AMJ, whereas little change is projected in JFM. By the end of the 21st century, AMFs will occur most frequently in OND, followed by JFM, and very few will occur in AMJ and JAS.

- RCP8.5 emission scenario

Results are similar to those projected under the RCP4.5 scenario but the projected changes are more pronounced.

- **Kreppa catchment (vhm233)**

In the reference period (1981-2010), simulated AMFs mainly occurred in JAS and very few in AMJ whereas none occurred in OND and JFM.

- RCP4.5 emission scenario

Very little change is projected to take place in the 21st century in this catchment regarding the frequency of occurrence of AMFs. The strong prevalence of JAS will persist during the entire projection period and even slightly increase in the first half of the 21st century.

- RCP8.5 emission scenario

Results are very similar to those projected with the RCP4.5 emission scenario and the strong prevalence of JAS will be maintained over the course of the 21st century.

- **Discussion**

Projected changes in the seasonal frequency of occurrence of AMFs are related to changes in the mechanisms generating these floods. The flood regime of the Þverá catchment is projected to become increasingly more dominated by rainfall in autumn and winter, possibly associated with some snowmelt, and less dominated by snowmelt in spring and early summer. The increase in rainfall in autumn, possibly associated with some snowmelt will also have an increasing influence on the frequency of occurrence of AMFs in the Markarfljót catchment, at the expense of snowmelt in spring and summer. The flood regime of the Kreppa catchment is projected to remain dominated by glacier melt in summer during the 21st century.

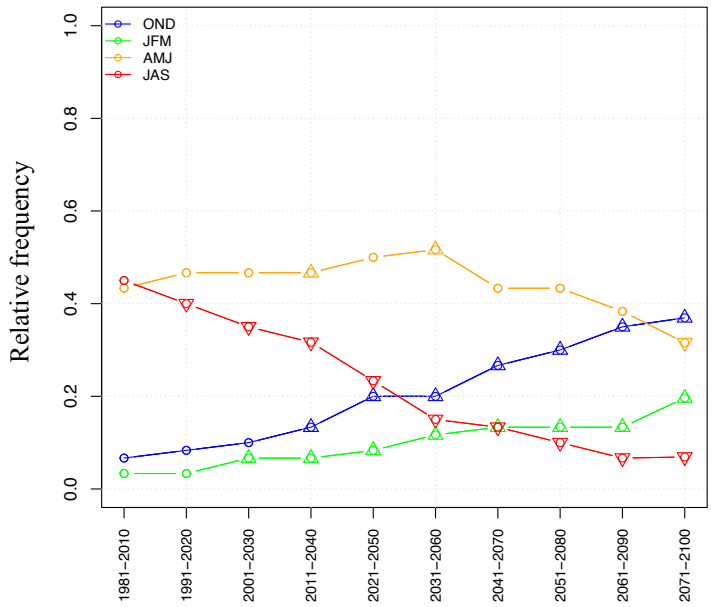

Fig. 54: Þverá catchment (vhm38): Projected median frequency of occurrence of AMFs in each season under the RCP4.5 emission scenario. OND (blue), JFM (green), AMJ (orange), JAS (red). The symbols on the ensemble median indicate whether a significant shift in the ensemble of seasonal frequencies has been detected between the reference and future periods (triangle point-up=freq. increase; triangle point down=freq. decrease; open circle=no significant change).

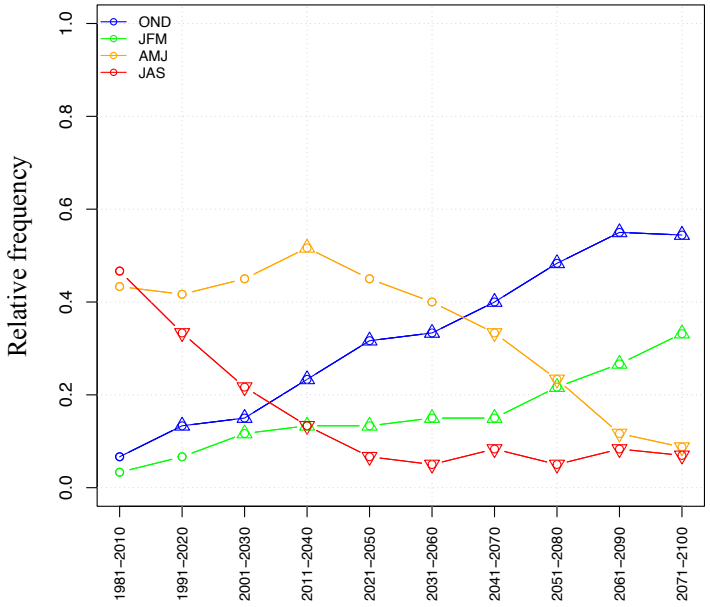

Fig. 55: Þverá catchment (vhm38): as Fig. 54 but under the RCP8.5 emission scenario.

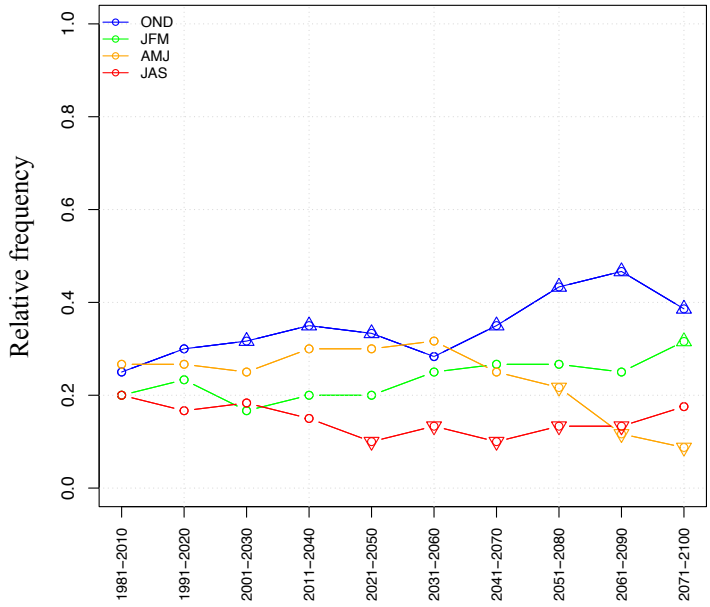

Fig. 56: Markarfljót catchment (vhm218): Projected median frequency of occurrence of AMFs in each season under the RCP4.5 emission scenario. OND (blue), JFM (green), AMJ (orange), JAS (red). The symbols on the ensemble median indicate whether a significant shift in the ensemble of seasonal frequencies has been detected between the reference and future periods (triangle point-up=freq. increase; triangle point down=freq. decrease; open circle=no significant change).

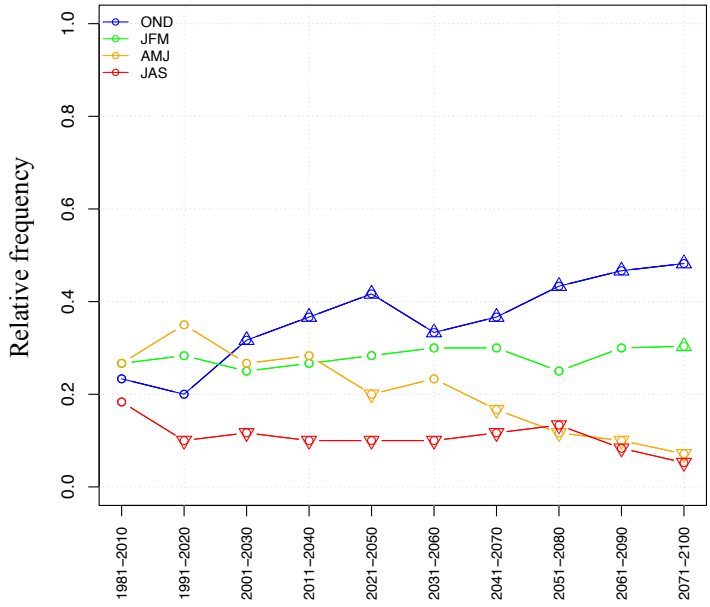

Fig. 57: Markarfljót catchment (vhm218): as Fig. 56 but under the RCP8.5 emission scenario.

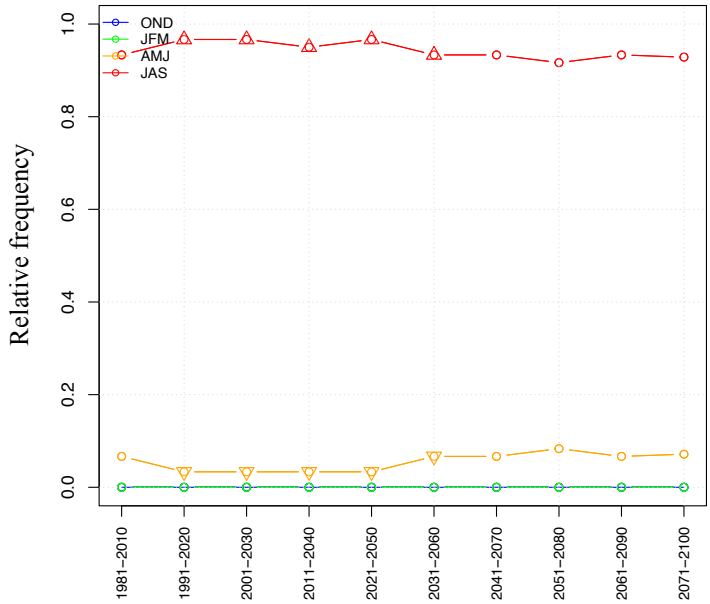

Fig. 58: Kreppa catchment (vhm233): Projected median frequency of occurrence of AMFs in each season under the RCP4.5 emission scenario. OND (blue), JFM (green), AMJ (orange), JAS (red). The symbols on the ensemble median indicate whether a significant shift in the ensemble of seasonal frequencies has been detected between the reference and future periods (triangle point-up=freq. increase; triangle point down=freq. decrease; open circle=no significant change).

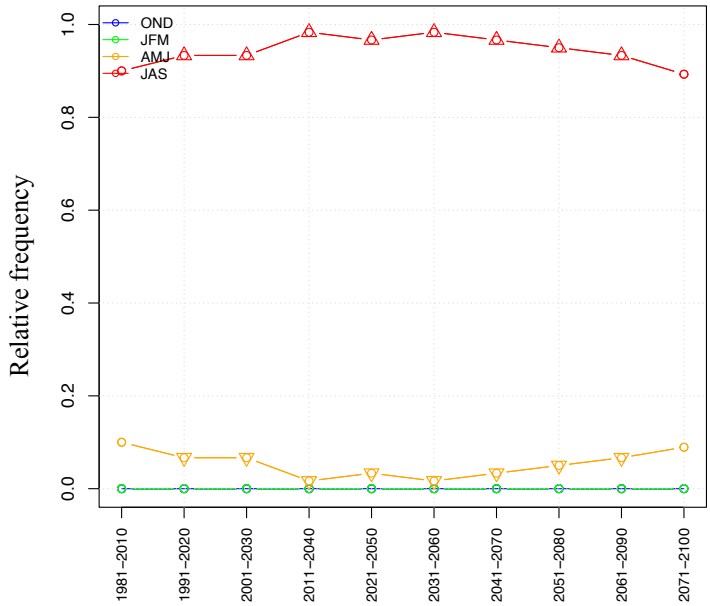

Fig. 59: Kreppa catchment (vhm233): as Fig. 58 but under the RCP8.5 emission scenario.

7-2 Changes in the magnitude of annual maximum floods

This section examines the impact of projected climate change on the magnitude of annual maximum floods (AMFs).

7-2-1 Changes in the magnitude of T-year floods

A Gumbel distribution was fitted to the AMFs series in each 30-year time-window (not shown) and the magnitude of the T-year floods estimated for the return periods T=10 and 50 years. The uncertainty associated with the T-year flood estimation is large and increases with T. Projected changes in the magnitude of the T-year floods between reference and future periods are presented in Figs. 60 to 65.

- **Þverá catchment (vhm38)**

See Figs. 60 and 61.

- RCP4.5 emission scenario

No significant change is projected until 2021-2050 and then, a significant decrease in the magnitude of the T-year floods is projected from 2031-2060 to 2051-2080. In this period of time, the median change is ranging from about −10 to −20%, relative to the 1981-2010 reference level. Beyond 2051-2080, the magnitude and direction of change of individual ensemble members become increasingly more spread and divergent, making the outcome very uncertain.

- RCP8.5 emission scenario

Similar conclusions can be drawn for this emission scenario. A significant decrease in the magnitude of T-year floods is projected in a few future time-windows only, from 2011-2040 to 2031-2060. Then, the trajectory of the projections becomes increasingly more divergent and the ensemble is split into two groups, one group projecting an increase and the other one a decrease, making the outcome very uncertain.

- Discussion

Snowmelt runoff in spring plays a primary role in the generation of AMFs in this catchment in the entire projection period, under the RCP4.5 scenario (see Fig. 54 in Section 7-1), which may explain why no significant change is detected in the magnitude of AMFs until about 2021-2050. Rainfall in autumn and winter will play an increasing role in the generation of AMFs in the 21st century but according to the results, the magnitude of these AMFs may or may not become larger than those triggered by snowmelt in spring in the reference period, depending on the ensemble member considered. The increasing spread in the projected change in T-year flood magnitude towards the end of the 21st century is likely related to the increasing uncertainty associated with the rainfall projections in autumn and winter (cf. Figs. 25, 26). Similar conclusions can be drawn for the RCP8.5 scenario except that the period with a significant decrease starts and ends earlier than under the RCP4.5 scenario, because spring snowmelt becomes less dominant earlier in the generation of AMFs.

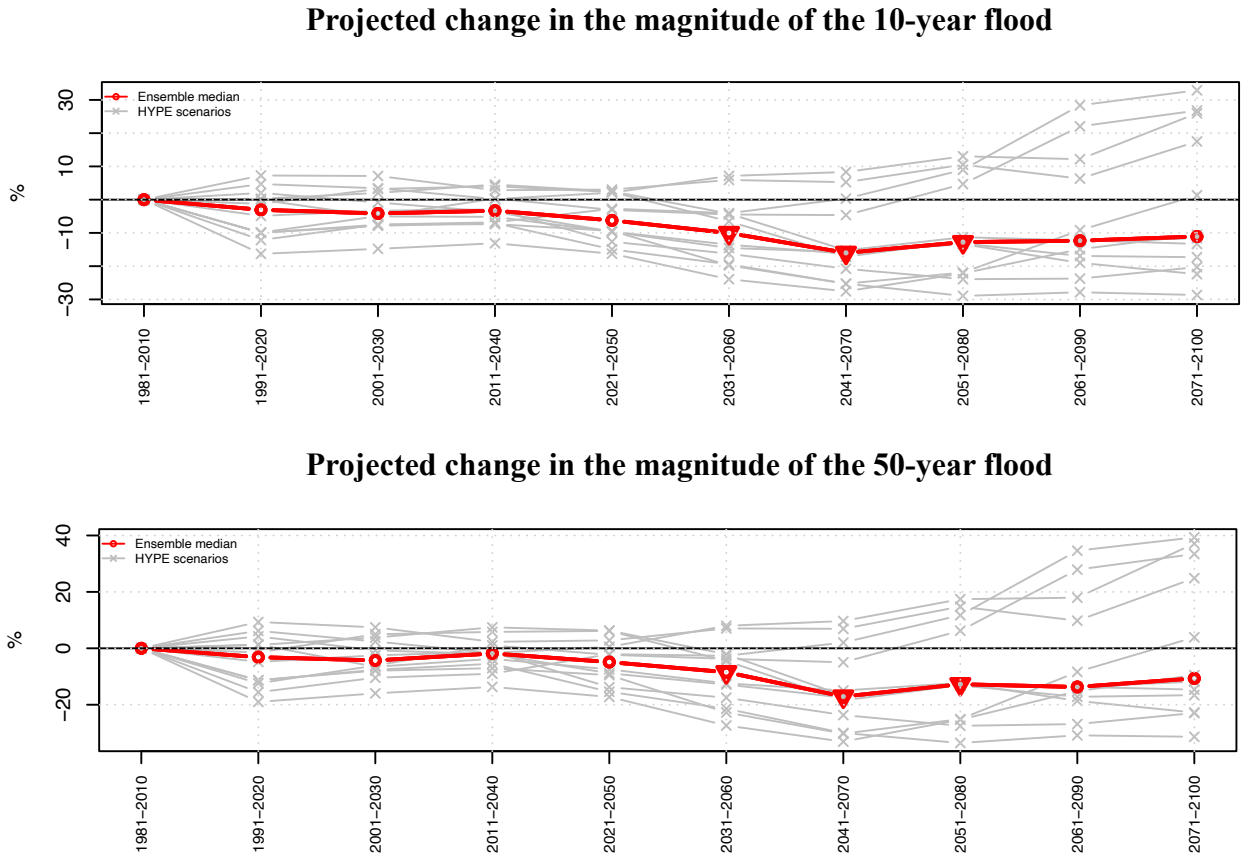

Fig. 60: Þverá catchment (vhm38): Projected changes in the magnitude of the T-year flood relative to the 1981-2010 reference level, under the RCP4.5 emission scenario: 10-year flood (top) and 50-year flood (bottom). Ensemble members (grey lines) and ensemble median (red line). The symbols on the ensemble median indicate whether a significant shift in the ensemble of T-year flood magnitudes has been detected between the reference and future periods, according to the Mann-Whitney test (triangle point-up= significant magnitude increase; triangle point down= significant magnitude decrease; open circle=no significant change).

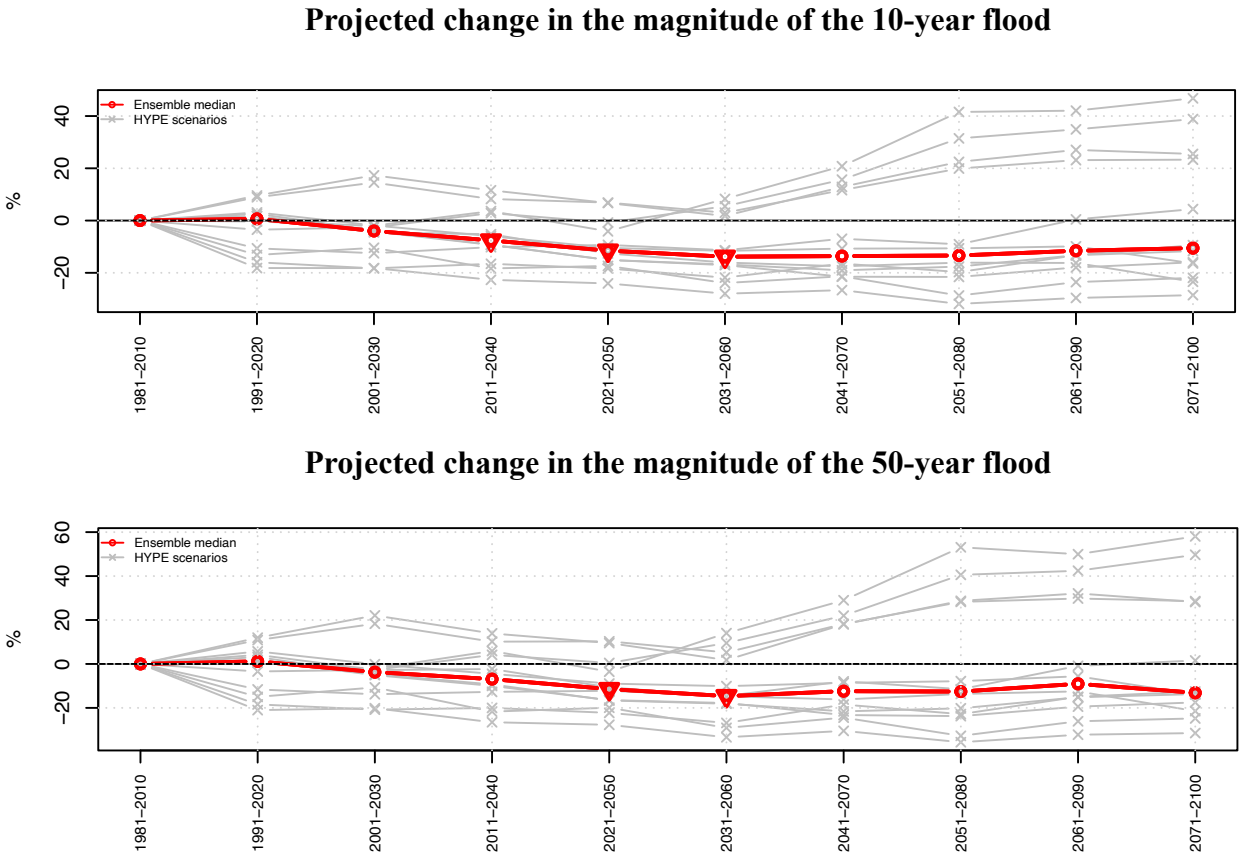

Fig. 61: Þverá catchment (vhm38): As Fig. 60 but under the RCP8.5 emission scenario.

- **Markarfljót catchment (vhm218)**

See Figs. 62 and 63.

- RCP4.5 emission scenario

No significant change is projected until 2041-2070 and thereafter, a significant increase in the magnitude of T-year floods is projected until the end of the century for both return periods. The increase in magnitude varies in similar proportions for the two return periods and reaches a median value of about +20% in 2071-2100, relative to the 1981-2010 reference level.

- RCP8.5 emission scenario

Similar results are observed under this emission scenario but the increase in magnitude is projected to start earlier (2021-2050). The increase in magnitude varies in similar proportions for the two return periods and reaches a median value of about +50% in 2071-2100, relative to the 1981-2010 reference level.

- Discussion

The projected increase in the magnitude of T-year floods, combined with an increase in the frequency of occurrence of AMFs in autumn at the expense of a decrease in spring and summer (see Section 7-1) is likely caused by a rainfall intensification in autumn and winter combined with an increase in the number of intermittent snowmelt events (see also Figs. 35, 36, 40, 41 and Appendix 9).

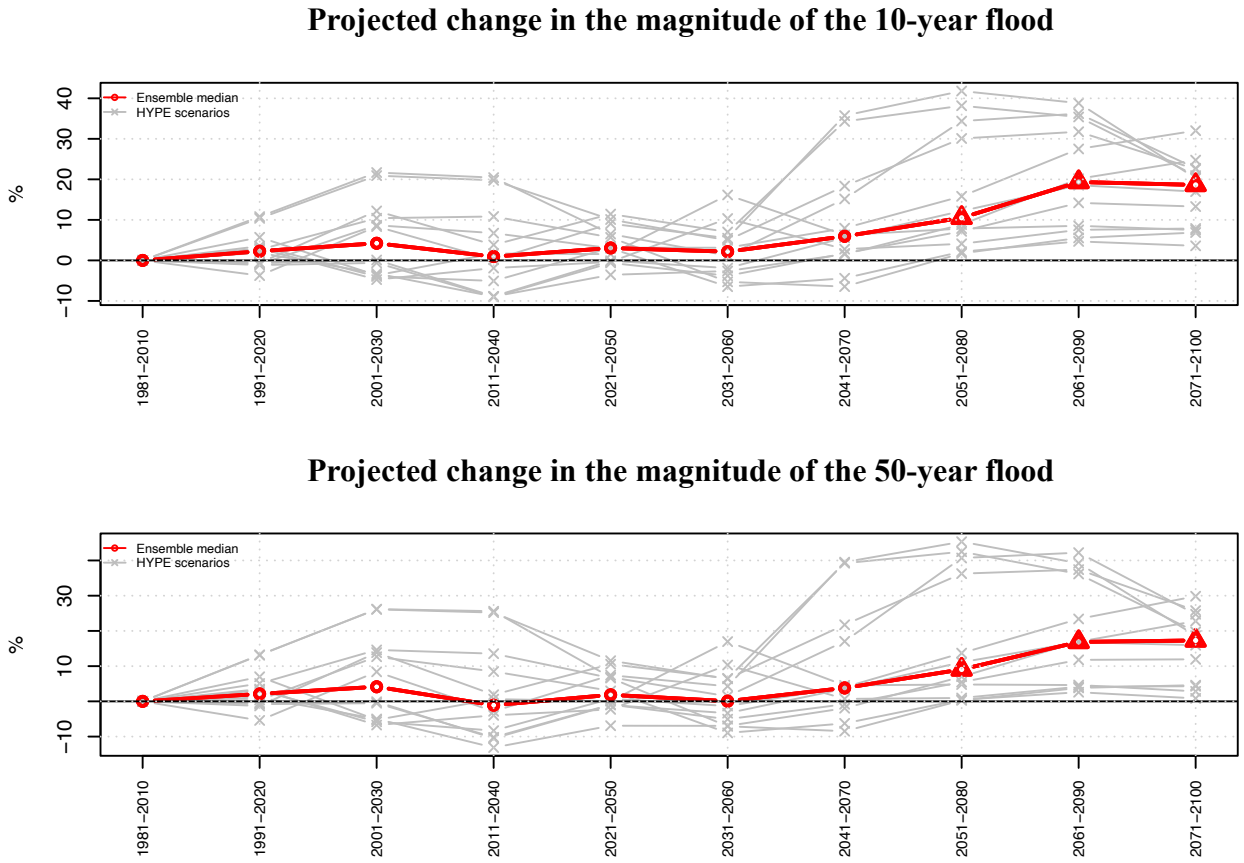

Fig. 62: Markarfljót catchment (vhm218): Projected changes in the magnitude of the T-year flood relative to the 1981-2010 reference level, under the RCP4.5 emission scenario: 10-year flood (top) and 50-year flood (bottom). Ensemble members (grey lines) and ensemble median (red line). The symbols on the ensemble median indicate whether a significant shift in the ensemble of T-year flood magnitudes has been detected between the reference and future periods, according to the Mann-Whitney test (triangle point-up= significant magnitude increase; triangle point down= significant magnitude decrease; open circle=no significant change).

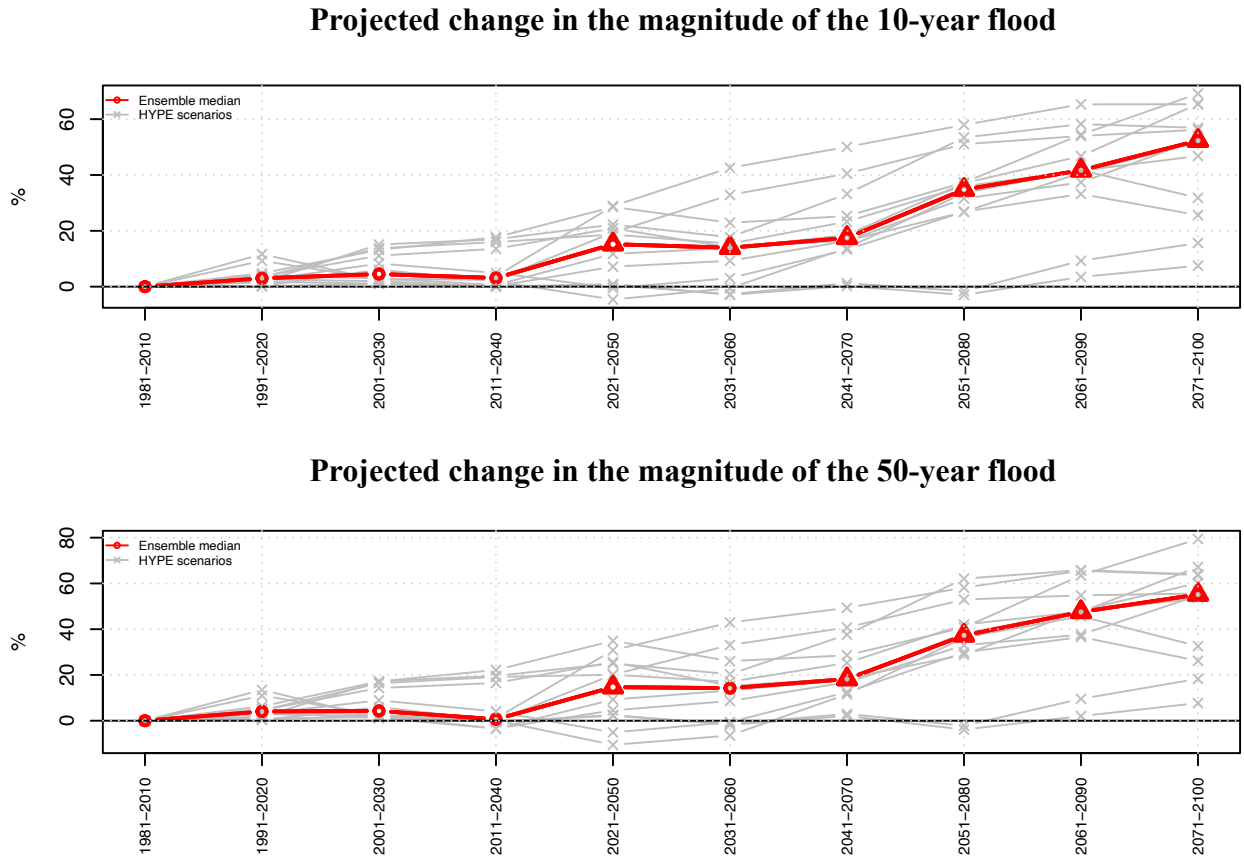

Fig. 63: Markarfljót catchment (vhm218): As Fig. 62 but under the RCP8.5 emission scenario.

- **Kreppa catchment (vhm233)**

See Figs. 64 and 65.

- RCP4.5 emission scenario

The magnitude of the 10-year flood is projected to significantly increase during the 21st century. The magnitude of the 50-year flood is projected to significantly increase until 2021-2050 and thereafter no significant change is detected in the ensemble, because the spread is increasing and the direction of change is diverging between individual members, making difficult to draw any robust conclusion. When significant, the increase does not exceed a median value of +10%.

- RCP8.5 emission scenario

The magnitude of the T-year flood is projected to significantly increase during most of the 21st century for both return periods. The peak of increase is projected in 2011-2040, with a median value of about +20%. Thereafter, the increase in T-year flood slowly decays and is no longer considered significant in 2071-2100.

- Discussion

AMFs in this catchment are triggered by glacier melt in summer (see Section 7-1). Therefore, an increase in glacier melt in summer due to warming is very likely responsible for the projected increase in the magnitude of T-year floods. Note also that the glacier is projected to progressively retreat with rising temperature, which may have some counteracting effects on extreme daily glacier melt after some point in time and could explain why the increase in T-year flood is projected to decay beyond 2011-2040. The uncertainty in the T-year flood estimates is also expected to increase with T which probably accounts for some of the differences in the results between the two return periods under the RCP4.5 emission scenario.

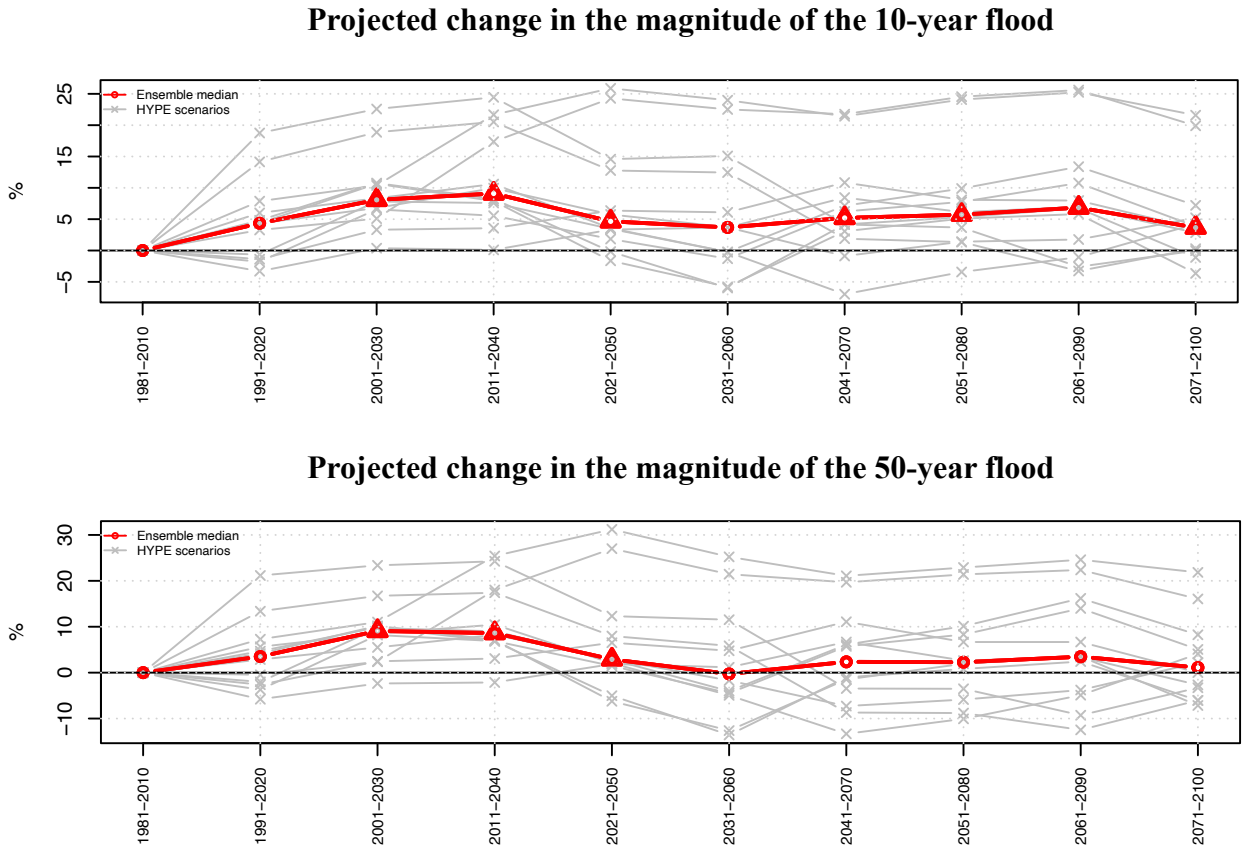

Fig. 64: Kreppa catchment (vhm233): Projected changes in the magnitude of the T-year flood relative to the 1981-2010 reference level, under the RCP4.5 emission scenario: 10-year flood (top) and 50-year flood (bottom). Ensemble members (grey lines) and ensemble median (red line). The symbols on the ensemble median indicate whether a significant shift in the ensemble of T-year flood magnitudes has been detected between the reference and future periods, according to the Mann-Whitney test (triangle point-up= significant magnitude increase; triangle point down= significant magnitude decrease; open circle=no significant change).

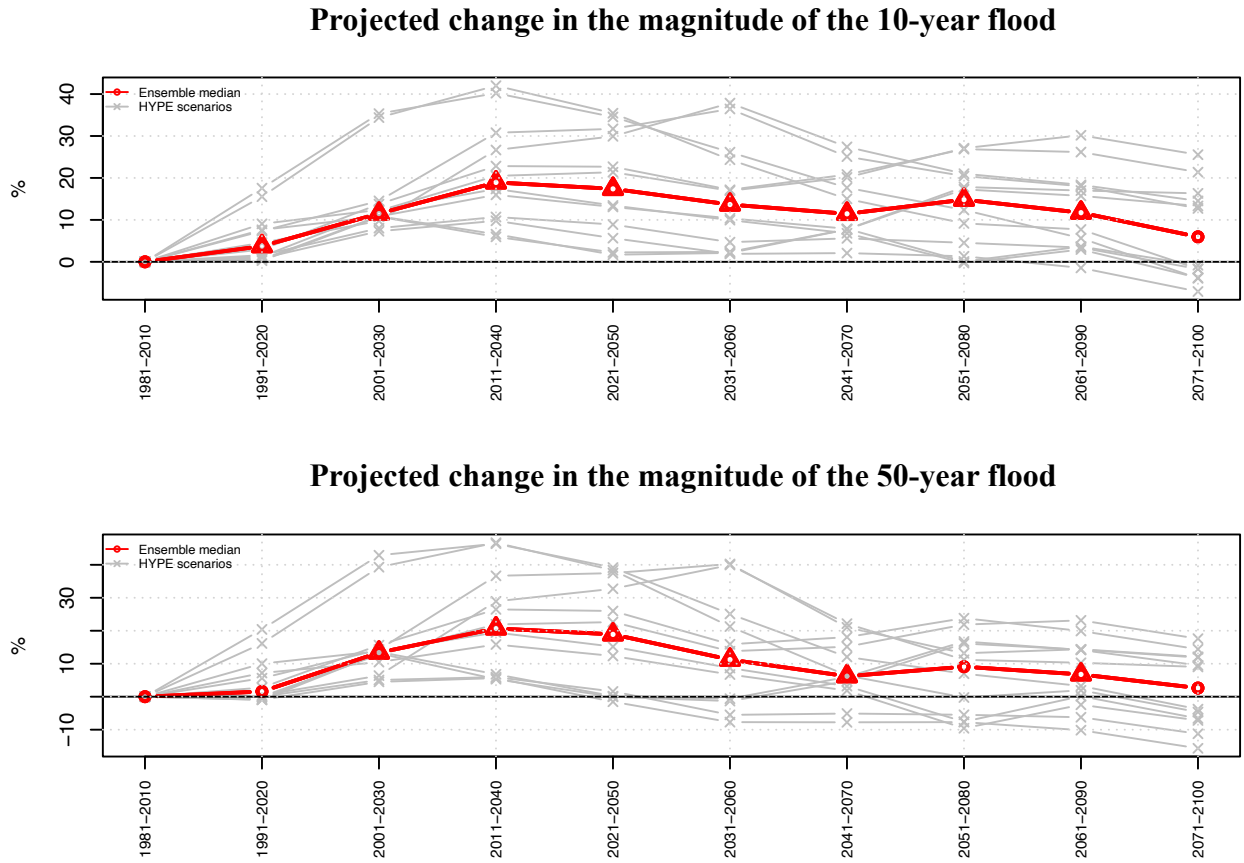

Fig. 65: Kreppa catchment (vhm233): As Fig. 64 but under the RCP8.5 emission scenario.

7-2-2 Changes in the return period of annual maximum floods

The flood magnitude (Q) is now fixed and the corresponding return period T(Q) estimated in each 30-year time-window and compared to T(Q) in the reference period (1981-2010). If the frequency distribution of AMFs is projected to shift towards larger flood discharges in the future, then a flood of magnitude Q will be exceeded more frequently in the future and its return period will decrease:

$$q_1=Q(T=T_i)_{1981\text{-}2010} < q_2=Q(T=T_i)_{future}$$
$$T_1=T(Q=q_1)_{1981\text{-}2010} > T_2=T(Q=q_1)_{future}$$

If the frequency distribution of AMFs is projected to shift towards lower flood discharges in the future, then a flood of magnitude Q will be exceeded less frequently in the future and its return period will increase:

$$q_1=Q(T=T_i)_{1981\text{-}2010} > q_2=Q(T=T_i)_{future}$$
$$T_1=T(Q=q_1)_{1981\text{-}2010} < T_2=T(Q=q_1)_{future}$$

The flood magnitude of reference (Q) is taken as the magnitude of the 10-year flood in the reference period (1981-2010). Changes between reference and future periods are considered significant when more than two-thirds of the ensemble members are shifted in the same direction (T increase or decrease). The temporal evolution of the T(Q) ensembles is presented in Figs. 66 to 68. Note that in order to keep the figures readable around the ensemble median, not all members appear in some figures because located beyond the plotted range.

- **Þverá catchment (vhm38)**

See Fig. 66.

- RCP4.5 emission scenario

The median of the projected return period is systematically greater than 10 years. However, it cannot be concluded that the return period of the reference 10-year flood will systematically increase in the future because the consensus among the ensemble members regarding the direction of change is low in a majority of projection periods, making the two-thirds majority criteria not fulfilled. As a result, the return period associated with the reference 10-year flood is projected to significantly increase in 2031-2060 and 2041-2070 only. As an example, in 2041-2070, the reference 10-year flood is projected to become a flood with a median return period of about 40 years.

- RCP8.5 emission scenario

Similar results are obtained with the RCP8.5 scenario. The large ensemble spread and the lack of consensus regarding the direction of change make it difficult to draw robust conclusions regarding the evolution of the return period of the reference 10-year flood in the future, except for two future periods (2001-2030 and 2021-2050) where a significant increase is projected. As an example, in 2021-2050, the reference 10-year flood is projected to become a flood with a median return period of about 25 years.

- Discussion

These results are in line with what was expected, given the projected evolution of the magnitude of the 10-year flood (cf. Figs 60 and 61). The increase in T(Q) in some future time-windows corresponds to a decrease in the magnitude of the T-year flood. Note that results in Fig. 66 are not in complete agreement with those in Figs. 60 and 61 regarding the future time-windows with a significant change. This is due to the use of a different criteria (two-thirds majority voting for T vs. Mann-Whitney test for the T-year flood) and to the growing uncertainty of the T estimate with T.

- **Markarfljót catchment (vhm218)**

See Fig. 67.

- RCP4.5 emission scenario

Results indicate that the return period associated with the reference 10-year flood is projected to significantly and progressively decrease from 2041-2070 to the end of the century, meaning that the reference 10-year flood will be exceeded more than once every 10 years on average in the future. For instance, in 2071-2100, the reference 10-year flood is projected to become a flood with a median return period of approximately 5 years. Before 2041-2070, no significant change is detected and the different members fluctuate around T=10 years.

- RCP8.5 emission scenario

A significant decrease in the return period associated with the reference 10-year flood is projected during the entire projection period. As an example, the reference 10-year flood is projected to become a flood with a median return period of about 2 years in 2071-2100.

- Discussion

These results are in line with what was expected, given the projected increase in the magnitude of the 10-year flood in the future (cf. Figs 62 and 63). Here too, results in Fig. 67 are not in complete agreement with those in Figs. 62 and 63 regarding the future periods with a significant change. This is due to the same reasons mentioned above.

- **Kreppa catchment (vhm233)**

See Fig. 68.

- RCP4.5 emission scenario

A significant decrease in the return period associated with the reference 10-year flood is projected during most of the 21st century, meaning that the reference 10-year flood will be exceeded more than once every 10 years on average in the future. As an example, the reference 10-year flood is projected to become a flood with a median return period of about 6 years in 2001-2030.

- RCP8.5 emission scenario

Results are similar to those observed in the RCP4.5 scenario. A significant decrease in the return period associated with the reference 10-year flood is projected during most of the 21st century. As an example, the reference 10-year flood is projected to become a flood with a median return period of about 4.5 years in 2001-2030.

- Discussion

These results reflect very well the projected increase in the magnitude of the 10-year flood in the future in this catchment (cf. Figs 64 and 65). The projected T reaches a minimum around 2011-2040 and then re-increases but remains under T=10 years in all projection time-windows.

7-3 Summary and discussion

Projected climate change, especially warming, is expected to have a significant impact on the flood regimes of the three studied catchments in the future, leading to a change in flood risk. The nature of this impact varies with the catchments. It concerns essentially changes in the seasonal frequency of occurrence of AMFs in the Þverá catchment, the magnitude of AMFs in the Kreppa catchment and both seasonal frequency of occurrence and magnitude of AMFs in the Markarfljót catchment. The direction of projected changes varies also with the catchments and depends on the initial dominating flood generating mechanisms. The changes are also projected to start more or less rapidly, depending on the catchment and emission scenario.

- In the Þverá catchment, the strong dominance of spring and early summer snowmelt on the timing of AMFs is projected to progressively decrease in the future, and the influence of rainfall and/or combined rainfall and snowmelt in autumn and winter increase, owing to the projected rise in temperature. The projected changes in the timing of AMFs are not clearly accompanied by changes in their magnitude (no clear shift in one direction for the ensemble of T-year floods). Several assumptions can be made: i) rainfall-triggered AMFs in autumn/winter in the future will be of the same order of magnitude as snowmelt-triggered AMFs in spring in the reference period; ii) the uncertainty associated with rainfall projections triggering these AMFs increases with the projection horizon and so does the estimation of projected T-year floods.
- The Kreppa catchment is projected to remain strongly dominated by AMFs triggered by glacier melt in summer. The magnitude of T-year floods is projected to increase in the future, owing to the increase in glacier melt with projected warming.
- In the Markarfljót catchment, AMFs occur in all seasons in the current climate and with a similar frequency. In the future, AMFs are projected to occur progressively more frequently in autumn and less frequently in spring and summer, whereas little change is projected in winter. Projected snow storage reduction will most likely lead to a decrease in the magnitude of spring floods, making them less likely to become AMFs in the future. The magnitude of T-year floods is projected to increase, likely because of an intensification of rainfall in autumn and winter, possibly combined with snowmelt.

Projected changes in the seasonal frequency of occurrence of AMFs appear to be relatively robust and the consensus among the ensemble members regarding the direction of change is usually high. Projected changes in the magnitude of T-year floods are often associated with large uncertainties and these results have to be treated with caution. The overall uncertainty in the estimation of T-year floods is related to uncertainties affecting extreme discharge projections (hydrological modelling uncertainties and climate projection uncertainties), uncertainties related to the fitting of the Gumbel distribution and uncertainties in the estimation of flood quantiles or return periods for large flood quantiles beyond the range of simulated flood values (statistical uncertainties).

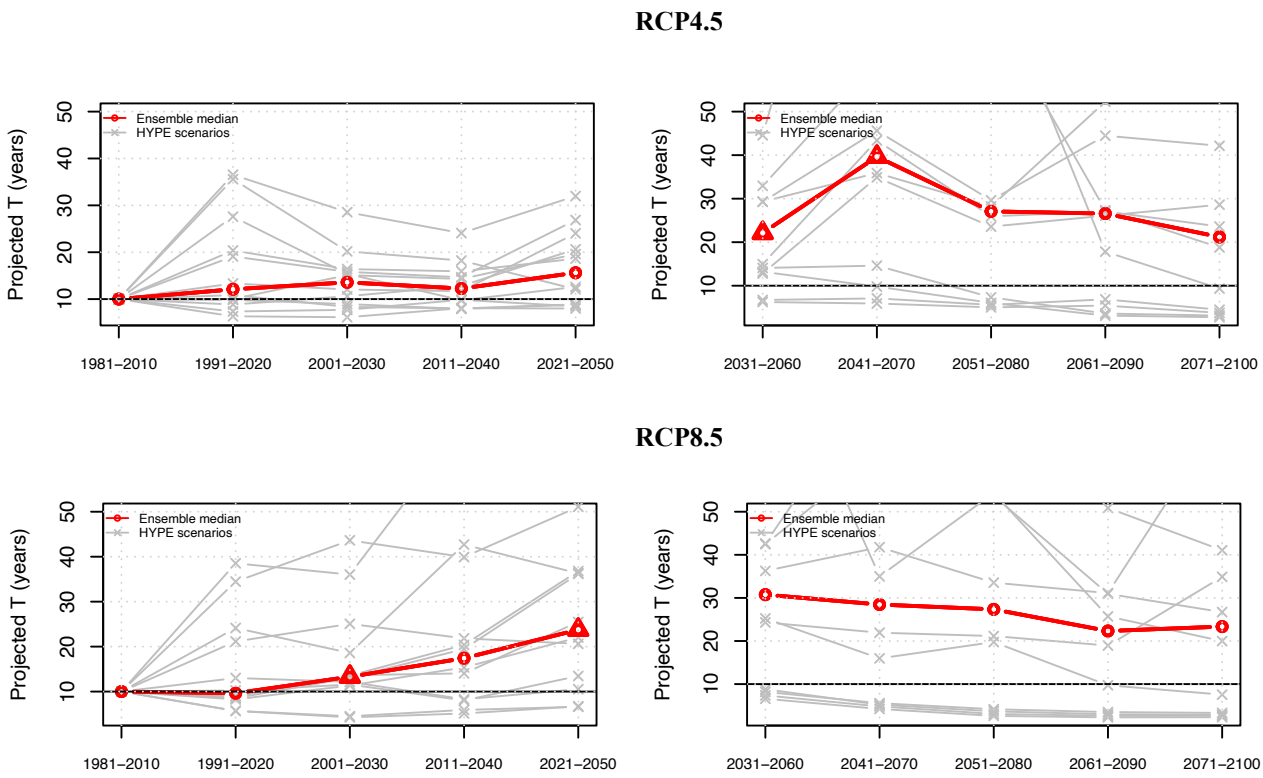

Fig. 66: Þverá catchment (vhm38): Projected return period (T) associated with the reference 10-year flood. Top-panel: RCP4.5 emission scenario; bottom-panel: RCP8.5 emission scenario. Ensemble members (grey lines) and ensemble median (red line). The symbols on the ensemble median indicate whether a significant shift in the T ensemble has been detected between the reference and future periods (triangle point-up= significant T increase; triangle point down= significant T decrease; open circle=no significant change).

RCP4.5

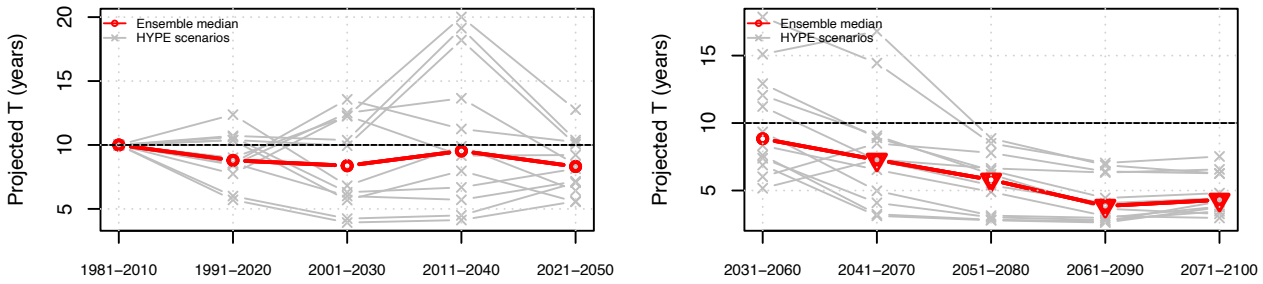

RCP8.5

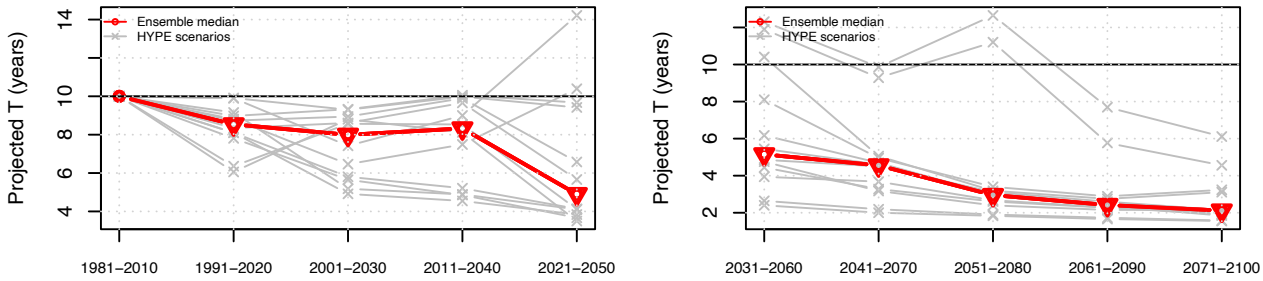

Fig. 67: Markarfljót catchment (vhm218): Projected return period (T) associated with the reference 10-year flood. Top-panel: RCP4.5 emission scenario; bottom-panel: RCP8.5 emission scenario. Ensemble members (grey lines) and ensemble median (red line). The symbols on the ensemble median indicate whether a significant shift in the T ensemble has been detected between the reference and future periods (triangle point-up= significant T increase; triangle point down= significant T decrease; open circle=no significant change).

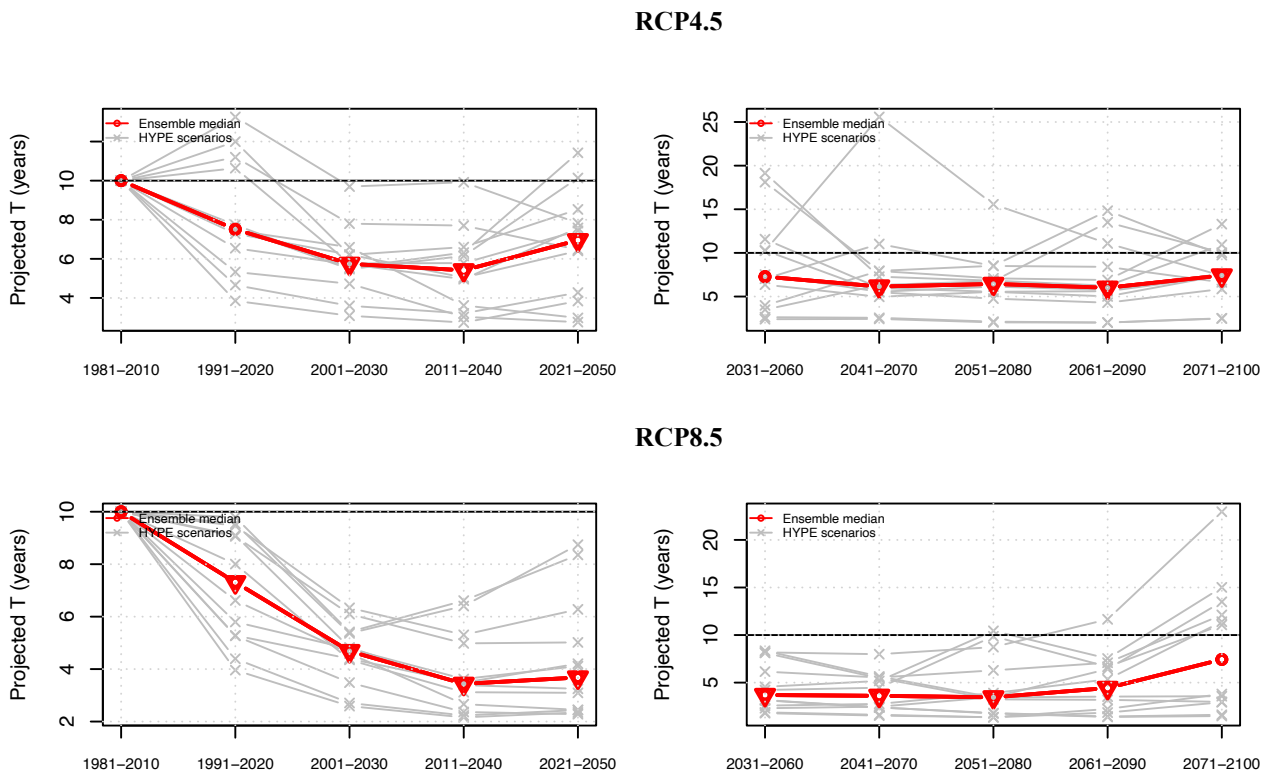

Fig. 68: Kreppa catchment (vhm233): Projected return period (T) associated with the reference 10-year flood. Top-panel: RCP4.5 emission scenario; bottom-panel: RCP8.5 emission scenario. Ensemble members (grey lines) and ensemble median (red line). The symbols on the ensemble median indicate whether a significant shift in the T ensemble has been detected between the reference and future periods (triangle point-up= significant T increase; triangle point down= significant T decrease; open circle=no significant change).

8 Summary and conclusions

This study presented an analysis of the impact of projected climate change in the 21st century on the hydrological characteristics of three river catchments located in various regions of Iceland. The Þverá catchment is located near the coast in the Westfjords; The Markarfljót catchment is located in the southern highlands, in the region of Myrdalsjökull ice cap and has a glacier coverage of around 13%; The Kreppa catchment is located in the northeast central highlands, in the region of Vatnajökull ice cap and has a glacier coverage of around 51%.

An ensemble of hydrological projections was obtained for the period 1981-2100 by forcing the HYPE hydrological model with locally-adjusted daily temperature and precipitation outputs from an ensemble of CORDEX climate projections, for two different greenhouse gas emission scenarios (RCPs 4.5 and 8.5). Projected changes affecting near surface air temperature, precipitation, snow storage, snow and glacier melt, and their impact on mean and extreme streamflow characteristics were analysed, considering moving 30-year time-windows. The reference period was taken as 1981-2010.

First, results indicated that simulated river discharges, obtained with HYPE calibrated and driven with the ICRA climate reanalysis, compared well against observed daily discharges in the reference period, but some weaknesses were observed in the simulation of annual maximum floods in the Þverá and Markarfljót catchments, which tended to be underestimated. The comparisons between daily discharge statistics obtained with HYPE forced with the ICRA reanalysis and with the locally-adjusted CORDEX climate series in the reference period showed good agreement, giving credibility to the modelling chain and its use for the impact study.

As expected, climate projections indicate that near surface air temperature is very likely to rise in the future, with a rate of 0.29°C/decade under the RCP4.5 emission scenario and 0.46°C/decade under the RCP8.5 emission scenario, on average over all months and catchments. This warming is of the same order of magnitude as in other studied catchments (Crochet 2020, 2021, 2022). Projections of precipitation are not as homogenous in space and time as temperature. Precipitation is characterised by decadal to multi-decadal oscillations reflecting natural climate variability and the different members of the ensemble do not always fluctuate in phase with each other, sometimes leading to large uncertainties regarding both direction and magnitude of changes in annual and seasonal means, depending on the time-windows under consideration. Despite the large spread affecting these projections, there is a general consensus that mean precipitation will increase in summer and autumn in the future, in the three catchments, especially under the RCP8.5 emission scenario, and decrease in winter in the Markarfljót catchment. No clear consensus regarding mean seasonal precipitation change was otherwise identified.

The projected warming, if it realises, will lead to an increase in the fraction of annual precipitation falling as rain at the expense of snow, which, in turn, will lead to less snow storage and shorter snow seasons. An increase in snowmelt is also expected in autumn and/or winter and will

contribute to destabilise the build-up of the snowpack which in turn will lead to a decrease in mean snowmelt in spring and summer. In the Kreppa catchment, however, snow storage outside the glacier is actually projected to increase due to the projected increase in land area concomitant with the retreat of glaciers. In the Kreppa and Markarfljót catchments, mean annual glacier melt is projected to increase and reach a peak, owing to the rise in temperature. The time-window when this peak is expected to be reached is very different for the two catchments. Thereafter, mean annual glacier melt will still increase but at a slower rate due to the retreat of glaciers and eventually decrease in the Markarfljót catchment, whereas in the Kreppa catchment, mean annual glacier melt will remain greater than in the reference period during the entire projection horizon.

Projected changes in mean seasonal rainfall, snowfall and snow and glacier melt will subsequently have an impact on the streamflow seasonality pattern of the three studied catchments. Results indicate that mean seasonal streamflow will likely increase in all seasons in the future in the Kreppa catchment, whereas in the Þverá and Markarfljót catchments, an increase is projected in autumn and winter, either an increase or a decrease is projected in spring depending on the future time-window and emission scenario under consideration, and a decrease is projected in summer.

Projected climate change will also have an impact on flood risk. Changes in the seasonal frequency of occurrence of annual maximum floods are expected in the Þverá and Markarfljót catchments with an increase in autumn/winter and a decrease in spring/summer, whereas no change is expected in the Kreppa catchment which will remain dominated by floods in summer. An increase in the magnitude of annual maximum floods is also projected in the Kreppa and Markarfljót catchments whereas no clear trend is emerging in the Þverá catchment.

In conclusion, projected climate change, if it realises, is expected to have a significant impact on the hydrological characteristics of the three studied catchments in the future. The main driver of these changes is warming. The magnitude of the hydrological response is expected to vary over the course of the 21st century and to be different from one catchment to another because their characteristics differ. Therefore, the development of adaptation strategies and the design of water-related infrastructures under changing hydro-climatic conditions will probably represent a considerable challenge in the future. The uncertainty associated with the hydrological projections must also be taken into account. The results of this study have shown how large the spread of the hydrological projections can be, even though one hydrological model only was used.

Acknowledgements

This work was supported by the Icelandic Road and Coastal Administration Research Fund.

The author acknowledges the World Climate Research Programme's Working Group on Regional Climate, and the Working Group on Coupled Modelling, former coordinating body of CORDEX and responsible panel for CMIP5. The author acknowledges the climate modelling groups (listed in Table 2 in this report) for producing and making available their model output. The author also acknowledges the Earth System Grid Federation infrastructure an international effort led by the U.S. Department of Energy's Program for Climate Model Diagnosis and Intercomparison, the European Network for Earth System Modelling and other partners in the Global Organisation for Earth System Science Portals (GO-ESSP).

DEMs (ArcticDEM) provided by the Polar Geospatial Center under NSF-OPP awards 1043681, 1559691, and 1542736.

The author wishes to thank the Swedish Meteorological and Hydrological Institute for making the HYPE model available.

Veðurstofa Íslands provided the ICRA climate reanalysis and discharge observations (IMO database, service no. 2019-11-01/01).

Data analysis was performed with the R software (R Core Team, 2016).

9 References

Aðalgeirsdóttir, G., Magnússon, E., Pálsson, F., Thorsteinsson, T., Belart, J.M.C., Jóhannesson, T., Hannesdóttir, H., Sigurðsson, O., Gunnarsson, A., Einarsson, B., Berthier, E., Steffensen Schmidt, L., Haraldsson, H. H., and Björnsson, H. (2020). Glacier Changes in Iceland From ~1890 to 2019. *Front. Earth Sci.* , 8, 1-15, doi: 10.3389/feart.2020.523646.

Arheimer, B. and Lindström, G. (2015). Climate impact on floods: changes in high flows in Sweden in the past and the future (1911–2100). *Hydrol. Earth Syst. Sci.*, 19, 771–784, 2015. doi:10.5194/hess-19-771-2015.

Arnalds, O. (2015). The Soils of Iceland. World Soils Book Series. Springer Netherlands.

Arnalds, Ó., and Óskarsson, H. (2009). Íslenskt jarðvegskort (Soil map of Iceland). Nátturufræðingurinn 78:107-121.

Árnason, K., and Matthíasson, I. (2017). CORINE - landflokkun 2012. Landgerðabreytingar á Íslandi 2006-2012. Landmælingar Íslands.

Benestad, R., Haensler, A., Hennemuth, B., Illy, T., Jacob, D., Keup-Thiel, E., Kotlarski, S., Nikulin, G., Otto, J., Rechid, D., Sieck, K., Sobolowski, S., Szabó, P., Szépszó, G., Teichmann, C., Vautard, R., Weber, T., Zsebeházi G. (2017). Guidance for EURO-CORDEX climate projections data use. EURO-CORDEX Guidelines Version 1.0 - 2017.08. (www.euro-cordex.net)

Björnsson, H., Sigurðsson, B. D., Davíðsdóttir, B., Ólafsson, J., Ástþórssson, Ó. S., Ólafsdóttir, S., Baldursson, T., and Jónsson, T. (2018). Loftslagsbreytingar og áhrif þeirra á Íslandi – Skýrsla vísindanefndar um loftslagsbreytingar 2018. Veðurstofa Íslands.

Brigode, P., Oudin, L., and Perrin, C. (2013). Hydrological model parameter instability: A source of additional uncertainty in estimating the hydrological impacts of climate change? *J. Hydrol.*, 476, 410-425. https://doi.org/10.1016/j.jhydrol.2012.11.012

Climate Change and Energy Systems. Impacts, risks and adaptation in the Nordic and Baltic countries. Th. Thorsteinsson and H. Björnsson Eds. TemaNord (2011):502, 226 pp.

Crochet, P. (2007). A study of regional precipitation trends in Iceland using a high quality gauge network and ERA-40. *J. Climate,* 20(18), 4659-4677.

Crochet, P. (2013). Sensitivity of Icelandic river basins to recent climate variations. *Jökull*, 63, 71-90.

Crochet, P. (2020). Flood frequency analysis in a changing climate - Climate change impact on design flood (160p). Report prepared for the Icelandic Road and Coastal Administration Research Fund. https://www.vegagerdin.is/link_to_report

Crochet, P. (2021). Impact of climate change on mean and high streamflow characteristics in Icelandic watersheds: a case study (166p). Report prepared for the Icelandic Road and Coastal Administration Research Fund. https://www.vegagerdin.is/link_to_report

Crochet, P. (2022). Hydrological response of Icelandic river basins to projected climate change during the 21st century. A case study (168p). Report prepared for the Icelandic Road and Coastal Administration Research Fund. https://www.vegagerdin.is/link_to_report

Dee, D. P., Uppala, S. M., Simmons, A. J., Berrisford, P., Poli, P., Kobayashi, S., Andrae, U., Balmaseda, M. A., Balsamo, G., Bauer, P., Bechtold, P., Beljaars, A. C. M., van de Berg, L., Bidlot, J., Bormann, N., Delsol, C., Dragani, R., Fuentes, M., Geer, A. J., Haimberger, L., Healy, S. B., Hersbach, H., Hólm, E. V., Isaksen, L., Kållberg, P., Köhler, M., Matricardi, M., McNally, A. P., Monge-Sanz, B. M., Morcrette, J.-J., Park, B.-K., Peubey, C., de Rosnay, P., Tavolato, C., Thépaut, J.-N., and Vitart, F. (2011). The ERA-Interim reanalysis: configuration and performance of the data assimilation system, *Q.J.R. Meteorol. Soc.*, 137(656), 553–597, doi:10.1002/qj.828.

Delignette-Muller, M.L., and Dutang, C. (2015). "fitdistrplus: An R Package for Fitting Distributions." *Journal of Statistical Software*, 64(4), 1–34.

Doherty, J. (2021). PEST: Model-independent parameter estimation. User manual part I: PEST, SENSAN and global optimisers. (7th Ed. with latest additions). Watermark Numerical Computing.

Einarsson, B., and Jónsson, S. (2010). The effect of climate change on runoff from two watersheds in Iceland. VÍ-2010-016 report, 34 pp. Veðurstofa Íslands.

Frans, C., Istanbulluoglu, E., Lettenmaier, D.P., Fountain, A.G., and Riedel, J. (2018). Glacier Recession and the response of summer streamflow in the Pacific Northwest United States, 1960-2099. *Water Resour. Res.*, 54, 6202-6225, https://doi.org/10.1029/2017WR021764

Giorgetta, M.A., Jungclaus, J., Reick, C., Legutke, S., Bader, J., Böttinger, M., Brovkin, V., Crueger, T., Esch, M., Fieg, K., Glushak, K., Gayler, V., Haak, H., Hollweg, H., Ilyina, T., Kinne, S., Kornblueh, L., Matei, D., Mauritsen, T., Mikolajewicz, U., Mueller, W., Notz, D., Pithan, F., Raddatz, T., Rast, S., Redler, R., Roeckner, E., Schmid, H., Schnur, R., Segschneider, J., Six, K.D., Stockhause, M., Timmreck, C., Wegner, J., Widmann, H., Weiners, K., Claussen, M., Marotzke, J., and Stevens, B. (2013). Climate and carbon cycle changes from 1850 to 2100 in MPI-ESM simulations for the coupled model intercomparison project phase 5. *Journal of Advances in Modeling Earth Systems* 5:572–597, https://doi.org/10.1002/jame.20038.

Giorgi, F., Jones, C., and Asrar, G. R. (2009). Addressing climate information needs at the regional level: the CORDEX framework, World Meteorological Organization (WMO) Bulletin, 58(3), 175-183.

Gosling, S. N., Taylor, R. G., Arnell, N.W., and Todd, M. C. (2011). A comparative analysis of projected impacts of climate change on river runoff from global and catchment-scale hydrological models. Hydrol. Earth Syst. Sci., 15, 279-294, doi:10.5194/hess-15-279-2011.

Gosseling, M. (2017). CORDEX climate trends for Iceland in the 21st century. VI-report 2017-009. Veðurstofa Íslands..

Gudmundsson, L., Bremnes, J. B., Haugen, J. E., and Engen-Skaugen, T. (2012). Technical Note: Downscaling RCM precipitation to the station scale using statistical transformations – a comparison of methods, *Hydrol. Earth Syst. Sci.*, 16, 3383–3390, https://doi.org/10.5194/hess-16-3383-2012.

Gudmundsson, L. (2016). qmap: Statistical transformations for post-processing climate model output. R package version 1.0-4.

Habets, F., Boé, J., Déqué, M., Ducharne, A., Gascoin, S., Hachour, A., Martin, E., Pagé, C., Sauquet, E., Terray, L., Thiéry, D., Oudin, L., and Viennot, P. (2013). Impact of climate change on the hydrogeology of two basins in northern France. *Climatic Change*, 121: 771-785. DOI 10.1007/s10584-013-0934-x

Hróðmarsson, H.B., and Þórarinsdóttir, T. (2018). Flóð íslanskra vatnsfalla, Flóðagreining rennslisraða. VÍ-2018-003 report, 144 pp. Veðurstofa Íslands.

IPCC, 2021: Summary for Policymakers. In: *Climate Change 2021: The Physical Science Basis. Contribution of Working Group I to the Sixth Assessment Report of the Intergovernmental Panel on Climate Change.* (2021). Masson-Delmotte, V., P. Zhai, A. Pirani, S.L. Connors, C. Péan, S. Berger, N. Caud, Y. Chen, L. Goldfarb, M.I. Gomis, M. Huang, K. Leitzell, E. Lonnoy, J.B.R. Matthews, T.K. Maycock, T. Waterfield, O. Yelekçi, R. Yu, and B. Zhou (eds.). Cambridge University Press, Cambridge, United Kingdom and New York, NY, USA, pp. 3−32, doi:10.1017/9781009157896.001.

Jacob, D., Elizalde, A., Haensler, A., Hagemann, S., Kumar, P., Podzun, R., Rechid, D., Remedio, A.R., Saeed, F., Sieck, K., Teichmann, C., and Wilhelm, C. (2012). Assessing the transferability of the regional climate model REMO to different coordinated regional climate downscaling experiment (CORDEX) regions. *Atmosphere* 3(1): 181-199. https://doi.org/10.3390/atmos3010181.

Jacob, D., Petersen, J., Eggert, B., Alias, A., Christensen, O.B., Bouwer, L.M., Braun, A., Colette, A., Déqué, M., Georgievski, G., Georgopoulou, E., Gobiet, A., Menut, L., Nikulin, G., Haensler, A., Hempelmann, N., Jones, C., Keuler, K., Kovats, S., Kröner, N., Kotlarski, S., Kriegsmann, A., Martin, E., van Meijgaard, E., Moseley, C., Pfeifer, S., Preuschmann, S., Radermacher, C., Radtke, K., Rechid, D., Rounsevell, M., Samuelsson, P., Somot, S., Soussana, J.-F., Teichmann, C., Valentini, R., Vautard, R., Weber, B., and Yiou, P. (2014). EURO-CORDEX: new high-resolution climate change projections for European impact research. *Reg Environ Change* 14:563–578. https://doi.org/10.1007/s10113-013-0499-2.

Jones, C. D., Hughes, J. K., Bellouin, N., Hardiman, S. C., Jones, G. S., Knight, J., Liddicoat, S., O'Connor, F. M., Andres, R. J., Bell, C., Boo, K.-O., Bozzo, A., Butchart, N., Cadule, P., Corbin, K. D., Doutriaux-Boucher, M., Friedlingstein, P., Gornall, J., Gray, L., Halloran, P. R., Hurtt, G., Ingram, W. J., Lamarque, J.-F., Law, R. M., Meinshausen, M., Osprey, S., Palin, E. J., Parsons, Chini, L., Raddatz, T., Sanderson, M. G., Sellar, A. A., Schurer, A., Valdes, P., Wood, N., Woodward, S., Yoshioka, M., and Zerroukat, M. (2011). The HadGEM2-ES implementation of CMIP5 centennial simulations. *Geosci. Model Dev*., 4, 543-570. doi:10.5194/gmd-4-543-2011.

Jóhannesson, T., and co-authors (2007). Effect of climate change on hydrology and hydro-resources in Iceland. OS-2007/011, 91 pp.

Kupiainen, M., Samuelsson, P., Jones, C., Jansson, C., Willén, U., Hansson, U., Ullerstig, A., Wang, S., and Döscher, R. (2011). Rossby Centre regional atmospheric model, RCA4. Rossby Centre Newsletter.

Lane, R.A., and Kay, A.L. (2021). Climate change impact on the magnitude and timing of hydrological extremes across Great Britain. *Front. Water, 3:684982*, https://doi.org/10.3389/frwa.2021.684982.

Lindström, G., Pers, C., Rosberg, J., Strömqvist, J. and Arheimer, B. (2010). Development and testing of the HYPE (Hydrological Predictions for the Environment) water quality model for different spatial scales. *Hydrol. Res.*, 41, 3-4, 295-319.

Massad, A.G. R., Þórarinsdóttir, T. and Roberts, M.J (2022). Design-flood estimates from daily runoff simulations using the Icelandic Reanalysis (ICRA): a first step towards estimating extremes in ungauged catchments. Technical report AGM/ofl/2022-01, 41 pp. Veðurstofa Íslands.

Nash, J.E., and Sutcliffe, J.V. (1970). River flow forecasting through conceptual models part I - A discussion of principles. *J. Hydrol.*, 10 (3), 282-290. doi:10.1016/0022-1694(70)90255-6.

Nawri, N., Pálmason, B., Petersen, G.N., Björnsson, H., and Þorsteinsson, S. (2017). The ICRA atmospheric reanalysis project for Iceland. VÍ Report, 2017-005. Veðurstofa Íslands.

Naz, B.S., Kao, S.C, Ashfaq, M., Rastogi, D., Mei, R., and Bowling, L.C. (2016). Regional hydrologic response to climate change in the conterminous United States using high-resolution hydroclimate simulations. *Glob. Planet. Chang.,* 143, 100-117.

Osuch, M., Romanowicz, R., and Wong, W.K. (2018). Analysis of low flow indices under varying climatic conditions in Poland. *Hydrol. Res.*, 49 (2), 373-389, https://doi.org/10.2166/nh.2017.021.

Porter, C., Morin, P., Howat, I., Noh, M.-J., Bates, B., Peterman, K, Keesey, S., Schlenk, M., Gardiner, J., Tomko, K., Willis, M., Kelleher, C., Cloutier, M., Husby, E., Foga, S., Nakamura, H., Platson, M., Wethington, M. Jr., Williamson, C., Bauer, G., Enos, J., Arnold, G., Kramer, W., Becker, P., Doshi, A., D'Souza, C., Cummens, P., Laurier, F., and Bojesen, M. (2018). "ArcticDEM", https://doi.org/10.7910/DVN/OHHUKH, Harvard Dataverse, V1, [Accessed Nov. 2019].

R Core Team (2016). R: A language and environment for statistical computing. R Foundation for Statistical Computing, Vienna, Austria. URL https://www.R-project.org/.

Rockel, B., Will, A., and Hense, A. (2008). The regional climate model COSMO-CLM (CCLM). *Meteorol Z,* 17(4), 347–348. doi:10.1127/0941-2948/2008/0309.

Samuelsson, P., Jones, C., Willén, U., Ullerstig, A., Gollvik, S., Hansson, U., Jansson, C., Kjellström, E., Nikulin, G., and Wyser, K. (2011). The Rossby Centre Regional Climate Model RCA3: model description and performance. *Tellus* 63A. doi:10.1111/j.1600-0870.2010.00478.x.

Somers, L.D., McKenzie, J.M., Mark, B.G., Lagos, P., Ng., G-H. C., Wickert, A.D., Yarleque, C., Baraër, M., and Silva, Y. (2019). Groundwater buffers decreasing glacier melt in an Andean watershed—but not forever. *Geophysical Research Letters*, 46 (22), 13016-13026, https://doi.org/10.1029/2019GL084730.

Stephenson, A.G. (2002). evd: Extreme Value Distributions. R News, 2(2):31-32, June 2002. URL: http://CRAN.R-project.org/doc/Rnews/.

van Meijgaard, E., van Ulft, L.H., Lenderink, G., de Roode, S.R., Wipfler, L., Boers, R., and Timmermans, R.M.A. (2012). Refinement and application of a regional atmospheric model for climate scenario calculations of Western Europe. Climate changes Spatial Planning publication: KvR 054/12, ISBN/EAN 978-90-8815-046-3, pp 44.

Velázquez, J. A., Schmid, J., Ricard, S., Muerth, M. J., Gauvin St- Denis, B., Minville, M., Chaumont, D., Caya, D., Ludwig, R., and Turcotte, R. (2013). An ensemble approach to assess hydrological models' contribution to uncertainties in the analysis of climate change impact on water resources, Hydrol. Earth Syst. Sci., 17, 565–578, doi:10.5194/hess-17-565-2013.

Vetter, T., Huang, S., Aich, V., Yang, T., Wang. X., Krysanova, V., and Hattermann, F. (2015). Multi-model climate impact assessment and intercomparison for three large-scale river basins on three continents. *Earth Syst. Dynam.*, 6, 17-43, https://doi.org/10.5194/esd-6-17-2015.

Vormoor, K., Lawrence, D., Heistermann, M., and Bronstert, A. (2015). Climate change impacts on the seasonality and generation processes of floods – projections and uncertainties for catchments with mixed snowmelt/rainfall regimes. *Hydrol. Earth Syst. Sci.*, 19, 913-931, doi:10.5194/hess-19-913-2015.

Wan, W, Zhao, J., Li, H.-Y., Mishra, A., Hejazi, M., Lu, H., Demissie, Y., and Wang, H. (2018). A holistic view of water management impacts on future droughts: A global multimodel analysis. *J. Geophys. Res.: Atmospheres*, 123, 5947-5972, https://doi.org/10.1029/2017JD027825.

Wanders, N., and Wada, Y. (2015). Human and climate impacts on the 21st century hydrological drought. *J. Hydrol,* 526, 208-220, https://doi.org/10.1016/j.jhydrol.2014.10.047.

Zhao, Q., Ding, Y., Wang, J., Gao, H., Zhang, S., Zhao, C., Xu, J., Han, H., and Shangguan, D. (2019). Projecting climate change impacts on hydrological processes on the Tibetan Plateau with model calibration against the glacier inventory data and observed streamflow. *J. Hydrol.*, 573, 60-81.

Appendix 1

Observed versus simulated Annual Maximum Floods

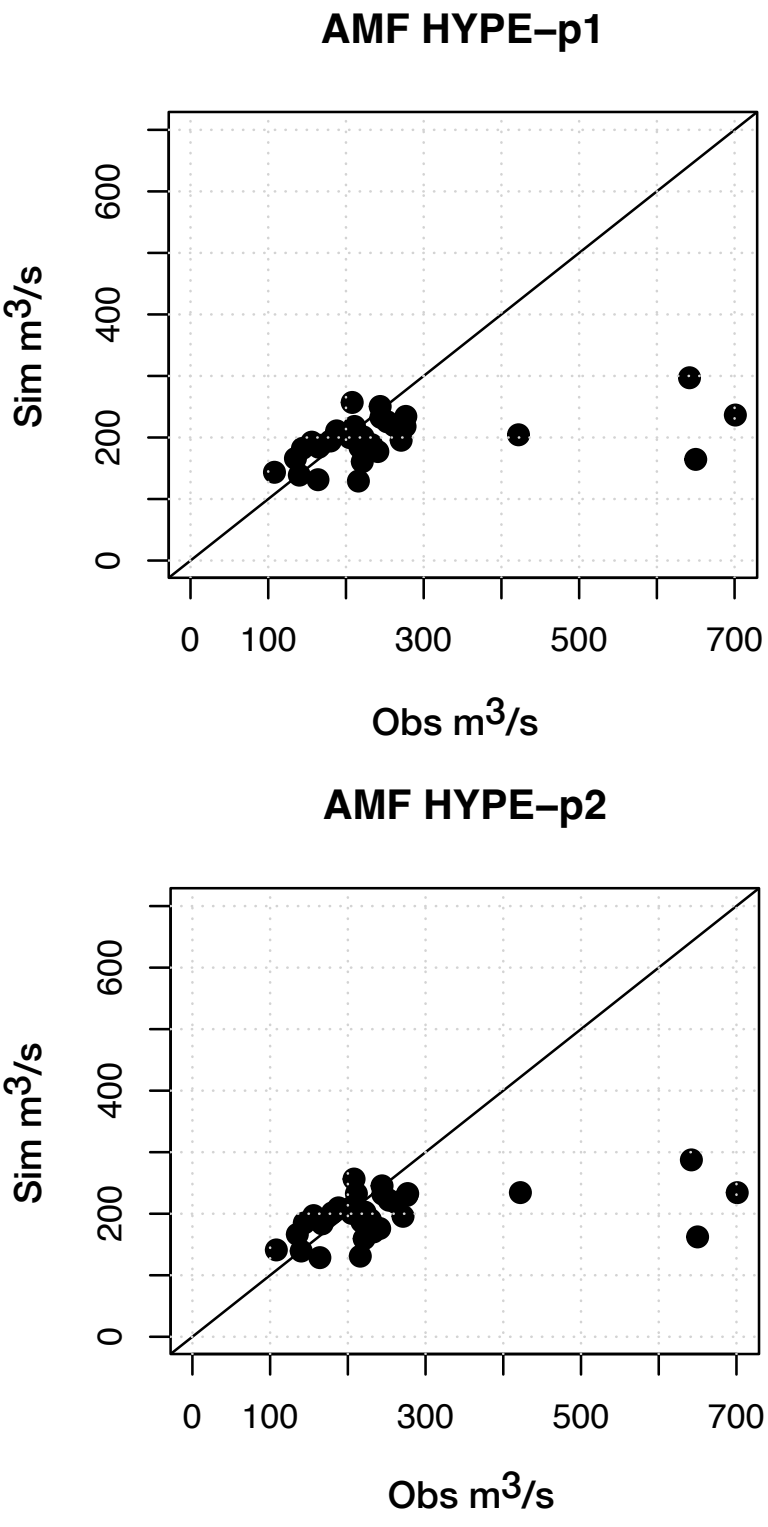

Fig. I-1: Catchment vhm233: Simulated vs. observed AMFs in the water years 1981-2016. Top: HYPE with parameter set calibrated in 1996-2002. Bottom: HYPE with parameter set calibrated in 2003-2009.

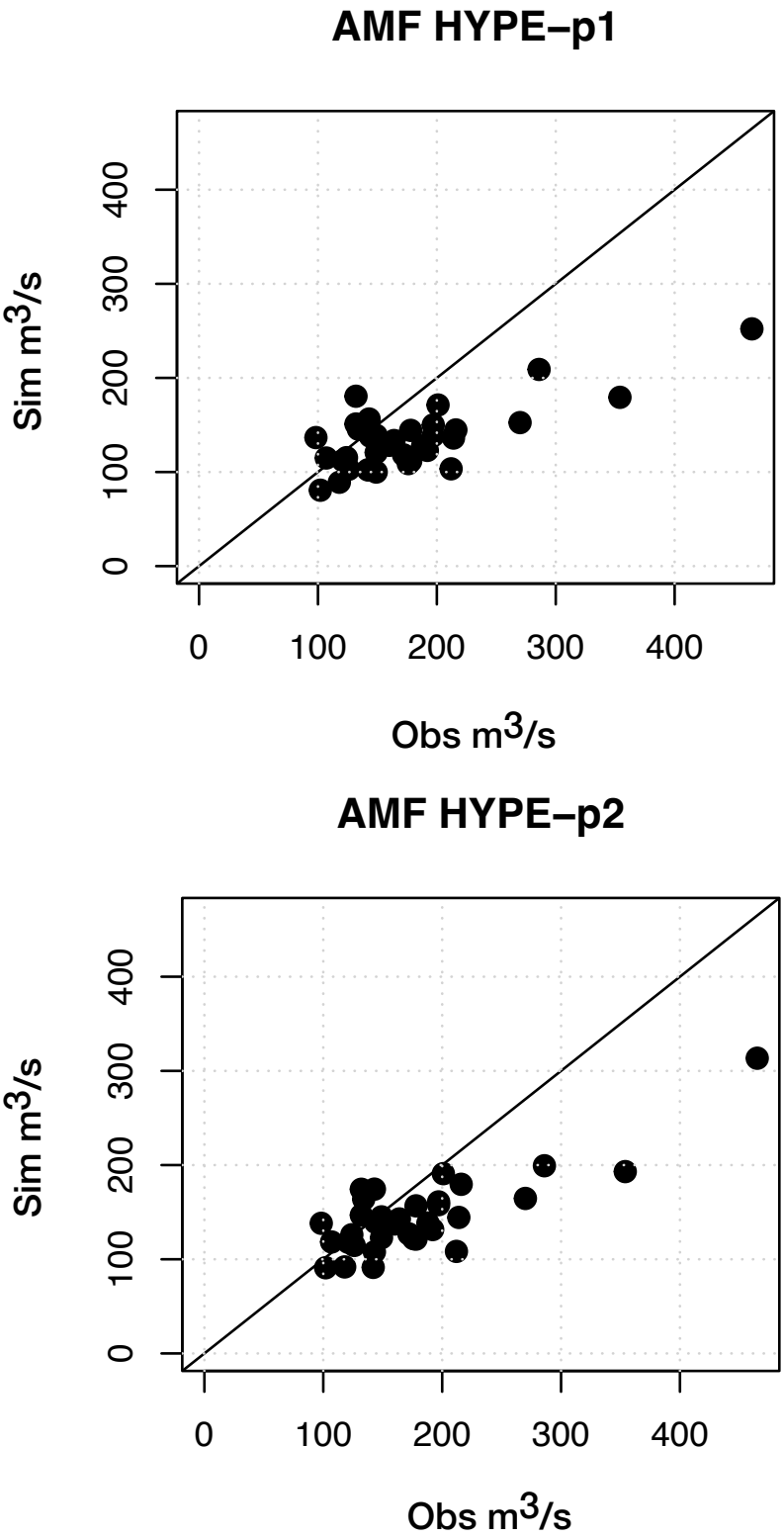

Fig. I-2: Catchment vhm218: Simulated vs. observed AMFs in the water years 1981-2016. Top: HYPE with parameter set calibrated in 1996-2002. Bottom: HYPE with parameter set calibrated in 2003-2009.

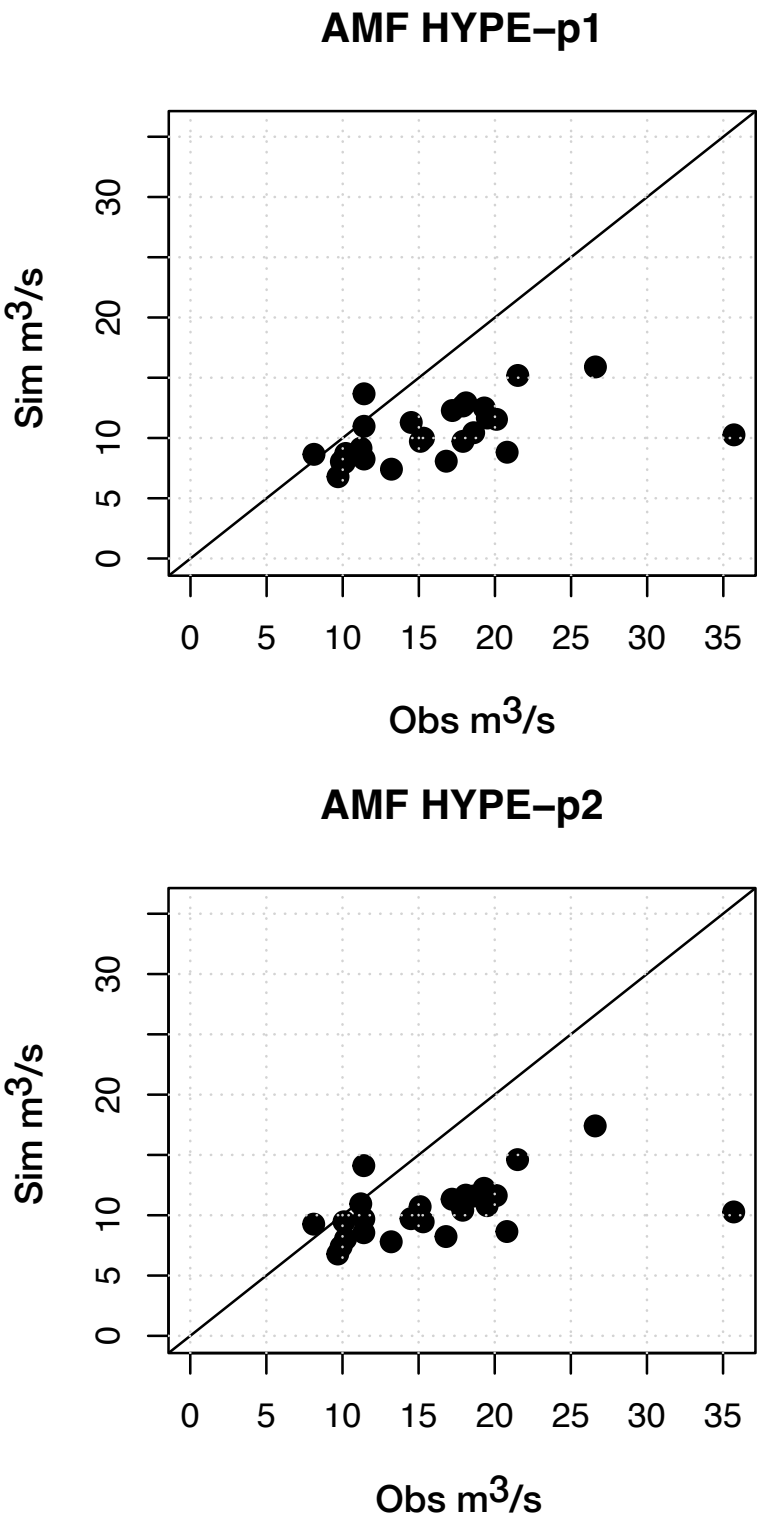

Fig. I-3: Catchment vhm38: Simulated vs. observed AMFs in the water years 1981-2016. Top: HYPE with parameter set calibrated in 1996-2002. Bottom: HYPE with parameter set calibrated in 2003-2009.

Appendix 2

CORDEX air temperature evaluation series: Error statistics before and after local adjustment

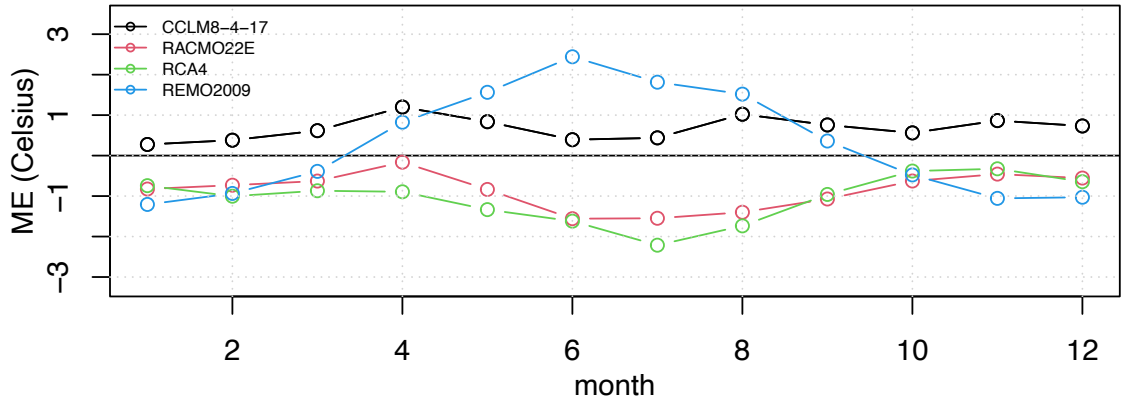

Fig. II-1: Catchment vhm233: Mean error (ME) between original CORDEX evaluation air temperature and ICRA air temperature. Period 1989-2008. Each colour corresponds to a RCM (cf. Table 3). The month=1 for January and 12 for December.

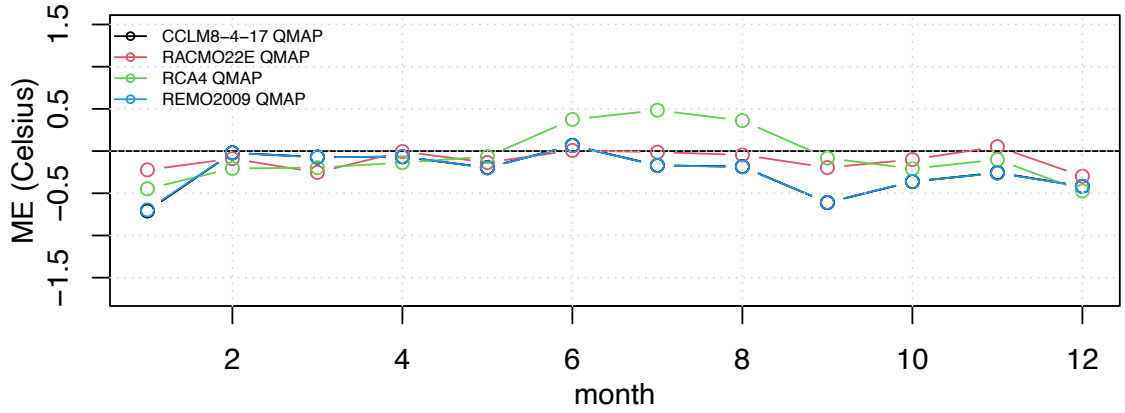

Fig. II-2: Catchment vhm233: Mean error (ME) between locally-adjusted CORDEX evaluation air temperature and ICRA air temperature. Period 1989-2008. The month=1 for January and 12 for December.

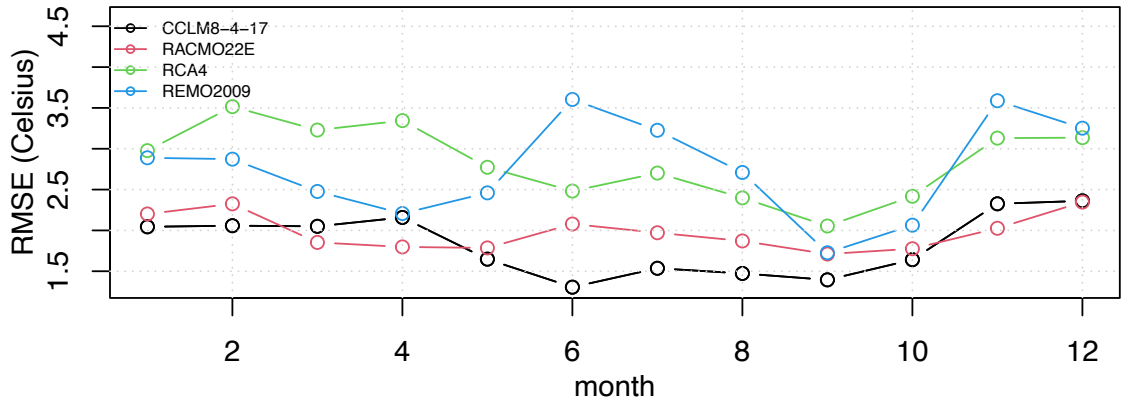

Fig. II-3: Catchment vhm233: Root-mean-square-error (RMSE) between original CORDEX evaluation air temperature and ICRA air temperature. Period 1989-2008. Each colour corresponds to a RCM (cf. Table 3). The month=1 for January and 12 for December.

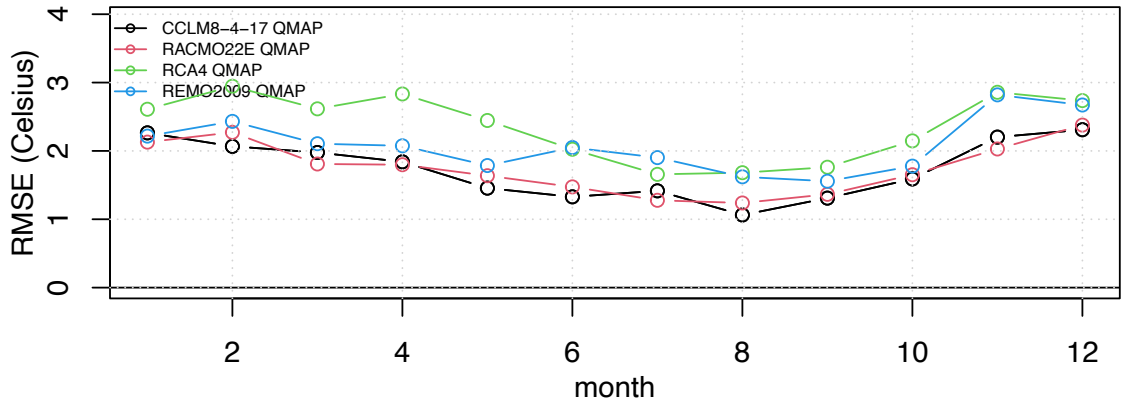

Fig. II-4: Catchment vhm233: Root-mean-square-error (RMSE) between locally-adjusted CORDEX evaluation air temperature and ICRA air temperature. Period 1989-2008. The month=1 for January and 12 for December.

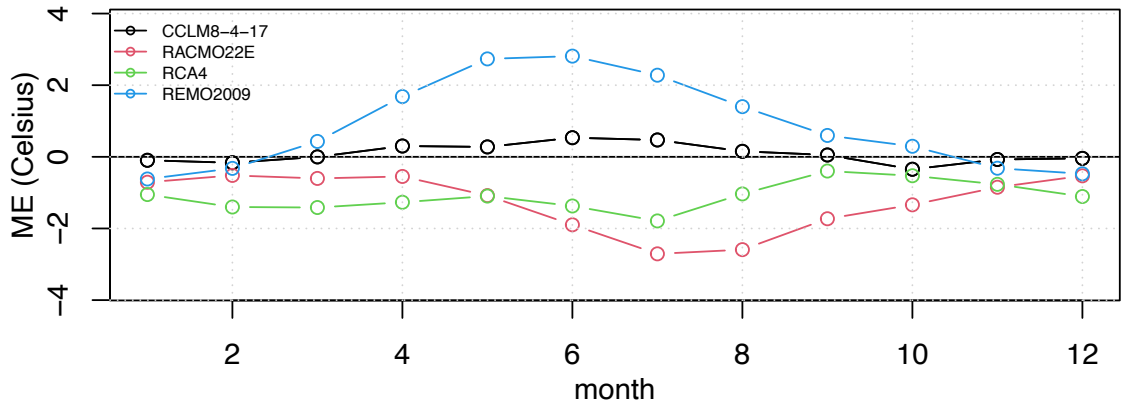

Fig. II-5: Catchment vhm218: Mean error (ME) between original CORDEX evaluation air temperature and ICRA air temperature. Period 1989-2008. Each colour corresponds to a RCM (cf. Table 3). The month=1 for January and 12 for December.

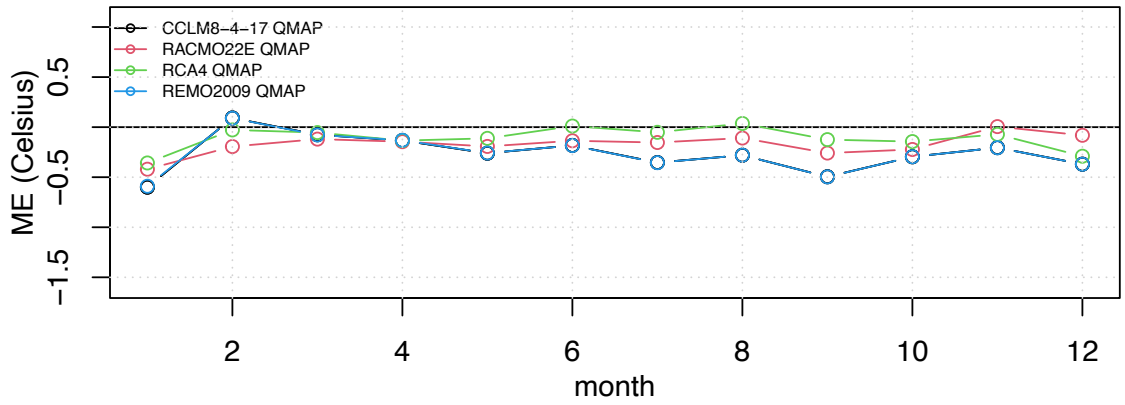

Fig. II-6: Catchment vhm218: Mean error (ME) between locally-adjusted CORDEX evaluation air temperature and ICRA air temperature. Period 1989-2008.The month=1 for January and 12 for December.

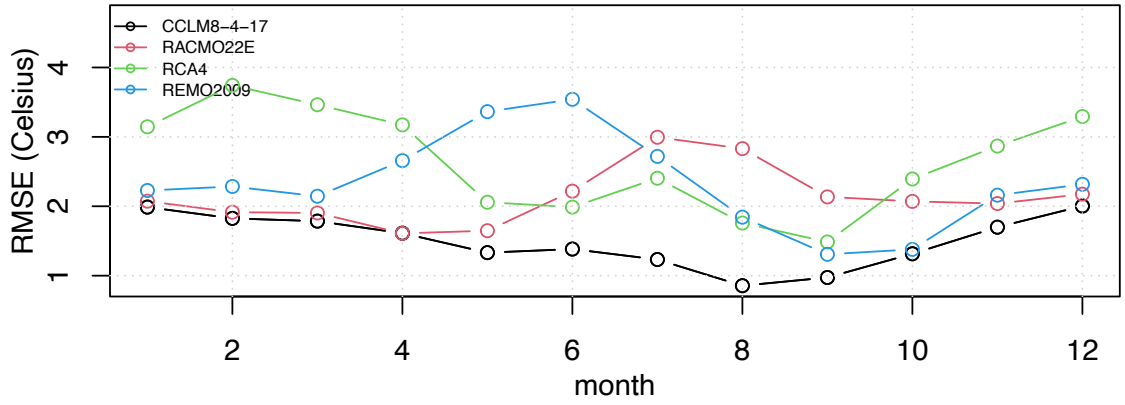

Fig. II-7: Catchment vhm218: Root-mean-square-error (RMSE) between original CORDEX evaluation air temperature and ICRA air temperature. Period 1989-2008. Each colour corresponds to a RCM (cf. Table 3). The month=1 for January and 12 for December.

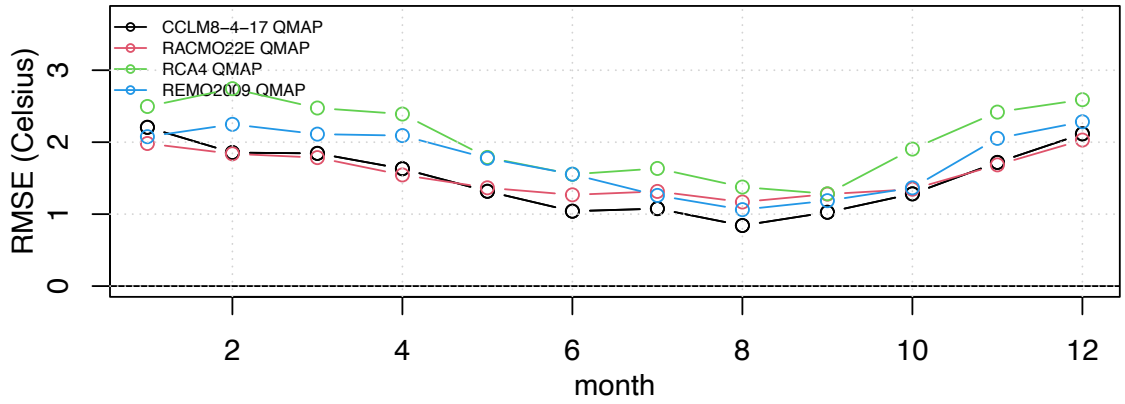

Fig. II-8: Catchment vhm218: Root-mean-square-error (RMSE) between locally-adjusted CORDEX evaluation air temperature and ICRA air temperature. Period 1989-2008. The month=1 for January and 12 for December.

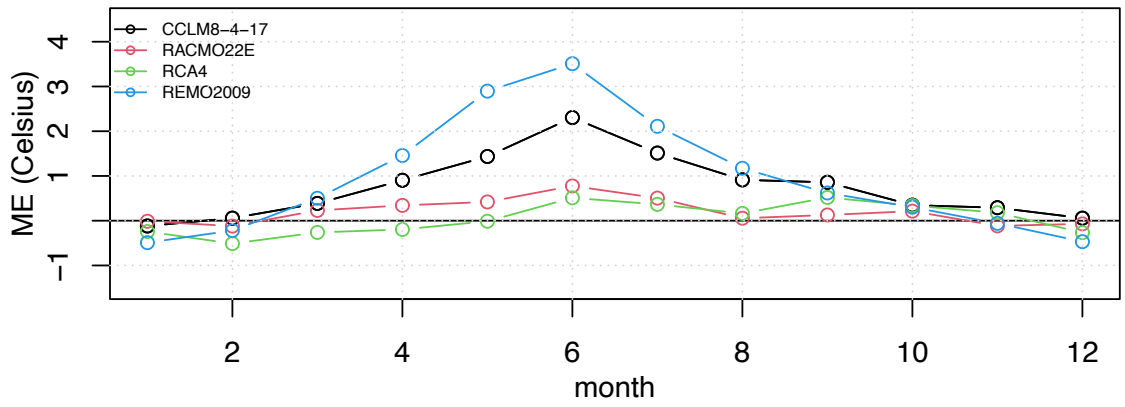

Fig. II-9: Catchment vhm38: Mean error (ME) between original CORDEX evaluation air temperature and ICRA air temperature. Period 1989-2008. Each colour corresponds to a RCM (cf. Table 3). The month=1 for January and 12 for December.

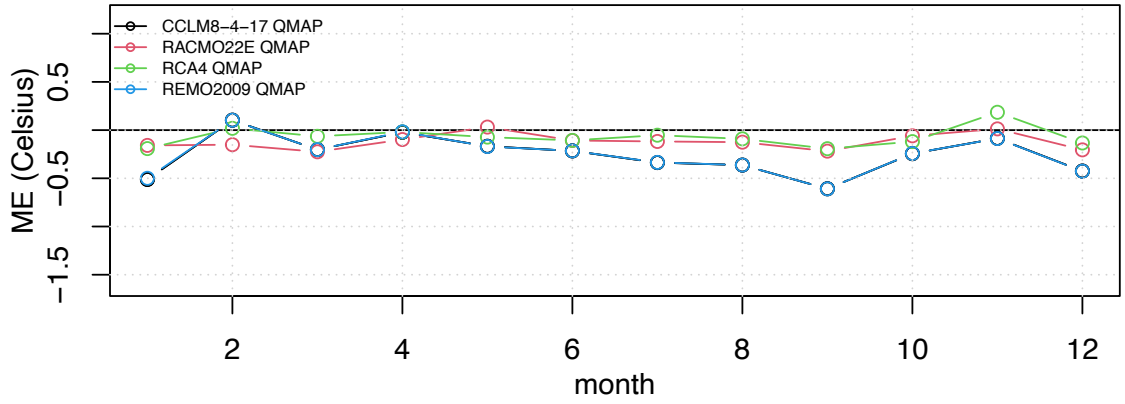

Fig. II-10: Catchment vhm38: Mean error (ME) between locally-adjusted CORDEX evaluation air temperature and ICRA air temperature. Period 1989-2008. The month=1 for January and 12 for December.

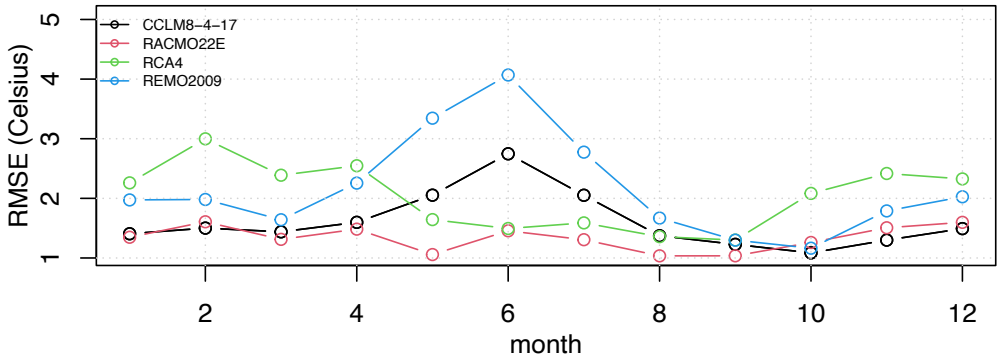

Fig. II-11: Catchment vhm38: Root-mean-square-error (RMSE) between original CORDEX evaluation air temperature and ICRA air temperature. Period 1989-2008. Each colour corresponds to a RCM (cf. Table 3). The month=1 for January and 12 for December.

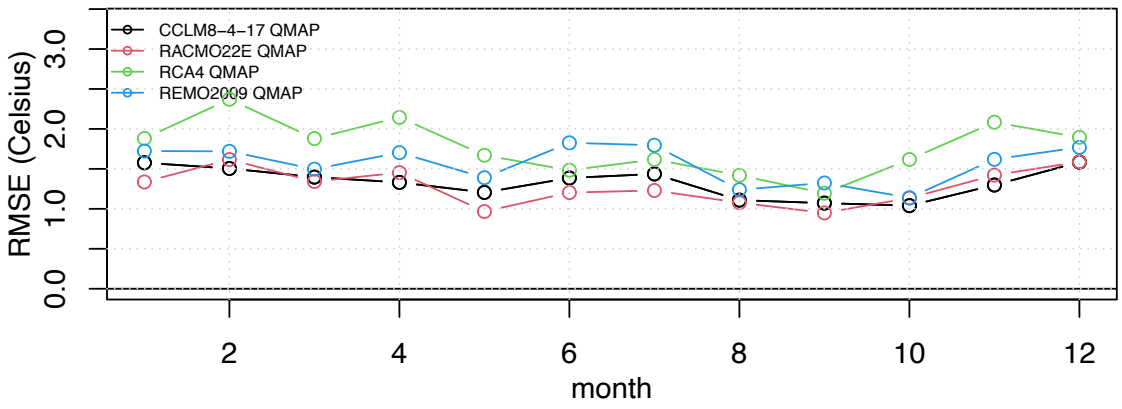

Fig. II-12: Catchment vhm38: Root-mean-square-error (RMSE) between locally-adjusted CORDEX evaluation air temperature and ICRA air temperature. Period 1989-2008. The month=1 for January and 12 for December.

Appendix 3

CORDEX precipitation evaluation series: Error statistics before and after local adjustment

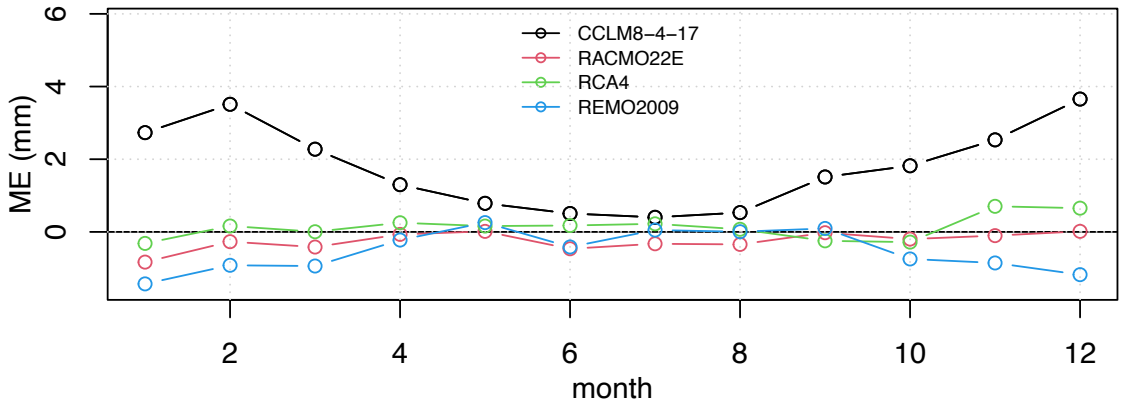

Fig. III-1: Catchment vhm233: Mean error (ME) between original CORDEX evaluation precipitation and ICRA precipitation (mm/d). Period 1989-2008. Each colour corresponds to a RCM (cf. Table 3). The month=1 for January and 12 for December.

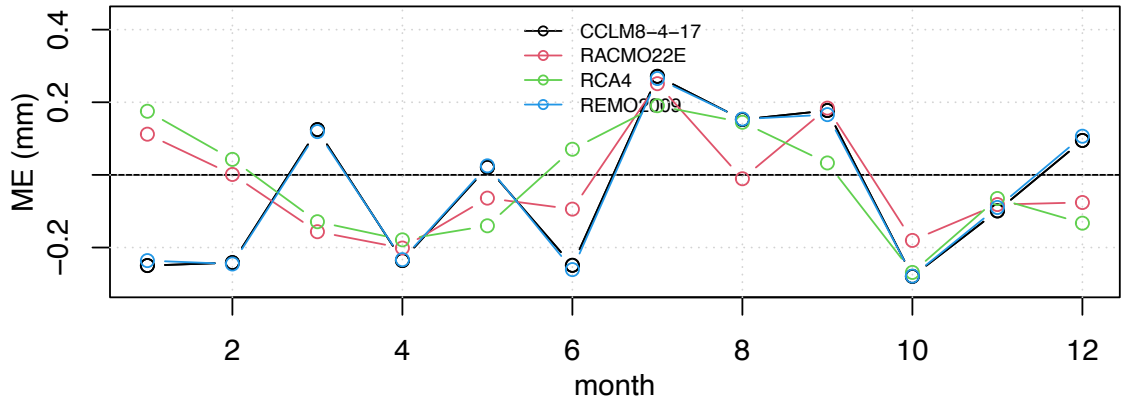

Fig. III-2: Catchment vhm233: Mean error (ME) between locally-adjusted CORDEX evaluation precipitation and ICRA precipitation (mm/d). Period 1989-2008. The month=1 for January and 12 for December.

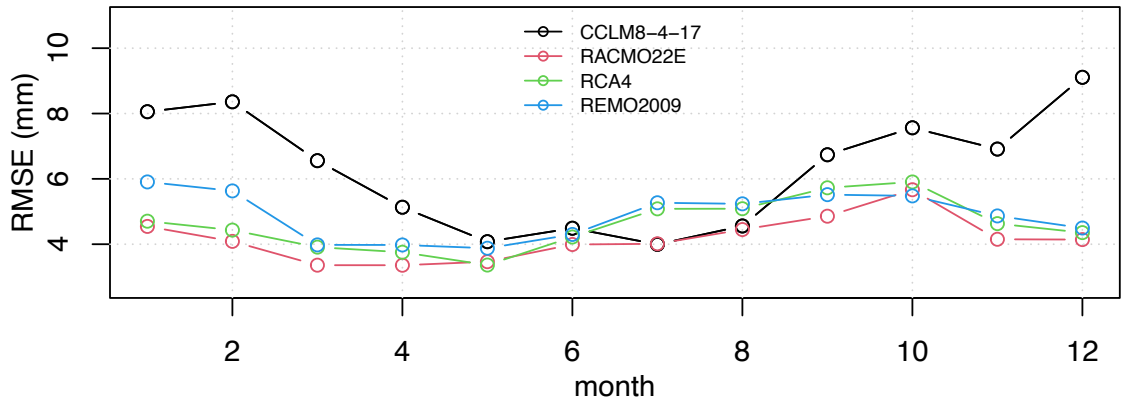

Fig. III-3: Catchment vhm233: Root-mean-square-error (RMSE) between original CORDEX evaluation precipitation and ICRA precipitation (mm/d). Period 1989-2008. Each colour corresponds to a RCM (cf. Table 3). The month=1 for January and 12 for December.

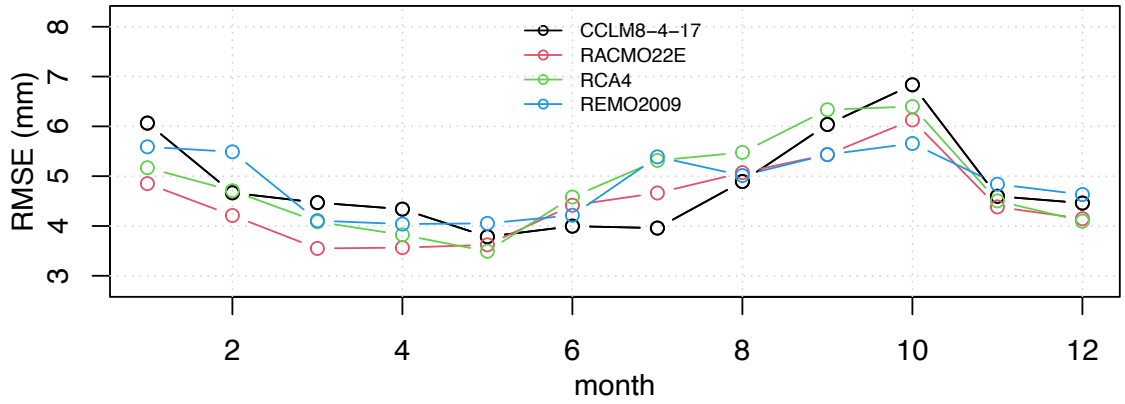

Fig. III-4: Catchment vhm233: Root-mean-square-error (RMSE) between locally-adjusted CORDEX evaluation precipitation and ICRA precipitation (mm/d). Period 1989-2008. The month=1 for January and 12 for December.

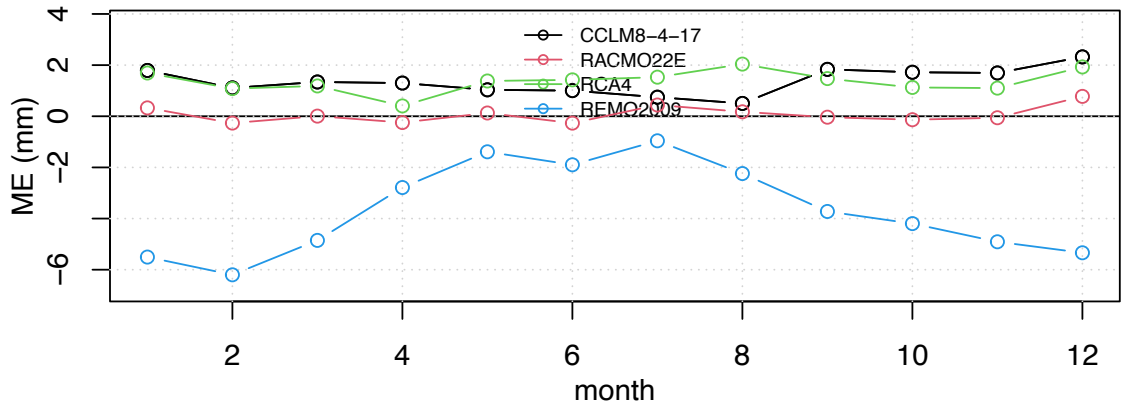

Fig. III-5: Catchment vhm218: Mean error (ME) between original CORDEX evaluation precipitation and ICRA precipitation (mm/d). Period 1989-2008. Each colour corresponds to a RCM (cf. Table 3). The month=1 for January and 12 for December.

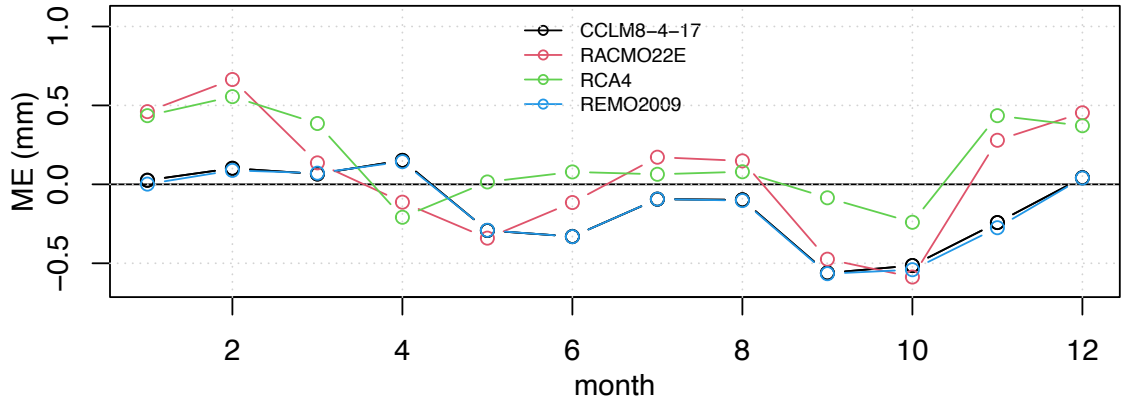

Fig. III-6: Catchment vhm218: Mean error (ME) between locally-adjusted CORDEX evaluation precipitation and ICRA precipitation (mm/d). Period 1989-2008. The month=1 for January and 12 for December.

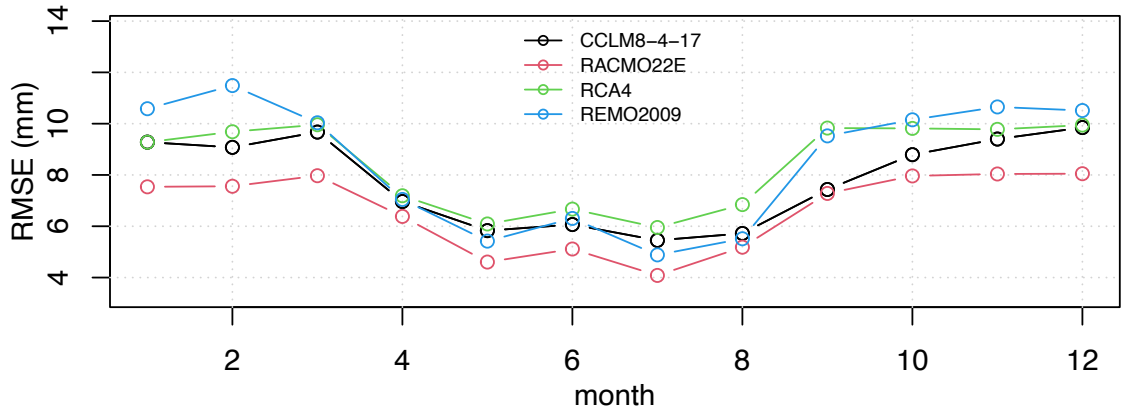

Fig. III-7: Catchment vhm218: Root-mean-square-error (RMSE) between original CORDEX evaluation precipitation and ICRA precipitation (mm/d). Period 1989-2008. Each colour corresponds to a RCM (cf. Table 3). The month=1 for January and 12 for December.

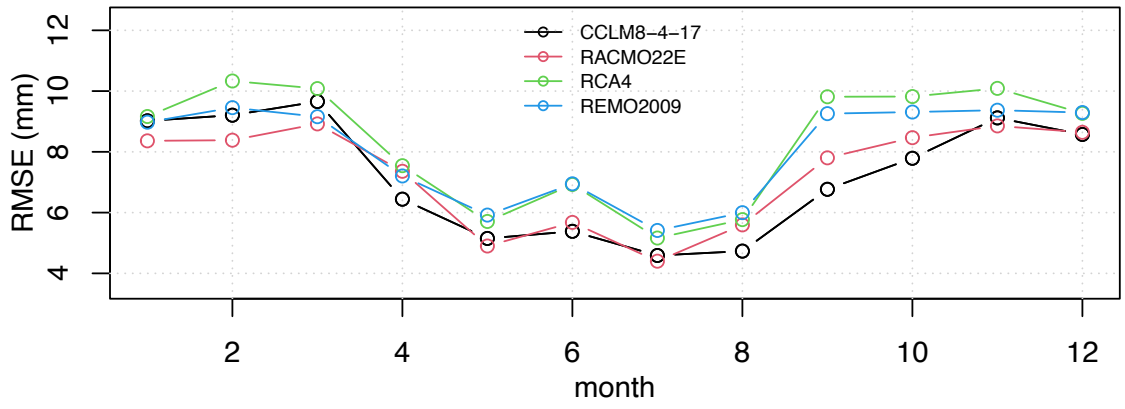

Fig. III-8: Catchment vhm218: Root-mean-square-error (RMSE) between locally-adjusted CORDEX evaluation precipitation and ICRA precipitation (mm/d). Period 1989-2008. The month=1 for January and 12 for December.

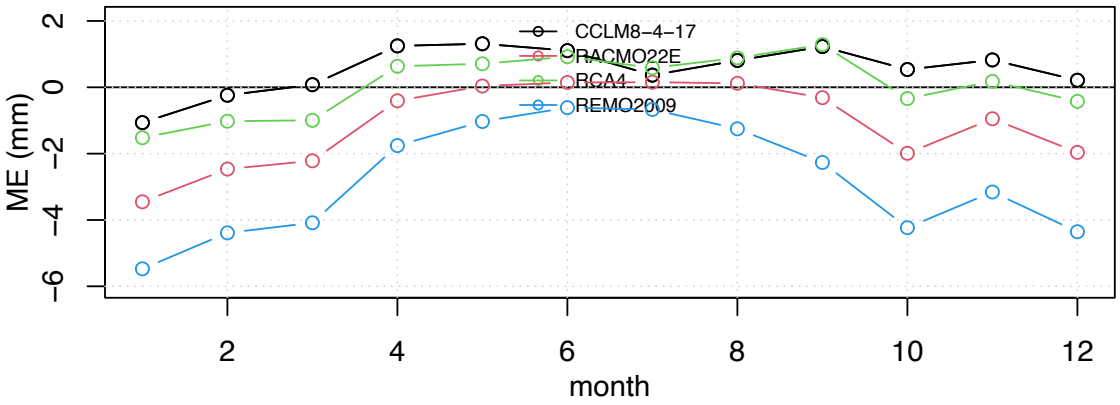

Fig. III-9: Catchment vhm38: Mean error (ME) between original CORDEX evaluation precipitation and ICRA precipitation (mm/d). Period 1989-2008. Each colour corresponds to a RCM (cf. Table 3). The month=1 for January and 12 for December.

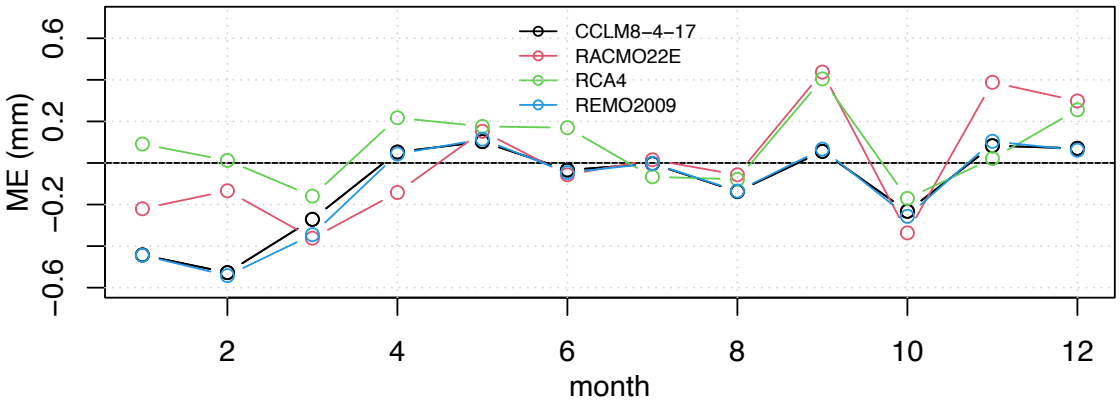

Fig. III-10: Catchment vhm38: Mean error (ME) between locally-adjusted CORDEX evaluation precipitation and ICRA precipitation (mm/d). Period 1989-2008. The month=1 for January and 12 for December.

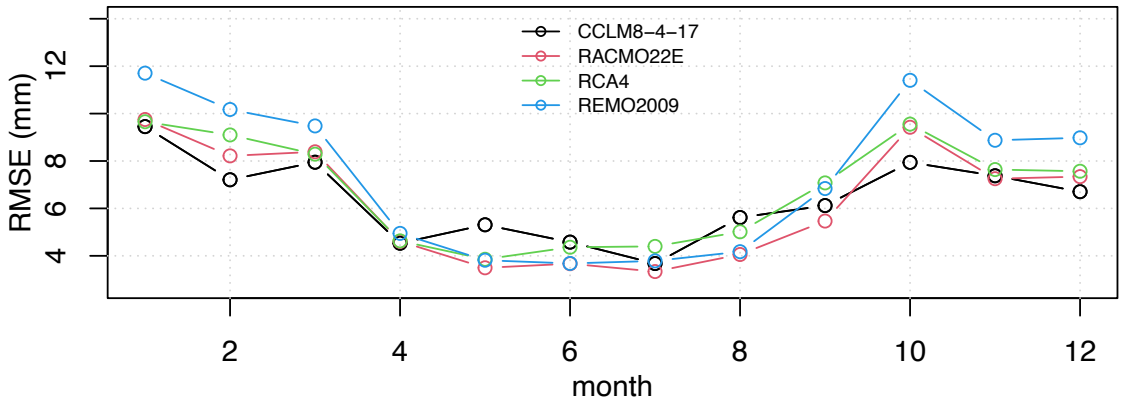

Fig. III-11: Catchment vhm38: Root-mean-square-error (RMSE) between original CORDEX evaluation precipitation and ICRA precipitation (mm/d). Period 1989-2008. Each colour corresponds to a RCM (cf. Table 3). The month=1 for January and 12 for December.

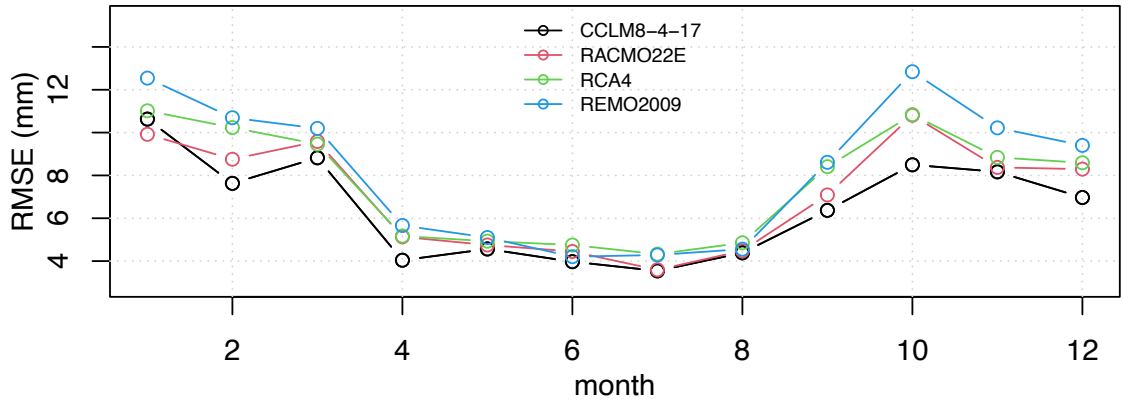

Fig. III-12: Catchment vhm38: Root-mean-square-error (RMSE) between locally-adjusted CORDEX evaluation precipitation and ICRA precipitation (mm/d). Period 1989-2008. The month=1 for January and 12 for December.

Appendix 4

Mean monthly near surface air temperature in the reference period (1981-2010)

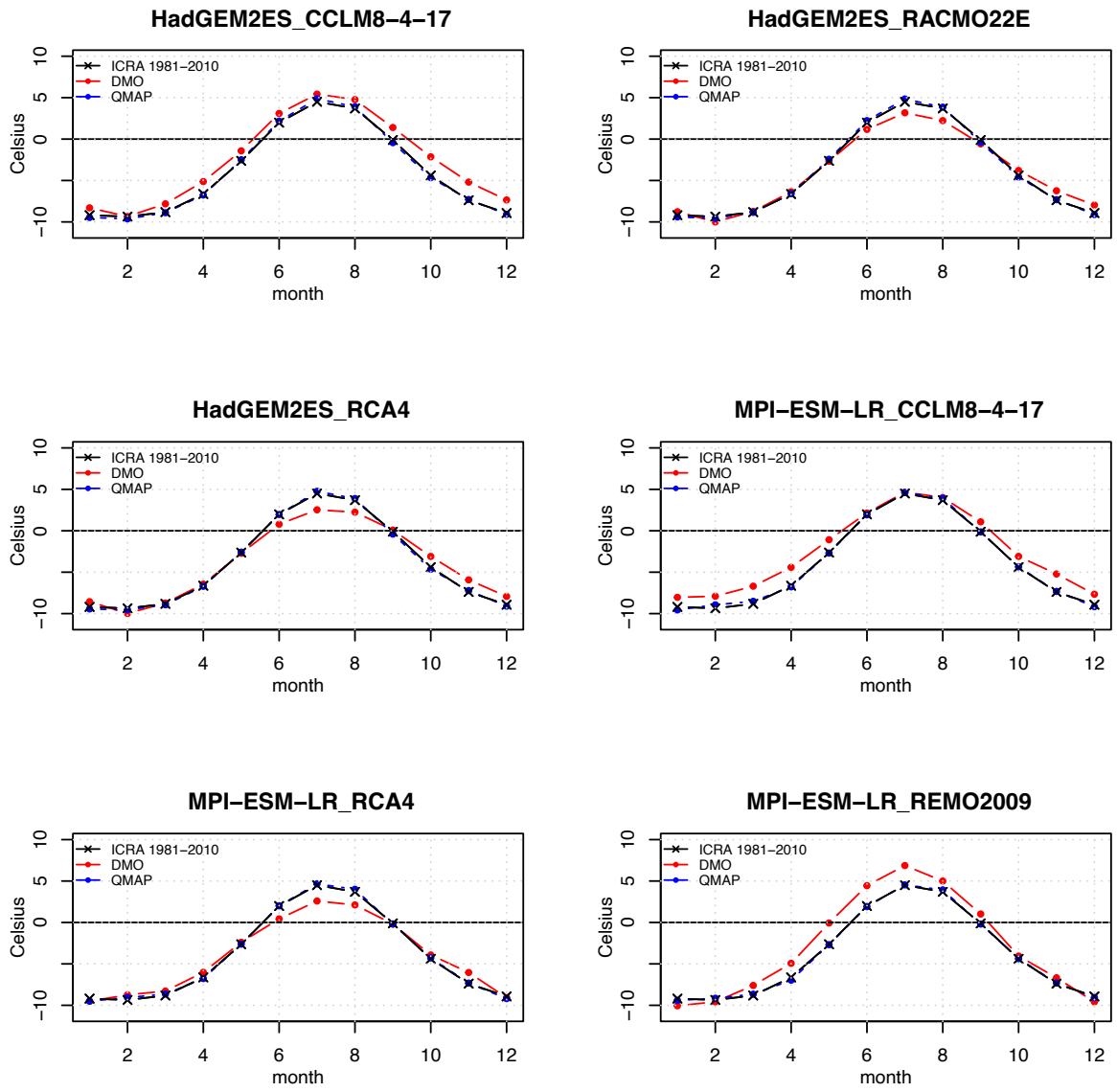

Fig. IV-1: Catchment vhm233: Mean monthly near surface air temperature in the reference period (1981-2010). Each panel corresponds to a GCM-RCM combination (cf. Table 3). ICRA-reference (black line), original CORDEX projections (red line), locally-adjusted CORDEX projections (blue line). For the CORDEX projections, the period 2006-2010 is taken from the RCP4.5 scenario. The month=1 for January and 12 for December.

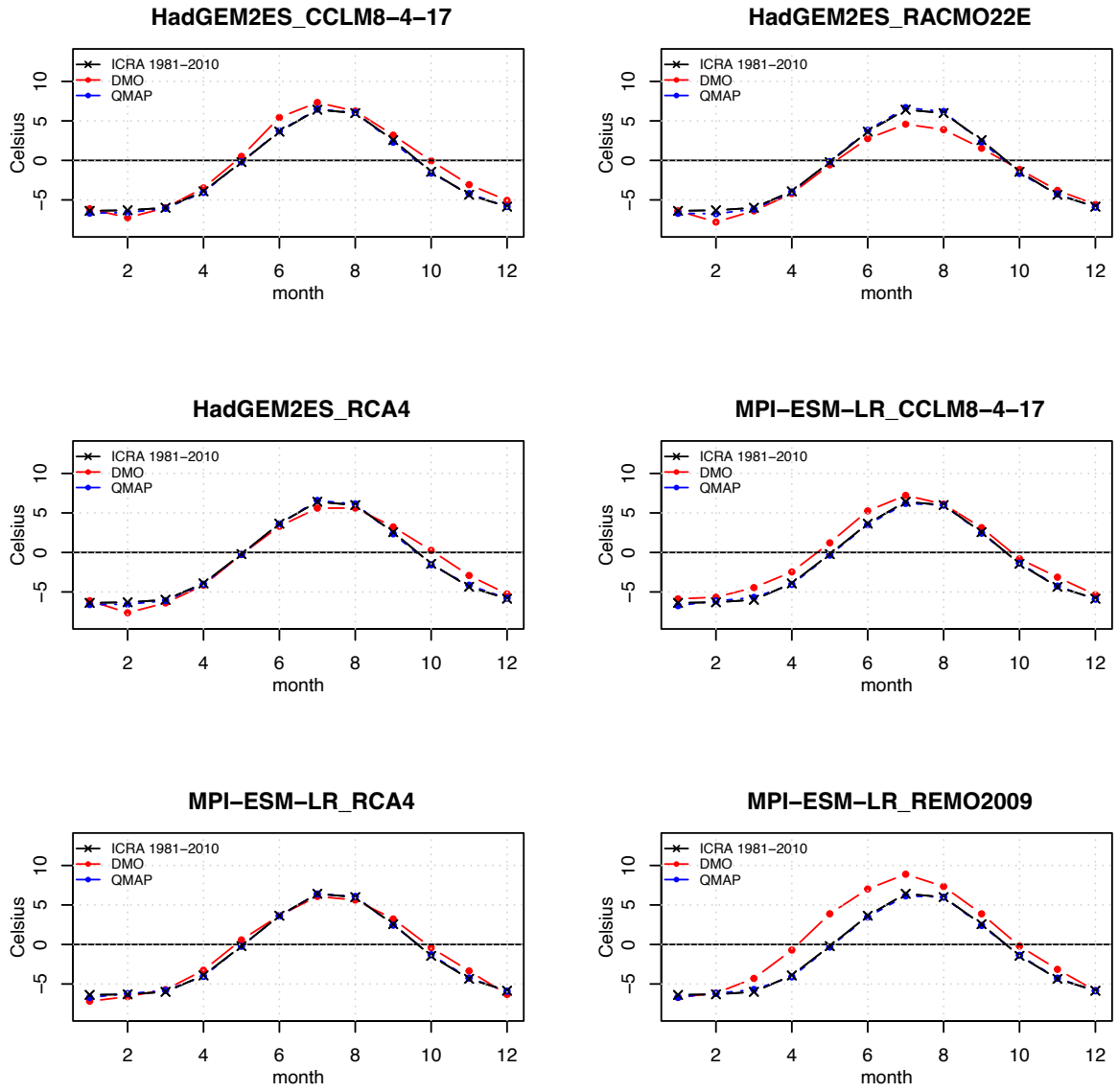

Fig. IV-2: Catchment vhm218: Mean monthly near surface air temperature in the reference period (1981-2010). Each panel corresponds to a GCM-RCM combination (cf. Table 3). ICRA-reference (black line), original CORDEX projections (red line), locally-adjusted CORDEX projections (blue line). For the CORDEX projections, the period 2006-2010 is taken from the RCP4.5 scenario. The month=1 for January and 12 for December.

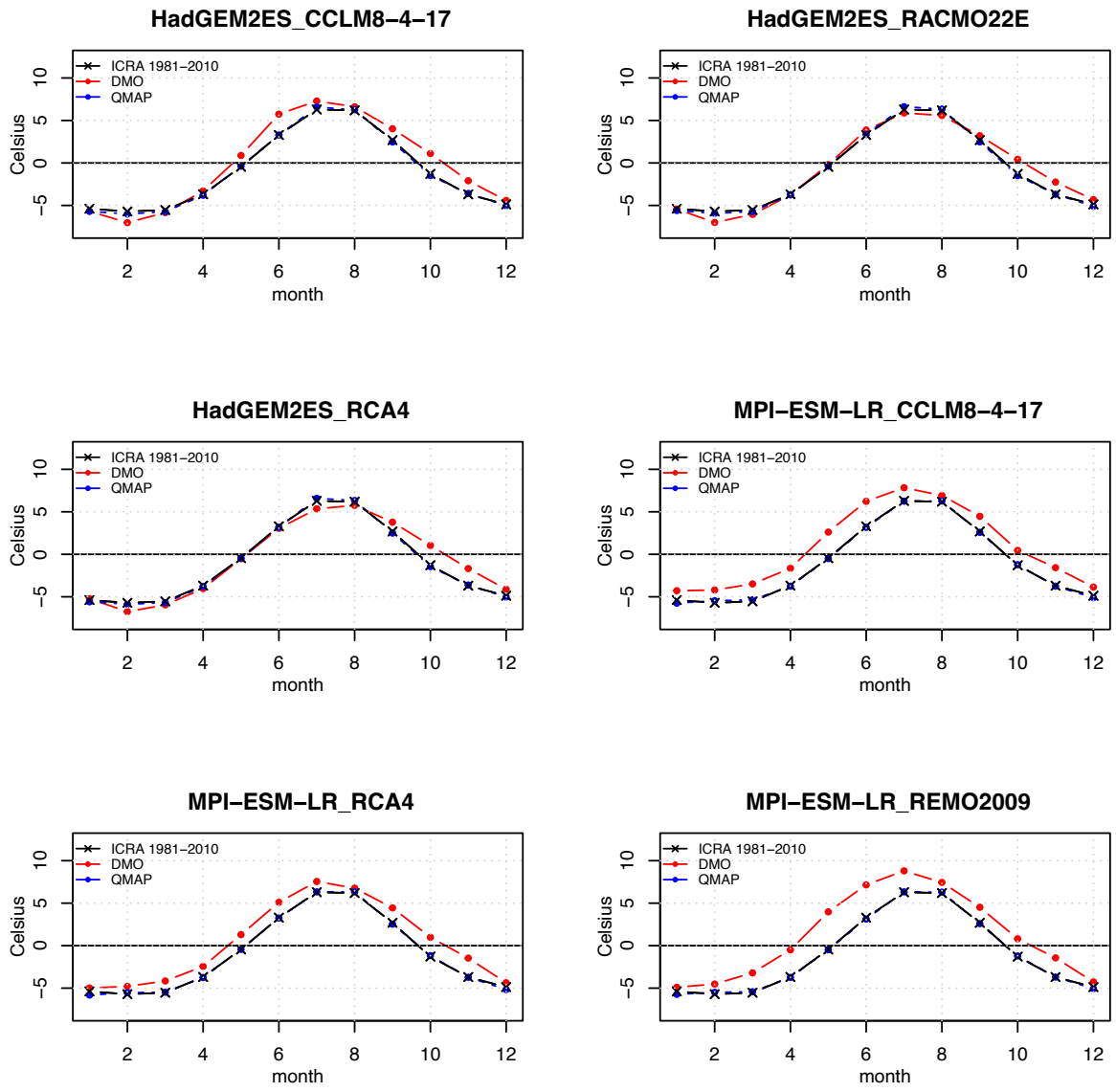

Fig. IV-3: Catchment vhm38: Mean monthly near surface air temperature in the reference period (1981-2010). Each panel corresponds to a GCM-RCM combination (cf. Table 3). ICRA-reference (black line), original CORDEX projections (red line), locally-adjusted CORDEX projections (blue line). For the CORDEX projections, the period 2006-2010 is taken from the RCP4.5 scenario. The month=1 for January and 12 for December.

Appendix 5

Mean monthly precipitation in the reference period (1981-2010)

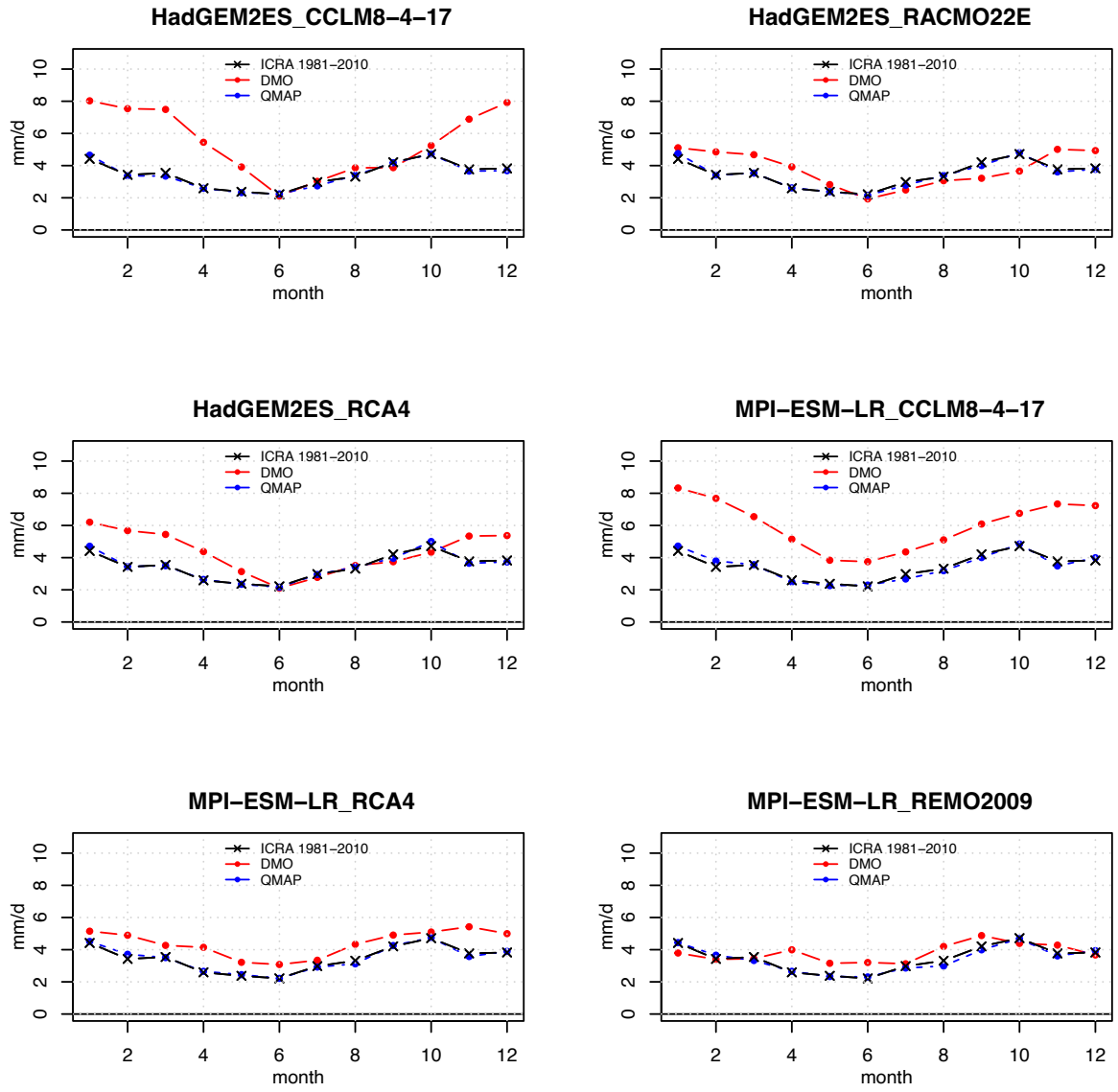

Fig. V-1: Catchment vhm233: Mean monthly precipitation (mm/d) in the reference period (1981-2010). Each panel corresponds to a GCM-RCM combination (cf. Table 3). ICRA-reference (black line), original CORDEX projections (red line), locally-adjusted CORDEX projections (blue line). For the CORDEX projections, the period 2006-2010 is taken from the RCP4.5 scenario. The month=1 for January and 12 for December.

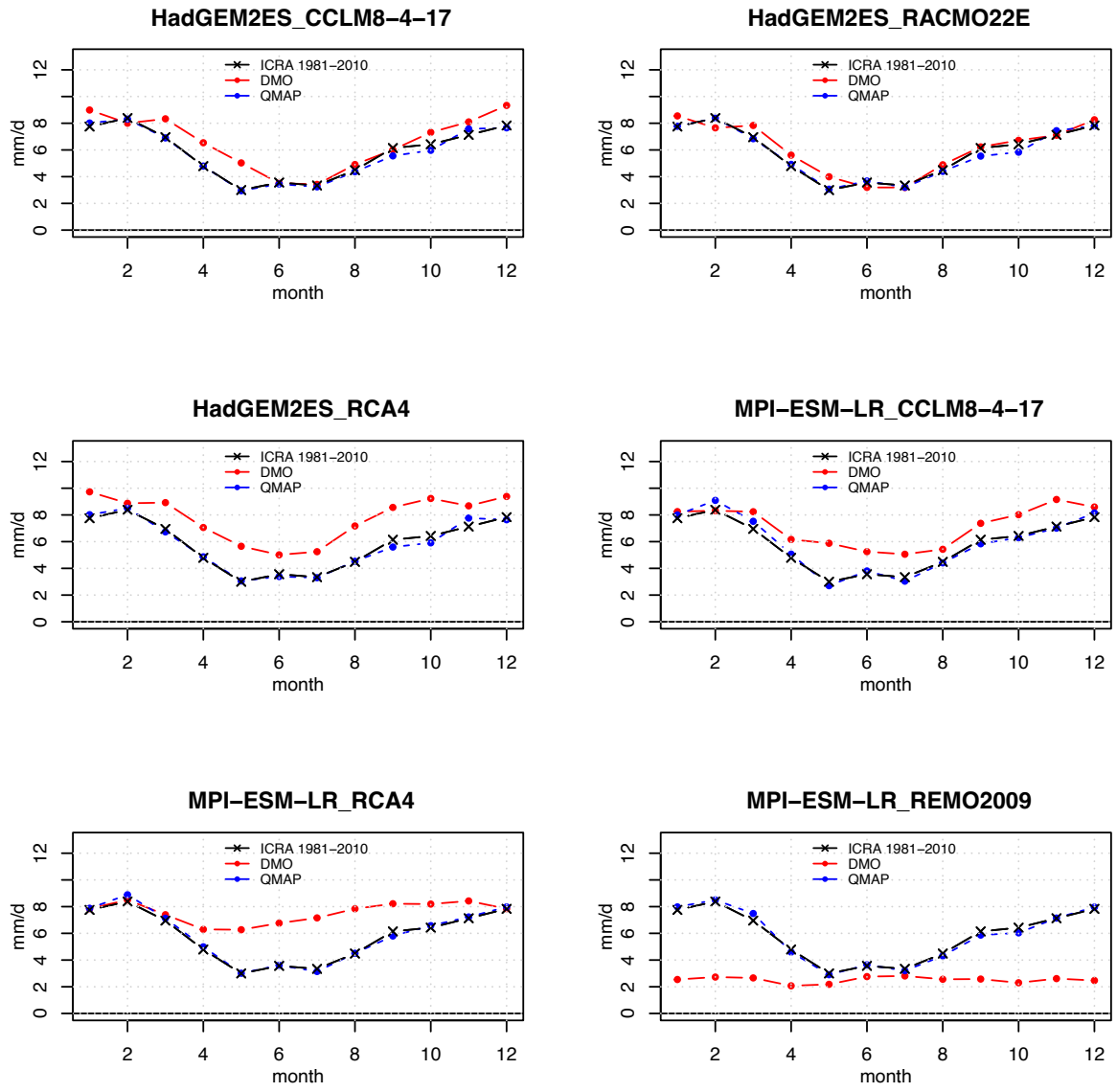

Fig. V-2: Catchment vhm218: Mean monthly precipitation (mm/d) in the reference period (1981-2010). Each panel corresponds to a GCM-RCM combination (cf. Table 3). ICRA-reference (black line), original CORDEX projections (red line), locally-adjusted CORDEX projections (blue line). For the CORDEX projections, the period 2006-2010 is taken from the RCP4.5 scenario. The month=1 for January and 12 for December.

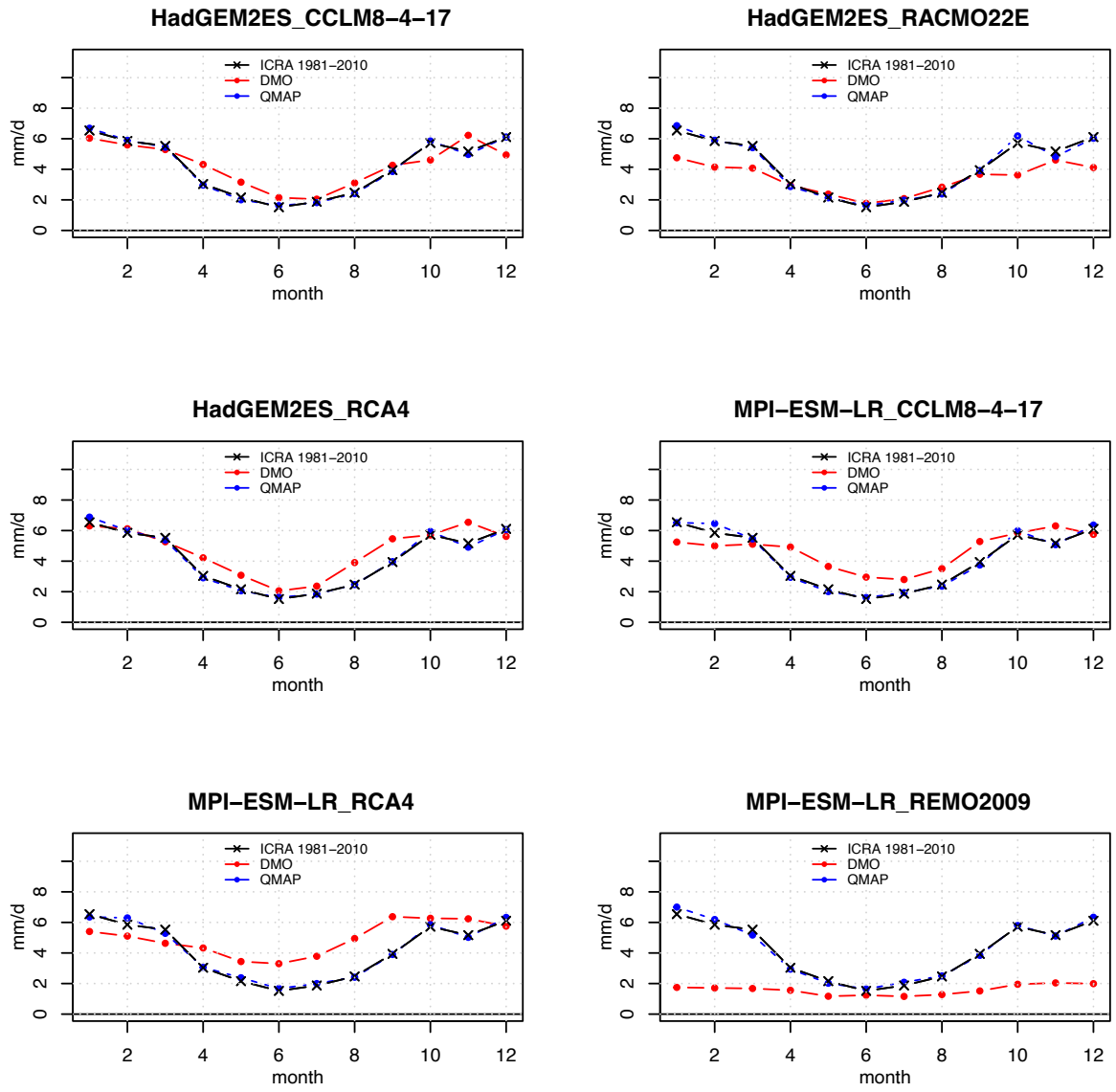

Fig. V-3: Catchment vhm38: Mean monthly precipitation (mm/d) in the reference period (1981-2010). Each panel corresponds to a GCM-RCM combination (cf. Table 3). ICRA-reference (black line), original CORDEX projections (red line), locally-adjusted CORDEX projections (blue line). For the CORDEX projections, the period 2006-2010 is taken from the RCP4.5 scenario. The month=1 for January and 12 for December.

Appendix 6

Projected locally-adjusted 30-year mean monthly near surface air temperature

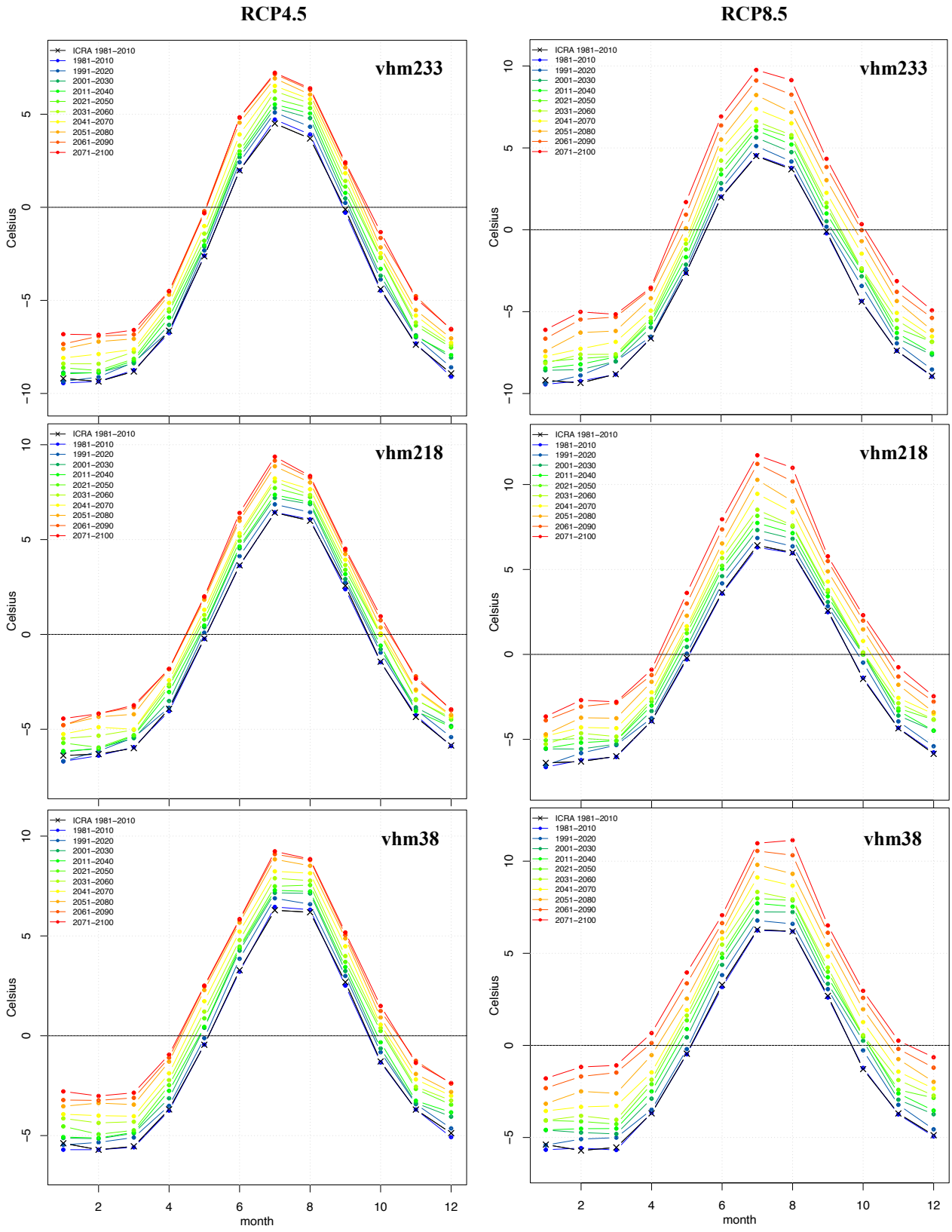

Fig. VI-1: Projected seasonality of mean monthly near surface air temperature (ensemble median) under the RCP4.5 emission scenario (left panel) and RCP8.5 emission scenario (right panel). Catchments vhm233 (top panel), vhm218 (middle panel), vhm38 (bottom panel). ICRA-reference (1981-2010) (black line). Each colour corresponds to a 30-year period: from dark blue (1981-2010) to red (2071-2100). The month=1 for January and 12 for December.

Appendix 7

Locally-adjusted monthly precipitation projections under the RCP4.5 emission scenario

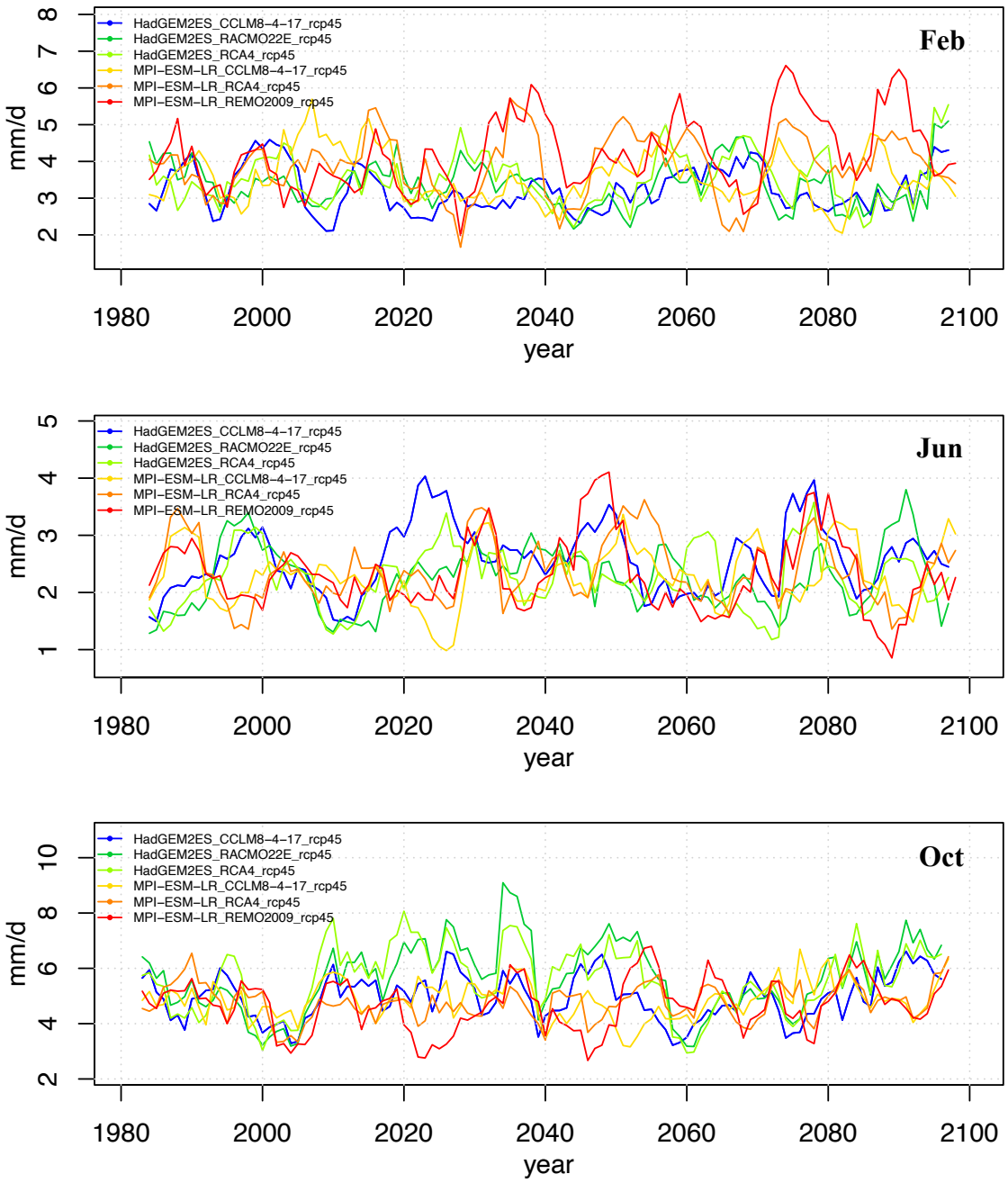

Fig. VII-1: Catchment vhm233: Projected monthly precipitation under the RCP4.5 emission scenario. Top (February); Middle (June); Bottom (October). A 5-year running mean was applied. Each colour corresponds to a GCM-RCM combination (cf. Table 3).

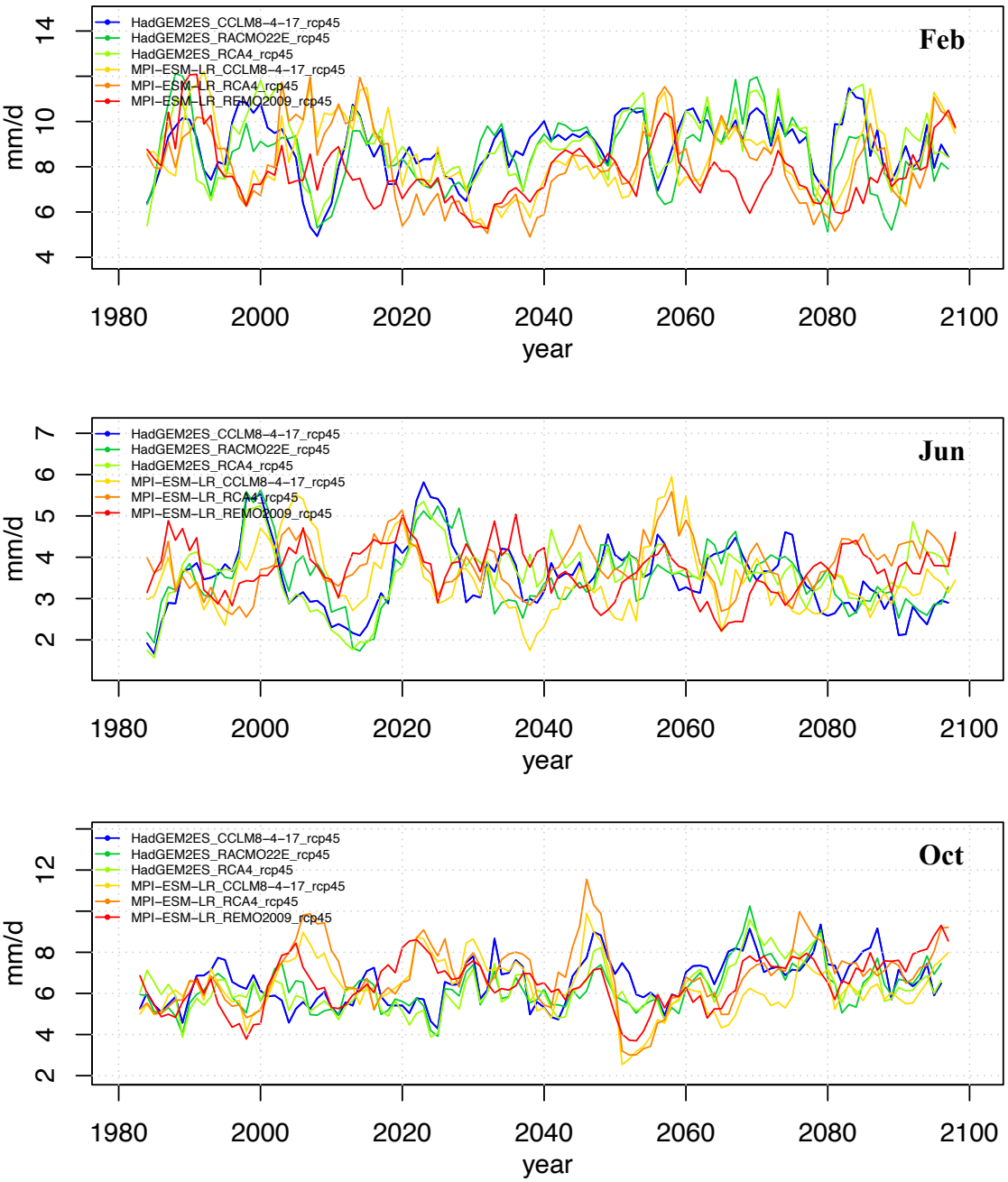

Fig. VII-2: Catchment vhm218: Projected monthly precipitation under the RCP4.5 emission scenario. Top (February); Middle (June); Bottom (October). A 5-year running mean was applied. Each colour corresponds to a GCM-RCM combination (cf. Table 3).

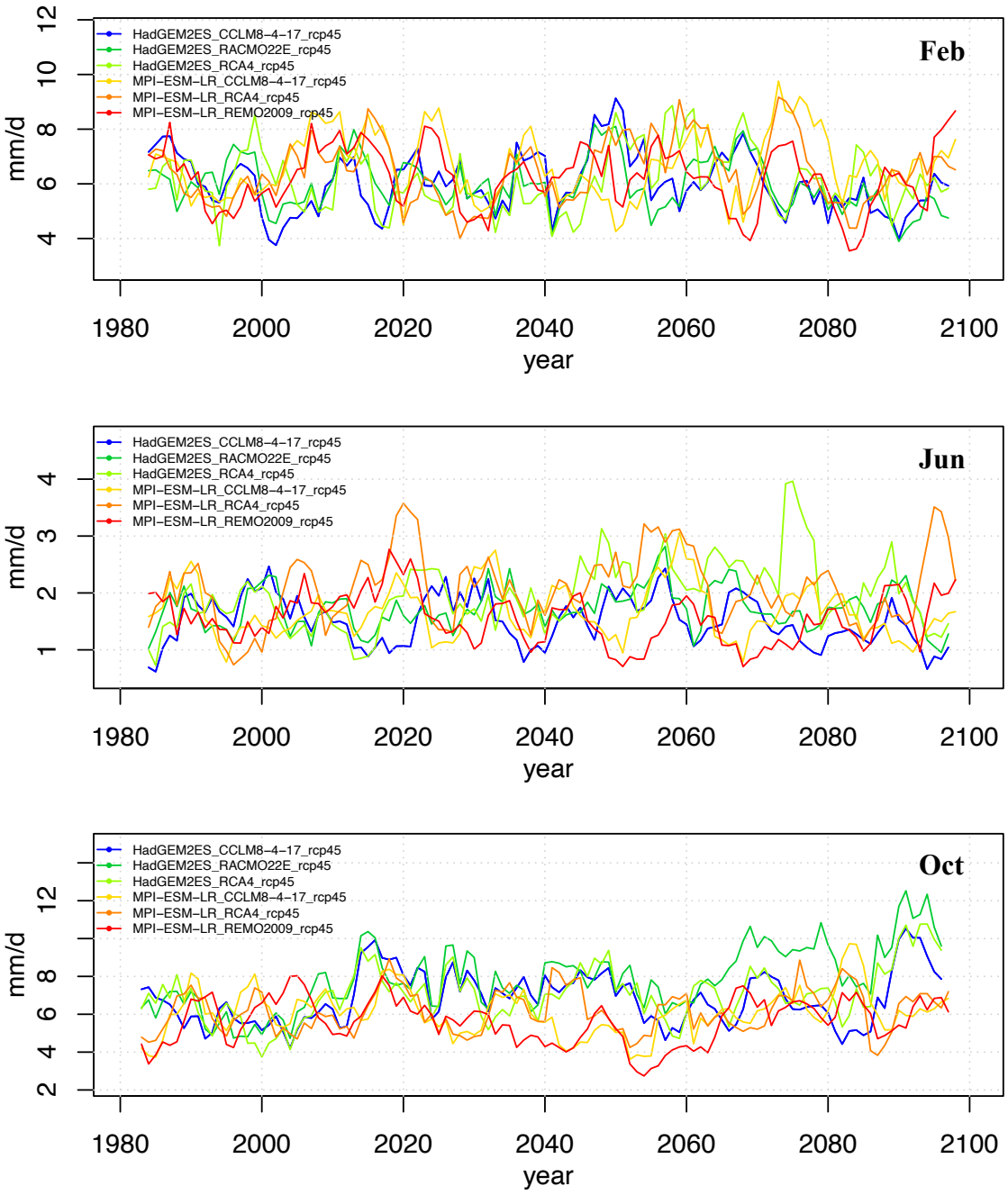

Fig. VII-3: Catchment vhm38: Projected monthly precipitation under the RCP4.5 emission scenario. Top (February); Middle (June); Bottom (October). A 5-year running mean was applied. Each colour corresponds to a GCM-RCM combination (cf. Table 3).

Appendix 8

Hydrological projections in the reference period (1981-2010): magnitude and seasonal frequency of occurrence of AMFs

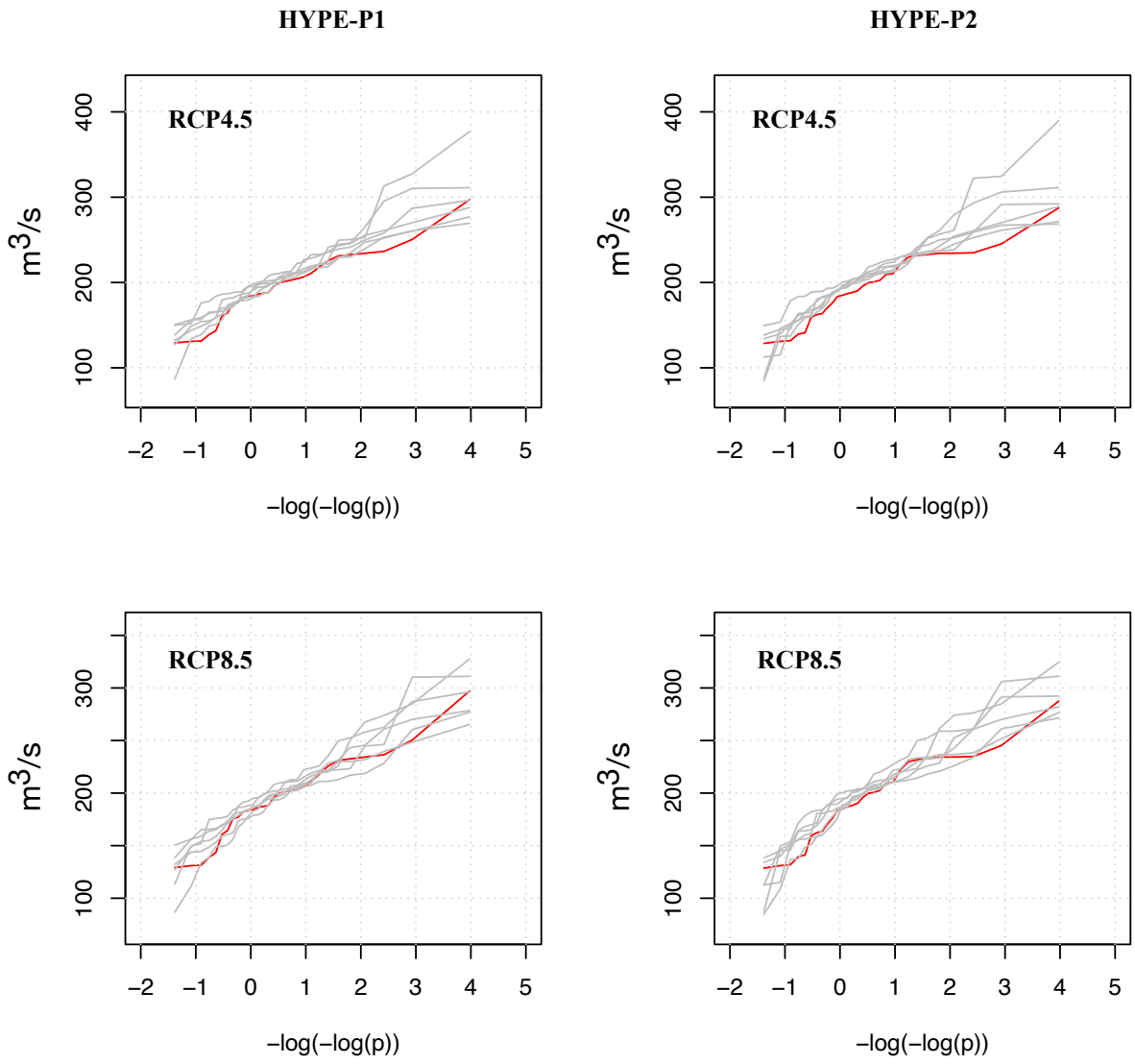

Fig. VIII-1: Catchment vhm233: Empirical cumulative distribution functions of AMFs in the reference period (1981-2010). Estimations derived from HYPE forced with the ICRA reanalysis (red line) and with the locally-adjusted CORDEX projections (grey lines). Top panel: HYPE forced with CORDEX RCP4.5 series. Bottom-panel: HYPE forced with CORDEX RCP8.5 series. Left-panel: HYPE with parameter set calibrated in 1996-2002. Right-panel: HYPE with parameter set calibrated in 2003-2009. The parameter p=1-1/T.

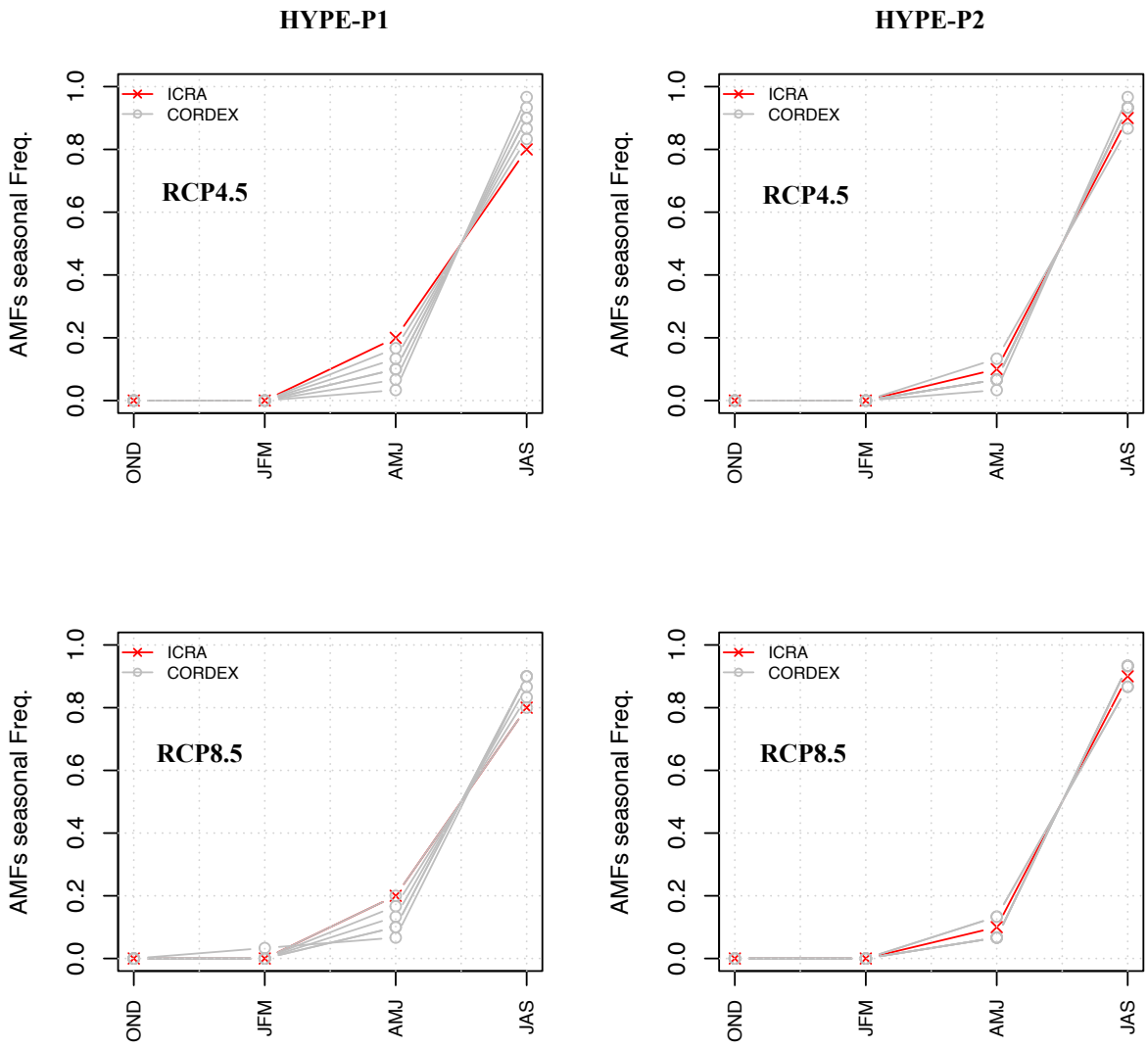

Fig. VIII-2: Catchment vhm233: Seasonal frequency of occurrence of AMFs in the reference period (1981-2010). Estimations derived from HYPE forced with the ICRA reanalysis (red line) and with the locally-adjusted CORDEX projections (grey lines). Top panel: HYPE forced with CORDEX RCP4.5 series. Bottom-panel: HYPE forced with CORDEX RCP8.5 series. Left-panel: HYPE with parameter set calibrated in 1996-2002. Right-panel: HYPE with parameter set calibrated in 2003-2009.

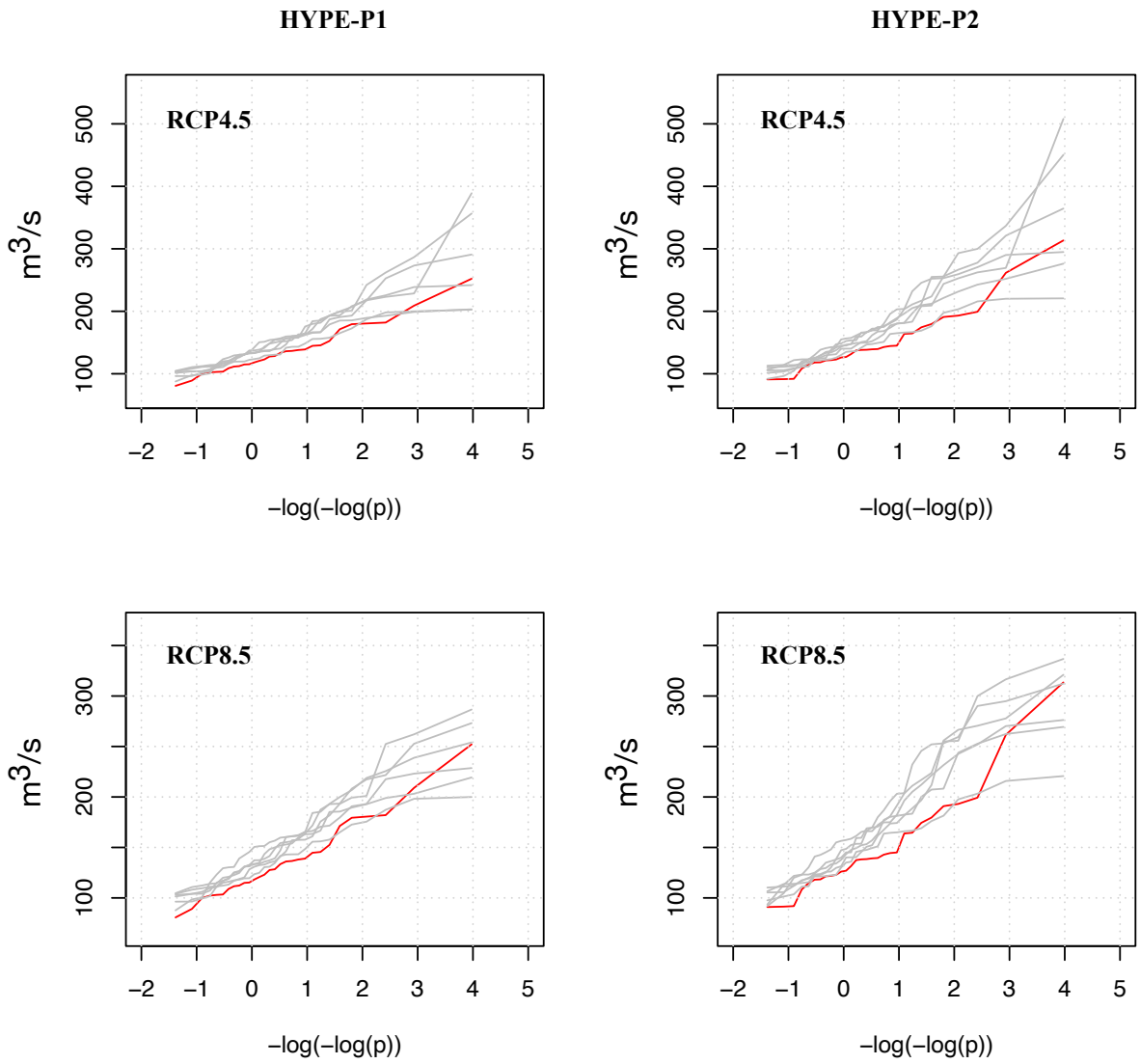

Fig. VIII-3: Catchment vhm218: Empirical cumulative distribution functions of AMFs in the reference period (1981-2010). Estimations derived from HYPE forced with the ICRA reanalysis (red line) and with the locally-adjusted CORDEX projections (grey lines). Top panel: HYPE forced with CORDEX RCP4.5 series. Bottom-panel: HYPE forced with CORDEX RCP8.5 series. Left-panel: HYPE with parameter set calibrated in 1996-2002. Right-panel: HYPE with parameter set calibrated in 2003-2009. The parameter p=1-1/T.

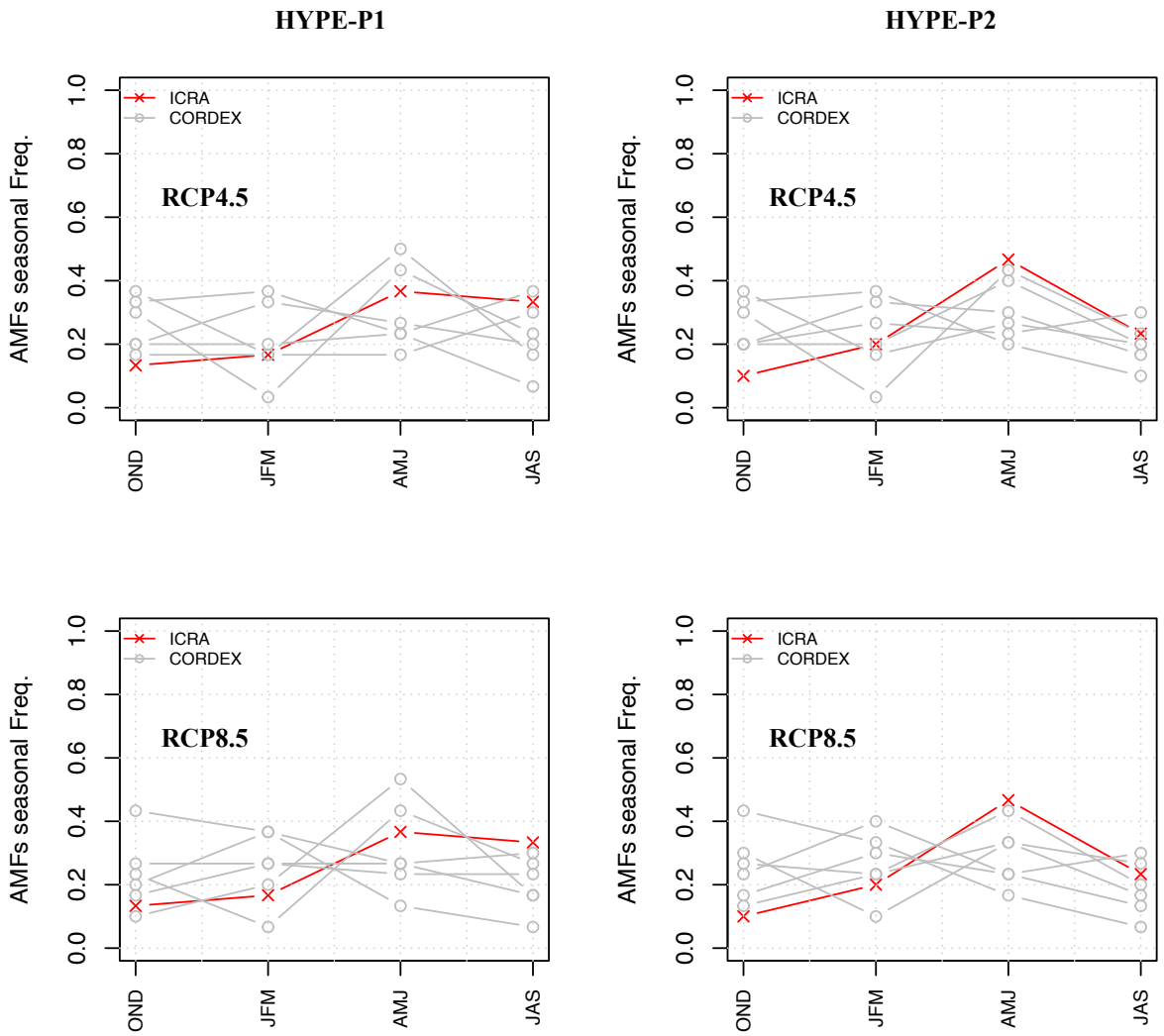

Fig. VIII-4: Catchment vhm218: Seasonal frequency of occurrence of AMFs in the reference period (1981-2010). Estimations derived from HYPE forced with the ICRA reanalysis (red line) and with the locally-adjusted CORDEX projections (grey lines). Top panel: HYPE forced with CORDEX RCP4.5 series. Bottom-panel: HYPE forced with CORDEX RCP8.5 series. Left-panel: HYPE with parameter set calibrated in 1996-2002. Right-panel: HYPE with parameter set calibrated in 2003-2009.

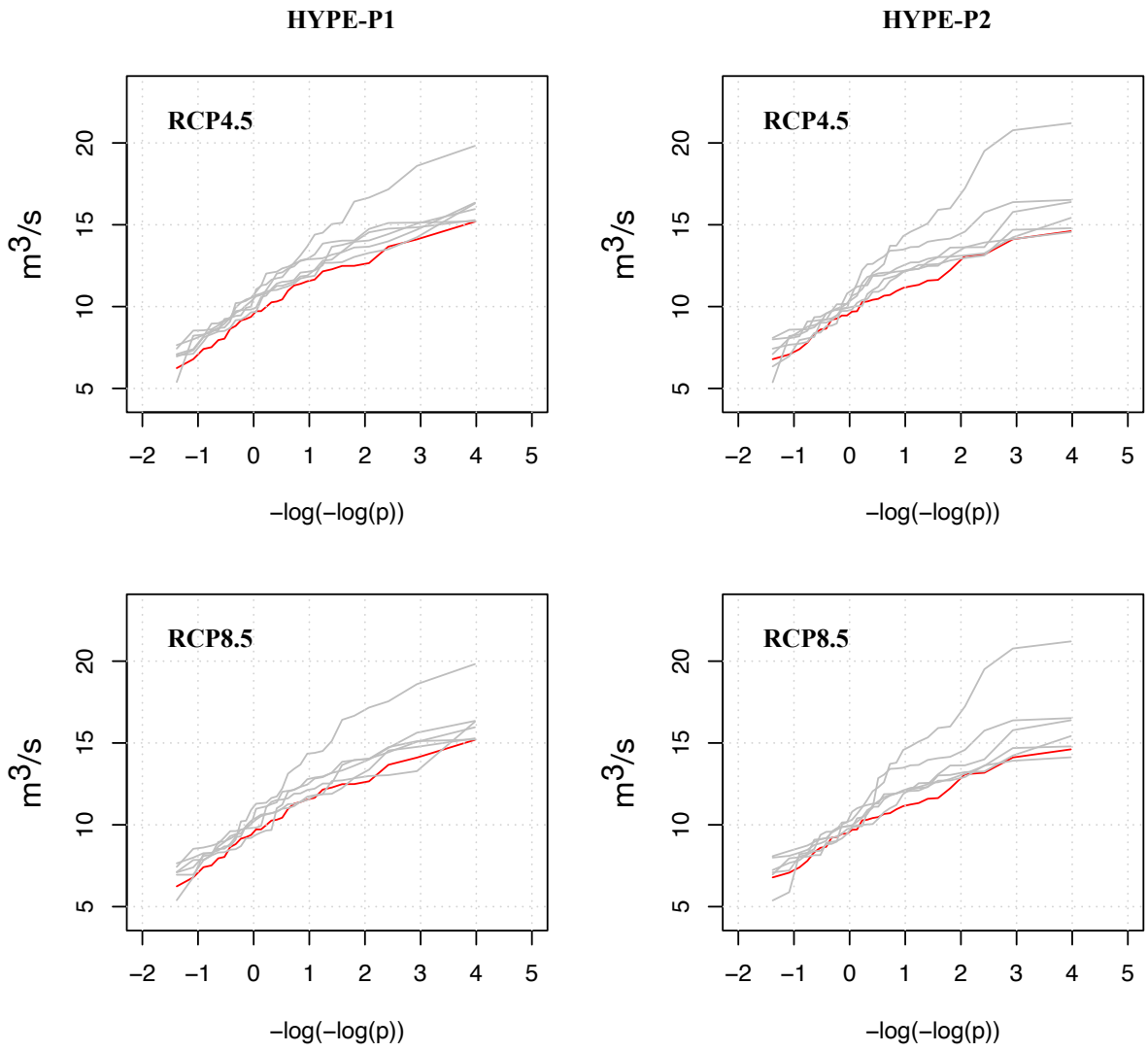

Fig. VIII-5: Catchment vhm38: Empirical cumulative distribution functions of AMFs in the reference period (1981-2010). Estimations derived from HYPE forced with the ICRA reanalysis (red line) and with the locally-adjusted CORDEX projections (grey lines). Top panel: HYPE forced with CORDEX RCP4.5 series. Bottom-panel: HYPE forced with CORDEX RCP8.5 series. Left-panel: HYPE with parameter set calibrated in 1996-2002. Right-panel: HYPE with parameter set calibrated in 2003-2009. The parameter p=1-1/T.

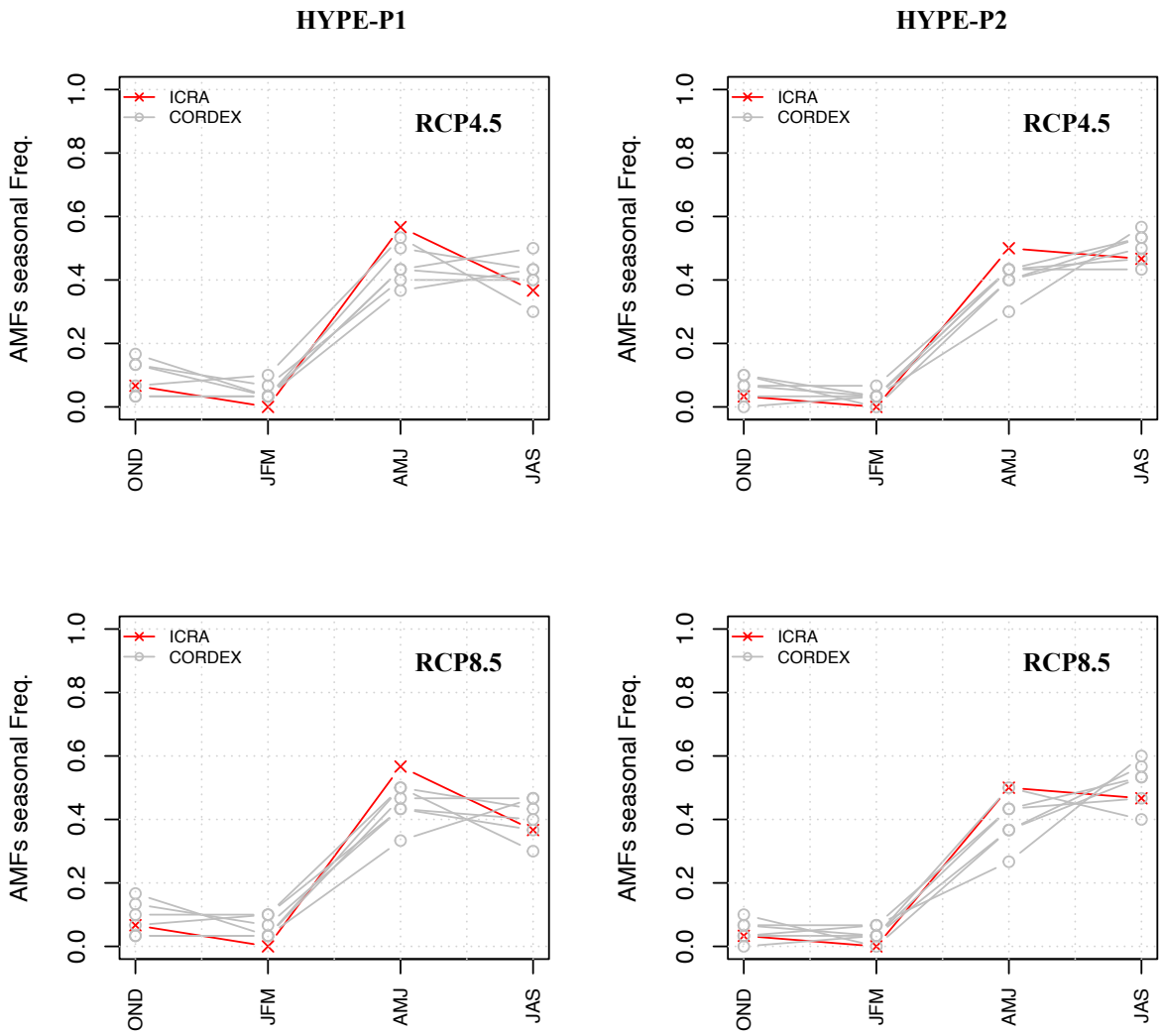

Fig. VIII-6: Catchment vhm38: Seasonal frequency of occurrence of AMFs in the reference period (1981-2010). Estimations derived from HYPE forced with the ICRA reanalysis (red line) and with the locally-adjusted CORDEX projections (grey lines). Top panel: HYPE forced with CORDEX RCP4.5 series. Bottom-panel: HYPE forced with CORDEX RCP8.5 series. Left-panel: HYPE with parameter set calibrated in 1996-2002. Right-panel: HYPE with parameter set calibrated in 2003-2009.

Appendix 9

Projected changes in mean snow and glacier melt in the Markarfljót catchment (vhm218)

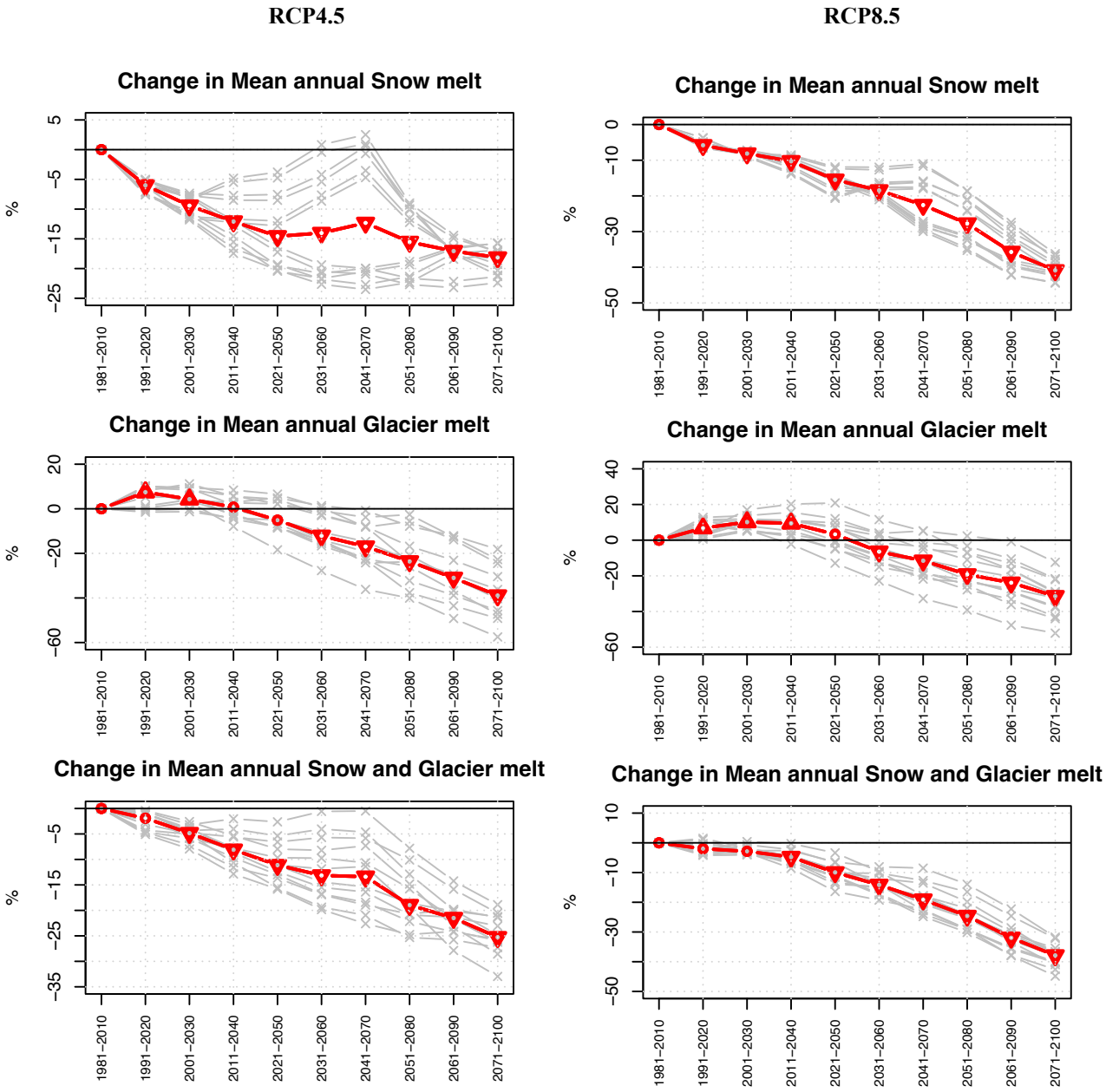

Appendix IX-1: Projected changes in 30-year mean annual snow and glacier melt, relative to the 1981-2010 reference period. Left-panel: RCP4.5 emission scenario. Right-panel: RCP8.5 emission scenario. Ensemble members (grey lines) and ensemble median (red line). The symbols on the ensemble median indicate whether the 30-year mean is projected to change significantly or to remain unchanged in future periods compared to the reference period, according to the Mann-Whitney test (triangle point-up=significant increase; triangle point down=significant decrease; open circle=no significant change).

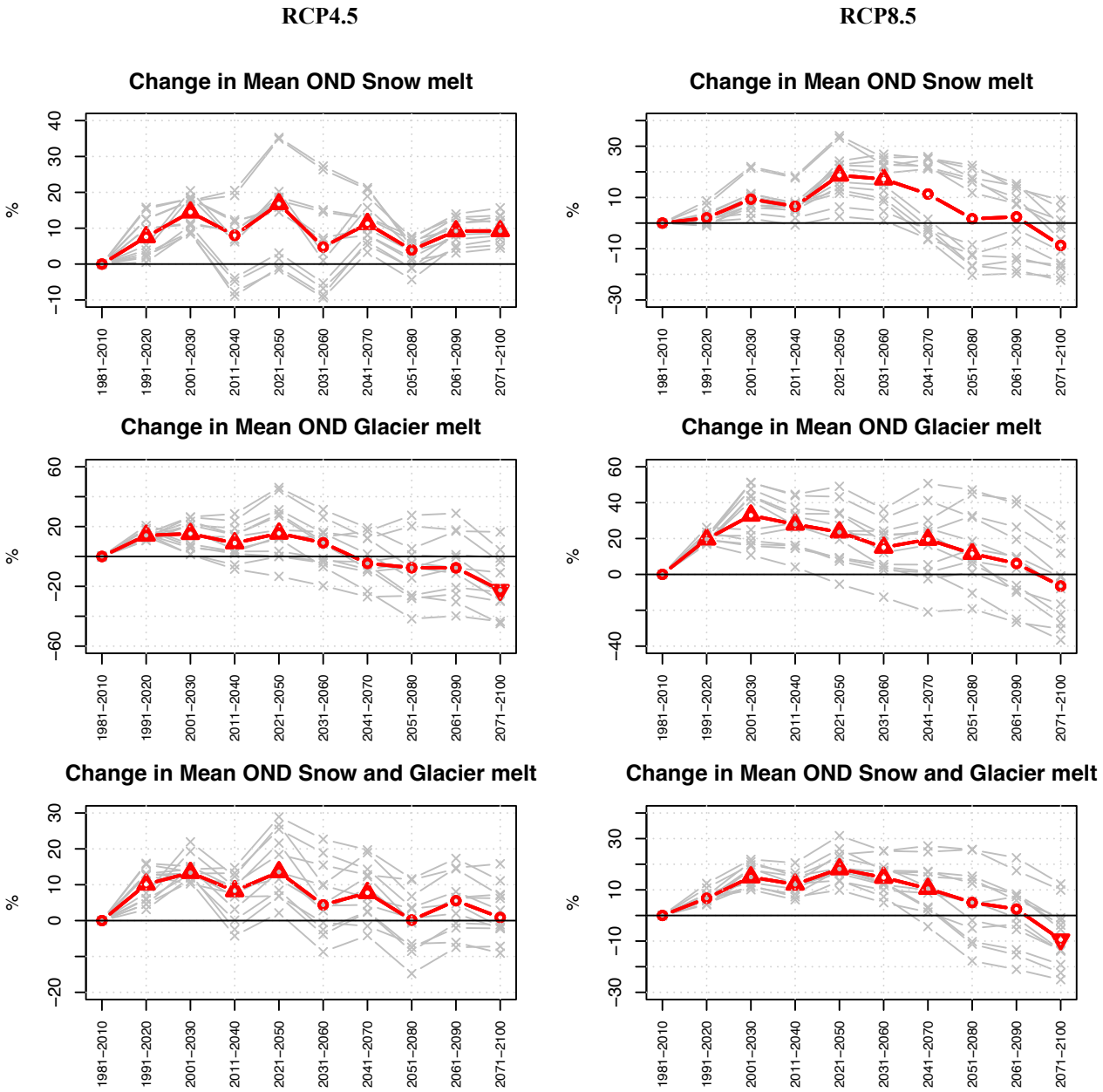

Appendix IX-2: Projected changes in 30-year mean OND snow and glacier melt, relative to the 1981-2010 reference period. Left-panel: RCP4.5 emission scenario. Right-panel: RCP8.5 emission scenario. Ensemble members (grey lines) and ensemble median (red line). The symbols on the ensemble median indicate whether the 30-year mean is projected to change significantly or to remain unchanged in future periods compared to the reference period, according to the Mann-Whitney test (triangle point-up=significant increase; triangle point down=significant decrease; open circle=no significant change).

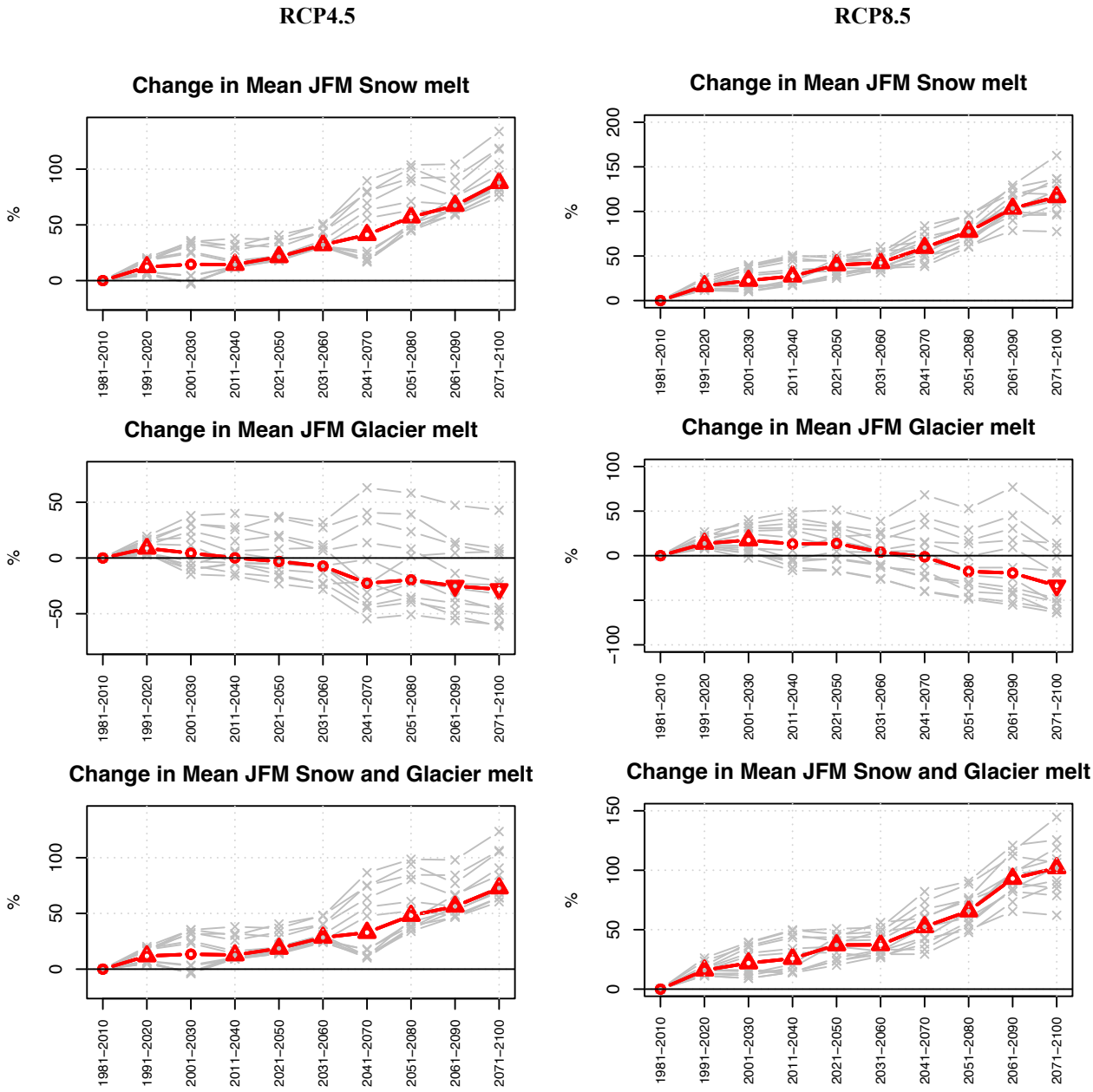

Appendix IX-3: Projected changes in 30-year mean JFM snow and glacier melt, relative to the 1981-2010 reference period. Left-panel: RCP4.5 emission scenario. Right-panel: RCP8.5 emission scenario. Ensemble members (grey lines) and ensemble median (red line). The symbols on the ensemble median indicate whether the 30-year mean is projected to change significantly or to remain unchanged in future periods compared to the reference period, according to the Mann-Whitney test (triangle point-up=significant increase; triangle point down=significant decrease; open circle=no significant change).

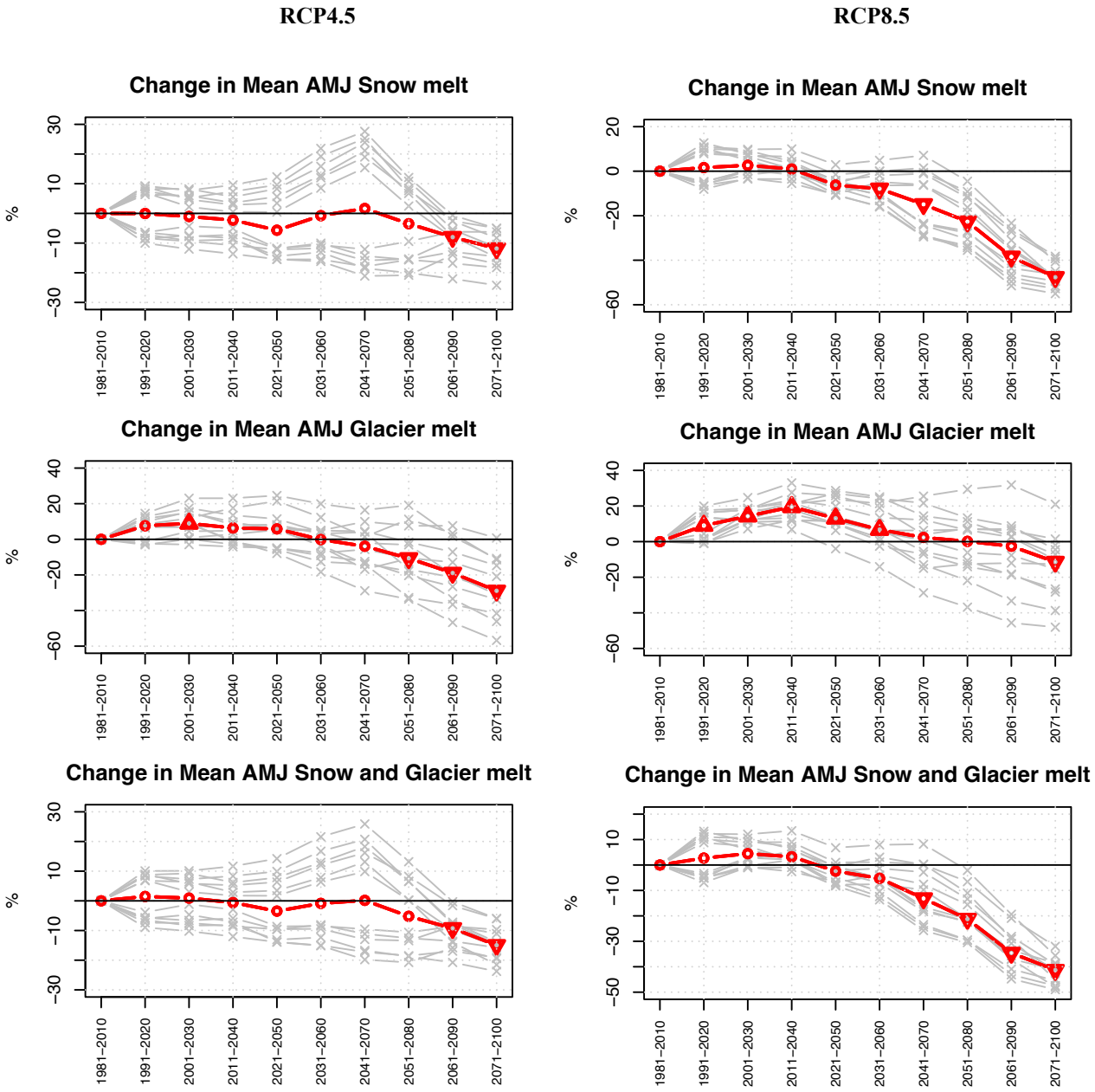

Appendix IX-4: Projected changes in 30-year mean AMJ snow and glacier melt, relative to the 1981-2010 reference period. Left-panel: RCP4.5 emission scenario. Right-panel: RCP8.5 emission scenario. Ensemble members (grey lines) and ensemble median (red line). The symbols on the ensemble median indicate whether the 30-year mean is projected to change significantly or to remain unchanged in future periods compared to the reference period, according to the Mann-Whitney test (triangle point-up=significant increase; triangle point down=significant decrease; open circle=no significant change).

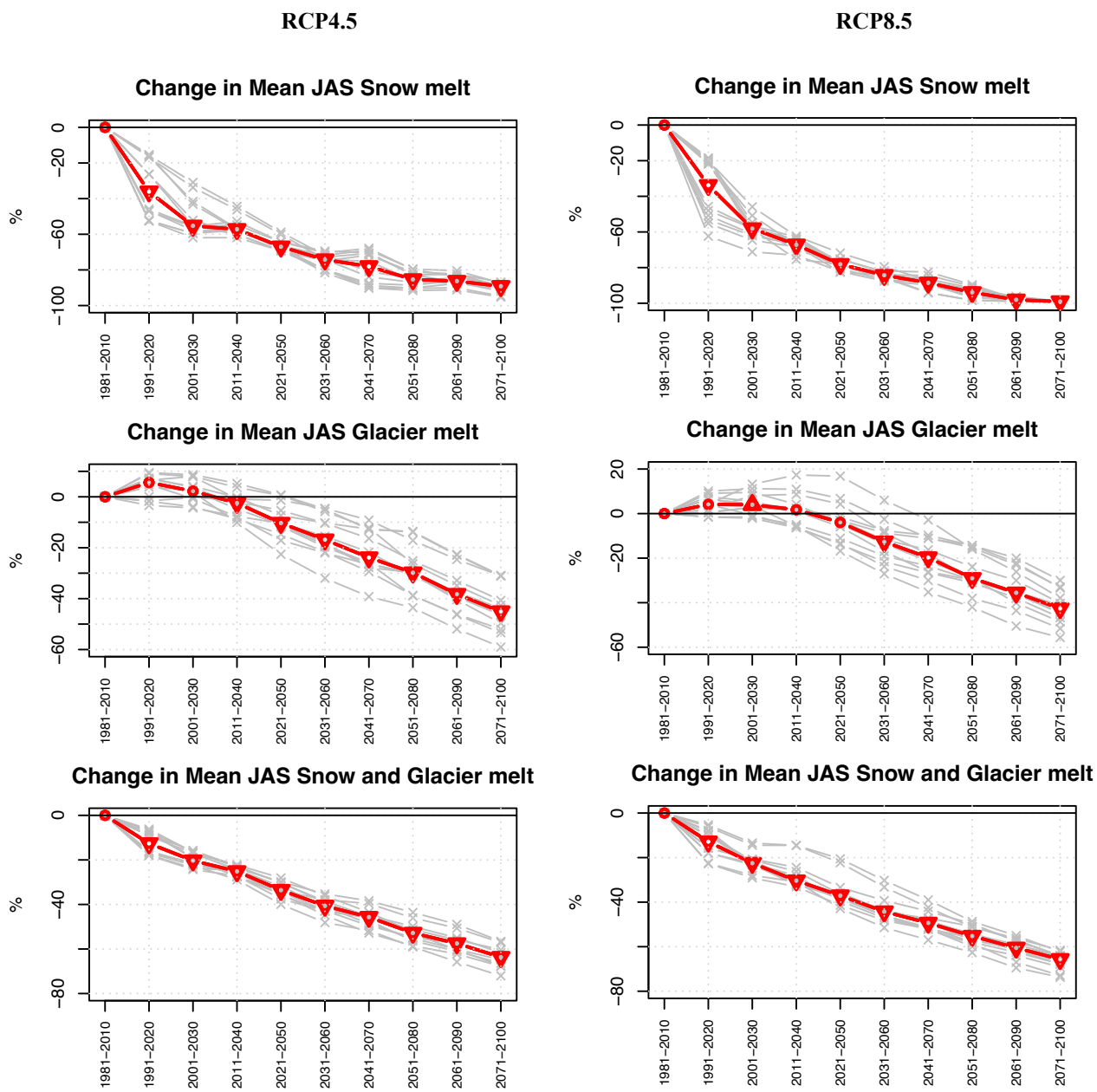

Appendix IX-5: Projected changes in 30-year mean JAS snow and glacier melt, relative to the 1981-2010 reference period. Left-panel: RCP4.5 emission scenario. Right-panel: RCP8.5 emission scenario. Ensemble members (grey lines) and ensemble median (red line). The symbols on the ensemble median indicate whether the 30-year mean is projected to change significantly or to remain unchanged in future periods compared to the reference period, according to the Mann-Whitney test (triangle point-up=significant increase; triangle point down=significant decrease; open circle=no significant change).

Appendix 10

Projected changes in mean snow and glacier melt in the Kreppa catchment (vhm233)

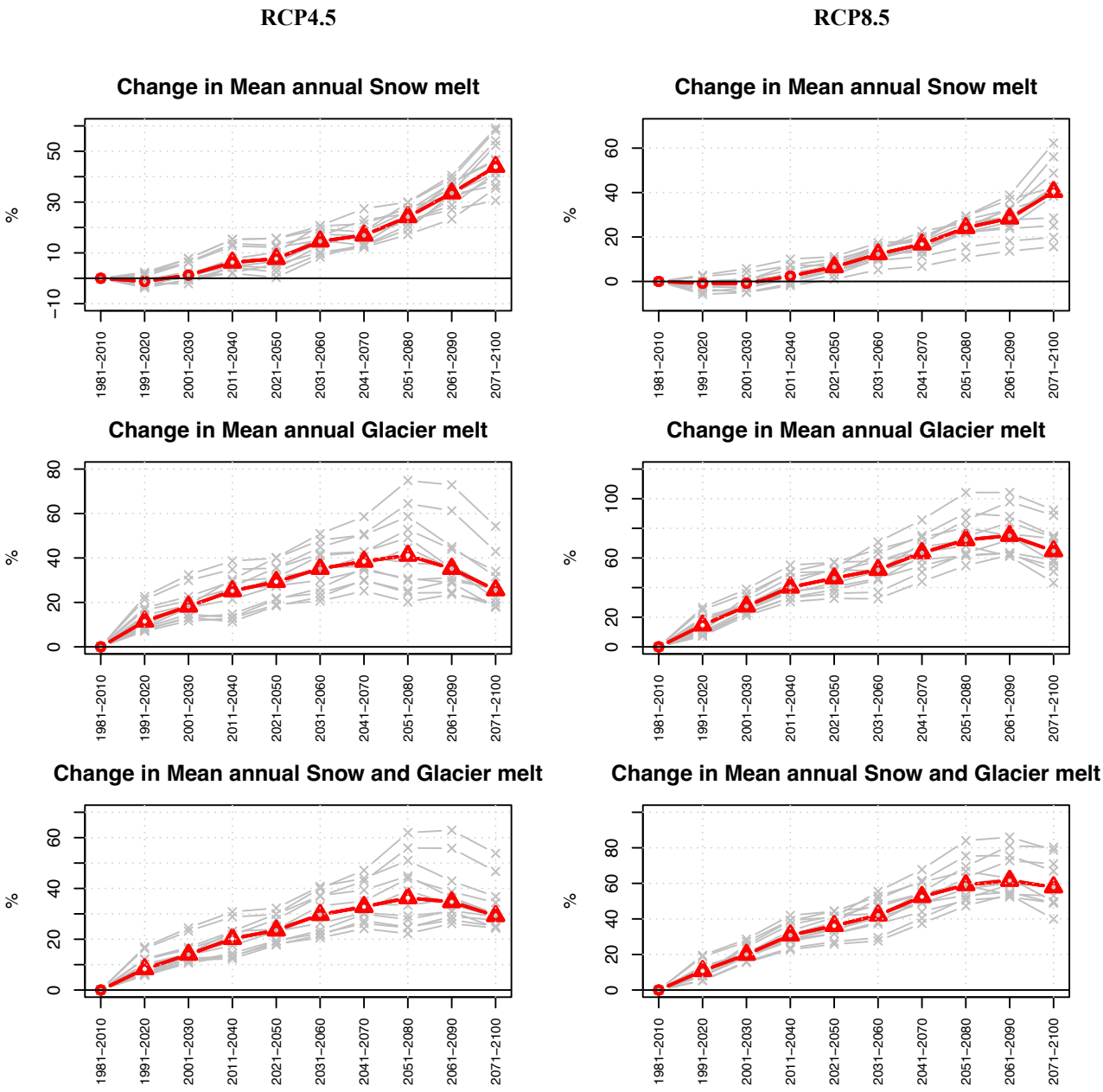

Appendix X-1: Projected changes in 30-year mean annual snow and glacier melt, relative to the 1981-2010 reference period. Left-panel: RCP4.5 emission scenario. Right-panel: RCP8.5 emission scenario. Ensemble members (grey lines) and ensemble median (red line). The symbols on the ensemble median indicate whether the 30-year mean is projected to change significantly or to remain unchanged in future periods compared to the reference period, according to the Mann-Whitney test (triangle point-up=significant increase; triangle point down=significant decrease; open circle=no significant change).

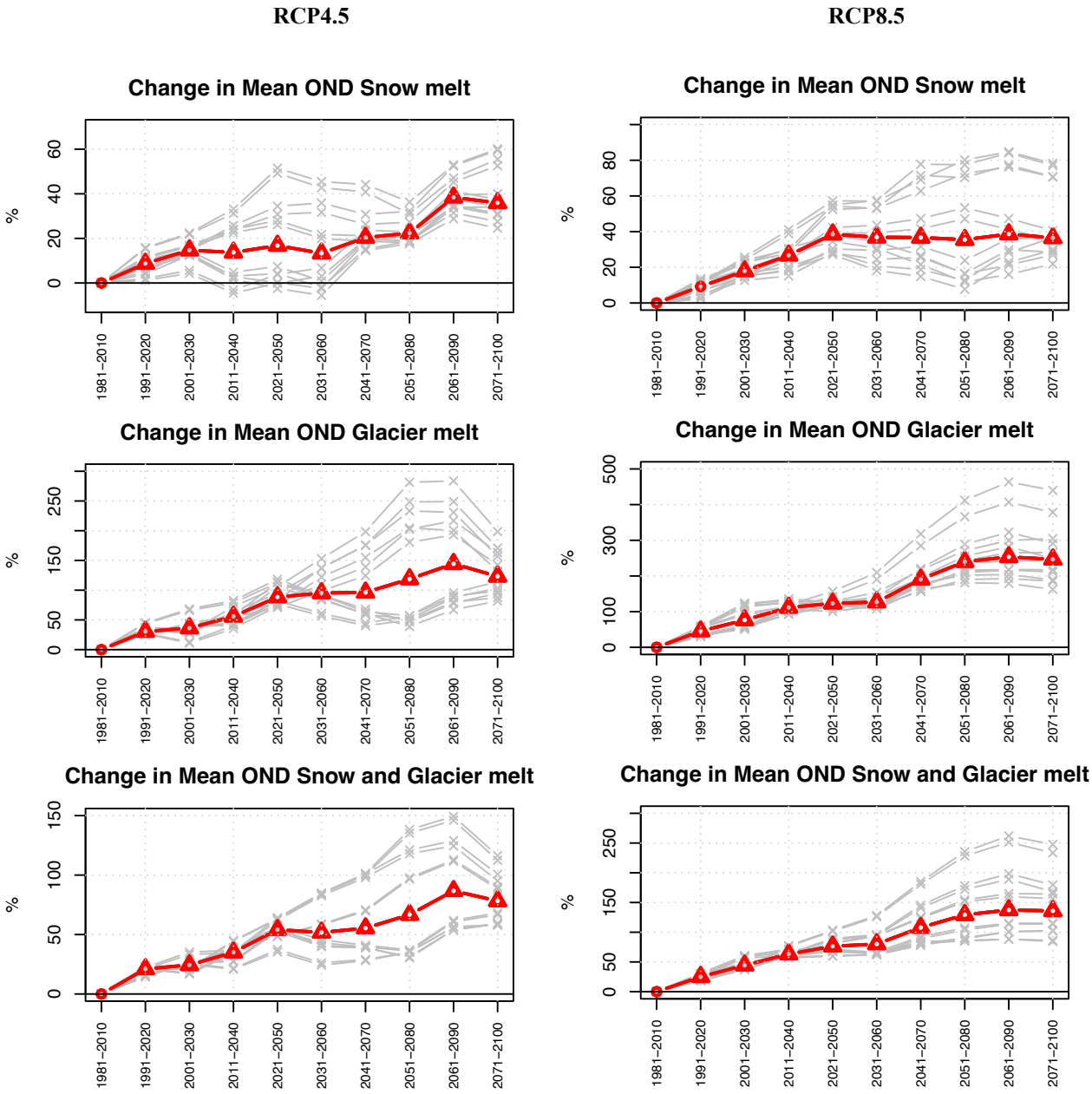

Appendix X-2: Projected changes in 30-year mean OND snow and glacier melt, relative to the 1981-2010 reference period. Left-panel: RCP4.5 emission scenario. Right-panel: RCP8.5 emission scenario. Ensemble members (grey lines) and ensemble median (red line). The symbols on the ensemble median indicate whether the 30-year mean is projected to change significantly or to remain unchanged in future periods compared to the reference period, according to the Mann-Whitney test (triangle point-up=significant increase; triangle point down=significant decrease; open circle=no significant change).

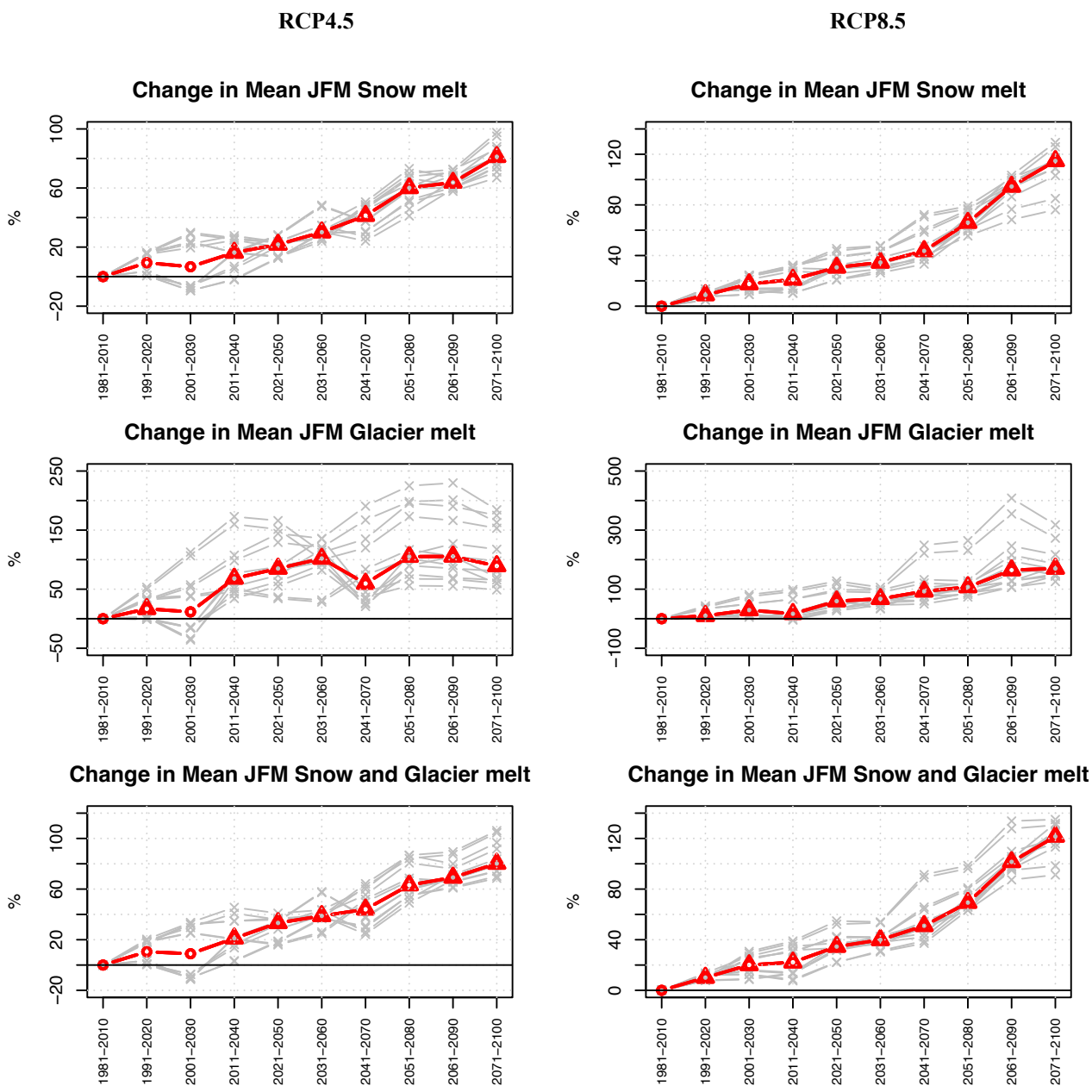

Appendix X-3: Projected changes in 30-year mean JFM snow and glacier melt, relative to the 1981-2010 reference period. Left-panel: RCP4.5 emission scenario. Right-panel: RCP8.5 emission scenario. Ensemble members (grey lines) and ensemble median (red line). The symbols on the ensemble median indicate whether the 30-year mean is projected to change significantly or to remain unchanged in future periods compared to the reference period, according to the Mann-Whitney test (triangle point-up=significant increase; triangle point down=significant decrease; open circle=no significant change).

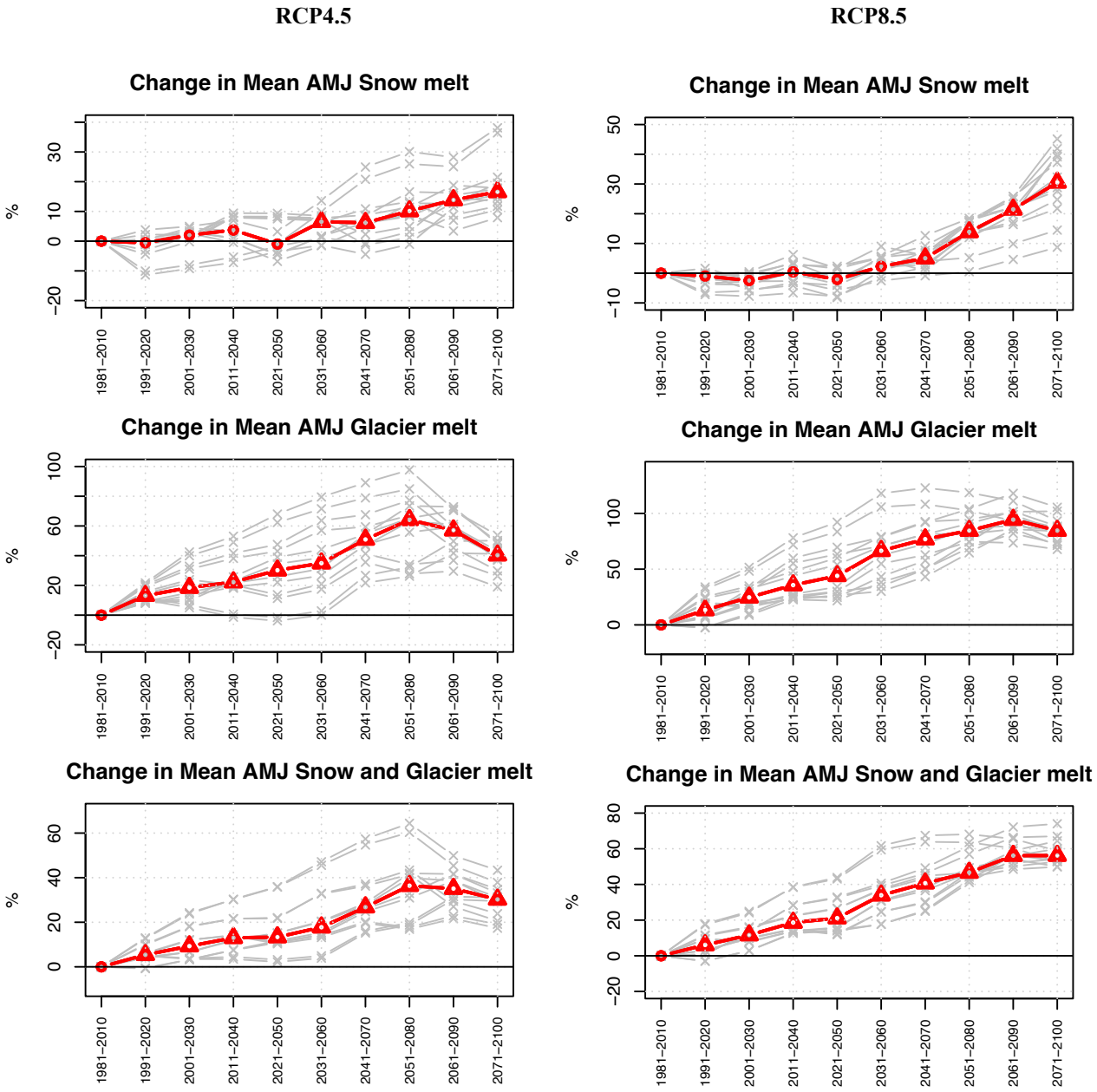

Appendix X-4: Projected changes in 30-year mean AMJ snow and glacier melt, relative to the 1981-2010 reference period. Left-panel: RCP4.5 emission scenario. Right-panel: RCP8.5 emission scenario. Ensemble members (grey lines) and ensemble median (red line). The symbols on the ensemble median indicate whether the 30-year mean is projected to change significantly or to remain unchanged in future periods compared to the reference period, according to the Mann-Whitney test (triangle point-up=significant increase; triangle point down=significant decrease; open circle=no significant change).

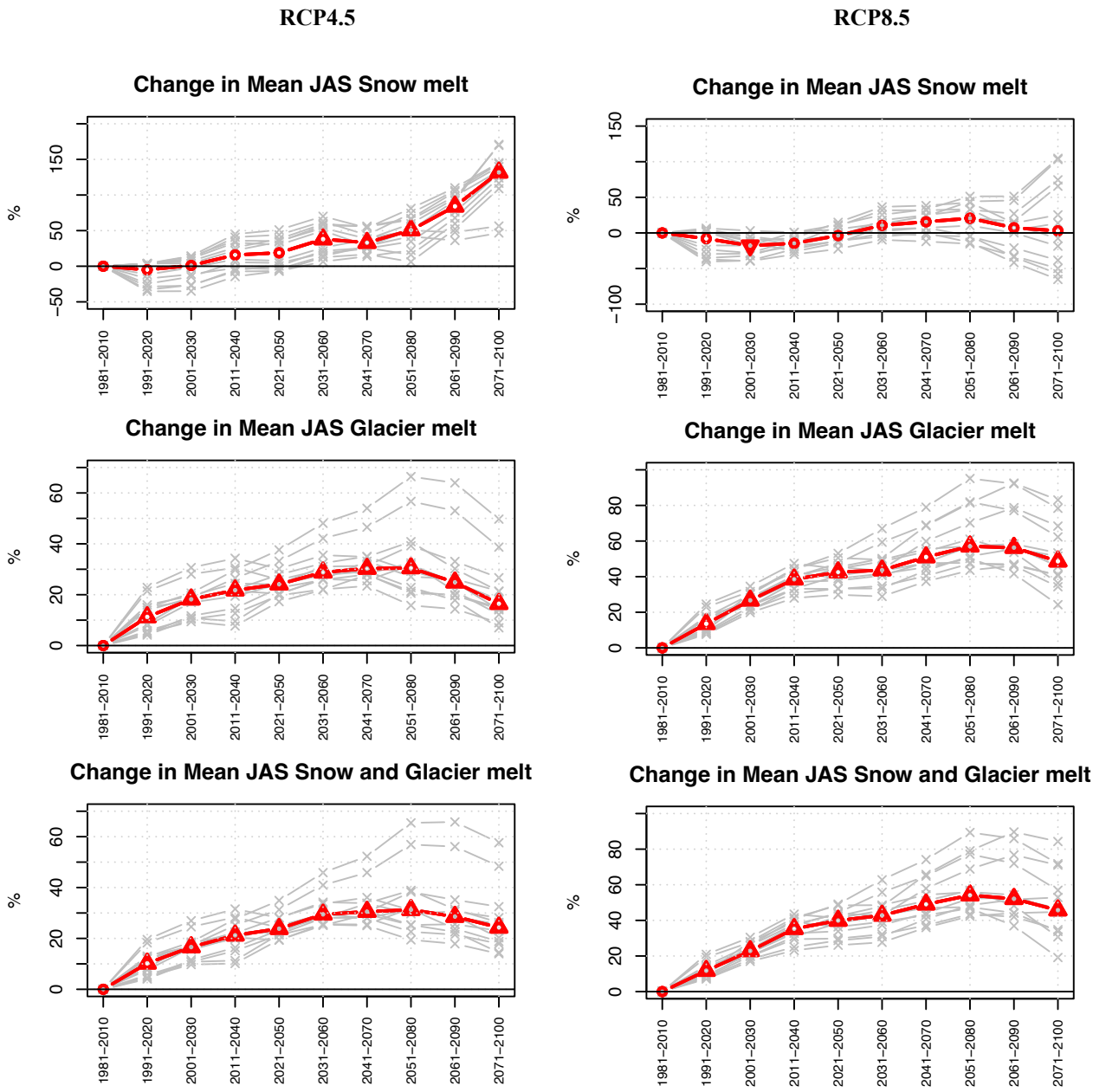

Appendix X-5: Projected changes in 30-year mean JAS snow and glacier melt, relative to the 1981-2010 reference period. Left-panel: RCP4.5 emission scenario. Right-panel: RCP8.5 emission scenario. Ensemble members (grey lines) and ensemble median (red line). The symbols on the ensemble median indicate whether the 30-year mean is projected to change significantly or to remain unchanged in future periods compared to the reference period, according to the Mann-Whitney test (triangle point-up=significant increase; triangle point down=significant decrease; open circle=no significant change).

Appendix 11

Projected seasonal frequency of occurrence of AMFs

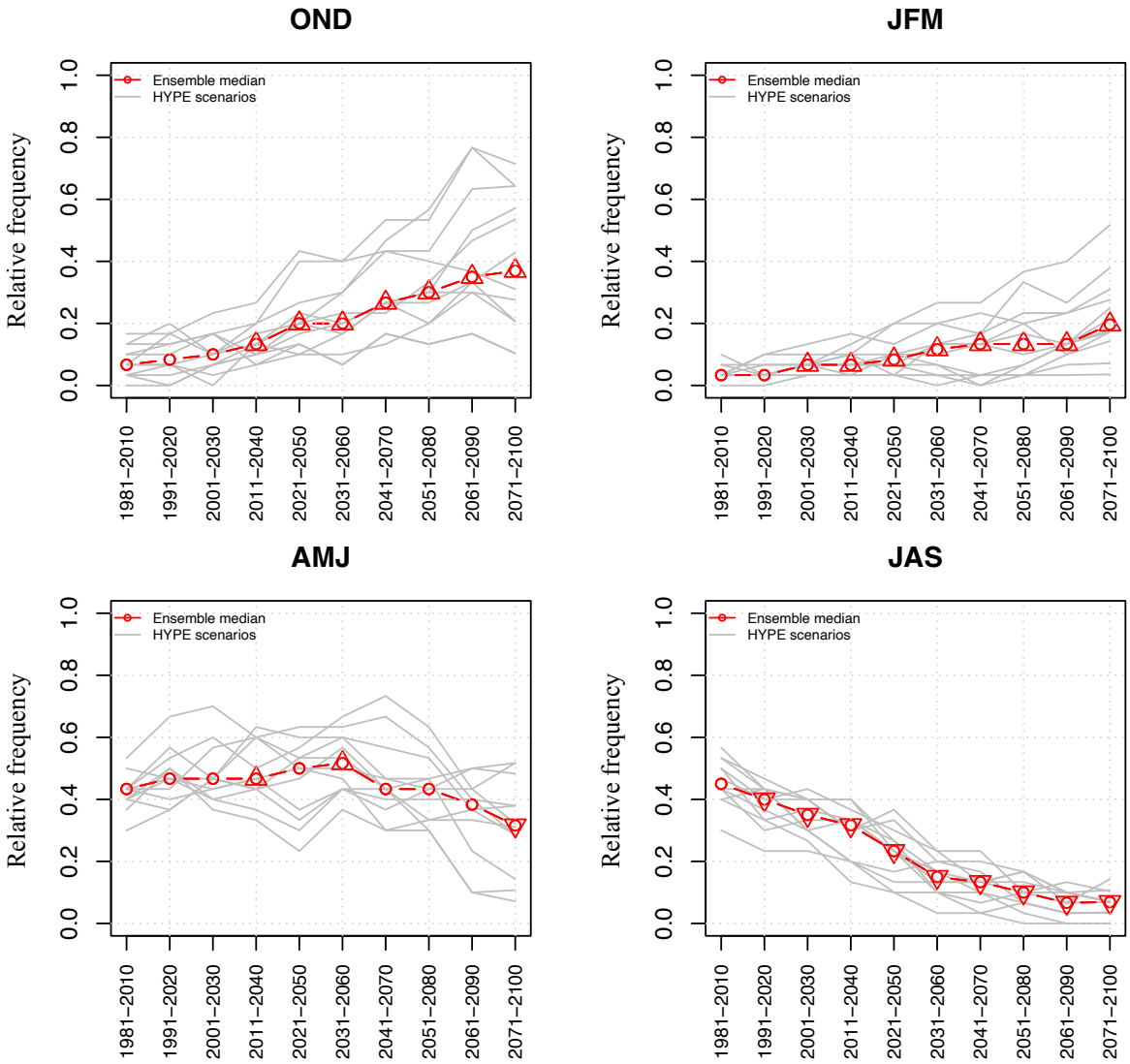

Fig. XI-1: Catchment vhm38: Projected seasonal frequency of occurrence of AMFs (RCP4.5 emission scenario). Ensemble members (grey lines) and ensemble median (red line). The symbols on the ensemble median indicate whether a significant shift in the ensemble of seasonal frequencies has been detected between the reference and future periods (triangle point-up=freq. increase; triangle point down=freq. decrease; open circle=no significant change).

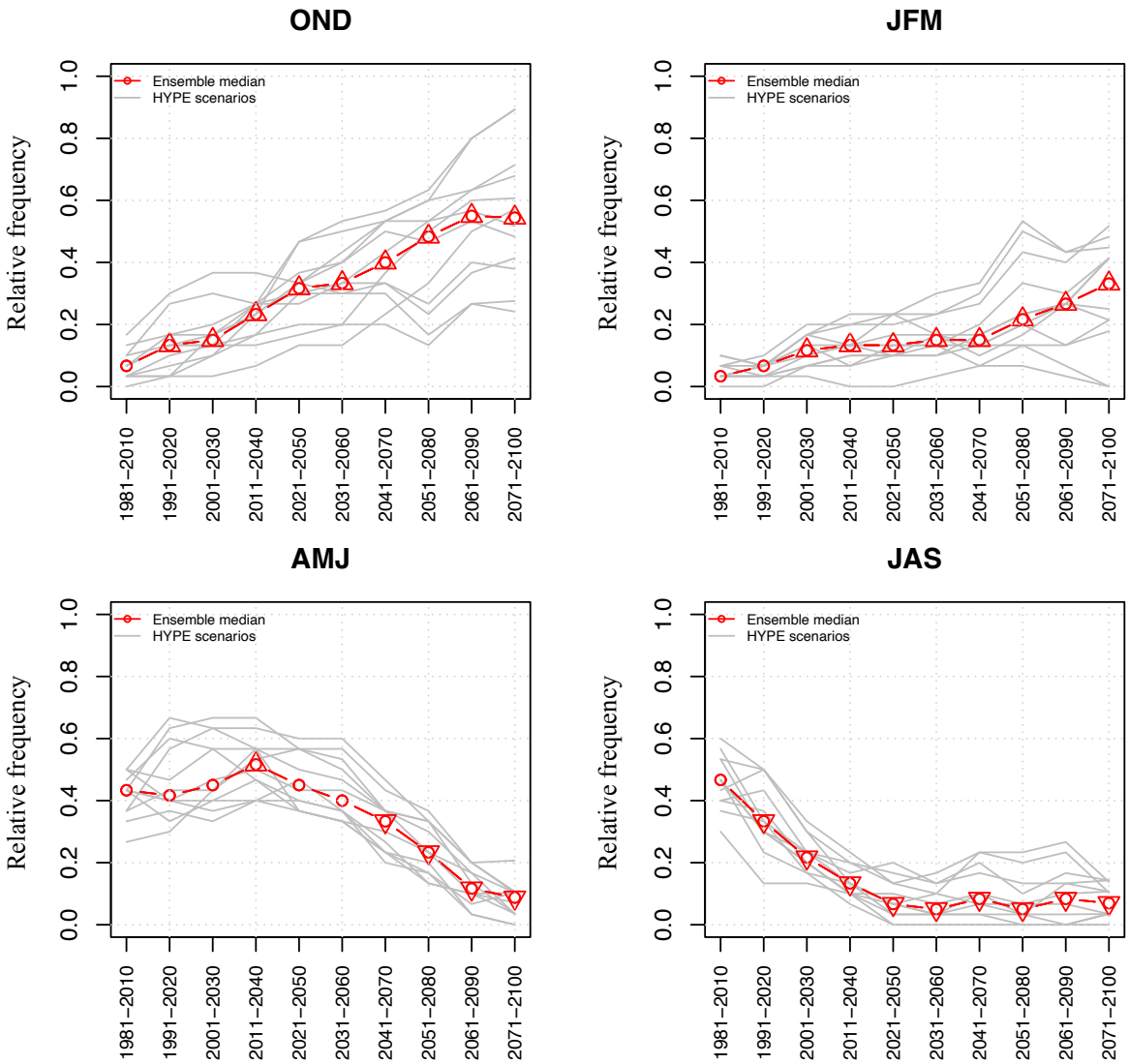

Fig. XI-2: Catchment vhm38: Projected seasonal frequency of occurrence of AMFs (RCP8.5 emission scenario). Ensemble members (grey lines) and ensemble median (red line). The symbols on the ensemble median indicate whether a significant shift in the ensemble of seasonal frequencies has been detected between the reference and future periods (triangle point-up=freq. increase; triangle point down=freq. decrease; open circle=no significant change).

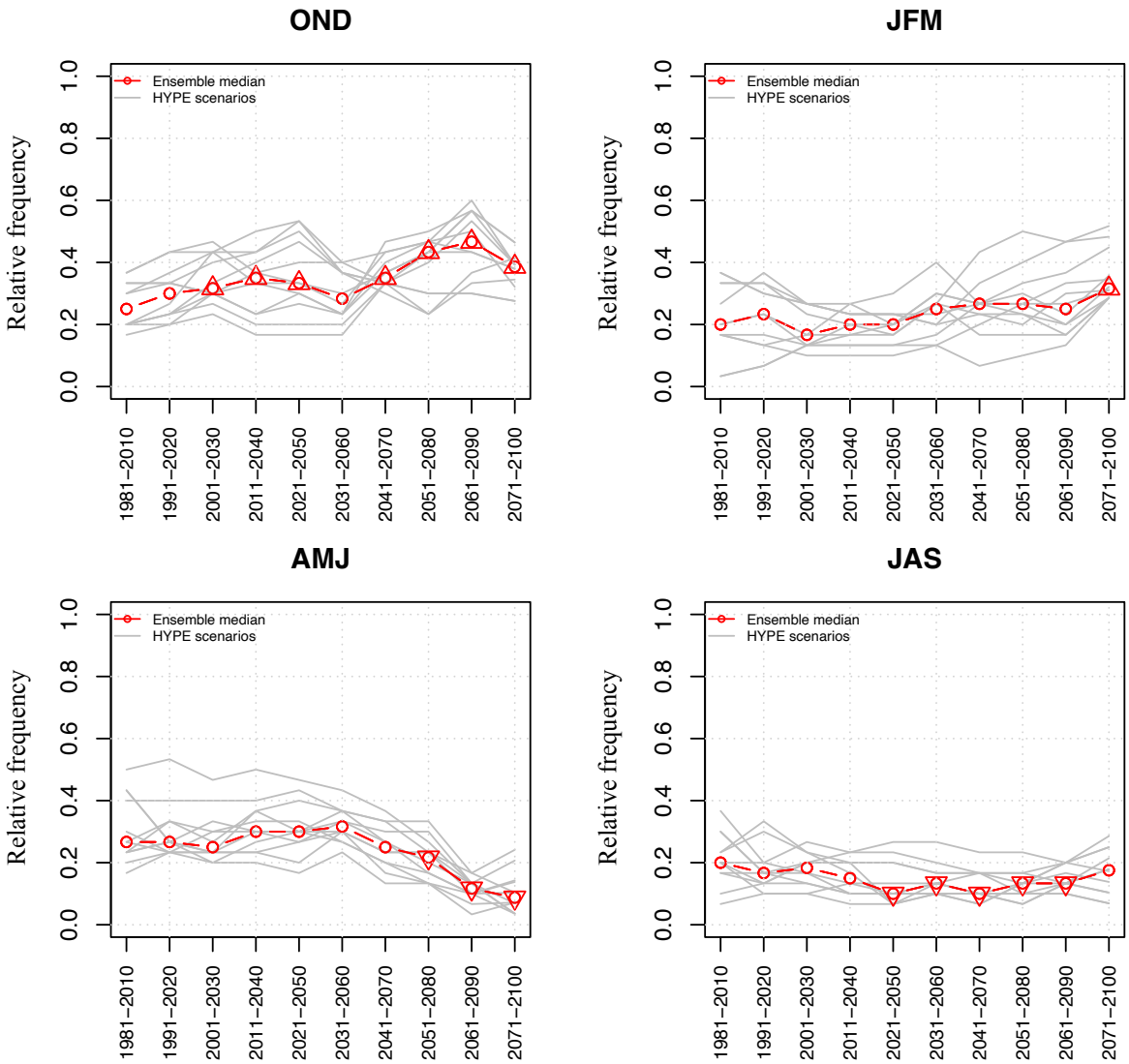

Fig. XI-3: Catchment vhm218: Projected seasonal frequency of occurrence of AMFs (RCP4.5 emission scenario). Ensemble members (grey lines) and ensemble median (red line). The symbols on the ensemble median indicate whether a significant shift in the ensemble of seasonal frequencies has been detected between the reference and future periods (triangle point-up=freq. increase; triangle point down=freq. decrease; open circle=no significant change).

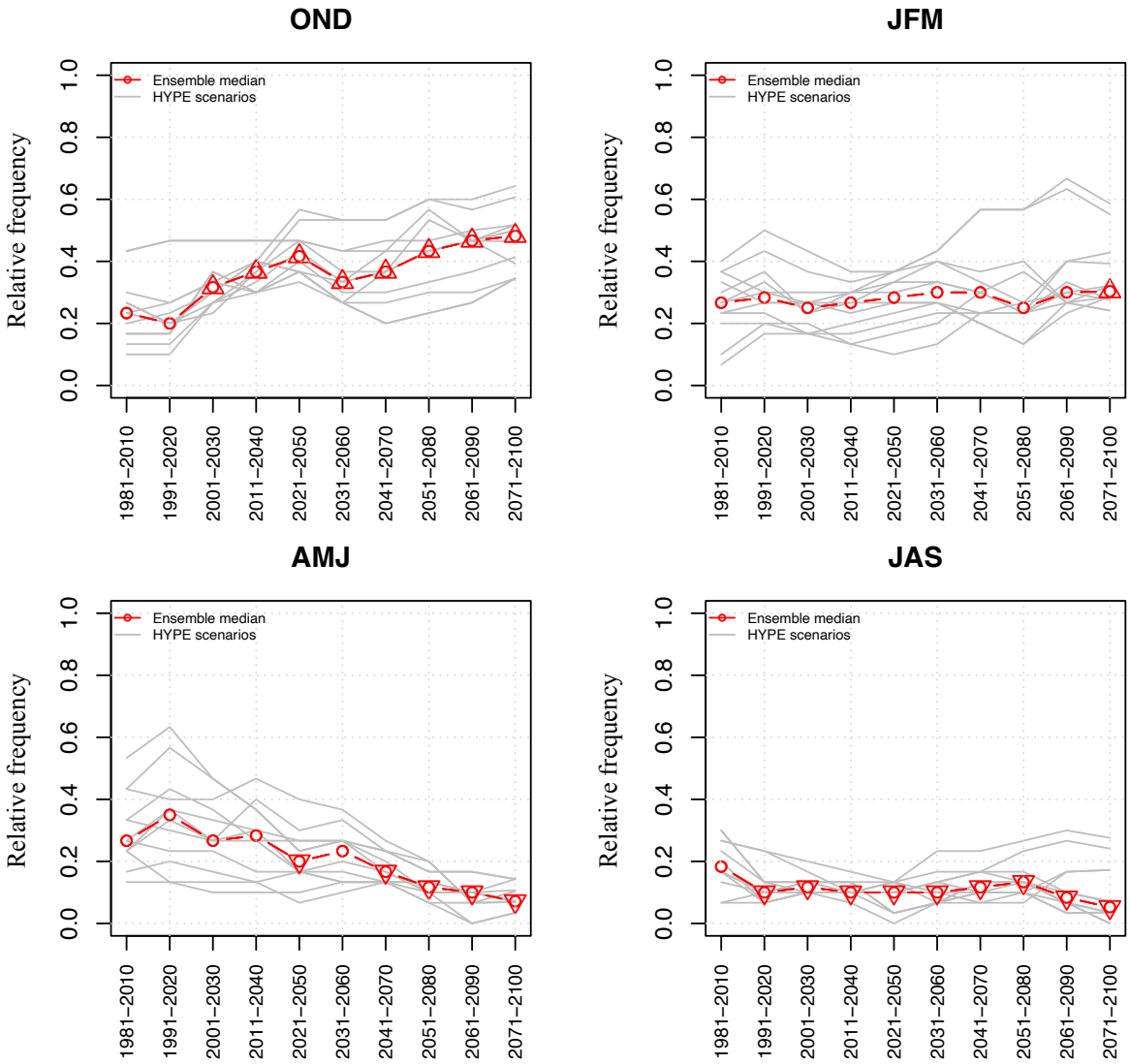

Fig. XI-4: Catchment vhm218: Projected seasonal frequency of occurrence of AMFs (RCP8.5 emission scenario). Ensemble members (grey lines) and ensemble median (red line). The symbols on the ensemble median indicate whether a significant shift in the ensemble of seasonal frequencies has been detected between the reference and future periods (triangle point-up=freq. increase; triangle point down=freq. decrease; open circle=no significant change).

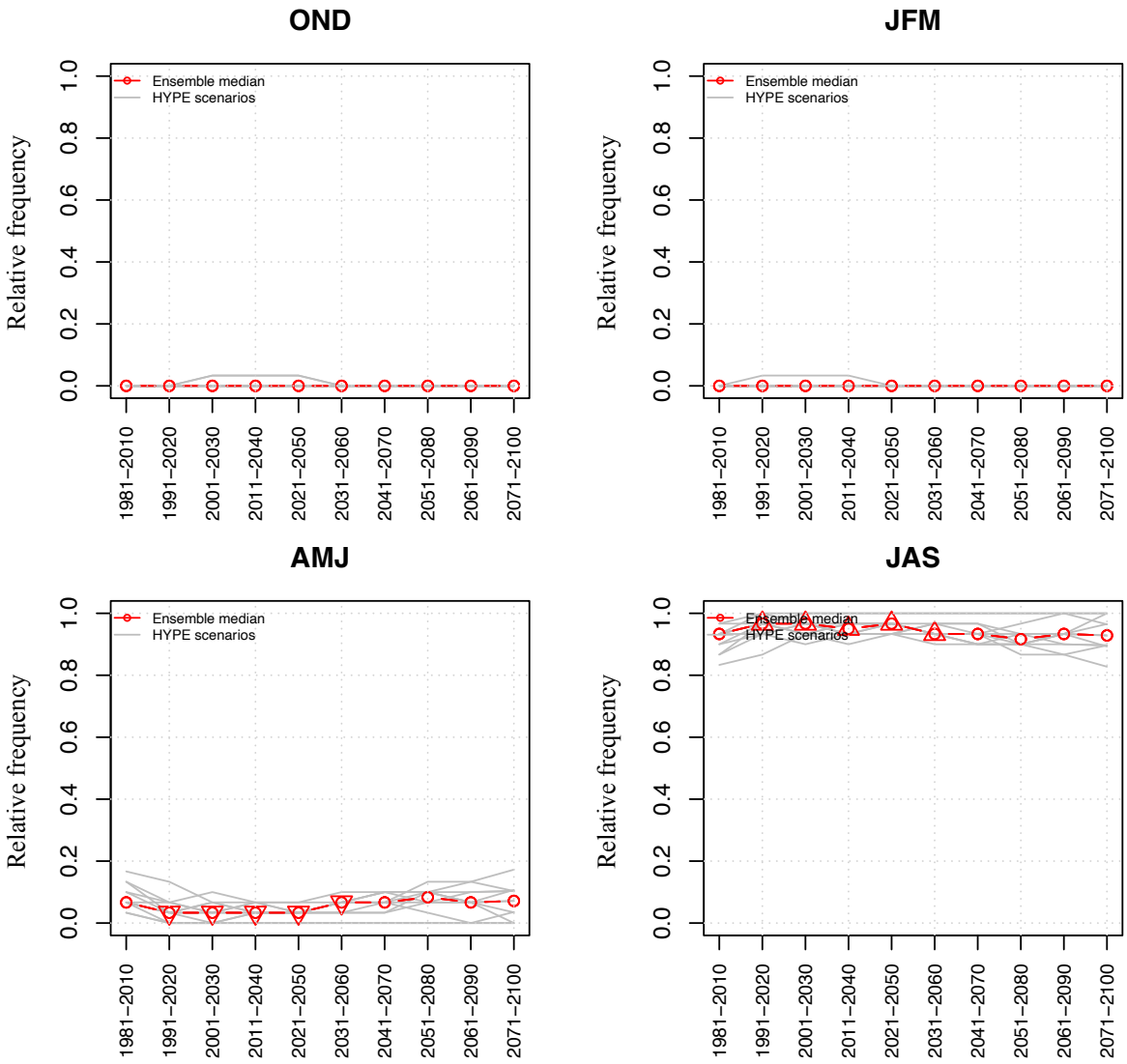

Fig. XI-5: Catchment vhm233: Projected seasonal frequency of occurrence of AMFs (RCP4.5 emission scenario). Ensemble members (grey lines) and ensemble median (red line). The symbols on the ensemble median indicate whether a significant shift in the ensemble of seasonal frequencies has been detected between the reference and future periods (triangle point-up=freq. increase; triangle point down=freq. decrease; open circle=no significant change).

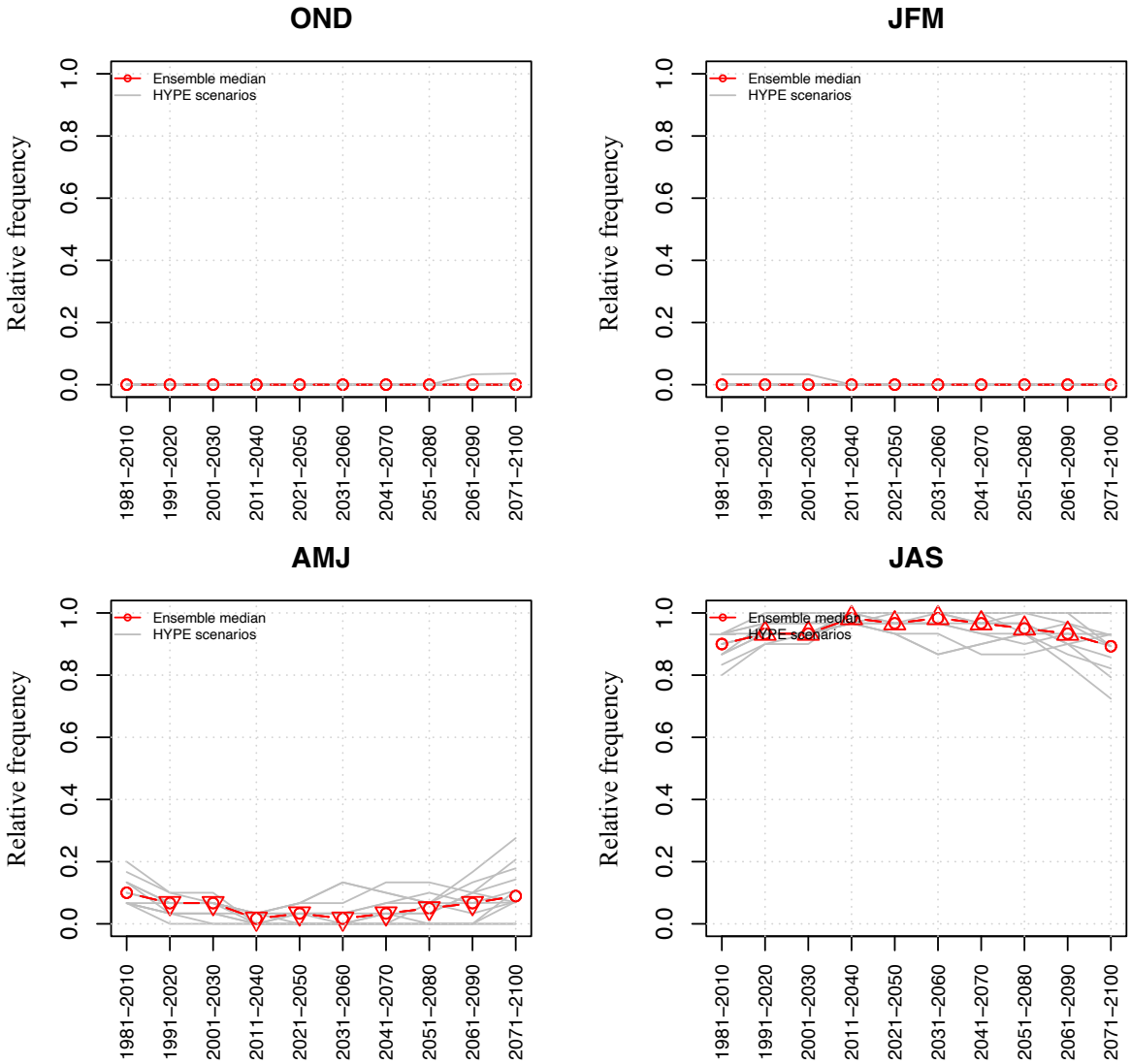

Fig. XI-6: Catchment vhm233: Projected seasonal frequency of occurrence of AMFs (RCP8.5 emission scenario). Ensemble members (grey lines) and ensemble median (red line). The symbols on the ensemble median indicate whether a significant shift in the ensemble of seasonal frequencies has been detected between the reference and future periods (triangle point-up=freq. increase; triangle point down=freq. decrease; open circle=no significant change).